Open quantum systems
—
Resolving issues beyond ultraweak system-bath coupling

vorgelegt von
M. Sc.
Tobias Becker
ORCID: 0009-0003-7839-2307

an der Fakultät II – Mathematik und Naturwissenschaften
der Technischen Universität Berlin
zur Erlangung des akademischen Grades

Doktor der Naturwissenschaften
- Dr. rer. nat. -

genehmigte Dissertation

Promotionsausschuss:

Vorsitzender:	Prof. Dr. Christian Thomsen
Gutachter:	Prof. Dr. André Eckardt
Gutachterin:	Prof. Dr. Janet Anders

Tag der wissenschaftlichen Aussprache: 20.03.2024

Berlin 2024

Publications in Peer-Reviewed Journals

[1] Tobias Becker, Ling-Na Wu and André Eckardt, Lindbladian approximation beyond ultraweak coupling, Physical Review E **104**, 014110 (2021).

[2] Tobias Becker, Alexander Schnell and Juzar Thingna, Canonically Consistent Quantum Master Equation, Physical Review Letters **129**, 200403 (2022).

[3] Tobias Becker, Ché Netzer and André Eckardt, Quantum Trajectories for Time-Local Non-Lindblad Master Equations, Physical Review Letters **131**, 160401 (2023).

Preprints and manuscripts in preparation

[4] Tobias Becker and André Eckardt, Optimal form of time-local non-Lindblad master equations, arxiv preprint (2023), arxiv:2312.15066.

[5] Camilo Santiago Tello Breuer, Tobias Becker and André Eckardt, Benchmarking quantum master equations beyond ultraweak coupling, arxiv preprint (2024), arxiv:2403.08320.

Zusammenfassung

Realistische Quantensysteme sind unweigerlich an deren Umgebung gekoppelt, wodurch die Beschreibung als geschlossenes Quantensystem zweifelhaft ist. Gleichzeitig erreicht die experimentelle Kontrolle einen Grad an Präzision, wodurch die Kopplung an die Umgebung sogar als Ressource für die Kontrolle von Quantensystemen genutzt werden kann. Aus diesem Grund gewinnt die Theorie offener Quantensysteme zunehmend an Aufmerksamkeit. Dabei ist das allgemeine Ziel eine Beschreibung für die Dynamik des Systems allein zu finden, wobei über die Freiheitsgrade der Umgebung, welche als thermisches Bad aufgefasst wird, gemittelt wird.

Häufig werden effektive Bewegungsgleichungen, sogenannte (Quanten-)Mastergleichungen, für den Dichteoperator des Systems herangezogen, welche von den mikroskopischen Details des Gesamtsystems abgeleitet werden. Im Allgemeinen erfordert dieses Vorgehen gewisse Näherungen, so wie zum Beispiel die schwache Kopplung zwischen dem System und dem Bad, wodurch die Genauigkeit von Mastergleichungen herausgefordert wird. In gleicher Weise, insbesondere für große Quantensysteme, ist die effiziente Lösung der Mastergleichungen mittels numerischer Simulationen relevant.

Das Standardverfahren zur Herleitung einer Mastergleichung geht von der Born-Markov-Näherung für schwache System-Bad Kopplung aus. Ausgehend von der störungstheoretischen Entwicklung bis zur zweiten Ordnung in der Kopplung, wird angenommen, dass das Bad in seinem Gleichgewichtszustand verbleibt und dass die Anregungen im Bad schnell genug zerfallen, sodass diese keinen Einfluss auf den Systemzustand zu einer späteren Zeit haben. Unter diesen Nährungen erhält man die zeitlich lokale Redfield-Gleichung.

Im Vergleich zu alternativen Näherungsverfahren, für welche oftmals die Redfield-Gleichung der Ausgangspunkt ist, liefert die Redfield-Gleichung in ihrem Geltungsbereich eine genauere Beschreibung. Für ultraschwache Kopplung im Gleichgewicht liefert die Redfield-Gleichung einen stationären Zustand, welcher mit dem thermischen Gibbs-Zustand der statistischen Mechanik übereinstimmt. Darüber hinaus liegt die Konsistenz mit statistischer Mechanik auch jenseits ultraschwacher Kopplung vor, zumindest für die Kohärenzen des Dichteoperators. Allerdings werden die Populationen der ungestörten Eigenzustände des Systems in zweiter Ordnung der Kopplung nicht akkurat hervorgesagt. Zudem ist bekannt, dass die Redfield-Gleichung in gewissen Parameterbereichen zu Zuständen negativer Besetzungswahrscheinlichkeit führt.

Aus diesen Gründen wird die Redfield-Gleichung für gewöhnlich auf Gorini-Kossakowski-Sudarhsan-Lindblad (GKSL) Form reduziert. Im Allgemeinen sind Mastergleichung von GKSL-Form von zentraler Bedeutung für die Theorie offener Quantensysteme, da diese vollständig positive Dynamik garantieren. Überdies kann die Dynamik des Dichteoperators unter einer GKSL-Mastergleichung effizient durch ein Ensemble von sogenannten Quantentrajektorien simuliert werden. Diese sind reine Quantenzustände und folgen stochastischer Dynamik, wobei deren kohärente Zeitentwicklung durch zufällig auftretende Quantensprünge unterbrochen

wird.

Um die Redfield-Gleichung auf GKSL-Form zu reduzieren, wird in der Regel die Drehwellennäherung, im Englischen als *rotating-wave approximation* (RWA) bekannt, angewandt, wodurch man die quantenoptische Mastergleichung erhält. Bei der RWA wird angenommen, dass schnell oszillierende Terme in der Redfield-Gleichung im Mittel verschwinden und vernachlässigt werden können. Für ultraschwache Kopplung ist die so erhaltene quantenoptische Mastergleichung so akkurat wie die Redfield-Gleichung. Jenseits ultraschwacher Kopplung ist die RWA allerdings nicht mehr gültig. Beispielsweise ist der vorhergesagte stationäre Zustand unabhängig von der Kopplungsstärke.

Abgesehen von existierenden alternativen Methoden bleibt die akkurate und effiziente Beschreibung von offenen Quantensystemen jenseits ultraschwacher Kopplung bislang ein ungelöstes Problem. Diese Arbeit präsentiert drei Hauptergebnisse, welche dazu dienen können, die Probleme jenseits ultraschwacher Kopplung zu lösen.

Das erste Projekt ist eine Alternative zur RWA und reduziert die Redfield-Gleichung auf GKSL-Form. Für diese Methode wird eine Transformation hergeleitet, welche die Redfield-Gleichung zunächst auf pseudo-Lindblad-Form bringt, welche strukturell mit der GKSL-Form übereinstimmt, jedoch auch Terme mit negativem Gewicht beinhaltet. Dabei sind verschiedene pseudo-Lindblad-Darstellungen möglich, welche durch Symmetrieparameter charakterisiert sind. Es wird die optimale pseudo-Lindblad-Darstellung mit einem minimalen Gewicht der negativen Terme gefunden. Die Näherung der Vernachlässigung der negativen Terme führt auf GKSL-Form und ist anwendbar in einem großen Parameterbereich jenseits ultraschwacher Kopplung.

Im zweiten Projekt wird eine Methode für Quantentrajektorien für pseudo-Lindblad-Gleichungen entwickelt. Anders als die bisher bekannten Methoden, welche zumindest eine effektive Verdopplung des Zustandsraumes erfordern, wird in diesem Algorithmus eine Trajektorie lediglich um ein klassisches Bit erweitert, welches das Vorzeichen des pseudo-Lindblad-Gewichts kodiert. Hierbei wird für kleine negative Gewichte eine gute statistische Konvergenz erreicht, weshalb die Methode mit einer zustandsabhängigen Minimierung kombiniert wird, um die Dynamik der Redfield-Gleichung effizient zu simulieren.

Das dritte zentrale Ergebnis dieser Arbeit ist die kanonisch konsistente Mastergleichung. Diese modifiziert die Redfield-Gleichung um einen Beitrag höherer Ordnung in der Kopplung, welcher die Dynamik steuert und zum korrekten stationären Zustand führt. Die Methode verbindet statistische Mechanik, und den damit beschriebenen exakten Gleichgewichtszustand, mit einer dynamischen Theorie. Die neue Mastergleichung liefert genaue Ergebnisse, nicht nur für den stationären Zustand, sondern auch für die transiente Dynamik. Darüber hinaus lässt sich für den gedämpften harmonischen Oszillator zeigen, dass die gefundene Mastergleichung Positivität garantiert. Mit dem gleichen numerischen Aufwand und derselben konzeptionellen Komplexität wie die der Redfield- und GKSL-Gleichungen, liefert die kanonisch konsistente Mastergleichung akkurate Dynamik auch jenseits ultraschwacher Kopplung.

Abstract

Realistic quantum systems are inevitably coupled to their environment, which challenges the description as closed quantum systems. At the same time, experimental platforms are now entering the realm, where such coupling to the environment can be precisely controlled and, thus, is seen as a resource for dissipative state engineering. To this end, the theory of open quantum systems is gaining great attention. Here, the general aim is to find a description for the reduced dynamics of the system by averaging over the degrees of freedom of the environment, which is typically modelled as a thermal bath.

Often, effective equations of motion, so-called quantum master equations, for the density operator of the system are formulated, which are derived from the microscopic details of the total system-bath compound. In general, these derivations require certain approximations, e.g., weak coupling between system and bath, which challenge the accuracy of quantum master equations. At the same time, and equally important, especially for large quantum systems, master equations should allow for efficient numerical simulations.

The standard approach to derive a quantum master equation is via the Born-Markov approximation for weak system-bath coupling. There, in a perturbative expansion to second order in the system-bath coupling, it is assumed that the bath remains in its equilibrium state, and that the bath excitations decay sufficiently fast, such that they do not have an influence on the system's state at later times. With this, one obtains the time-local Redfield equation.

As compared to other approximative approaches, for which the Redfield equation is often the starting point, in its applicable regime, the Redfield equation yields a more accurate description. For ultraweak coupling in equilibrium, the predicted steady state coincides with the thermal Gibbs state of statistical mechanics. Furthermore, the consistency with statistical mechanics also applies beyond ultraweak coupling, at least, to the coherences of density operator. Nevertheless, the populations of the unperturbed system's eigenstates are not accurately predicted in second order of the coupling. Moreover, in certain parameter regimes, the Redfield equation is known to yield negatively populated states.

To this end, the Redfield equation is often reduced to Gorini-Kossakowski-Sudarshan-Lindblad (GKSL) form. In general, quantum master equations of GKSL form play a central role in the theory of open quantum systems, as they guarantee completely positive dynamics. Furthermore, for GKSL master equations, the dynamics of the density operator can be efficiently simulated by an ensemble of so-called quantum trajectories, which are pure states that obey stochastic dynamics, and for which the coherent time evolution is interrupted by spontaneously occurring quantum jumps.

Usually, the Redfield equation is reduced to the quantum-optical master equation of GKSL form by further employing the rotating-wave approximation (RWA). Within the RWA, rapidly oscillating terms in the Redfield equation are assumed to average out and are neglected.

For ultraweak coupling, the quantum-optical master equation is as accurate as the Redfield equation. However, beyond ultraweak coupling the RWA is no longer valid. For instance, the predicted steady state is independent of the coupling strength.

Despite existing alternative approaches, an accurate and efficient description of open quantum systems beyond ultraweak system-bath coupling is still an open problem. In this thesis, three main results are presented intending to solve the problems beyond ultraweak system-bath coupling.

In the first project, an alternative approximation is proposed to reduce the Redfield equation to GKSL form. For this approach, a transformation is derived that brings the Redfield equation into pseudo-Lindblad form, which is analogous to the GKSL form, except it also includes terms with negative weights. Different pseudo-Lindblad representations are possible, which are controlled by symmetry parameters. The optimal pseudo-Lindblad representation is found with a minimal weight of the negative contribution. The truncation of the negative contribution leads to the GKSL form, which is an approximation, applicable in a large parameter regime beyond ultraweak coupling.

In the second project, a quantum-trajectory approach for pseudo-Lindblad equations is derived. While existing approaches require at least a doubling of the state space, the algorithm presented here only requires one auxiliary classical bit for the trajectory that encodes the sign of the pseudo-Lindblad weight. The statistical convergence is good for small negative weights and is combined with a state-dependent minimization procedure to efficiently simulate the dynamics of the Redfield equation.

In the third project, the canonically consistent quantum master equation is proposed, which modifies the Redfield equation by a contribution of higher order in the coupling that steers the dynamics towards the correct steady state. It is based on incorporating the exact equilibrium state, dictated by statistical mechanics, into the dynamical theory. The new master equation yields accurate results not only for the stationary state, but also for the dynamics. Furthermore, for the damped harmonic oscillator in thermal equilibrium, it is proven to guarantee positivity. The canonically consistent master equation accurately describes the dynamics beyond the ultraweak coupling regime of Redfield and quantum-optical master equations, while it retains the same conceptual and numerical complexity.

Contents

1 Introduction

Quantum mechanics is the fundamental theory of physics. It states that quantum systems are described by vectors in the Hilbert space that follow deterministic dynamics dictated by the Hamiltonian of the system. There is immense progress in the experimental control of quantum systems with many degrees of freedom. Prominent platforms are for instance, ultracold quantum gases, trapped ions, superconducting circuits, quantum dots, nitrogen-vacancy centers et cetera. However, isolated quantum systems are an idealized description. Instead, realistic quantum systems are always open systems that couple to the degrees of freedom of the environment.

The theory of open quantum systems is a necessity for not perfectly isolated systems and furthermore is relevant for quantum control. The control over the dissipative channels can be used to guide the system into engineered nonequilibrium states. It can be used to influence transport properties, such as heat and particle exchange between quantum reservoirs [1–3].

In combination with driving, e.g., by time-periodic forces or by coupling the system to several independent baths, open systems give rise to new unprecedented phases of matter. In equilibrium, below a critical temperature, bosons form a Bose-Einstein condensate [4]. In contrast, in nonequilibrium, the condensate can be fragmented into different energy eigenstates, because there is no natural order for quantum states that would be dictated by the energies [5–7]. Nonequilibrium Bose-Einstein condensation has been realized, e.g., for Dye molecules in solution pumped with photons using a microcavity. Here, the steady-state populations show nonequilibrium Bose condensation in higher excited states [8–11].

Driven-dissipative dynamics is also present in quantum optics, where the interaction of matter with light is considered [12, 13]. The interplay of drive, relaxation and loss forms correlated excitations of light and matter (polaritons), such as strongly coupled electron-photon excitations in a semiconductor microcavity [14], or correlated photon-Rydberg excitations in an optical microcavity [15]. Light-matter interaction can also be designed in quantum circuits with artificial atoms. For instance, the measured resonance lineshape of Josephson junctions, each comprising of capacitive-inductive circuits, deviates from static predictions and necessitates a dynamical theory [16].

The examples above show that there is an increasing interest in the out-of-equilibrium dynamics for quantum system with many degrees of freedom. For those many-body systems, the description of quantum states is very challenging, because the dimensionality of the state

space growths exponentially with the system size and the particle number. For the environment, one resorts to a statistical description which reduces the complexity. Environments are modelled as a thermal baths that are described by a few state variables, such as temperature and chemical potential. However, an accurate modelling for the out-of-equilibrium dynamics is challenging because, conceptually, quantum dynamics is formulated for isolated systems, in which all degrees of freedom of the system and the bath enter. The general goal for the theory of open quantum systems is to derive an effective equation of motion for the reduced dynamics of the open system, by averaging over the bath's degrees of freedom. This is referred to as quantum master equation for the reduced density operator of the system.

From first principles of quantum mechanics, master equations are typically derived perturbatively in orders of the system-bath coupling. For weak coupling between system and bath, a second-order master equation is justified [17]. Here, it is assumed that the open system varies slowly as compared to the fast relaxation dynamics of the bath. This clear separation of time scales is fundamental to obtain a time-local master equation. It is usually formulated using the Born-Markov assumption [18–23]. The system creates excitations in the equilibrium state of the bath. As compared to the slow variation of the open system, the bath excitations decay fast and it is assumed that they do not influence the system at latter times. The Born assumption is that the bath effectively remains in its equilibrium state and that there are no correlations between system and bath. Furthermore, the Markov assumption is that time-nonlocal contributions in the generator can be neglected. Under these assumptions one obtains the time-local Redfield equation [24–27]. An equivalent formulation is known as the second-order time-convolutionless master equation [28, 29] derived from the Nakajima-Zwanzig equation [30, 31].

The Redfield equation has been benchmarked to alternative approaches, e.g., coarse-grained master equations [32–34], the partial-rotating-wave approximation [35, 36], and the quantum-optical master equation [18–22], and is shown to be the most accurate one [37]. In equilibrium, the stationary state of the Redfield equation yields coherences that are consistent with statistical mechanics [38–44, 17]. For ultraweak coupling, that is in zeroth order of the system-bath coupling, the steady state coincides with the canonical Gibbs state of thermal equilibrium.

However, the Redfield equation is not free of problems. On the one hand, beyond ultraweak coupling, the predicted eigenstate populations in equilibrium deviate from the expectation of statistical mechanics given by the reduced Gibbs state [38–42]. On the other hand, the Redfield equation is known to yield unphysical negatively populated states, which commonly happens in parameter regimes where the Born-Markov approximation is not longer valid [45–47].

To this end, a certain algebraic form of quantum master equations, i.e., master equations of Gorini-Kossakowski-Sudarshan-Lindblad (GKSL) form are commonly favoured and play a central role in the theory of open quantum systems. Master equations of GKSL form preserve hermiticity, normalization and complete positivity of the quantum state, for which the latter

is a long-standing debate of open quantum system dynamics [48–50]. Furthermore, master equations of GKSL form are closely related to stochastic processes and can be efficiently simulated by an ensemble of pure state trajectories that evolve stochastically [51–57].

For a microscopic description, commonly, the quantum-optical master equation is used [18–22]. This GKSL master equation describes the exponential decay of coherences and spontaneously occurring quantum jumps between the eigenstates of the system. The stationary state is independent of the coupling strength and in equilibrium, it yields the canonical Gibbs state. Consequently the quantum-optical master equation is an ultraweak coupling approximation, which is valid in the limit of vanishing coupling [17].

The quantum-optical master equation follows from the Redfield equation by further employing the rotating-wave approximation (RWA), first proposed by Rabi *et al.* in Ref. [58] and later by Jaynes and Cummings in Ref. [59]. The RWA assumes that only those terms in the Redfield equation with slow varying phases would contribute to the dynamics, whereas the rapidly oscillating terms would average out and are neglected. In addition to the Born-Markov assumption, in the RWA it is assumed that the open system varies slowly as compared to the intrinsic time scale of the system. However, this additional step requires ultraweak system-bath coupling, which is small compared to the energy level splittings of the system. The RWA and with this the quantum-optical master equation is no longer valid beyond ultraweak coupling or if the eigenstates come close in energy [60–62]. For instance, in many-body systems energy eigenstates become quasi-degenerate, which yields slow intrinsic dynamics and also violates the RWA. Furthermore, in time-periodically driven open quantum systems the RWA is only valid for high frequency driving [63–66].

The question arises: What is an accurate modelling for the reduced dynamics of the system beyond ultraweak coupling, in regimes where the RWA breaks down? At the same time, and equally important, the theoretical description should allow for efficient numerical simulations. One solution would be to omit the RWA and use Redfield equation in regimes where positivity holds or is only marginally violated [24–27]. However, the Redfield equation is not of GKSL form and does not directly allow for an efficient time evolution via quantum trajectories [67–73].

In the literature, many alternative approaches have been proposed. For instance, there are quasi-exact stochastic approaches for open quantum systems, e.g., hierarchical equations of motion [74–76], hierarchy of pure states (HOPS) [77], quantum state diffusion [56, 78], or quasi-adiabatic propagator path integrals [79–81]. The idea of these approaches is to augment the system's state space by auxiliary degrees of freedom and to solve the open system dynamics via a stochastic unraveling. However, typically these approaches exploit elaborative numerical tools for adequate convergence, which is not at the focus of this thesis [82–85].

Apart from the Redfield and quantum-optical master equations, there are alternative master equation approaches: For instance, the exact Hu-Paz-Zhang master equation [86], which is

only applicable to the damped harmonic oscillator.

Another approach is the reaction-coordinate mapping [87, 88], where the system is augmented by a collective bath mode. There, for baths with a narrow spectral width, the coupling to the residual bath can be treated in the ultraweak coupling limit. However, the extended state space challenges the numerical simulation and, furthermore, for baths with a broad spectrum, the residual coupling is not ultraweak.

An alternative formalism that intends to include correlations between system and bath has been formulated in Ref. [89]. It leads to a formal master equation that is the starting point for a weak-correlation expansion. However, this correlation-picture approach does not yield a master equation of GKSL form.

Recently, an alternative approximation to reduce the Redfield equation to GKSL form has been proposed [90]. This approach is valid on the same order as the Redfield equation, however, it does not yield the accurate coherences in second order of the coupling.

The concepts of open quantum systems can even be adapted to the ultrastrong coupling regime [17]. In this regime, when the coupling strength dominates all energy scales, a perturbative expansion for ultraweak inverse coupling has been applied to derive the corresponding equilibrium state [17]. Furthermore, this expected equilibrium state is the stationary state of the master equation derived for the ultrastrong coupling regime [91].

In summary, there is ongoing development and interest for quantum master equations and efficient simulations beyond ultraweak coupling, in regimes where the rotating-wave approximation breaks down, and in regimes where the Redfield equation is inaccurate or yields negatively populated states. For instance, it is controversially discussed, whether the reduced dynamical map should be described by a GKSL master equation, or if one should allow for a more general class of generators [46, 92–94]. Existing master equations beyond ultraweak coupling in general face the problems that they not guarantee positive evolution, that they are inconsistent with statistical mechanics, that they are not model independent, or that they not allow for the efficient simulation of quantum trajectories. In this thesis we present different approaches intending to resolve these problems.

In Chapter 2, the concepts of open quantum systems are introduced. The derivations of the second-order master equations, i.e., the Redfield and quantum-optical master equations are presented and the problems beyond ultraweak coupling are pointed out. Throughout this thesis, the concepts are benchmarked against the exact dynamics of the damped harmonic oscillator.

In Chapter 3, the Redfield equation is mapped to what is referred to as *pseudo-Lindblad* equation, which has the structure of a GKSL equation, except that it also possesses dissipators with negative weights. It turns out that the mapping is not unique, but instead leads to a class of equivalent pseudo-Lindblad equations represented by symmetry parameters. The optimal pseudo-Lindblad equation is found, which minimizes the negative relaxation weights. With

this, an alternative to the RWA is proposed by truncating the negative contribution. By analytically analysing the truncated term, and within numerical simulations, also for a many-body system using quantum trajectories, it is shown that this approach works well in a large parameter regime, where the RWA is no longer valid.

In Chapter 4, the quantum-trajectory unraveling scheme for GKSL master equations is generalized to pseudo-Lindblad equations. This is referred to as *pseudo-Lindblad quantum-trajectory* (PLQT) approach, which is relevant for the remaining parameter space, where the negative contribution in the Redfield equation is small but cannot be neglected. This new approach is derived by extending the state space in a minimal fashion, for which the trajectories are equipped with one additional classical bit, which encodes the sign of the pseudo-Lindblad dissipator weight. The algorithm shows good statistical convergence for small negative weights. To this end, we combine the PLQT approach with the pseudo-Lindblad mapping of the Redfield equation using a state-dependent minimization of the negative dissipator weights.

In Chapter 5, the inconsistency between the Redfield equation and statistical mechanics beyond ultraweak coupling is resolved. In a rigorous second-order expansion, which combines a dynamical description with statistical mechanics in a holistic way, the *canonically consistent quantum master equation* (CCQME) is proposed. It modifies the Redfield equation with a contribution that is effectively of fourth order in the coupling and that steers the dynamics towards the correct steady state. By benchmarking it with exact dynamics, we demonstrate that the CCQME significantly improves upon the dynamics of the Redfield equation and quantum-optical master equation. For the damped harmonic oscillator, we prove that the CCQME guarantees positive evolution, albeit without being of GKSL form.

In Chapter 6, a prelude to future directions for the regime of ultrastrong coupling and time-periodically driven open quantum systems is outlined. In Chapter 7, the results of this thesis are summarized and concluding remarks are given.

2 Open quantum systems and their description beyond ultraweak coupling

Quantum systems that are not isolated, but instead couple to environmental degrees of freedom are referred to as open quantum systems. Typically, the coupling between system and bath is considered to be weak and the bath is modelled as a continuum of either fermions or bosons in thermal equilibrium. One then aims to derive an effective equation of motion for the reduced dynamics of the system in a perturbative expansion in the coupling.

In this chapter, after introducing the correlations in thermal baths, together with the spectral density and coupling density, the derivation of the second-order Redfield equation is stated. In contrast to the often used Born-Markov approximation, it is shown that the Redfield equation follows rigorously in second-order perturbation theory, which is corroborated by considering the exact master equation of the damped harmonic oscillator.

Often, the Redfield equation is further reduced to the quantum-optical master equation by performing the rotating-wave approximation. However, the quantum-optical master equation is only valid for ultraweak coupling and in particular, the stationary state is independent of the coupling and, thus, only valid if the coupling approaches zero.

Because the Redfield equation is known to possibly violate positivity, it is only since recently that is has gained more attention. As well-known result, we reiterate that any second-order master equation is inconsistent for finite coupling, which is not related to the fact that the Redfield equation is not of GKSL form. As novel result, for the damped harmonic oscillator, we identify this inconsistency in the uncertainty principle for momentum and displacement, which is, furthermore, the reason why positivity may be violated for finite coupling and low bath temperatures.

Subsequent discussions in Chapters 3 to 5, are based on the preliminaries and the notations specified in this chapter. Throughout, the thesis we work in units, where energies are identified with frequencies by formally setting Planck's constant to one, i.e., $\hbar = 1$. Similarly, temperatures are identified with energies by formally setting Boltzmann's constant to one, i.e., $k_{\mathrm{B}} = 1$.

2.1 The canonical form to couple system and bath

The microscopic Hamiltonian of the total system-bath compound is denoted as

$$H_{\mathrm{tot}} = H_{\mathrm{S}} + H_{\mathrm{SB}} + H_{\mathrm{B}}, \tag{2.1}$$

with H_{S} and H_{B} acting solely on the system and bath, respectively. System and bath are coupled via the interaction Hamiltonian H_{SB} acting on the joint Hilbert space of system and bath, which is schematically depicted in Fig. 2.1. Without loss of generality, the interaction can be written in the canonical form, e.g., by doing a Schmidt decomposition,

$$H_{\mathrm{SB}} = \sum_{\alpha} (S_\alpha \otimes B_\alpha^\dagger + S_\alpha^\dagger \otimes B_\alpha), \tag{2.2}$$

with S_α referred to as coupling operator solely acting on the system and B_α being some bath operator. Here, multiple coupling operators S_α for $\alpha = 1, 2, \ldots$ shall be considered, only, for system driven out of equilibrium by multiple reservoirs, for which we write $H_{\mathrm{B}} = \sum_\alpha H_{\mathrm{B}\alpha}$. To keep the notation simple, in this thesis often only one channel with interaction Hamiltonian $H_{\mathrm{SB}} = S \otimes B^\dagger + S^\dagger \otimes B$ is considered. Generalizations, e.g., for quantum master equations with multiple coupling channels, are easily found by reintroducing the summation over α.

We assume that the bath is a collection of non-interacting particles, for which we denote the single-particle annihilators as b_k. The bath Hamiltonian is assumed to be quadratic in b_k and has the diagonal form

$$H_{\mathrm{B}} = \sum_k \omega_k b_k^\dagger b_k, \tag{2.3}$$

where b_k and $b_k^\dagger$ is the annihilation operator creation operator for single particle modes labelled by k with eigenenergy ω_k. It is reasonable to assume that the coupling to individual bath modes

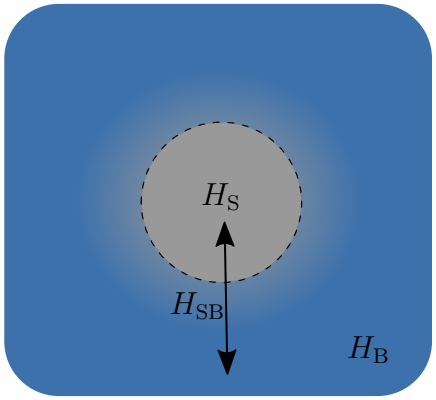

Figure 2.1: Illustration of a general open quantum system with total Hamiltonian $H_{\mathrm{tot}} = H_{\mathrm{S}} + H_{\mathrm{SB}} + B_{\mathrm{B}}$ describing system, bath and system-bath interaction with H_{S}, H_{B} and H_{SB}, respectively.

scales inversely with the number of bath modes, since the bath is assumed to be macroscopic. Consequently, the bath operator B can be considered to be linear in the bath modes b_k [23],

$$B = \sum_k c_k b_k, \tag{2.4}$$

where c_k is generally complex and determines the coupling strength between the system and individual bath modes. In particular, higher order contributions are suppressed. The coupling operator S defines the particular type of interaction. A simple example is given by a system with a single annihilation operator a, such as the harmonic oscillator. On the one hand, modelling a non-Hermitian coupling operator, e.g., $S = a$ yields a coupling channel $H_{\mathrm{SB}} = \sum_k c_k a \otimes b_k^\dagger + \mathrm{H.c.}$, which describes exchange of excitations between system and bath. On the other hand, a Hermitian coupling operator, e.g., $S = a^\dagger + a$ yields a coupling channel $H_{\mathrm{SB}} = S \otimes (B^\dagger + B) = \sum_k c_k (a + a^\dagger) \otimes (b_k^\dagger + b_k)$, which allows for processes that annihilate (create) excitations in both system and bath, respectively. All interactions considered in this thesis allow for an exchange of excitations between system and bath. As a consequence of a time-independent total Hamiltonian, the total energy of the system-bath compound is fix. We consider baths in thermal equilibrium that are described by some finite temperature, for which β denotes the inverse temperature.

2.2 Temporal correlations in a thermal bath

Bath correlations are essential in the description of open quantum systems and are relevant for the reduced dynamics of the system. The total system-bath state at time t is given by $\varrho_{\mathrm{tot}}(t) = U_{\mathrm{tot}}(t)\varrho_{\mathrm{tot}}(0)U_{\mathrm{tot}}^\dagger(t)$, with the unitary time evolution operator of the total system-bath compound $U_{\mathrm{tot}}(t) = \exp[-\mathrm{i}(H_{\mathrm{S}} + H_{\mathrm{SB}} + H_{\mathrm{B}})t]$. By tracing over the bath degrees of freedom, the reduced density matrix of the system $\varrho(t) = \mathrm{tr}_{\mathrm{B}}\, \varrho_{\mathrm{tot}}(t)$ involves different kinds of bath correlation functions. In a perturbative treatment, to first non-trivial order in the system-bath coupling Hamiltonian, such as in the Redfield formalism, only two-point correlations of the interaction Hamiltonian H_{SB} appear [Section 2.4]. For the generic decomposition $H_{\mathrm{SB}} = S \otimes B^\dagger + S^\dagger \otimes B$, we are interested in the temporal bath correlations $\langle \boldsymbol{B}(t)^\dagger B\rangle$ and $\langle \boldsymbol{B}(t) B^\dagger\rangle$, where $\langle\cdot\rangle = \mathrm{tr}_{\mathrm{B}}(\cdot\varrho_{\mathrm{B}})$ denotes the expectation value in the equilibrium bath state ϱ_{B}. They describe the two-time correlation between B at the initial time $t_0 = 0$ and $B^\dagger$ at time $t_0 + t$. Here, $\boldsymbol{B}(t) = e^{\mathrm{i}H_{\mathrm{B}}t} B e^{-\mathrm{i}H_{\mathrm{B}}t}$ is the Heisenberg operator with respect to the bath Hamiltonian H_{B}. A detailed discussion on how this bath correlation appears in the reduced dynamics of the system, is given in the derivation of the Redfield equation in Section 2.4. In this section, general properties of the bath correlation are discussed.

2.2.1 Model interaction by a continuous function - spectral density

A naive calculation of the bath correlation involves all microscopic properties of the bath. Let b_k ($b_k^\dagger$) be the annihilation (creation) operator for a bath mode of energy ω_k, such that the bath Hamiltonian can be written as in Eq. (2.3). The bath may either have bosonic or fermionic character depending on the commutation relation of the bath modes. Throughout this thesis, we concentrate on bosonic baths. However, analogous expressions can be found for fermionic baths. In the eigenbasis of the bath, the Heisenberg operator $\boldsymbol{B}(t) = e^{\mathrm{i}H_\mathrm{B}t}Be^{-\mathrm{i}H_\mathrm{B}t}$ reads

$$\boldsymbol{B}(t) = \sum_{k=1}^{\infty} c_k e^{-\mathrm{i}\omega_k t} b_k. \tag{2.5}$$

Since in a thermal state modes of different energy are not correlated $\langle b_k^\dagger b_{k'}\rangle = \delta_{k,k'}\langle b_k^\dagger b_k\rangle = \delta_{k,k'}n_k$ the bath correlation is given by

$$\langle \boldsymbol{B}^\dagger(t)B\rangle = \sum_{k=1}^{\infty} |c_k|^2 \exp[\mathrm{i}\omega_k t] n_k, \tag{2.6}$$

where n_k is the population of the k-th mode. Often, another representation is given that does not require to specify c_k and ω_k for all k, where the sum over the discrete modes is replaced by an integral over a function. By defining the spectral density

$$\tilde{J}(\omega) = \pi \sum_{k=1}^{\infty} |c_k|^2 \delta(\omega_k - \omega), \tag{2.7}$$

the correlation function then takes the form

$$\left\langle \boldsymbol{B}^\dagger(t)B\right\rangle = \int_0^\infty e^{\mathrm{i}\omega t}\tilde{J}(\omega)n_\beta(\omega)\frac{d\omega}{\pi}, \tag{2.8}$$

with the thermal distribution function $n_\beta(\omega) = [\exp(\beta\omega) \mp 1]^{-1}$, where the upper sign applies to a bosonic bath and the lower sign applies to a fermionic bath, respectively.

The spectral density can be understood as the frequency resolved system-bath coupling strength.[1] The additional factor of π is not essential but will be convenient as it will cancel for most bath models. Here, the notation $\tilde{J}(\omega)$ is used to define the spectral density for positive arguments. Analogously, using the commutation relation $b_k b_k^\dagger = 1 \pm b_k^\dagger b_k$ the interchanged correlator is obtained

$$\left\langle \boldsymbol{B}(t)B^\dagger\right\rangle = \int_0^\infty e^{-\mathrm{i}\omega t}\tilde{J}(\omega)[1 \pm n_\beta(\omega)]\frac{d\omega}{\pi}, \tag{2.9}$$

[1] For the quantum-optical master equation, the relevant frequencies are related to transitions between energy eigenstates, where the transition rate R_{qk} is proportional to the spectral density $\tilde{J}(E_q - E_k)$ [Section 2.5.1].

again for bosons (upper sign) and fermions (lower sign), respectively. Often one considers a system-bath interaction of the form $H_{\mathrm{SB}} = S \otimes (B^\dagger + B)$, in which one considers only one Hermitian coupling operator S. Using[2] $1 + 2n_\beta(\omega) = \coth(\beta\omega/2)$ and $\langle \boldsymbol{B}(t)^\dagger B^\dagger \rangle = \langle \boldsymbol{B}(t) B \rangle = 0$ because $\langle b_k^\dagger b_{k'}^\dagger \rangle = \langle b_k b_{k'} \rangle = 0$ in a thermal bath, the bath-bath correlation function is given by

$$\begin{aligned} C(t) &= \big\langle (\boldsymbol{B}^\dagger(t) + \boldsymbol{B}(t))(B^\dagger + B) \big\rangle = \big\langle \boldsymbol{B}^\dagger(t) B \big\rangle + \big\langle \boldsymbol{B}(t) B^\dagger \big\rangle \,, \\ &= \int_0^\infty \cos(\omega t) \tilde{J}(\omega) \coth(\beta\omega/2) \frac{d\omega}{\pi} - \mathrm{i} \int_0^\infty \sin(\omega t) \tilde{J}(\omega) \frac{d\omega}{\pi}, \end{aligned} \tag{2.10}$$

which is the quantum version of the fluctuation-dissipation theorem, where the first term is the temperature dependent symmetrized correlation function and the second term is the response function from the antisymmetric part of the correlation [95–97].

The explicit calculation of the rapidly oscillating integrals in Eq. (2.10) can be challenging. Alternatively, one may use the symmetry of the Bose function[3] $1 + n_\beta(\omega) = -n_\beta(-\omega)$ and define $J(\omega)$ as antisymmetric continuation of the spectral density for negative arguments,

$$J(\omega) \equiv \tilde{J}(\omega)\Theta(\omega) - \tilde{J}(-\omega)\Theta(-\omega) = \begin{cases} \tilde{J}(\omega) & \text{for } \omega < 0, \\ 0 & \text{for } \omega = 0, \\ -\tilde{J}(-\omega) & \text{for } \omega < 0, \end{cases} \tag{2.11}$$

with the Heaviside step function Θ,[4] to write $C(t)$ as Fourier transform,

$$\begin{aligned} C(t) &= \int_0^\infty e^{\mathrm{i}\omega t} \tilde{J}(\omega) n_\beta(\omega) \frac{d\omega}{\pi} - \int_{-\infty}^0 \tilde{J}(-\omega) n_\beta(\omega) \frac{d\omega}{\pi}, \\ &= \int_{-\infty}^\infty e^{\mathrm{i}\omega t} J(\omega) n_\beta(\omega) \frac{d\omega}{\pi}. \end{aligned} \tag{2.12}$$

For certain spectral densities, namely for those with isolated poles in the complex plane [Section 2.2 below], the Fourier transform can be obtained analytically. A detailed discussion for spectral densities can be found in Ref. [23].

It is emphasized that no approximation has been made, which can be seen by reinserting the definition of the spectral density. Moreover, for practical calculations, it is helpful to model the spectral density (2.7) by a smooth function corresponding to the assumption of a large bath. If one would keep the discrete character, only those system energies that match exactly to one of the bath modes would couple to the bath and all others remain unaffected by the

[2] For fermionic baths, one finds $C(t) = \int_0^\infty \cos(\omega t) \tilde{J}(\omega) \frac{\mathrm{d}\omega}{\pi} - \mathrm{i} \int_0^\infty \sin(\omega t) \tilde{J}(\omega) \tanh(\beta\omega/2) \frac{\mathrm{d}\omega}{\pi}$.

[3] With the symmetry of the Bose function the correlation function is rewritten as, $\langle \boldsymbol{B}(t) B^\dagger \rangle = \int_{-\infty}^0 e^{\mathrm{i}\omega t} [-\tilde{J}(-\omega)] n_\beta(\omega)$

[4] The Heaviside step function is defined as, $\Theta(x) = \begin{cases} 1 & , x > 0 \\ 0 & , x \leq 0 \end{cases}$.

bath. Even if this procedure would be possible, which is not the case, since one would have to control infinitely many bath parameters, one would recover the coherent dynamics of the total system-bath compound, which is not dissipative. The spectral density is a measurable quantity. This thesis is mainly focused on Ohmic baths with Drude cutoff at frequency ω_D,

$$J(\omega) = \gamma \frac{\omega}{1+\omega^2/\omega_D^2}, \tag{2.13}$$

where γ is either dimensionless and describes the system-bath coupling strength relative to the energy scales of the system, or defines an inverse relaxation time. To decide the latter, one makes the dimensional analysis for the system-bath Hamiltonian and the bath-bath correlation,

$$[H_{\mathrm{SB}}] = [S][B] = [\hbar][\omega] \quad \Rightarrow \quad [B] = \frac{[\hbar][\omega]}{[S]}, \tag{2.14}$$

$$[J][\omega] = [C] = [B]^2 = \frac{[\hbar]^2[\omega]^2}{[S]^2} \quad \Rightarrow \quad [J] = \frac{[\hbar]^2[\omega]}{[S]^2}, \tag{2.15}$$

where $[\cdot]$ shall denote the dimension of a physical quantity and where all factors of $\hbar$ are explicitly taken into account. The dimension is easily understood for the quantum-optical master equation, for which $\frac{|\langle q|S|k\rangle|^2}{\hbar^2} 2J(\Delta_{qk})n_\beta(\Delta_{qk})$ corresponds to the rate for the transition from state $|q\rangle$ to $|k\rangle$ [Sections 2.5.1 and 3.13]. Here, the additional factor of $\frac{1}{\hbar^2}$ comes from the perturbative expansion of the master equation up to second order.

In Section 2.6, we discuss the damped harmonic oscillator with position-position coupling to the bath, for which one deduces $[J] = [\hbar]$ energy/length^2 $= [\hbar]$ mass/time^2. The corresponding Ohmic-Drude spectral density is $J(\omega) = \hbar M\gamma\omega/(1+\omega^2/\omega_D^2)$, where γ defines an inverse time scale.

2.2.2 Matsubara series for the correlation function $C(t)$

If the bath is large compared to the system and the coupling is sufficiently small compared to the baths relaxation time scale, the bath approximately stays in equilibrium. Therefore, the reduced dynamics of the system is influenced by short-lived excitations of the equilibrium state, which are described by the correlation function $C(t)$.

It is only for certain models, for which the bath correlation can be obtain analytically [98]. In this section, we make use of the fact that Eq. (2.12) can be understood as the Fourier transform of $J(\omega)n_\beta(\omega)$. For well-behaved $J(\omega)n_\beta(\omega)$, the integrand decays exponentially in the upper complex plane and, thus, by closing the contour, it can be solved using the residue theorem,

$$C(t) = 2\mathrm{i}\sum_n \mathrm{Res}(J(\omega)n_\beta(\omega), \omega = z_n)e^{\mathrm{i}z_n t}, \tag{2.16}$$

where z_n are complex isolated poles of the integrand. Here, the cancellation of the factor of π is emphasized, which motivates the definition of the spectral density in Eq. (2.7) and the factor of $\frac{1}{\pi}$ in Eq. (2.8), respectively. Also, for poles z_n with positive imaginary part, the bath correlation decays exponentially. Further below, it is seen explicitly that this is the case for thermal baths. This is important for the Markovian approximation, which is based on the assumption that the decay time of the bath correlation is short compared to the relaxation time.

The Bose function $n_\beta(\omega) = [\exp(\beta\omega - 1]^{-1}$ is singular at the complex Matsubara energies $\mathrm{i}\nu_n = \mathrm{i}2\pi n/\beta$ with $n \in \mathbb{Z}$. The residues are found to be $\mathrm{Res}(n_\beta(\omega), \omega = \mathrm{i}\nu_n) = 1/\beta$.[5] For a well-behaved spectral density that is differentiable in the complex plane, the bath correlation is then found to be

$$C(t) = 2\mathrm{Res}(J(\omega), \omega = \mathrm{i}\omega_\mathrm{D})\, \mathrm{i}n_\beta(\mathrm{i}\omega_\mathrm{D})\, e^{-\omega_D t} + \frac{2}{\beta}\sum_{n=1}^{\infty} \mathrm{i}J(\mathrm{i}\nu_n)e^{-\nu_n t}. \tag{2.17}$$

Here, it is assumed that the spectral density has one isolated pole at $z_0 = \mathrm{i}\omega_\mathrm{D}$. A generalization for several poles is straightforward. Also, the term *well-behaved* refers to the series expansion, which is expected to be finite for all times $t > 0$. This is true for the Drude bath, for which $\mathrm{Res}(J(\omega), \omega = \mathrm{i}\omega_\mathrm{D}) = \gamma\omega_\mathrm{D}^2/2$ and $\mathrm{i}J(\mathrm{i}\nu_n) = -\gamma\nu_n/(1 - \nu_n^2/\omega_D^2)$. It is emphasized that the bath correlation is ill-defined for a purely Ohmic bath that is in the limit of $\omega_\mathrm{D} \to \infty$. For a consistent description, a cutoff energy as a regularization parameter has to be introduced. The formula above cannot be applied for spectral densities with exponential decay $\tilde{J}(\omega) = \gamma\omega \exp[-\omega/\omega_\mathrm{D}]$, since its antisymmetric continuation $J(\omega) = \gamma\omega \exp[-|\omega|/\omega_\mathrm{D}]$ is not differentiable for $\omega = 0$ and the residue theorem cannot be applied. Similarly, it does not apply to a spectral density with a hard cutoff, which is also not differentiable at the cutoff.

2.2.3 Temperature-dependent coupling density $G(\Delta)$

Typically, for open quantum systems the bath is assumed to remain in a thermal state. The interaction between system and bath leads to short lived excitation in the bath. The bath correlation is assumed to decay on a time scale that is short compared to the dynamics of the system. In the Markovian limit, the excitations the system creates in the bath decay fast enough, such that they do not act back on the system at a later time. In this regime, the dynamics of the system is described by a time local generator. In a perturbative treatment up to second order in the interaction Hamiltonian H_SB, the Redfield master equation (2.42) is obtained. There, the bath correlation $C(\tau)$ appears in a convolution $\mathbb{S}_t = \int_0^t C(\tau) e^{-\mathrm{i}H_\mathrm{S}\tau} S e^{\mathrm{i}H_\mathrm{S}\tau} d\tau$.

[5] To analyze the pole structure of the Bose function, it is rewritten in terms of the hyperbolic cotangent $n_\beta(\omega) = (\coth(\beta\omega/2) - 1)/2$. The Laplace series of the hyperbolic cotangent reads $\coth(\beta\omega/2) = 1/(\beta\omega/2)\sum_{n=-\infty}^{\infty} 1/(1 + \nu_n^2/\omega^2)$, with $\nu_n = 2\pi n/\beta$. Analogously for the hyperbolic tangent $\tanh(\beta\omega/2) = 1/(\beta\omega/2)\sum_{n=-\infty}^{\infty} 1/(1 + [\frac{\pi(2n+1)}{\beta}]^2/\omega^2)$, which is relevant for fermionic baths [99].

Represented in the eigenbasis of the system, the matrix elements of the convoluted operator read $\langle q|\mathbb{S}_t|k\rangle = G_t(\omega_q - \omega_k)\langle q|S|k\rangle$, where ω_q and $|q\rangle$, respectively, are the eigenfrequencies and eigenstates of H_S. Here,

$$G_t(\Delta) \equiv \int_0^t e^{-\mathrm{i}\Delta\tau} C(\tau)\mathrm{d}\tau, \tag{2.18}$$

defines the temperature-dependent coupling density [100].[6] In the asymptotic limit of large times we define $\lim_{t\to\infty} G_t(\Delta) = G(\Delta)$, which corresponds to the half-sided Fourier transform of the bath correlation. By inserting the integral expression (2.12), one arrives at

$$G(\Delta) = J(\Delta)n_\beta(\Delta) + \mathrm{i}\,\mathcal{P}\int_{-\infty}^{\infty} \frac{J(\omega)n_\beta(\omega)}{\omega-\Delta}\frac{d\omega}{\pi} \equiv G'(\Delta) + \mathrm{i}G''(\Delta), \tag{2.19}$$

where the time integral is performed by making use of the Sokhotskyi-Plemelj formular [21]

$$\int_0^\infty e^{\mathrm{i}E\tau}\mathrm{d}\tau = \pi\delta(E) + \mathrm{i}\mathcal{P}\frac{1}{E}, \tag{2.20}$$

also referred to as Kramers-Kronig relation. It states that the real- and imaginary part of the coupling density are related via a Cauchy-principal integral indicated by $\mathcal{P}$. The latter is, yet, a different manifestation of the residue theorem, where the poles are disregarded from the integration path.[7] Using $J(-\Delta) = -J(\Delta)$ and $n_\beta(\Delta) = 1/(e^{\beta\Delta}-1)$, the real part of the coupling density obeys

$$\frac{G(\Delta)}{G(-\Delta)} = e^{-\beta\Delta}, \tag{2.21}$$

which is known as the detailed balance condition [101].

In the following, some basic properties of $G''(\Delta)$ are discussed, which stem directly from the integral representation. By using the antisymmetry of the spectral density $J(\Delta)$, the region of integration can be limited to positive frequencies only,

$$\begin{aligned} G''(\Delta) &= \mathcal{P}\int_0^\infty \frac{J(\omega)}{\omega^2-\Delta^2}\big[\omega(n_\beta(\omega)+n_\beta(-\omega)) + \Delta(n_\beta(\omega)-n_\beta(-\omega))\big]\frac{d\omega}{\pi}, \\ &= \underbrace{-\int_0^\infty \frac{J(\omega)}{\omega}\frac{d\omega}{\pi}}_{G''_\mathrm{RN}} \underbrace{+\mathcal{P}\int_0^\infty \frac{J(\omega)}{\omega^2-\Delta^2}\left[\Delta - \frac{\Delta^2}{\omega}\right]\frac{d\omega}{\pi}}_{G''_0(\Delta)} + \underbrace{2\Delta\mathcal{P}\int_0^\infty \frac{J(\omega)n_\beta(\omega)}{\omega^2-\Delta^2}\frac{d\omega}{\pi}}_{G''_\mathrm{th}(\Delta)}, \end{aligned} \tag{2.22}$$

[6] Sometimes it is also referred to as *spectral noise power*, e.g., in Ref. [76]. However, in this work the integration always starts at time $t = 0$. Therefore, the coupling density is the half-sided Fourier transform and in general a complex quantity.

[7] The Cauchy-principal integral is defined as $\mathcal{P}\int_{-\infty}^{\infty}\frac{J(\omega)n_\beta(\omega)}{\omega-\Delta}\frac{\mathrm{d}\omega}{\pi} = \int_{-\infty}^{\Delta-0^+}\frac{J(\omega)n_\beta(\omega)}{\omega-\Delta}\frac{\mathrm{d}\omega}{\pi} + \int_{\Delta+0^+}^{\infty}\frac{J(\omega)n_\beta(\omega)}{\omega-\Delta}\frac{\mathrm{d}\omega}{\pi}$ where the limit $0^+ \to 0$ is implicit.

where we used the symmetries of the Bose function $n_\beta(\omega)+n_\beta(-\omega) = -1$ and $n_\beta(\omega)-n_\beta(-\omega) = 2n_\beta(\omega)+1$. Above, G''_{RN} is the reorganization energy [23], which is a constant shift of the coupling density and is discussed in more detail in Section 2.4.3. One also identifies zero-point fluctuation $G''_0(\Delta)$ and thermal noise $G''_{\mathrm{th}}(\Delta)$.[8] Note, the identification of the latter as thermal noise is based on the fact that it vanishes for zero temperature. For zero temperature in Eq. (2.19), one has $n_\beta(\omega) = -\Theta(-\omega)$, such that only $G''_{\mathrm{RN}} + G''_0(\Delta)$ contributes to the imaginary part. For a Drude bath, $J(\omega) = \gamma\omega/(1+\omega^2/\omega_D^2)$, one finds [Appendix A]

$$G''_{\mathrm{RN}} = -\frac{\gamma\omega_D}{2} < 0, \tag{2.23}$$

$$G''_0(\Delta) = \frac{\gamma\Delta}{1+\Delta^2/\omega_D^2}\Big(-\frac{1}{\pi}\ln\Big[\frac{|\Delta|}{\omega_D}\Big] + \frac{1}{2}\frac{\Delta}{\omega_D}\Big), \tag{2.24}$$

$$G''_{\mathrm{th}}(\Delta) = \frac{\gamma\Delta}{1+\Delta^2/\omega_D^2}\underbrace{\Big(\frac{1}{\pi}\ln\Big[\frac{|\Delta|}{\omega_D}\Big] + \frac{T}{\omega_D} + \frac{1}{\pi}\psi(\omega_D/(2\pi T)) - \frac{1}{\pi}\mathrm{Re}\,\psi(\mathrm{i}|\Delta|/(2\pi T))\Big)}_{\leq 0}, \tag{2.25}$$

which is expressed with the temperature $T = 1/\beta$ and the Digamma function ψ. An interesting

[8] The terms *zero-point fluctuation* and *thermal noise* are vaguely used in the literature and might not agree with the definition given in this manuscript. Though a very similar discussion of the fluctuations and thermal noise is given in Refs. [102, 20].

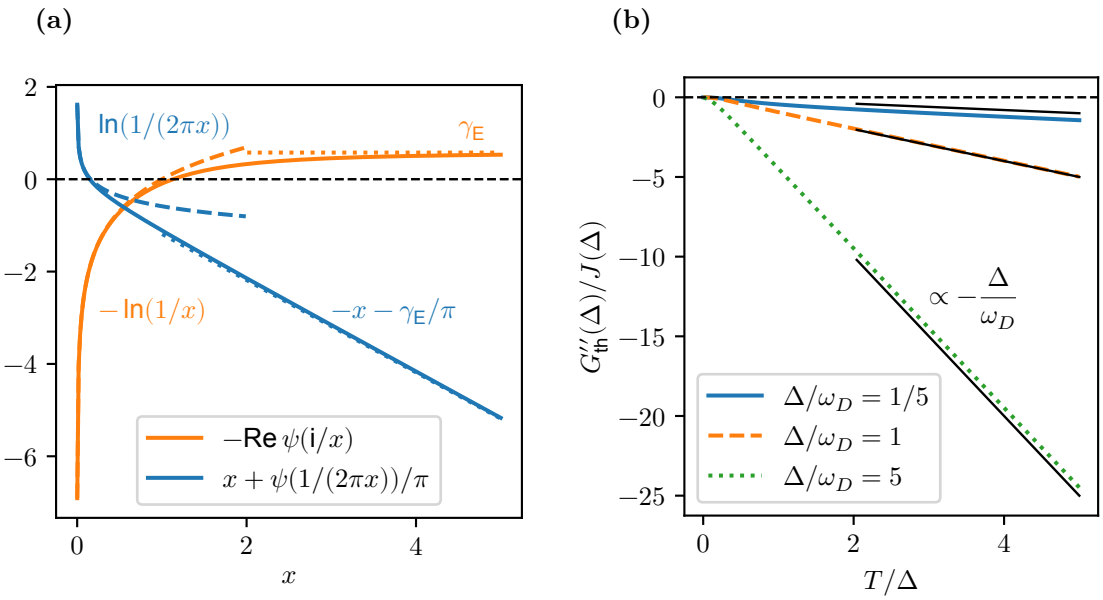

Figure 2.2: In (a) Digamma-functions $-\mathrm{Re}\,\psi(\mathrm{i}/x)$ in orange and $x+\psi(1/(2\pi x))/\pi$ in blue with asymptotic behaviour for small x (low temperature) and large x (high temperature), respectively. In (b) thermal noise $G''_{\mathrm{th}}(\Delta)/J(\Delta)$ for Drude spectral density as a function of temperature T/Δ and for different values of $\Delta/\omega_D = \frac{1}{5}, 1$ and 5 in blue solid, orange dashed and green dotted, respectively. The black lines indicate the approximation $G''_{\mathrm{th}}(\Delta)/J(\Delta) \simeq -T/\omega_D$.

interpretation of the zero-point fluctuation and thermal noise has been found in Ref. [103], where they are shown to be essential to describe finite coherences in the long-time limit. Using $\psi(\omega_D/(2\pi T)) \simeq \ln\left[\frac{\omega_D}{2\pi T}\right]$ and $\mathrm{Re}\,\psi(\mathrm{i}|\Delta|/(2\pi T)) \simeq \ln\left[\frac{|\Delta|}{2\pi T}\right]$, which is valid for low temperature and depicted in Fig. 2.2(a), one finds that the thermal noise vanishes at zero temperature. For high temperature, use $\psi(\omega_D/(2\pi T)) \simeq -2\pi T/\omega_D - \gamma_\mathrm{E}$ and $\mathrm{Re}\,\psi(\mathrm{i}\Delta/(2\pi T)) \simeq -\gamma_\mathrm{E}$, where γ_E is the Euler-Mascheroni constant, to arrive at

$$G''_\mathrm{th}(\Delta) \simeq \frac{\gamma\Delta}{1+\Delta^2/\omega_D^2}\left(\frac{1}{\pi}\ln\left[\frac{|\Delta|}{\omega_D}\right] - \frac{T}{\omega_D}\right), \tag{2.26}$$

which is depicted in Fig. 2.2(b).

Often, pure Ohmic baths $J(\omega) = \gamma\omega$ are considered by taking the cutoff at infinity, for which the real part of the coupling density $G'(\Delta) = \gamma\omega n_\beta(\omega)$ still acquires finite values. However, for finite temperature the imaginary part is divergent. A detailed discussion is carried out in Section 3.5.2.

2.3 Completely positive evolution and the relation to GKSL master equations

Quantum mechanics is a probability theory. That is, measuring an observable O on a quantum state ϱ yields one of the eigenvalues o_n with probability $P(o_n) = \langle o_n|\varrho|o_n\rangle$, with eigenstate $|o_n\rangle$ of O to the eigenvalue o_n. Here, for simplicity, it is assumed that o_n is a non-degenerate eigenvalue and that $|o_n\rangle$ is normalized. The quantity $P(o_n) = \langle o_n|\varrho|o_n\rangle$ can be interpreted as the population fraction of $|o_n\rangle$ in the quantum state ϱ.

In order to yield adequate probabilities, the state ϱ has to obey three conditions: First, the quantum state has to be Hermitian $\varrho = \varrho^\dagger$, such that the populations $P(o_n) = \langle o_n|\varrho|o_n\rangle \in \mathbb{R}$ are real. Second, the quantum state needs to be normalized $\mathrm{tr}\,\varrho = 1$, from which one also deduces that the probabilities add up to one, $\sum_n P(o_n) = 1$. Third, the quantum state has to be positive,[9]

$$\varrho \geq 0, \tag{2.27}$$

which is defined as $\langle\psi|\varrho|\psi\rangle \geq 0$ for all pure states $|\psi\rangle$ in the Hilbert space. In a dynamical description

$$\varrho(0) \mapsto \Phi_t[\varrho(0)] = \varrho(t), \tag{2.28}$$

[9] Operators that obey $\varrho \geq 0$ are called positive-semidefinite, which includes the zero operator, of which all matrix elements are zero. Typically, we are interested in positive-definite quantum states $\varrho > 0$, where at least one quantum state is populated.

where Φ_t shall denote the dynamical map that maps the initial state $\varrho(0)$ to the time evolved state $\varrho(t)$, especially, the third condition is difficult to guarantee.

For open quantum system Choi's theorem [48] guarantees positive evolution via the stronger assumption of completely positive evolution [49, 50, 104, 21]. The evolution of the dynamical map is completely positive if, and only if, it maps positive operators in an augmented Hilbert space onto positive operators. That is when the dynamical map acts on the tensor product $\mathcal{H}_\mathrm{S} \otimes \mathcal{H}_\mathrm{A}$ of the system's Hilbert space $\mathcal{H}_\mathrm{S}$ and some ancillary Hilbert space $\mathcal{H}_A$ of arbitrary but finite dimension according to

$$\sum_\alpha \varrho_\alpha \otimes A_\alpha \mapsto \sum_\alpha \Phi_t[\varrho_\alpha] \otimes A_\alpha. \tag{2.29}$$

with positive operators $\varrho_\alpha \in \mathcal{H}_\mathrm{S}$ and $A_\alpha \in \mathcal{H}_A$.

The theorem states that the dynamical map Φ_t is completely positive and trace preserving, if, and only if, the generator $\mathcal{G}$,

$$\Phi_t = \exp[\mathcal{G}t], \tag{2.30}$$

can be written as GKSL superoperator [49, 50]

$$\mathcal{G}[\varrho(t)] = -\mathrm{i}[H, \varrho(t)] + \sum_{i=1}^{D^2-1} \left(L_i \varrho(t) L_i^\dagger - \frac{1}{2}\{L_i^\dagger L_i, \varrho(t)\} \right). \tag{2.31}$$

Here, H is some Hermitian Hamiltonian, and L_i is a basis of traceless operators of $\mathcal{H}_\mathrm{S}$ with Hilbert space dimension D. It is emphasized that the theorem does not make a statement about the detailed form of the Hamiltonian H and the jump operators L_i and, thus, cannot be used to derive a particular master equation. Instead, master equations are derived perturbatively in orders of the system-bath coupling, which is at the focus of the next section.

2.4 Perturbative master equations

For open quantum systems that are coupled to their environment, an effective description for the reduced dynamics of the system is of great interest. For ultraweak coupling between system and bath, GKSL master equations yield an adequate approximation. Away from equilibrium, the properties of open quantum systems depend on the details of the coupling and the environment. Therefore, a microscopic derivation of a master equation is crucial, rather than the use of phenomenological master equations [105–108].

In this section, we review the derivation of the Redfield equation by performing a second-order perturbative expansion in the system-bath coupling. Derivations are outlined, e.g., in Refs. [18–23].

2.4.1 Perturbative treatment of the system-bath coupling

Considering an open quantum system with total Hamiltonian $H_{\mathrm{tot}} = H_0 + H_{\mathrm{SB}}$, with unperturbed Hamiltonian $H_0 = H_{\mathrm{S}} + H_{\mathrm{B}}$ for the system (S) and bath (B), respectively, and the system-bath coupling H_{SB}, the dynamics of the total system-bath state follows Schrödinger's equation. Represented in interaction picture the dynamics is solely generated by the interaction

$$\partial_t \left(e^{\mathrm{i}H_0 t} \varrho_{\mathrm{tot}}(t) e^{-\mathrm{i}H_0 t} \right) = -\mathrm{i} \left[\boldsymbol{H}_{\mathrm{SB}}(t), e^{\mathrm{i}H_0 t} \varrho_{\mathrm{tot}}(t) e^{-\mathrm{i}H_0 t} \right], \tag{2.32}$$

with $\boldsymbol{H}_{\mathrm{SB}}(t) = e^{\mathrm{i}H_0 t} H_{\mathrm{SB}} e^{-\mathrm{i}H_0 t}$. We formally obtain the solution by integration with respect to time, which we express explicitly using the exponential function,

$$e^{\mathrm{i}H_0 t} \varrho_{\mathrm{tot}}(t) e^{-\mathrm{i}H_0 t} = T \exp \left[-\mathrm{i} \int_0^t [\boldsymbol{H}_{\mathrm{SB}}(\tau), \cdot] d\tau \right] \varrho_{\mathrm{tot}}(0), \tag{2.33}$$

where T denotes the time ordering. Here, the exponential of the commutator is defined as $\exp[H, \cdot] = \sum_{n=0}^{\infty} \frac{1}{n!} [H, \cdot]^n$, with nested commutators $[H, \cdot]^n[\varrho] = \underbrace{[H, [H, \ldots [H}_{n-\text{fold}}, \varrho] \ldots]]$. For open quantum systems, we are interested in the effective dynamics of the reduced state of the system. This is a challenging task because as seen from the right hand side of Eq. (2.33) the dynamics does not factorize between system and bath but clearly shows how correlations build up over time. For coarse-graining the dynamics,[10] we trace over the bath degrees of freedom. On the left-hand side of Eq. (2.33) this is easily possible due to the cyclic property of the (partial) trace, $\mathrm{tr}_{\mathrm{B}}\, e^{\mathrm{i}(H_{\mathrm{S}}+H_{\mathrm{B}})t} \varrho_{\mathrm{tot}}(t) e^{-\mathrm{i}(H_{\mathrm{S}}+H_{\mathrm{B}})t} = e^{\mathrm{i}H_{\mathrm{S}}t} \varrho(t) e^{-\mathrm{i}H_{\mathrm{S}}t}$, where $\varrho(t) \equiv \mathrm{tr}_{\mathrm{B}}\, \varrho_{\mathrm{tot}}(t)$ defines the reduced state of the system. Here, and throughout this thesis, we consider an initial state that is factorized between system and bath

$$\varrho_{\mathrm{tot}}(0) = \varrho(0) \otimes \varrho_{\mathrm{B}}, \tag{2.34}$$

with $\varrho_{\mathrm{B}} = e^{-\beta H_{\mathrm{B}}}/Z_{\mathrm{B}}$ being the (initial) equilibrium state of the bath. This may be seen as a dynamical quench in which system and bath at initial time $t = 0$ are put into contact and correlations only build up over time. For the dynamics of initial correlations, we refer to the correlation picture approach in Ref. [89], or the dynamics of the damped harmonic oscillator in Refs. [110, 111]. Using the series expansion of the exponential in orders of the interaction, we arrive at,

$$e^{\mathrm{i}H_{\mathrm{S}}t} \varrho(t) e^{-\mathrm{i}H_{\mathrm{S}}t} = \varrho(0) - \int_0^t \mathrm{d}\tau_1 \int_0^{\tau_1} \mathrm{d}\tau_2\, \mathrm{tr}_B [\boldsymbol{H}_{\mathrm{SB}}(\tau_1), [\boldsymbol{H}_{\mathrm{SB}}(\tau_2), \varrho(0) \otimes \varrho_{\mathrm{B}}]] + \ldots, \tag{2.35}$$

[10] From reference [109], "*In physics a fine-grained description of a system is a detailed description of its microscopic behaviour. A coarse-grained description is one in which some of this fine detail has been smoothed over.*"

where the right-hand side defines the reduced dynamical map $\varrho(0) \mapsto e^{\mathrm{i}H_\mathrm{S}t}\varrho(t)e^{-\mathrm{i}H_\mathrm{S}t}$ as a series expansion in orders of the interaction H_SB. Because of symmetry reasons, only even orders contribute to the series expansion above.[11] However, any truncation of this series leads to divergences with respect to time [112, 40]. In second order, this divergence is linear in t, such that it can be cured by taking the time-derivative to obtain a first-order differential equation. After reordering the terms one arrives at

$$\partial_t \varrho(t) \simeq -\mathrm{i}[H_\mathrm{S}, \varrho(t)] + \mathcal{R}_t^{(2)}[e^{-\mathrm{i}H_\mathrm{S}t}\varrho(0)e^{\mathrm{i}H_\mathrm{S}t}], \tag{2.36}$$

where fourth- and higher order contributions are neglected. We comment on higher order expansions in Chapter 5. Here the time-dependent Redfield superoperator is introduced,

$$\mathcal{R}_t^{(2)}[e^{-\mathrm{i}H_\mathrm{S}t}\varrho(0)e^{\mathrm{i}H_\mathrm{S}t}] = -\int_0^t \mathrm{tr}_\mathrm{B}[H_\mathrm{SB}, [\boldsymbol{H}_\mathrm{SB}(-\tau), e^{-\mathrm{i}H_\mathrm{S}t}\varrho(0)e^{\mathrm{i}H_\mathrm{S}t} \otimes \varrho_\mathrm{B}]]d\tau, \tag{2.37}$$

which acts on the freely evolving system state. For an equilibrium bath one has $e^{-\mathrm{i}H_\mathrm{B}t}\varrho_\mathrm{B}e^{\mathrm{i}H_\mathrm{B}t} = \varrho_\mathrm{B}$. In a reduced description, one looses information about the bath dynamics. Nevertheless, with all orders included, the reduced dynamical map (2.35) is formally exact and does not assume the bath to remain in its initial equilibrium state. In particular, the resulting master equation can describe non-Markovian dynamics, where excitations in the bath have some finite lifetime and influence the system at a later time. Another example is the exact master equation for the damped harmonic oscillator, for which all relevant quantities are calculated from the initial equilibrium state of the bath.

On short time scales, Eq. (2.36), is an adequate description for the reduced dynamics and only assumes weak coupling between system and bath. However, typically we consider large baths with a continuous spectrum that steer the system towards a genuine steady state. To this end, it is convenient to find a time-local equation of motion, i.e., master equation, that does not explicitly depend on the initial state. Additionally, the integration of time-local master equations is simpler compared to time-non-local ones. Time-local master equations can be exact and may also describe non-Markovian evolution,[12] as discussed in Section 2.6. Given

[11] In this thesis, we consider interaction Hamiltonians $H_\mathrm{SB} = S \otimes B^\dagger + \mathrm{H.c.}$, where $B = \sum_k c_k b_k$ ($B^\dagger = \sum_k c_k^* b_k^\dagger$) creates (annihilates) excitations in the bath. Tracing over the bath yields correlation functions $\mathrm{tr}_\mathrm{B}(\boldsymbol{B}(\tau_1)^\dagger \boldsymbol{B}(\tau_2)\ldots\varrho_\mathrm{B})$, of arbitrary order. For a bath that is initially in an equilibrium state, this contributes only if the number of excitations is conserved. Therefore, only even orders contribute to the series expansion.

[12] Transcript of discussion between W. G. Unruh and J. P. Paz at the NATO Advanced Research Workshop, Spain (1991) [113]: Unruh: *Your master equation is local in time. For an arbitrary spectral density I would strongly expect that the equations are strongly non-local in time. Why aren't yours?* - Paz: *There are two observations one can intuitively make for the model described by equation (12.1)* [action of harmonic oscillator coupled to a bath]. *On the one hand we expect that a general environment will produce non-Markovian effects and that the master equation will be non local in time. On the other hand, the (reduced) evolution operator must be gaussian since the problem is linear. The crucial observation is that if one admits a gaussian evolution operator, the master equation is always local provided the matrix mixing "old" and "new" coordinates in the propagator can be inverted. Taking this into account, it is surprising to me that*

the exact dynamical map, and provided it is invertible, any time non-local master equation, such as the one in Eq. (2.36), can be represented with a time-local generator that depends on the initial state [114]. In Eq. (2.36), we approximate the inverse of the dynamical map $\varrho(0) \simeq e^{\mathrm{i}H_\mathrm{S}t}\varrho(t)e^{-\mathrm{i}H_\mathrm{S}t}$ and arrive at the Redfield equation

$$\partial_t \varrho(t) \simeq -\mathrm{i}[H_\mathrm{S}, \varrho(t)] + \mathcal{R}_t^{(2)}[\varrho(t)]. \tag{2.38}$$

The latter approximation has to be understood in the dynamical equation. In particular, the resulting dynamics under the Redfield equation differs from the free evolution, $\varrho(t) = T\exp\left[\int_0^t(-\mathrm{i}[H_\mathrm{S},\cdot] + R_\tau^{(2)}[\cdot])\mathrm{d}\tau\right][\varrho(0)] \neq e^{-\mathrm{i}H_\mathrm{S}t}\varrho(0)e^{\mathrm{i}H_\mathrm{S}t}$. Thus, it is shown that the Redfield equation follows rigorously from a perturbative expansion by neglecting fourth-order corrections in the dynamical map [115]. This can be seen from the zeroth-order approximation for the inverse of the dynamical map. Higher, i.e., second-order corrections, would contribute to the generator in fourth order of the coupling. If strong correlations between system and bath build up, this approximation is no longer valid. In Chapter 5, we suggest the canonically consistent master equation that takes into account higher order corrections to include strong correlations. Alternatively, the Redfield equation can be derived in the Born-Markov formalism. The latter *Markov* approximation assumes a fast decay of the bath excitations.

Relation to the Born-Markov approximation

The derivation of the second-order Redfield master equation given above follows the idea of a rigorous perturbative expansion in the coupling Hamiltonian. There are, yet, different derivations of the Redfield equation that make strong assumptions. For instance, often it is assumed that the total system-bath state factorizes for all times and that all memory effects are neglected. This is widely known as the Born-Markov approximation and is revisited in this section. As first step, and similarly to the derivation above, the Schrödinger equation is formally integrated, $e^{\mathrm{i}H_0t}\varrho_\mathrm{tot}(t)e^{-\mathrm{i}H_0t} = \varrho_\mathrm{tot}(0) - \mathrm{i}\int_0^t[\boldsymbol{H}_\mathrm{SB}(\tau), e^{\mathrm{i}H_0\tau}\varrho_\mathrm{tot}(\tau)e^{-\mathrm{i}H_0\tau}]d\tau$. This is used to replace the state $\varrho(t)$ on the right-hand side of Schrödinger's equation and one obtains a time non-local second-order master equation

$$\partial_t\left(e^{\mathrm{i}H_0t}\varrho_\mathrm{tot}(t)e^{-\mathrm{i}H_0t}\right) = -\mathrm{i}[\boldsymbol{H}_\mathrm{SB}(t), \varrho_\mathrm{tot}(0)] - \int_0^t[\boldsymbol{H}_\mathrm{SB}(t), [\boldsymbol{H}_\mathrm{SB}(\tau), e^{\mathrm{i}H_0\tau}\varrho_\mathrm{tot}(\tau)e^{-\mathrm{i}H_0\tau}]]d\tau. \tag{2.39}$$

As in the derivation above, the first term which is of first order in H_SB, is often neglected because it can be cancelled by shifting the interaction Hamiltonian.[13]

the existence of a local master equation has not been noticed until so recently.

[13] By considering the shifted interaction Hamiltonian $H_\mathrm{SB} \to H_\mathrm{SB} - H_\mathrm{shift}\otimes\mathbb{1}_\mathrm{B}$ with $H_\mathrm{shift} = \mathrm{tr}_B[H_\mathrm{SB}\varrho_\mathrm{B}]$, and after tracing over bath degrees of freedom, the first term in Eq. (2.39) would yield, $\mathrm{tr}_\mathrm{B}\left[\boldsymbol{H}_\mathrm{SB}(t) - \boldsymbol{H}_\mathrm{shift}(t)\otimes\mathbb{1}, \varrho(0)\otimes\varrho_\mathrm{B}\right] = \mathrm{tr}_\mathrm{B}\left[\boldsymbol{H}_\mathrm{SB}(t)\varrho(0)\otimes\varrho_\mathrm{B}\right] - \mathrm{tr}_\mathrm{B}\left[\varrho(0)\otimes\varrho_\mathrm{B}\boldsymbol{H}_\mathrm{SB}(t)\right] - [\boldsymbol{H}_\mathrm{shift}(t), \varrho(0)] = \left[\mathrm{tr}_B[\boldsymbol{H}_\mathrm{SB}(t)\varrho_\mathrm{B}], \varrho(0)\right] -$

Here, the Born-Markov approximation is to replace $e^{\mathrm{i}H_0\tau}\varrho_{\mathrm{tot}}(\tau)e^{-\mathrm{i}H_0\tau} \simeq e^{\mathrm{i}H_\mathrm{S}t}\varrho(t)e^{-\mathrm{i}H_\mathrm{S}t}\otimes\varrho_\mathrm{B}$, for which by tracing over the bath one obtains the Redfield master equation. Here the Born approximation assumes factorization for all times and that the bath remains unaffected by the system. The Markov approximation neglects memory effects and assumes a fast decay of the integral kernel, which translates into a short lifetime of the bath-bath autocorrelation. There, it is assumed that within the typical relaxation time bath excitations decay sufficiently fast and do not cause any back action onto the system. The term *Markov approximation* is then inherited from classical mechanics where non-local integral kernels are a direct manifestation of non Markovian dynamics.

One might wonder how the Born-Markov approximation is related to the perturbative expansion in the derivation above. To this end, note that by reinserting the formally integrated state iteratively into Eq. (2.39), one obtains the integral representation of the time-ordered exponential in Eq. (2.33). Therefore, the derivation within the Born-Markov assumption starts from an equivalent formulation of the dynamical map. However, in contrast to the previous derivation, in the representation (2.39) the dynamics does not only depend on the initial state but on the whole history of states. This is the reason, why in this formulation one has to make the Born approximation, i.e., the factorization of the state of system and bath for all times, whereas in the perturbative expansion it is sufficient to make a statement only about the initial condition. In contrast to the Born approximation, second-order master equations can certainly describe correlations between system and bath, which is discussed in more detail in Chapter 5. Also, it is a strong assumption that the bath remains in its initial equilibrium state even though one allows for a finite lifetime of excitations. Instead, the bath dynamics is traced out but implicitly considered in the derivation above.

In general, integro-differential equations are difficult to solve. For quantum master equations, where the memory kernel is not merely a scalar function but a superoperator, the numerical integration can become very difficult. Above, the Markov approximation is used to obtain a time-local generator. In detail, on the level of the dynamical equation, the Markov approximation is equivalent to the approximation for the inverse dynamical map, i.e., to lowest order in the interaction we can write $\varrho(\tau) \simeq e^{\mathrm{i}H_\mathrm{S}(t-\tau)}\varrho(t)e^{-\mathrm{i}H_\mathrm{S}(t-\tau)}$. In general, if the inverse of the map exists, the integral kernel can be formulated as a time-local generator [114]. In quantum mechanics, the definition of Markovianity is more subtle than in classical mechanics and the Redfield equation is commonly known to be non-Markovian [41, 37, 91]. Therefore, the term *Markov approximation* is often misleading. Also, the Born and Markov approximations are both motivated from the assumption that the bath remains unaffected by the system. Therefore, one cannot rigorously distinguish between Born and Markov and one always has to tie them together. It is emphasized that the Redfield equation follows rigorously in a perturbative treatment to second order in the system-bath coupling. This is also explicitly shown for

$[\boldsymbol{H}_\mathrm{shift}(t), \varrho(0)] = 0$, and, thus, cancels out.

the damped-harmonic oscillator in Section 2.6. Also, the rigorous derivation for weak coupling outlined above is the starting point for the canonically consistent master equation in Chapter 5.

In the next section, we obtain the explicit superoperator of the Redfield equation by carrying out the trace over the bath degrees of freedom.

2.4.2 Time-dependent Redfield equation

Above, by a rigorous perturbative expansion to second order in the system bath coupling, one obtains an effective description for the reduced dynamics of the system for which the Redfield superoperator $\mathcal{R}^{(2)}$ in Eq. (2.37) is the central quantity. To evaluate the trace over the bath degrees of freedom we assume a system-bath-interaction Hamiltonian [Section 2.1]

$$H_{\mathrm{SB}} = S \otimes B^\dagger + S^\dagger \otimes B, \tag{2.40}$$

where S is the coupling operator acting on the system and B on the bath, respectively. The action of H_{SB} creates correlations between system and bath. In principle, one may allow for multiple coupling operators S_α and B_α, which is relevant for nonequilibrium processes and is outlined in Section 3.6. By expanding the commutators in Eq. (2.37), one arrives at

$$\begin{aligned}
\mathcal{R}_t^{(2)}[\varrho(t)] &= \int_0^t \mathrm{d}\tau\, \mathrm{tr}_{\mathrm{B}} \Big[\boldsymbol{H}_{\mathrm{SB}}(-\tau)\varrho(t) \otimes \varrho_{\mathrm{B}} H_{\mathrm{SB}} - H_{\mathrm{SB}} \boldsymbol{H}_{\mathrm{SB}}(-\tau)\varrho(t) \otimes \varrho_{\mathrm{B}} \Big] + \mathrm{H.c.}, \\
&= \Bigg[\left(\int_0^t \mathrm{d}\tau \left\langle \boldsymbol{B}(\tau) B^\dagger \right\rangle \boldsymbol{S}(-\tau) \right) \varrho(t) S^\dagger - S^\dagger \left(\int_0^t \mathrm{d}\tau \left\langle \boldsymbol{B}(\tau) B^\dagger \right\rangle \boldsymbol{S}(-\tau) \right) \varrho(t) \\
&\quad + \left(\int_0^t \mathrm{d}\tau \left\langle \boldsymbol{B}^\dagger(\tau) B \right\rangle \boldsymbol{S}^\dagger(-\tau) \right) \varrho(t) S - S \left(\int_0^t \mathrm{d}\tau \left\langle \boldsymbol{B}^\dagger(\tau) B \right\rangle \boldsymbol{S}^\dagger(-\tau) \right) \varrho(t) \Bigg] \\
&\quad + \mathrm{H.c.}\ .
\end{aligned} \tag{2.41}$$

For a Hermitian coupling operator $S = S^\dagger$, the Redfield superoperator reads

$$\mathcal{R}_t^{(2)}[\varrho(t)] = \mathbb{S}_t \varrho(t) S - S \mathbb{S}_t \varrho(t) + \mathrm{H.c} = \mathbb{S}_t \varrho S + S \varrho \mathbb{S}_t^\dagger - S \mathbb{S}_t \varrho - \varrho \mathbb{S}_t^\dagger S, \tag{2.42}$$

with convoluted coupling operator

$$\mathbb{S}_t = \int_0^t C(\tau)\, \mathbf{S}(-\tau) d\tau, \tag{2.43}$$

and bath correlation $C(\tau) = \left\langle \boldsymbol{B}(\tau) B^\dagger \right\rangle + \left\langle \boldsymbol{B}^\dagger(\tau) B \right\rangle$ (2.10). For the convoluted operator $\mathbb{S}_t$ the eigenbasis $|q\rangle$ of the system Hamiltonian H_{S} is preferred. For the matrix elements, one

obtains

$$\langle q|\mathbb{S}_t|k\rangle = \underbrace{\int_0^t C(\tau)e^{-\mathrm{i}\Delta_{qk}\tau}d\tau}_{=G_t(\Delta_{qk})}\ \langle q|S|k\rangle\,, \tag{2.44}$$

with the coupling density (2.19) evaluated at the frequencies $\Delta_{qk} = E_q - E_k$, associated with the energy level splittings. The quantities $G_t(\Delta_{qk})$ appear in the tensor elements $\langle q|\mathcal{R}_t^{(2)}[|n\rangle\langle m|]|k\rangle$ of the Redfield superoperator. Even though some literature refers to them as transition rates, in general, this term might be misleading: On the one hand, there exist different notations, i.e., for golden rule type expressions $G'(\Delta) = 2\pi J(\Delta)n_\beta(\Delta)$ or different definitions of the coupling strength $G(\Delta) \propto \gamma^2$, e.g., in Ref. [63]. On the other hand, a simple physical interpretation for the coupling density might be possible only for the quantum-optical master equation [Section 2.5]. Furthermore, the relevance of the coupling density is discussed for the equilibrium steady state in Section 2.5.2.

It has been found that the time-dependent Redfield equation is more accurate for the dynamics as compared to the quantum-optical master equation and dynamical coarse graining, where the dynamical generator is averaged over adequately chosen time interval [32, 37]. For long-time dynamics or steady-state analysis, often, one relies on the time-independent Redfield equation. In the second Markov approximation, it is assumed that the bath correlation decays fast enough, such that the time-dependent convoluted operator may be replaced by the time-independent one for asymptotic times

$$\mathbb{S} = \int_0^\infty C(\tau)\,\boldsymbol{S}(-\tau)d\tau. \tag{2.45}$$

This approximation affects the transient dynamics but does not alter the steady state. As compared to the time-dependent coupling density, for the time-independent coupling density analytic expressions can be obtained for a much broader class of bath models [Section 2.2].

The Redfield superoperator not only includes dissipative terms. Instead, it also describes a shift of the coherent dynamics [21, 116]. A more detailed discussion is outlined in Section 3.2. One central shift is discussed in the next section. It is relevant for renormalization purposes and can be cancelled by a shift of the system Hamiltonian referred to as reorganization Hamiltonian.

2.4.3 Reorganization Hamiltonian

In the eigenbasis of the system, one obtains for the matrix elements of the asymptotic convoluted operator $\mathbb{S} = \sum_{qk}[G'(\Delta_{qk}) + \mathrm{i}G''(\Delta_{qk})]\,\langle q|S|k\rangle\,|q\rangle\langle k|$. The imaginary part of the bath correlation function $G''(\Delta) = G''_{\mathrm{RN}} + G''_0(\Delta) + G''_{\mathrm{th}}(\Delta)$ (2.22), involves the reorganization energy

G''_{RN}, which is a constant offset. One can write

$$\mathbb{S} = \tilde{\mathbb{S}} + \mathrm{i}G''_{\mathrm{RN}}\, S, \tag{2.46}$$

where the tilde denotes the convoluted operator without the reorganization energy. Equivalently, the reorganization energy can be introduced for the bath correlation $C(t) = \tilde{C}(t) + \mathrm{i}G''_{\mathrm{RN}}\delta(t)$,[14] such that the identity above $\mathbb{S}_t = \tilde{\mathbb{S}}_t + \mathrm{i}G''_{\mathrm{RN}}\, S$, also holds for the time-dependent convoluted operator. The name reorganization energy stems from the fact that it does not contribute to the dissipation but modifies the coherent dynamics by shifting the Hamiltonian.[15] The Redfield equation can be written as

$$\partial_t \varrho(t) = -\mathrm{i}[H_{\mathrm{S}} + G''_{\mathrm{RN}}S^2, \varrho(t)] + S\varrho(t)\tilde{\mathbb{S}}^\dagger + \tilde{\mathbb{S}}\varrho(t)S - S\tilde{\mathbb{S}}\varrho(t) - \varrho(t)\tilde{\mathbb{S}}^\dagger S, \tag{2.47}$$

for which the dissipation is governed by $\tilde{\mathbb{S}}$ only. Note that the reorganization Hamiltonian $G''_{\mathrm{RN}}S^2$ is not diagonal in H_{S} and is different from the Lamb-shift Hamiltonian of the quantum-optical master equation. For a Drude bath, one finds $G''_{\mathrm{RN}} = -\frac{M}{2}\gamma\omega_D < 0$ (2.23).

The reorganization Hamiltonian is well-known for the Brownian motion of a particle in a potential $V(q)$ with displacement operator q. Starting from the system Hamiltonian $H_{\mathrm{S}} = p^2/(2M) + V(q)$ and coupling $S = q$ to a thermal bath, the reorganization Hamiltonian is a potential renormalization $V(q) \to V(q) - \frac{M}{2}\gamma\omega_D q^2$. For a harmonic potential $V(q) = \frac{M\Omega^2}{2}q^2$, the effective frequency of the open quantum system is lowered, $\Omega^2 \to \Omega^2 - \gamma\omega_D$. Thus, also for weak coupling, e.g., for a broad spectral density, $\omega_D \gg \Omega$, the effective frequency may become imaginary and the spectrum is unbounded from below. This is known as the overdamped case [117].

Furthermore, typically the cutoff frequency ω_D is seen as regularization parameter to avoid divergences for the Cauchy principle integrals in Eq. (2.22) for large frequencies. To counteract the frequency shift described above, the total system-bath Hamiltonian is renormalized,

$$H_{\mathrm{tot}} = H_{\mathrm{S}} + H_{\mathrm{RN}} + H_{\mathrm{SB}} + H_{\mathrm{B}}, \tag{2.48}$$

with $H_{\mathrm{SB}} = S \otimes (B^\dagger + B)$. Here, $H_{\mathrm{RN}} = -G''_{\mathrm{RN}}S^2$ is the renormalization of the system Hamiltonian and is the counterterm to compensate for the reorganization energy. For the damped harmonic oscillator, the counterterm is introduced by completing the square for the system-bath coupling Hamiltonian and is further discussed in Section 2.6. Throughout this work, we consider the renormalization term, which cancels the reorganization energy. For the

[14] From the definition of the coupling density in Section 2.2.3 it is $G''_t(\Delta = 0) = \int_0^t \mathrm{Im}[C(\tau)]d\tau = G''_{\mathrm{RN}} + \int_0^t \mathrm{Im}[\tilde{C}(\tau)]d\tau$, where we defined the shifted bath correlation function $\tilde{C}(t) = C(t) - \mathrm{i}G''_{\mathrm{RN}}\delta(t)$.

[15] The physical dimension of G''_{RN} agrees with the physical dimension of the spectral density and is given by $[G''_{\mathrm{RN}}] = \mathrm{energy}/[S]^2$ (2.15). To define an adequate energy, when the coupling operator S is not dimensionless, G''_{RN} can be rescaled as $G''_{\mathrm{RN}}[S]^2$. Because this is trivial and in order to keep the consistency with the literature, e.g., in Ref. [23], G''_{RN} is referred to as reorganization energy.

damped harmonic oscillator, discussed in Section 2.6, the renormalized total Hamiltonian is widely known as Caldeira-Leggett model.

In addition to the reorganization Hamiltonian, there is a Lamb-shift Hamiltonian, which shifts the coherent evolution and is included in the latter terms of Eq. (2.47). The Lamb shift is well-known for the quantum-optical master equation, which is at the focus of the next section.

2.5 Quantum-optical master equation

For the dynamics of open quantum systems, master equations of GKSL form play a central role. They guarantee a positive evolution, which is reviewed in Section 2.3, and can be solved efficiently by quantum trajectories. Especially, the quantum-optical master equation, which can be derived from the microscopic properties of the total system-bath compound, is often employed.

The quantum-optical master equation allows for an intuitive understanding of the dynamics. In particular, the eigenbasis of the system Hamiltonian is the preferred basis, for which the off-diagonal elements of the density matrix decay exponentially and are dynamically decoupled from the diagonal elements, which obey a rate equation. Furthermore, in equilibrium, the rates obey the detailed balance condition, such that the steady state is given by the canonical Gibbs state.

However, the quantum-optical master equation requires the rotating-wave approximation (RWA), which is only valid for ultraweak coupling. Considering a quantum system with ultraweak external perturbation, it is assumed that the timescale of the system and the interaction with the environment are well separated. Starting from the dynamical generator, which is either the total Hamiltonian or the master equation for the reduced state of the system, the different timescales are identified in the interaction-picture representation as oscillating phase factors. The RWA assumes that only those terms with slow varying phases would contribute to the dynamics, whereas the rapidly oscillating terms would average out and are neglected. In the following, the RWA is discussed in more detail.

2.5.1 Rotating-wave approximation (RWA)

To resolve the positivity violation of the Redfield equation, commonly, it is reduced to GKSL form by applying the rotating-wave approximation to arrive at the quantum-optical master equation. The RWA has first been proposed by Rabi *et al.* in Ref. [58] for a semi-classical description of the radiation field. This was followed by a full quantum mechanical description of light-matter interaction by Jaynes and Cummings in Ref. [59].

it is instructive to discuss the RWA on the level of the Hamiltonian. To this end, we consider an interaction Hamiltonian $H_{\mathrm{SB}} = (a + a^\dagger) \otimes (B^\dagger + B)$, with a being an eigenoperator of

the system Hamiltonian H_S to eigenfrequency ω, i.e., $e^{-\mathrm{i}H_\mathrm{S}t}ae^{\mathrm{i}H_\mathrm{S}t} = e^{i\omega t}a$. In the interaction picture, the operators acquire oscillating phase factors, $\boldsymbol{H}_\mathrm{SB}(-t) = e^{\mathrm{i}\omega t}a\otimes\boldsymbol{B}(-t)^\dagger + e^{-\mathrm{i}\omega t}a^\dagger\otimes\boldsymbol{B}(-t) + e^{\mathrm{i}\omega t}a\otimes\boldsymbol{B}(-t) + e^{-\mathrm{i}\omega t}a^\dagger\otimes\boldsymbol{B}(-t)^\dagger$, with $\boldsymbol{B}(-t) = \sum_k c_k e^{\mathrm{i}\omega_k t}b_k$. For the first two terms, the oscillations $e^{\pm\mathrm{i}(\omega-\omega_k)t}$ are slow as compared to the oscillations $e^{\pm\mathrm{i}(\omega+\omega_k)t}$ for the two latter terms. In the RWA, it is assumed that only the slow varying terms contribute to the dynamics,

$$\boldsymbol{H}_\mathrm{SB}(-t) \approx e^{\mathrm{i}\omega t}a\otimes\boldsymbol{B}(-t)^\dagger + e^{-\mathrm{i}\omega t}a^\dagger\otimes\boldsymbol{B}(-t), \tag{2.49}$$

and the terms with the rapid oscillations average out and can be neglected. In this approximation, the interaction Hamiltonian describes the exchange of excitations between the system and the environment, which is also reflected by the resulting master equation. In particular, the Redfield superoperator (2.41) then reduces to GKSL form,

$$\begin{aligned}\mathcal{R}_t^{(2)}[\varrho(t)] \approx &-\mathrm{i}\Big[G_t''(-\omega)a^\dagger a + G_t''(\omega)aa^\dagger, \varrho(t)\Big] \\ &+2G_t'(-\omega)\Big(a\varrho(t)a^\dagger - \frac{1}{2}\{a^\dagger a, \varrho(t)\}\Big) + 2G_t'(\omega)\Big(a^\dagger\varrho(t)a - \frac{1}{2}\{aa^\dagger, \varrho(t)\}\Big),\end{aligned} \tag{2.50}$$

with the two jump operators a and $a^\dagger$ that annihilate and create excitations in the system with strength $G_t'(-\omega)$ and $G_t'(\omega)$, respectively. The imaginary part of the coupling density gives rise to a Lamb-shift Hamiltonian, which commutes with H_S and modifies the coherent dynamics by shifting the eigenenergies.

In the general case, when the coupling operator is not necessarily an eigenoperator of the system Hamiltonian H_S, the RWA is performed on the level of the Redfield equation. To this end, the Redfield equation is represented in the eigenbasis of the system Hamiltonian, $H_\mathrm{S}\,|q\rangle = E_q\,|q\rangle$, with the matrix elements of the coupling operator denoted by $S_{qk} = \langle q|S|k\rangle$.[16] For the convoluted coupling operator, one obtains $\mathbb{S}_t = \sum_{qk} G_t(\Delta_{qk})S_{qk}L_{qk}$, with jump operators $L_{qk} = |q\rangle\langle k|$ and $\Delta_{qk} = E_q - E_k$. For simplicity only, we consider a single Hermitian coupling operator with $H_\mathrm{SB} = S\otimes(B^\dagger + B)$ and resulting Redfield equation in (2.42). Because the Redfield superoperator is quadratic in the coupling operator, the summation runs over four indices q, k and q', k' for the two frequencies Δ_{qk} and $\Delta_{q'k'}$ and can be brought to the form

$$\begin{aligned}\mathcal{R}_t^{(2)}[\varrho(t)] = &-\mathrm{i}\left[\sum_{qk,q'k'} S_{qk}S_{k'q'}\frac{G_t(\Delta_{qk}) - G_t(\Delta_{q'k'})^*}{2\mathrm{i}}L_{q'k'}^\dagger L_{qk}, \varrho(t)\right] \\ &+\sum_{qk,q'k'} S_{qk}S_{k'q'}\left(G_t(\Delta_{qk}) + G_t(\Delta_{q'k'})^*\right)\left[L_{qk}\varrho(t)L_{q'k'}^\dagger - \frac{1}{2}\Big\{L_{q'k'}^\dagger L_{qk}, \varrho(t)\Big\}\right],\end{aligned} \tag{2.51}$$

[16] If the spectrum is degenerate, instead the coupling operator $S = \sum_\omega S(\omega)$ is decomposed into jump operators $S(\omega) = \sum_{E_k - E_q = \omega}\Pi(E_q)\,S\,\Pi(E_k)$, where $\Pi(E)$ is the projector onto the eigenspace belonging to the eigenvalue E [21].

where the first term is a commutator with a Hermitian Lamb-shift Hamiltonian and the second term is interpreted as the dissipator. Transforming to the interaction picture, the jump operators require oscillating phase factors, $e^{-\mathrm{i}H_\mathrm{S}t}L_{qk}e^{\mathrm{i}H_\mathrm{S}t} = e^{-\mathrm{i}\Delta_{qk}t}L_{qk}$. Therefore, in the interaction picture the terms in the Redfield equation oscillate with phase factors $e^{-\mathrm{i}(\Delta_{qk}-\Delta_{q'k'})t}$. In the RWA it is assumed that only the slowly varying terms with $\Delta_{qk} = \Delta_{q'k'}$ contribute to the dynamics and the rapidly oscillating terms with $\Delta_{qk} \neq \Delta_{q'k'}$ average out and can be neglected. Taking only the terms with $(qk) = (q'k')$, one arrives at the quantum-optical master equation $\partial_t\varrho(t) = -\mathrm{i}[H_\mathrm{S}, \varrho(t)] + \mathcal{R}_t^\mathrm{RWA}[\varrho(t)]$ with superoperator[17] [19–21]

$$\mathcal{R}_t^\mathrm{RWA}[\varrho(t)] = -\,\mathrm{i}[H_\mathrm{LS}^\mathrm{RWA}, \varrho(t)] + \sum_{qk} R_{kq}\Big(L_{qk}\varrho(t)L_{qk}^\dagger - \frac{1}{2}\{L_{qk}^\dagger L_{qk}, \varrho(t)\}\Big), \tag{2.52}$$

with $L_{qk} = |q\rangle\langle k|$ and $R_{kq} = 2\,G'(\Delta_{qk})|S_{qk}|^2$ being the jump operators and the associated weights, respectively. The dissipator is of GKSL form and describes quantum jumps between individual energy eigenstates. Here, the rate for the transition $|q\rangle \to |k\rangle$ between energy eigenstates is given by $R_{kq} = 2G'(\Delta_{qk})|\,\langle q|S|k\rangle|^2$ and is independent of the imaginary part of the coupling density. The imaginary part only contributes to the Lamb-shift Hamiltonian

$$H_\mathrm{LS}^\mathrm{RWA} = \sum_{qk} G''(\Delta_{qk})|S_{qk}|^2\,|k\rangle\langle k|\,, \tag{2.53}$$

which is diagonal in the energy basis and modifies the coherent dynamics only by shifting the eigenenergies. The shift of the eigenenergies affects the transient dynamics in second order of the coupling, but not the steady state and is often neglected. The dynamics of the populations (diagonal elements of the density matrix) and coherences (off-diagonal elements of the density matrix) is discussed Section 3.13.

In contrast to a rigorous perturbative expansion in orders of the coupling strength, for the RWA, there is no control parameter that decides on the accuracy of the approximation. In Ref. [118], for time-periodically driven Hamiltonian systems, the authors put analytical bounds on the error of the RWA and show that it scales with the interaction divided by the driving frequency. For master equations, the RWA is only valid for ultraweak coupling [41, 119]. In particular, the resulting equilibrium state is independent of the coupling and is only valid if the coupling approaches zero.

In this thesis, the accuracy of perturbative master equations is assessed by benchmarking the resulting stationary state against the equilibrium state of statistical mechanics. This has been formulated as one of the fundamental requirements for quantum master equations in Ref. [94]. In the next section, it is shown that the Redfield- and the quantum-optical master equations

[17] In general, there might be different pairs of indices $(qk), (q'k')$ for which $\Delta_{qk} = \Delta_{q'k'}$, which all have to be considered for the RWA. This is the case, for instance, for the harmonic oscillator with equidistant energy levels. However, to keep the notation simple, we exclude the degenerate case from the consideration here.

yield the accurate equilibrium state for ultraweak coupling. However, both master equations yield stationary states that deviate from the equilibrium state in second order of the coupling and, thus, both master equations are inconsistent beyond the ultraweak coupling limit.

2.5.2 Equilibrium steady state

In equilibrium, one obtains all relevant information from the thermodynamic properties of the system. With the methods of statistical mechanics, the equilibrium state is defined as the state with maximal entropy given certain constraints, such as the conservation of the probability and, for instance, also conservation of the mean energy or the mean particle number. However, the transient dynamics towards the equilibrium state is of great interest in modern physics. Here to mention is the eigenstate thermalization hypothesis, which is a conjecture that generic quantum many-body systems eventually equilibrate [120], provided they are not in the many-body localized phase [121].

In the theory of open quantum systems, we can define stationary states, which are fixed points of the quantum master equation. These can, but do not have to correspond to equilibrium states. Namely, the framework of quantum master equations also enables the study of nonequilibrium steady states for systems that are driven by several thermal reservoirs or an external periodic drive. Also, the approximations that are needed to derive the perturbative quantum master equation, lead to deviations from the expected equilibrium state.

In this section, we focus on open quantum systems coupled to a single thermal reservoir described by the Redfield and the quantum-optical master equation. It is shown that for ultraweak coupling the predicted steady state coincides with the thermodynamic equilibrium. Beyond ultraweak coupling, the steady state depends on the very details of the microscopic system. In the following, we review the well-known result that any second-order master equation is inadequate for the description of finite coupling steady states [122, 40].

In general, the predicted steady state is a fixed point solution of the master equation which is reached for asymptotic times,

$$0 = \partial_t \varrho(t)\big|_{t\to\infty} = -\mathrm{i}[H_\mathrm{S}, \varrho(t)] + \mathcal{R}[\varrho(t)]\Big|_{t\to\infty}, \tag{2.54}$$

where H_S is the Hamiltonian of the system and $\mathcal{R}$ shall denote the exact, non-perturbative superoperator, which dictates the relaxation and coupling to the bath. In most scenarios, we make a series expansion of the master equation in the coupling strength, $\mathcal{R} \equiv \mathcal{R}^{(2)} + \mathcal{R}^{(4)} + \mathcal{R}^{(6)} + \ldots$, where $\mathcal{R}^{(2)}$ is the second-order master equation, which is Redfield or Lindblad, $\mathcal{R}^{(4)}$ is the fourth-order master equation and so on. Similarly, we may identify the different orders of the steady state solution, $\varrho(t)|_{t\to\infty} \equiv \varrho^{(0)} + \varrho^{(2)} + \varrho^{(4)} + \ldots$, where $\varrho^{(0)}$ is the ultraweak coupling limit, which is independent of the coupling strength, $\varrho^{(2)}$ is the second-order contribution and so on. Evaluating Eq. (2.54) for each order separately, one obtains the hierarchy of coupled

equations,

$$0 = -\mathrm{i}[H_\mathrm{S}, \varrho^{(0)}], \tag{2.55}$$
$$0 = -\mathrm{i}[H_\mathrm{S}, \varrho^{(2)}] + \mathcal{R}^{(2)}[\varrho^{(0)}], \tag{2.56}$$
$$0 = -\mathrm{i}[H_\mathrm{S}, \varrho^{(4)}] + \mathcal{R}^{(2)}[\varrho^{(2)}] + \mathcal{R}^{(4)}[\varrho^{(0)}]. \tag{2.57}$$
$$\vdots$$

Here, one realizes that the 2ν-th equation couples to the next higher $(2\nu+2)$-th order. Consequently, for an accuracy on 2ν-th order, the master equation in order $(2\nu+2)$ must be known [40]. This inconsistency is discussed for the equilibrium dispersion of the momentum operator in Section 2.6.2.

It is important to note that in general, without further specification of the master any second-order master equation is not capable to consistently capture finite coupling effects.

As discussed in more detail, the quantum-optical master equation only gives the zeroth-order contribution, which is independent of the coupling. The Redfield equation gives the correct coherences in second order but fails for the populations, as discussed in Ref. [41] and later in this section. Over the last decades many different second-order master equations have been proposed, such as the coarse grained master equation [32] or the universal-Lindblad equation [90], which are of GKSL form and do not violate positivity. However, by following the statement above, these are not able to consistently describe the finite-coupling-steady state.

Before turning to the predicted steady-state solutions of the Redfield and quantum-optical master equations, let us discuss the expected equilibrium state for ultraweak coupling. For a system coupled to a thermal reservoir, we can define the canonical Gibbs state,

$$\varrho^{(0)} = \frac{e^{-\beta H_\mathrm{S}}}{Z_\mathrm{S}}, \tag{2.58}$$

with system Hamiltonian H_S, partition function $Z_\mathrm{S} = \mathrm{tr}_\mathrm{S}\, e^{-\beta H_\mathrm{S}}$ and inverse bath temperature $\beta = 1/T$. In particular, it is independent of how system and bath interact and is only accurate in the limit of vanishing coupling (ultraweak coupling). To understand how this state might result from the dynamics, let $H_\mathrm{tot} = H_\mathrm{S} + H_\mathrm{SB} + H_\mathrm{B}$ describe the open quantum system with interaction H_SB and bath Hamiltonian H_B.

In equilibrium, that is in the limit of asymptotic times, it is reasonable to assume that the total system-bath compound is described by a canonical Gibbs state $\varrho_\mathrm{tot} = e^{-\beta H_\mathrm{tot}}/Z_\mathrm{tot}$, with $Z_\mathrm{tot} = \mathrm{tr}_\mathrm{S}\,\mathrm{tr}_B\, e^{-\beta H_\mathrm{tot}}$. This can, for instance, be motivated by the eigenstate thermalization hypothesis [120, 123]. By tracing out the bath degrees of freedom, the exact steady state is

then given by [124, 125, 17, 44]

$$\varrho = \mathrm{tr}_\mathrm{B} \frac{e^{-\beta H_\mathrm{tot}}}{Z_\mathrm{tot}}, \tag{2.59}$$

which, in this thesis, is referred to as reduced Gibbs state. The exact reduced Gibbs state may be Taylor expanded to arrive at

$$\varrho = \varrho^{(0)} + \varrho^{(2)} + \mathcal{O}(\varrho^{(4)}), \tag{2.60}$$

with zeroth order given by the system's Gibbs state (2.58) and leading order correction

$$\varrho^{(2)} = \varrho^{(0)} \,\mathrm{tr}_\mathrm{B}[\varrho_B D^{(2)}] - \varrho^{(0)} \,\mathrm{tr}_\mathrm{S}\,\mathrm{tr}_\mathrm{B}[\varrho_B D^{(2)}], \tag{2.61}$$

with

$$D^{(2)} = -\int_0^{-\mathrm{i}\beta} \int_0^{\tau_1} \boldsymbol{H}_\mathrm{SB}(\tau_1)\boldsymbol{H}_\mathrm{SB}(\tau_2) d\tau_1 d\tau_2, \tag{2.62}$$

as outlined in Appendix B.

To see to which extent the Redfield theory agrees with this expectation, we consider the Redfield superoperator $\mathcal{R}^{(2)}[\varrho] = \mathbb{S}\varrho S - S\mathbb{S}\varrho + \mathrm{H.c.}$ in the asymptotic limit with time-independent $\langle n|\mathbb{S}|m\rangle = G(\Delta_{nm})S_{nm}$. In zeroth-order of the hierarchy, that is from Eq. (2.55), it follows that $\varrho^{(0)} = \sum_m p_m^{(0)} |m\rangle\langle m|$ is diagonal in H_S. The detailed form of the populations $p_m^{(0)}$ follows from the second-order equation (2.56). By projecting onto the diagonals and using $\langle n|[H_\mathrm{S}, \varrho^{(2\nu)}]|n\rangle = 0$ one arrives at

$$0 = \langle n|\mathcal{R}^{(2)}[\sum_m p_m^{(0)} |m\rangle\langle m|]|n\rangle = \sum_m |S_{mn}|^2 \big(2G'(\Delta_{nm})p_m^{(0)} - 2G'(\Delta_{mn})p_n^{(0)}\big), \tag{2.63}$$

which is the stationary solution of the Pauli-rate equation. One verifies easily that Eq. (2.63) coincides with the stationary solution of the quantum-optical master equation (2.52), i.e., $0 = \mathcal{R}^\mathrm{RWA}[\varrho^{(0)}]$. The equation above simplifies by noting the detailed balance condition $R_{mn}/R_{nm} = e^{-\beta\Delta_{nm}}$ (2.21), for which all terms vanish separately and yield the populations $p_n^{(0)} = e^{-\beta E_n}/\sum_m e^{-\beta E_m}$. Thus, the predicted steady state for ultraweak coupling is the canonical Gibbs state and agrees with the expected equilibrium state.

Given $\varrho^{(0)} = e^{-\beta H_\mathrm{S}}/Z_\mathrm{S}$, one might infer the second order contribution $\varrho^{(2)}$ from Eq. (2.56) by formal inversion of $\mathrm{i}\Delta[\varrho^{(2)}] = \mathcal{R}^{(2)}[\varrho^{(0)}]$, with $\Delta[\cdot] = [H_\mathrm{S}, \cdot]$. For the matrix elements one has $\mathrm{i}\Delta_{nm}\varrho_{nm}^{(2)} = \langle n|\mathcal{R}^{(2)}[\varrho^{(0)}]|m\rangle$, such that one immediately obtains the coherences, i.e., the

off-diagonal matrix elements

$$\varrho^{(2)}_{nm} \overset{n\neq m}{=} \langle n|\frac{\mathcal{R}^{(2)}[\varrho^{(0)}]}{\mathrm{i}\Delta_{nm}}|m\rangle\,, \tag{2.64}$$

$$= \frac{1}{\mathrm{i}\Delta_{nm}}\sum_i S_{ni}S_{im}\Big([G(\Delta_{ni})+G(\Delta_{mi})^*]\frac{e^{-\beta E_i}}{Z_\mathrm{S}} - G(\Delta_{in})^*\frac{e^{-\beta E_n}}{Z_\mathrm{S}} - G(\Delta_{im})\frac{e^{-\beta E_m}}{Z_\mathrm{S}}\Big). \tag{2.65}$$

By further using the detailed balance condition Eq. (2.21) for the real parts of $G(\Delta)$, $G'(\Delta_{ni}) = G'(\Delta_{in})e^{-\beta(E_n-E_i)}$, we observe that the real parts of the coupling density cancel and one arrives at

$$\varrho^{(2)}_{nm} \overset{n\neq m}{=} \frac{1}{\Delta_{nm}}\sum_i S_{ni}S_{im}\Big([G''(\Delta_{ni})-G''(\Delta_{mi})]\frac{e^{-\beta E_i}}{Z_\mathrm{S}} + G''(\Delta_{in})\frac{e^{-\beta E_n}}{Z_\mathrm{S}} - G''(\Delta_{im})\frac{e^{-\beta E_m}}{Z_\mathrm{S}}\Big). \tag{2.66}$$

In Ref. [41], it is shown that this expression is in agreement with Eq. (2.61). Further details are given in Appendix B.

Here, the relevance of consistent bath models should be noted. Often the imaginary part of the coupling density is neglected by arguing it would only cause a modification of the coherent dynamics and appear solely as Lamb shift. Following the arguments above, neglecting the imaginary part is indeed adequate in the ultraweak-coupling limit, for which the steady state is given by the canonical Gibbs state, and follows from the detailed balance condition of the real part $G'(\Delta)$. However, for finite coupling the imaginary parts are crucial as they give the second-order contribution. In other words, studying finite coupling effects within the Redfield theory and neglecting the imaginary parts, one does not get the correct second-order result. Only by considering a consistent bath model that includes the imaginary part of the coupling density, one can describe finite coupling effects.

On the other hand, the populations on second order cannot be directly inferred from the Redfield equation (2.42). Namely, in order to correctly determine the second-order populations, the fourth order master equation has to be known, which goes beyond the Redfield theory [126, 127]. Alternatively they are obtained from the coherences in an analytical continuation approach [41]. This problem of the Redfield theory has been pointed out by many authors [38, 45, 46, 39, 47, 37]. It is plausible that the inconsistency of the second order populations is the reason why the Redfield equation violates positivity in certain parameter regimes. That is, the violation of positivity is not necessarily a consequence of the fact that the Redfield equation is not of GKSL form, as also suggested by A. Shaji and E. Sudarshan in Ref. [93]. The aspect of positivity is discussed in more detail for the exact master equation of the damped harmonic oscillator in the next section and for the canonically consistent master equation in Chapter 5, which are both not of GKSL form, but still fulfil positivity.

2.6 The damped harmonic oscillator - an exactly solvable open quantum system

One of the few exactly solvable open quantum systems is the damped harmonic oscillator [86, 111, 113, 128]. It describes a particle with mass M in a quadratic potential with oscillator frequency Ω, whose displacement q is coupled to a continuum of oscillator modes. The total system-bath Hamiltonian is given by

$$H_{\mathrm{tot}} = \frac{p^2}{2M} + \frac{M\Omega^2}{2}q^2 + \sum_k^\infty \left[\frac{p_k^2}{2m_k} + \frac{m_k\omega_k^2}{2}\left(q_k - \frac{c_k}{m_k\omega_k^2}q\right)^2\right], \tag{2.67}$$

with displacement q and the canonically associated momentum p of the central oscillator. The coupling between system and bath is of the form

$$H_{\mathrm{SB}} = q \otimes B, \tag{2.68}$$

with bath operator $B = \sum_k^\infty -c_k q_k$ where the coefficients c_k are spring constants that determine the coupling strength between the individual bath modes and the system. Yet, there is another term appearing in the total system-bath Hamiltonian

$$H_{\mathrm{RN}} = \sum_k^\infty \frac{c_k^2}{2m_k\omega_k^2}\,q^2 = \int_0^\infty \frac{J(\omega)}{\omega}\frac{d\omega}{\pi}\,q^2, \tag{2.69}$$

with spectral density, $J(\omega) = \pi\sum_k \frac{c_k^2}{2m_k\omega_k}\delta(\omega-\omega_k)$. It is the reorganization Hamiltonian, which compensates the frequency shift caused by the reorganization energy, $G''_{\mathrm{RN}} = -\int_0^\infty \frac{J(\omega)}{\omega}\frac{d\omega}{\pi}$, as discussed in Section 2.4.3 and reference [129]. For a Drude bath, $J(\omega) = M\gamma\omega/(1+\omega^2/\omega_D^2)$ with cutoff ω_D, one finds $G''_{\mathrm{RN}} = -\frac{M}{2}\gamma\omega_D$.

Importantly, the Heisenberg equation of motions that originate from a quadratic Hamiltonian such as the one in Eq. (2.67) are linear coupled equations that can be solved exactly. However, the exact solution to the problem is still non-trivial and an explicit form for the reduced density matrix of the central oscillator, i.e., in terms of analytic functions, can only be given for the equilibrium state [128, 117], which is also discussed in Section 2.6.2. In Ref. [86], an exact master equation for the damped harmonic oscillator has been formulated, which we revisit below. Its form, often referred to as Hu-Paz-Zhang master equation, is closely related to the Redfield equation. From the direct comparison of the exact master equation and the perturbative Redfield equation one gains more insight in the applicability of the Redfield formalism. For instance, the dynamics for the number of excitations under different time-independent master equations, which is studied, e.g., in Ref. [130], is depicted in Fig. 2.3. One can observe that the Redfield dynamics captures the oscillatory behaviour of the exact solution, whereas the quantum-optical master equation gives rise to monotonically decreasing

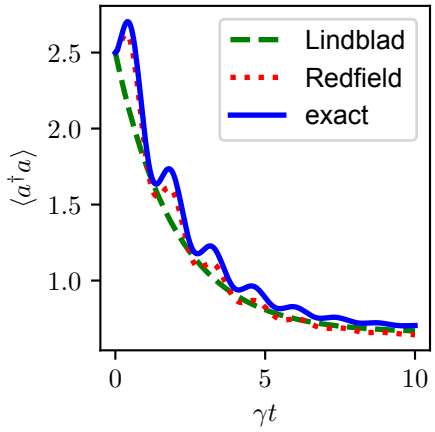

Figure 2.3: Dynamics for the number of excitations compared for different time-independent master equations, i.e., quantum optical (Lindblad) in dashed green, Redfield in dotted red and exact master equation in solid blue. The parameters are coupling strength $\gamma = 0.5\,\Omega$, a Drude spectral density with cutoff $\omega_D = \Omega$, and the bath temperature $T = 0.5\,\Omega$. The initial state is a Gaussian state $\varrho(t=0) = |\psi\rangle\langle\psi|$ with real space representation $\langle q|\psi\rangle = \frac{1}{(2\pi\sigma_q^2)^{1/4}} \exp\left[-(q-\langle q\rangle)^2/4\sigma_q^2\right]$ and mean displacement $\langle q\rangle = 2/\sqrt{M\Omega}$ and width $\sigma_q^2 = 0.5/M\Omega$.

behaviour.

2.6.1 Condition of positivity for the Caldeira-Leggett master equation

The Redfield formalism presented in Section 2.4 can directly be applied to the damped harmonic oscillator and one obtains the equation of motion for the reduced dynamics of the system

$$\partial_t \varrho(t) = -\mathrm{i}\Big[\frac{p^2}{2M} + \frac{M\Omega^2}{2}q^2, \varrho(t)\Big] + (\mathbb{S}\varrho(t)q - q\mathbb{S}\varrho(t) + \mathrm{H.c})\,, \tag{2.70}$$

with $\mathbb{S} = \int_0^\infty C(t)\boldsymbol{q}(-t)\mathrm{d}t$ and $C(t) = \langle \boldsymbol{B}(t)B\rangle$, which is the temporal correlation of the forces in the bath.

The representation above is rather compact but lacks for an intuitive interpretation of the single terms. In the following, we derive a different representation widely known as the Caldeira-Leggett master equation, in which one identifies the frequency shift, damping terms and diffusion terms. Noting the explicit time dependence of the Heisenberg position operator, one can solve the integrals for the convoluted operator $\mathbb{S}$ and finds

$$\boldsymbol{q}(-t) = \cos(\Omega t)\, q - \sin(\Omega t)\frac{p}{M\Omega}, \tag{2.71}$$

$$\mathbb{S} = \frac{1}{2}\Big(G^+ q - \mathrm{i}G^- \frac{p}{M\Omega}\Big), \tag{2.72}$$

with $G^{\pm} \equiv G(\Omega) \pm G(-\Omega)$ and temperature dependent coupling density $G(\pm\Omega)$ defined in Section 2.2.3, where the real part known as Redfield relaxation strength $G'(\Omega)$ and the imaginary part is given by zero-point fluctuation $G''_0(\Omega)$ plus thermal noise $G''_{\mathrm{th}}(\Omega) = -G''_{\mathrm{th}}(-\Omega)$. Note that there is no reorganization energy G''_{RN}, as it is cancelled by the renormalization term.

The Redfield equation (2.42) with the convoluted operator (2.72) reads

$$\begin{aligned}\partial_t \varrho(t) = &-\mathrm{i}\Big[\frac{p^2}{2M} + \frac{M\Omega^2}{2}q^2, \varrho(t)\Big] + \frac{1}{2}\Big(G^{+}q\varrho(t)q + G^{+*}q\varrho(t)q - G^{+}q^2\varrho(t) - G^{+*}\varrho(t)q^2 \\ &+ \frac{\mathrm{i}G^{-}}{M\Omega}qp\varrho(t) + \frac{\mathrm{i}G^{-*}}{M\Omega}q\varrho(t)p - \frac{\mathrm{i}G^{-}}{M\Omega}p\varrho(t)q - \frac{\mathrm{i}G^{-*}}{M\Omega}\varrho(t)pq\Big).\end{aligned} \tag{2.73}$$

Here, the terms quadratic in q give rise to a frequency shift as well as a GKSL contribution of the form

$$-[q,[q,\varrho]] = 2\left(q\varrho q - \frac{1}{2}\{q^2,\varrho\}\right), \tag{2.74}$$

whereas the terms involving products of q and p can be written as

$$[q,\{p,\varrho(t)\}] = qp\varrho(t) + q\varrho(t)p - p\varrho(t)q - \varrho(t)pq, \tag{2.75}$$

$$[q,[p,\varrho(t)]] = qp\varrho(t) - q\varrho(t)p - p\varrho(t)q + \varrho(t)pq. \tag{2.76}$$

One, thus, arrives at

$$\begin{aligned}\partial_t \varrho(t) = &-\mathrm{i}\left[\frac{p^2}{2M} + \frac{M(\Omega^2+\gamma_q^{(2)})}{2}q^2, \varrho(t)\right] \\ &- M^2 D_p^{(2)}[q,[q,\varrho(t)]] - \frac{\mathrm{i}}{2}\gamma_p^{(2)}[q,\{p,\varrho(t)\}] + MD_q^{(2)}[q,[p,\varrho(t)]],\end{aligned} \tag{2.77}$$

which is known as Caldeira-Leggett master equation [129]. In the Redfield formalism, the four real coefficients are identified to be

$$\gamma_q^{(2)} \equiv \frac{G''(\Omega)+G''(-\Omega)}{M} = \Omega^2\frac{2}{M}\mathcal{P}\int_0^\infty \frac{J(\omega)/\omega}{\Omega^2-\omega^2}\frac{d\omega}{\pi}, \tag{2.78}$$

$$D_p^{(2)} \equiv \frac{G'(\Omega)+G'(-\Omega)}{2M^2} = \frac{J(\Omega)}{2M^2}\coth(\beta\Omega/2), \tag{2.79}$$

$$\gamma_p^{(2)} \equiv -\frac{G'(\Omega)-G'(-\Omega)}{M\Omega} = \frac{J(\Omega)}{M\Omega}, \tag{2.80}$$

$$D_q^{(2)} \equiv -\frac{G''(\Omega)-G''(-\Omega)}{2M^2\Omega} = \frac{1}{M^2}\mathcal{P}\int_0^\infty \frac{J(\omega)}{\Omega^2-\omega^2}\coth(\beta\omega/2)\frac{d\omega}{\pi}, \tag{2.81}$$

which agree with the ones from Refs. [131, 21]. In Section 2.2.3, we calculate the integrals for

the Drude bath and find explicitly, $\frac{2}{M}\Omega^2\mathcal{P}\int_0^\infty \frac{J(\omega)/\omega}{\Omega^2-\omega^2}\frac{d\omega}{\pi} = \frac{J(\Omega)\Omega}{M\omega_D}$ and $\frac{\Omega}{M}\mathcal{P}\int_0^\infty \frac{J(\omega)}{\omega^2-\Omega^2}\coth(\beta\omega/2)\frac{d\omega}{\pi} = \frac{1}{M}\left(J(\Omega)\frac{1}{\pi}\ln\left[\frac{\omega_D}{\Omega}\right] + G''_{\rm th}(\Omega)\right)$.

Note that above $\gamma_q^{(2)}$ is temperature-independent and plays the role of a renormalized squared frequency. This renormalization depends on the bare frequency Ω and, thus, cannot be compensated by a global potential renormalization discussed in Section 2.4.3. Also, the frequency of the oscillator is increased, i.e., oscillations are faster and the spectrum is shifted to larger energies. In general, as compared to the Redfield form, the benefit of Eq. (2.77) is that the temperature independent damping coefficient, which for a Drude bath reduces to $\gamma_p^{(2)} = \gamma/(1+\Omega^2/\omega_D^2) \geq 0$, can be distinguished from the temperature-dependent, diffusion parameters $D_q^{(2)}$ and $D_p^{(2)} \geq 0$.

Often, the algebraic form of the master equation (2.77) is also used as a phenomenological description where the parameters are chosen such that the relation between fluctuations and dissipation ensures relaxation towards a thermal state. In this spirit, recently, for generic parameters γ_p, D_p, and D_q, in Ref. [132], a sufficient condition for positivity of the equilibrium state has been identified,

$$1 \leq \frac{4M^2}{\Omega^2\gamma_p^2} D_p\Big(D_p + \gamma_p D_q\Big) \equiv h_{\rm krit}. \tag{2.82}$$

It allows, in particular, for better understanding for the validity of perturbative master equations. Also, because the Hu-Paz-Zhang master equation is not of GKSL form, the dynamics does not obey complete positivity [Section 2.3]. However, this must be distinguished from positivity, which may still hold as it depends on the very details of the coefficients (2.82) and, in general, also on the initial state as discussed, e.g., in Ref. [133]. For the Redfield equation, the condition above can be reformulated as follows,

$$1 \leq \coth(\beta\Omega/2)\Big[\coth(\beta\Omega/2) - \frac{2}{M\Omega^2}\left(J(\Omega)\frac{1}{\pi}\ln\left[\frac{\omega_D}{\Omega}\right] + G''_{\rm th}(\Omega)\right)\Big] \equiv h^{(2)}_{\rm krit}, \tag{2.83}$$

which reflects a complex interplay of coupling strength γ, inverse temperature β and cutoff energy ω_D. For high temperature, we use $\coth(\beta\Omega/2) \simeq \frac{2}{\beta\Omega} \gg 1$, neglect $\ln[\omega_D/\Omega] = O(1)$, and approximate $G''_{\rm th} \simeq -\frac{J(\Omega)}{\beta\omega_D}$ [Fig. 2.2 (b)], to simplify the condition above to $\frac{4}{\beta^2\Omega^2}(1+\frac{J(\Omega)/(M\Omega)}{\omega_D}) \geq 1$, which is met independently of the coupling strength, see Fig. 2.4. For zero temperature, we use $\coth(\beta\Omega/2) \simeq 1$, $G''_{\rm th}(\Omega) = 0$, and the the condition simplifies to $\ln(\omega_D/\Omega) \leq 0$ which holds for $\omega_D \leq \Omega$, only.

In Fig. 2.4, the inequality is analyzed as a function of coupling strength and temperature. As expected, the Redfield formalism breaks down for finite coupling and low temperature.

Loosely speaking, the inequality condition above, which is found explicitly for the harmonic oscillator, states that if the thermal fluctuations are larger than the dissipation the steady state is positive definite. In other words, if the relation between fluctuations and dissipation

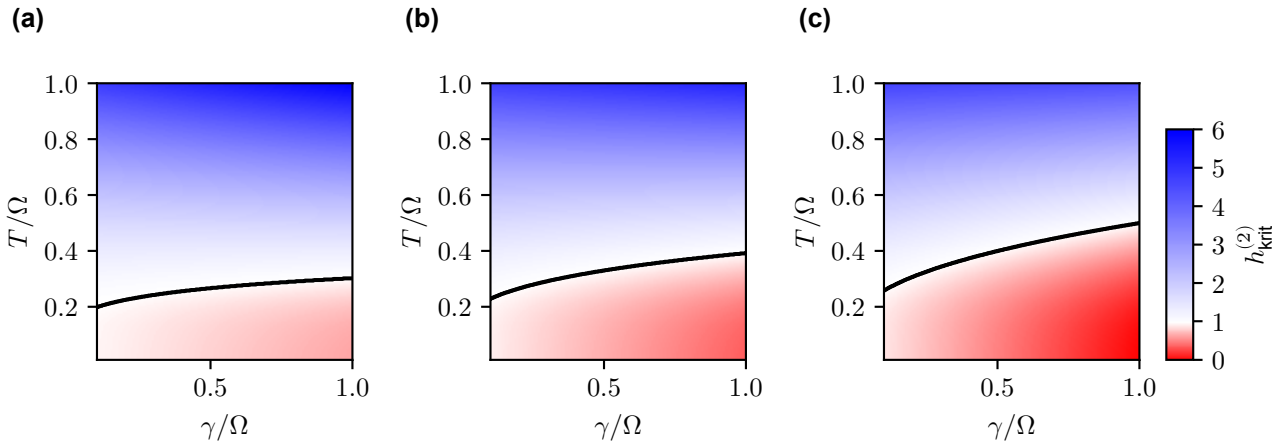

Figure 2.4: Check positivity condition for Redfield equation, i.e., $1 \leq h^{(2)}_{\mathrm{krit}}$ from Ref. [131], as a function of coupling strength and temperature for different Drude cutoff frequencies $\omega_D = 2\,\Omega$ in (a), $\omega_D = 3\,\Omega$ in (b) and $\omega_D = 5\,\Omega$ in (c), respectively.

is not met, the steady state violates positivity, this is further discussed in Section 2.6.2.

It is easy to check that Eq. (2.77) is hermiticity preserving and trace preserving. However, it should be underlined that it is not of GKSL form and does not yield a completely positive time evolution. This is still not the case in the Markovian limit, in which the time-dependent coefficients are replaced by their asymptotic values. The general necessity for completely positive maps is strongly debated and it might be argued that a reasonable quantum map should only guarantee the weaker condition of positivity [46, 92, 93]. Whereas for the damped harmonic oscillator, the exact Hu-Paz-Zhang master equation does preserve positivity, the Redfield equation, which turns out to be of the very same form, violates positivity for low temperatures and strong coupling [Fig. 2.4]. Thus, the notion of positivity is rather subtle and depends on the very details of the parameters $\gamma_q(t)$, $\gamma_p(t)$, $D_q(t)$ and $D_p(t)$, which are discussed in more detail.

2.6.2 Gaussian equilibrium - an analytical approach

In this section, the equilibrium state of the damped harmonic oscillator is studied analytically. We find a one-to-one correspondence between the equilibrium dispersions $\langle q^2 \rangle$ and $\langle p^2 \rangle$ and the asymptotic coefficients γ_q, γ_p, D_q, D_p of the exact Hu-Paz-Zhang master equation. Furthermore, we show that this also applies to the Redfield equation, which is, to the best of our knowledge, a new result. This analytical approach explicitly shows, why the Redfield equation violates positivity in the long-time limit.

In the limit of ultraweak coupling, thermal equilibrium is dictated by statistical mechanics of the system alone. For finite coupling, when the detailed-balance condition is broken, the predicted equilibrium state follows as stationary state of the master equation. Often, it is obtained numerically or perturbatively in the coupling [Section 2.5.2].

For the damped harmonic oscillator, the steady state of the Caldeira-Leggett master equation (2.77) can be obtained analytically [131]. This applies to the steady state of any phenomenological Caldeira-Leggett master equation [131], the Redfield master equation, and the exact Hu-Paz-Zhang master equation. This can be used to benchmark with the equilibrium state. In particular, for ultraweak coupling, which yields the canonical Gibbs state, the exact reduced Gibbs state [124, 125, 134], or the ultrastrong coupling limit [135], respectively. It is well-known that the equilibrium state of the Caldeira-Leggett master equation is given by a Gaussian state, which is a consequence of the fact that the total Hamiltonian is quadratic [128, 117, 111]. The matrix elements in real space are given by

$$\langle q|\varrho_G|q'\rangle = \frac{1}{\sqrt{2\pi\,\langle q^2\rangle}} e^{-\frac{1}{2}\left(\frac{r^2}{\langle q^2\rangle}+\langle p^2\rangle x^2\right)}, \tag{2.84}$$

with $r=(q+q')/2$ and $x=q-q'$. The expectation values of the displacement and momentum operators vanish, i.e., $\langle q\rangle = \langle p\rangle = 0$. In order to find the equilibrium dispersions $\langle q^2\rangle$ and $\langle p^2\rangle$,[18] we write the Caldeira-Leggett master equation (2.77) in position representation $\partial_t \varrho(t,x,r) = \mathcal{L}(x,r)\varrho(t,x,r)$, where the generator takes the form [111]

$$\mathcal{L}(t,x,r) = \mathrm{i}\frac{1}{M}\partial_x\partial_r - \mathrm{i}M\gamma_q(t)rx - \gamma_p(t)x\partial_x - \mathrm{i}MD_q(t)x\partial_r - M^2D_p(t)x^2. \tag{2.85}$$

In the limit of asymptotic times $\lim_{t\to\infty}\mathcal{L}(t,x,r) = \mathcal{L}(x,r)$, we replace the coefficients with their asymptotic values γ_p, γ_q, D_q, D_p. The steady state $\varrho_G(x,r) = \lim_{t\to\infty}\varrho(t,x,r)$ then obeys

$$0 = \mathcal{L}(x,r)\varrho_G(x,r) = \left(\mathrm{i}M\left[\frac{\langle p^2\rangle/M^2 - D_q}{\langle q^2\rangle} - \gamma_q\right]rx - \left[M^2D_p - \gamma_p\langle p^2\rangle\right]x^2\right)\varrho_G(x,r). \tag{2.86}$$

The right-hand side becomes zero, if, and only if both square brackets vanish. With that one obtains the equilibrium dispersions as a function of the generating coefficients,

$$\langle p^2\rangle = M^2\frac{D_p}{\gamma_p}, \tag{2.87}$$

$$\langle q^2\rangle = \frac{D_p/\gamma_p - D_q}{\gamma_q}. \tag{2.88}$$

Conversely, given the exact equilibrium dispersions, this relation can be used to define the asymptotic coefficients D_q and D_p of the exact master equation [Eqs. (2.107) and (2.108)].

[18] In other contexts $\langle q^2\rangle$ and $\langle p^2\rangle$ are referred to as *width* or *variance* in real space and momentum space, respectively. The term *dispersion* is also used for the relation between energy and momentum. In this work, the term *dispersion* only refers to the expectation values $\langle q^2\rangle$ and $\langle p^2\rangle$, respectively, which is taken from H. Grabert and U. Weiss, e.g., in Ref. [128].

In a weak coupling expansion, the leading order contributions for the coefficients are $\gamma_q \simeq \Omega^2 + \gamma_q^{(2)}$, $\gamma_p \simeq \gamma_p^{(2)} + \gamma_p^{(4)}$, $D_q \simeq D_q^{(2)}$ and $D_p \simeq D_p^{(2)} + D_p^{(4)}$. Inserted into the equations above and by Taylor expanding the denominators one finds

$$\langle p^2 \rangle \simeq M^2 \frac{D_p^{(2)}}{\gamma_p^{(2)}} + \langle p^2 \rangle^{(2)}, \tag{2.89}$$

$$\langle q^2 \rangle \simeq \frac{1}{\Omega^2} \left(\frac{D_p^{(2)}}{\gamma_p^{(2)}} - D_q^{(2)} - \frac{D_p^{(2)} \gamma_q^{(2)}}{\gamma_p^{(2)} \Omega^2} + \langle p^2 \rangle^{(2)} \right), \tag{2.90}$$

which is a result of this thesis. For ultraweak coupling, one then identifies the zeroth-order dispersions

$$M\Omega^2 \langle q^2 \rangle^{(0)} = \frac{1}{M} \langle p^2 \rangle^{(0)} = M \frac{D_p^{(2)}}{\gamma_p^{(2)}} = \frac{\Omega}{2} \coth(\beta\Omega/2), \tag{2.91}$$

which obey the equipartition theorem.

Beyond ultraweak coupling, the equilibrium state in second order is influenced by the fourth-order master equation. This is explicitly seen for the momentum dispersion

$$\langle p^2 \rangle^{(2)} = M^2 \frac{1}{\gamma_p^{(2)}} \left(D_p^{(4)} - \frac{\gamma_p^{(4)} D_p^{(2)}}{\gamma_p^{(2)}} \right), \tag{2.92}$$

which is linear in $\gamma_p^{(4)}$ and $D_q^{(4)}$, respectively. However, in Redfield theory, there are no fourth-order coefficients, i.e., $\gamma_p^{(4)} = D_q^{(4)} = 0$, such that $\langle p^2 \rangle^{(2)}_{\text{Redfield}} = 0$. The problem is, that the Redfield theory treats momentum and displacement inconsistently, which can be seen by evaluating Eqs. (2.87) and (2.88) for the Redfield coefficients: On the one hand, beyond ultraweak coupling the state becomes more localized in real space, $\langle q^2 \rangle_{\text{Redfield}} = \frac{(1/2M\Omega)\coth(\beta\Omega/2) - D_q^{(2)}}{\Omega^2 + \gamma_q^{(2)}}$. On the other hand, the momentum dispersion $\langle p^2 \rangle_{\text{Redfield}} = \frac{M\Omega}{2} \coth(\beta\Omega/2)$, is independent of the coupling strength, as this cancels out.

In the following, it is seen that this inconsistency leads to a violation of the positivity condition (2.83) of Ref. [131]. For the Hu-Paz-Zhang master equation, positivity is not guaranteed by the algebraic structure because it is not of GKSL form. Instead, positivity depends on the very details of the coefficients via Eq. (2.82). Since there is a one-to-one correspondence between the coefficients and the equilibrium dispersions, equivalently, the positivity condition is here reformulated as

$$1 \leq \frac{4}{\Omega^2} \frac{1}{M} \langle p^2 \rangle M \gamma_q \langle q^2 \rangle. \tag{2.93}$$

For the exact master equation, i.e, for the exact dispersions it is shown numerically in Fig. D.2 that the positivity condition holds. In the Redfield theory, beyond ultraweak coupling, the

displacement dispersion is reduced [Eq. (E.1)]. In the positivity condition (2.93), this would be compensated by an increase of the momentum dispersion [Eq. (E.2)]. However, since the Redfield theory does not capture the increase of the momentum dispersion, the condition is violated. This shows that the violation of positivity of the Redfield equation can directly be related to the inconsistent treatment of the state in second order. Namely, expanding the exact solution in second order, no violation of positivity is found.

Remarkably, often it is possible to infer finite-coupling effects, without the need of an rigorous fourth-order expansion [41]. This is also the case for the dispersions above, as we show in Section 5.1. This problem of the Redfield formalism is also the starting point of the canonically consistent master equation proposed in Chapter 5.

2.6.3 Green's function for the damped harmonic oscillator

For an exact treatment, we start from the Heisenberg equation of motion for the position of the central oscillator, $\partial_t \boldsymbol{q}(t) = \mathrm{i}[\boldsymbol{H}_{\mathrm{tot}}, \boldsymbol{q}(t)]$. Since the interaction Hamiltonian and bath Hamiltonian commute with $\boldsymbol{q}(t)$ this reduces to the simple relation between position and momentum $\partial_t \boldsymbol{q}(t) = \boldsymbol{p}(t)/M$. Together with the Heisenberg equation for the momentum $\boldsymbol{p}(t)$, this leads to a second order differential equation, $\ddot{\boldsymbol{q}}(t) + \Big(\Omega^2 + \frac{1}{M}\sum_k \frac{c_k^2}{m_k\omega_k^2}\Big)\boldsymbol{q}(t) = \frac{1}{M}\sum_k c_k \boldsymbol{q}_k(t)$, where the bath degrees of freedom appears as a force term on the right-hand site. In turn, for the bath degrees of freedom, one obtains an equation of motion for which the central oscillator serves as a force term, $\ddot{\boldsymbol{q}}_k(t) + \omega_k^2 \boldsymbol{q}_k(t) = \frac{c_k}{m_k}\boldsymbol{q}(t)$. This has the form of a driven harmonic oscillator with input $\boldsymbol{q}(t)$ and the solution is $\boldsymbol{q}_k(t) = \int_0^t (c_k/m_k\omega_k)\sin(\omega_k(t-s))\boldsymbol{q}(s)\mathrm{d}s + \boldsymbol{q}_k(0)\cos(\omega_k t) + (\boldsymbol{p}_k(0)/m_k\omega_k)\sin(\omega_k t)$. Inserting this in the dynamical equation for the central oscillator this leads to an explicit, second order differential equation as outlined, for instance, in Ref. [136],

$$\begin{aligned}\ddot{\boldsymbol{q}}(t) + \Big(\Omega^2 + \frac{1}{M}\sum_k \frac{c_k^2}{m_k\omega_k^2}\Big)\boldsymbol{q}(t) - \frac{1}{M}\sum_k \int_0^t \frac{c_k^2}{m_k\omega_k}\sin(\omega_k(t-s))\boldsymbol{q}(s)\mathrm{d}s \\ = \frac{1}{M}\sum_k c_k\Big[\boldsymbol{q}_k(0)\cos(\omega_k t) + \frac{\boldsymbol{p}_k(0)}{m_k\omega_k}\sin(\omega_k t)\Big].\end{aligned} \tag{2.94}$$

Now, by performing integration by parts $\int_0^t \sin(\omega_k(t-s))\boldsymbol{q}(s)ds = (1/\omega_k)(\boldsymbol{q}(t) - \cos(\omega_k t)\boldsymbol{q}(0)) - (1/\omega_k)\int_0^t \cos(\omega_k(t-s)\dot{\boldsymbol{q}}(s)ds$ in the last term on the left-hand side two things are achieved. Firstly, the boundary term cancels the frequency shift $\frac{1}{M}\sum_k c_k^2/m_k\omega_k^2$ from the potential renormalization H_{RN} and secondly one can identify a damping term proportional to the velocity $\dot{\boldsymbol{q}}$,

$$\ddot{\boldsymbol{q}}(t) + \int_0^t \kappa(t-\tau)\dot{\boldsymbol{q}}(\tau)d\tau + \Omega^2\boldsymbol{q}(t) = \frac{1}{M}\boldsymbol{\xi}(t), \tag{2.95}$$

with time-dependent damping kernel[19]

$$\kappa(t) \equiv \frac{1}{M}\sum_k \frac{c_k^2}{m_k\omega_k^2}\cos(\omega_k t), \tag{2.96}$$

$$= \frac{2}{M}\int_0^\infty \frac{J(\omega)}{\omega}\cos(\omega t)\frac{d\omega}{\pi}, \tag{2.97}$$

and the force

$$\boldsymbol{\xi}(t) \equiv -M\kappa(t)\boldsymbol{q}(0) + \underbrace{\sum_k \left(c_k\cos(\omega_k t)\boldsymbol{q}_k(0) + \frac{c_k}{m_k\omega_k}\sin(\omega_k t)\boldsymbol{p}_k(0)\right)}_{\equiv\boldsymbol{\xi}_{\rm B}(t)}. \tag{2.98}$$

The Heisenberg equation of motion Eq. (2.95) has the form of a classical Langevin equation with non-Markovian integral kernel and fluctuating force $\boldsymbol{\xi}_{\rm B}(t)$. The latter is related to the bath correlation function, $\langle\boldsymbol{\xi}_{\rm B}(t)\boldsymbol{\xi}_{\rm B}(0)\rangle = C(t)$ [137]. Here, the fluctuation-dissipation relation, which connects the damping kernel and the fluctuating force, guarantees equilibration [138].

In the following, we consider the antisymmetric part of the autocorrelation function,

$$\chi(t) \equiv \mathrm{i}M\langle[\boldsymbol{q}(t),\boldsymbol{q}(0)]\rangle, \tag{2.99}$$

which is independent of the fluctuating force because of the commutation relation $[\boldsymbol{\xi}(t),\boldsymbol{q}(0)] = 0$. The quantity $\chi(t)$ has the dimension of time[20] and is a Green's function, which for the damped harmonic oscillator satisfies, $\ddot{\chi}(t) + \int_0^t \kappa(t-\tau)\dot{\chi}(\tau)\mathrm{d}\tau + \Omega^2\chi(t) = 0$. Note that the expression is formulated in the Heisenberg picture and the expectation value for $\chi(t) = \mathrm{i}M\,\mathrm{tr}(\varrho(0)[\boldsymbol{q}(t),\boldsymbol{q}(0)])$ has to be understood with respect to the time-independent initial state. However, the commutator is a complex number and, thus, has a trivial operator character, which is a manifestation of the canonical commutation relation of position and momentum in quantum mechanics. Consequently, $\chi(t)$ is independent of the state. This is different for the temperature-dependent antisymmetric part $\langle\{\boldsymbol{q}(t),\boldsymbol{q}(0)\}\rangle$, for the evaluation of which one usually assumes a thermal Gibbs state of the total-system bath compound [111, 128].

The equation of motion for $\chi(t)$ is solved analytically in Laplace space which is defined by the transformation,

$$\bar{\chi}(z) \equiv \int_0^\infty \chi(t)e^{-zt}dt, \tag{2.100}$$

with the initial conditions $\chi(0) = 0$ and $\dot{\chi}(0) = 1$. For the transformation to Laplace space, one performs integration by parts for the first derivative, $\int_0^\infty \dot{\chi}(t)\exp(-zt)dt = 0 - \chi(0) -$

[19] Note, at time $t = 0$ the damping kernel yields the reorganization energy $\kappa(t=0) = -\frac{2}{M}G''_{\rm RN}$.

[20] Including all factors of $\hbar$ it is $\chi(t) = \mathrm{i}(M/\hbar)\,\langle[\boldsymbol{q}(t),\boldsymbol{q}(0)]\rangle$ and by dimensional analysis, it is found that $\chi(t)$ has the dimension of time.

$\int_0^\infty(-z)\exp(-zt)\chi(t)\mathrm{d}t = z\bar{\chi}(z)$ and for the second derivative $\int_0^\infty \ddot{\chi}(t)\exp(-zt)\mathrm{d}t = -1 + z^2\bar{\chi}(z)$. With this, one obtains an algebraic expression for $\bar{\chi}(z)$,

$$\bar{\chi}(z) = \frac{1}{z^2 + z\bar{\kappa}(z) + \Omega^2}, \tag{2.101}$$

where $\bar{\kappa}(z) = \int_0^\infty \kappa(t)\exp(-zt)dt$ is the Laplace transform of the damping kernel. Pictorially speaking, the Green's function is the inverse of the propagator, which is a well-known result in field theory. For a Drude spectral density, $J(\omega) = M\gamma\omega/(1+\omega^2/\omega_D^2)$, the Laplace transform can be easily carried out to give, $\bar{\kappa}(z) = \gamma\omega_D/(\omega_D + z)$, which has the dimension of inverse time.[21] The Green's function $\chi(t)$ is found by inverse Laplace transform of Eq. (2.101),

$$\chi(t) = c_1 e^{-\lambda_1 t} + c_2 e^{-\lambda_2 t} + c_3 e^{-\lambda_3 t}, \tag{2.102}$$

which is a real valued oscillating function with exponential decay. The latter expression is found by using the residue theorem and noting the three isolated poles λ_i of $\bar{\chi}(z)$ with corresponding residues c_i [111],

$$\lambda_1 = \lambda_2^* = \alpha + i\eta, \qquad c_1 = c_2^* = \frac{\mathrm{i}}{2\eta}\frac{\alpha + \mathrm{i}\eta - \omega_D}{\alpha + \mathrm{i}\eta - \delta}, \tag{2.103}$$

$$\lambda_3 = \delta, \qquad c_3 = \frac{-\delta + \omega_D}{(\alpha-\delta)^2 + \eta^2}, \tag{2.104}$$

where α, η and δ follow from the roots of $z^3 + z^2\omega_D + z(\Omega^2 + \gamma\omega_D) + \omega_D\Omega^2 = 0$ and are discussed in more detail in Appendix C.

2.6.4 Weak coupling expansion of the exact Hu-Paz-Zhang master equation and relation to Redfield theory

For the damped harmonic oscillator, it can be shown that the exact, non-perturbative master equation can be written in the form of Eq. (2.77), which goes back to Hu, Paz, and Zhang in Ref. [86]. It is a special property of the damped harmonic oscillator that all the non-Markovian dynamics is fully encoded in the time dependence of the parameters $\gamma_q(t)$, $\gamma_p(t)$, $D_q(t)$ and $D_p(t)$ without the need for non-local integral kernels in the master equation [113, 139].

A rigorous derivation of the exact master equation is carried out, e.g., in Ref. [140, 86] and involves the functional integral approach, which is different from perturbative expansions considered in this thesis. Therefore, in this section, the exact time-dependent coefficients $\gamma_q(t)$, $\gamma_p(t)$, $D_q(t)$ and $D_p(t)$ are merely stated. Furthermore, we show that by Taylor expanding the coefficients for asymptotic times up to second order in the coupling the exact coefficients reduce to the Redfield coefficients $\gamma_q^{(2)}$, $\gamma_p^{(2)}$, $D_q^{(2)}$ and $D_p^{(2)}$ in Eqs. (2.78) to (2.81). Even

[21] The Laplace transform of the cosine is $\int_0^\infty \cos(\omega t)e^{-zt}\mathrm{d}t = z/(\omega^2 + z^2)$.

though, the exact coefficients are well-known in literature, e.g., in Ref. [128, 86, 113, 111], the rigorous perturbative expansion outlined below is, to best of our knowledge, a novel result.

The time dependent parameters $\gamma_q(t)$, $\gamma_p(t)$, $D_q(t)$, $D_p(t)$ result from a path integral approach and are stated, for instance, in Ref. [111]. Since the total Hamiltonian of the damped harmonic oscillator is quadratic, they solely depend on two-point correlations. The renormalized squared frequency $\gamma_q(t)$ and the relaxation rate $\gamma_p(t)$ follow from the antisymmetric part of the correlation function,

$$\gamma_q(t) = \frac{\ddot{\chi}(t)^2 - \dot{\chi}(t)\dddot{\chi}(t)}{\dot{\chi}(t)^2 - \chi(t)\ddot{\chi}(t)} = \frac{\sum_{i<j} \lambda_i\lambda_j\, c_i c_j \left[\lambda_i - \lambda_j\right]^2 e^{-(\lambda_i+\lambda_j)t}}{\sum_{i<j} c_i c_j \left[\lambda_i - \lambda_j\right]^2 e^{-(\lambda_i+\lambda_j)t}} \overset{t\to\infty}{\longrightarrow} \alpha^2 + \eta^2, \tag{2.105}$$

$$\gamma_p(t) = \frac{\chi(t)\dddot{\chi}(t) - \dot{\chi}(t)\ddot{\chi}(t)}{\dot{\chi}(t)^2 - \chi(t)\ddot{\chi}(t)} = \frac{\sum_{i<j} (\lambda_i + \lambda_j)\, c_i c_j \left[\lambda_i - \lambda_j\right]^2 e^{-(\lambda_i+\lambda_j)t}}{\sum_{i<j} c_i c_j \left[\lambda_i - \lambda_j\right]^2 e^{-(\lambda_i+\lambda_j)t}} \overset{t\to\infty}{\longrightarrow} 2\alpha, \tag{2.106}$$

and are independent of fluctuations in the bath, i.e., they are temperature independent. Here, the asymptotic values are found by identifying the slowest decaying term for $\alpha < \delta$. For $\alpha \geq \delta$, however, as we discuss in Appendix D, there is no asymptotic regime and it is $\gamma_q(t), \gamma_p(t) \sim \tan(\eta t)$.

The diffusion coefficients of the exact master equation read [111],

$$D_q(t) = \frac{1}{M}\left[\frac{1}{2}\ddot{K}_q(t) - K_p(t) + \gamma_q(t)K_q(t) + \frac{\gamma_p(t)}{2}\dot{K}_q(t)\right] \overset{t\to\infty}{\longrightarrow} -\frac{1}{M^2}\langle p^2\rangle + \gamma_q\langle q^2\rangle, \tag{2.107}$$

$$D_p(t) = \frac{1}{M}\left[\frac{1}{2}\dot{K}_p(t) + \frac{\gamma_q(t)}{2}\dot{K}_q(t) + \gamma_p(t)K_p(t)\right] \overset{t\to\infty}{\longrightarrow} \frac{1}{M^2}\gamma_p\langle p^2\rangle. \tag{2.108}$$

Here, the temperature-dependence is encoded in the frequency-integrals [117]

$$K_q(t) = \frac{1}{M}\int_0^\infty J(\omega)\coth(\beta\omega/2)\left|\int_0^t e^{-\mathrm{i}\omega\tau}\chi(\tau)d\tau\right|^2 \frac{d\omega}{\pi} \overset{t\to\infty}{\longrightarrow} M\langle q^2\rangle, \tag{2.109}$$

$$K_p(t) = \frac{1}{M}\int_0^\infty J(\omega)\coth(\beta\omega/2)\left|\int_0^t e^{-\mathrm{i}\omega\tau}\dot{\chi}(\tau)d\tau\right|^2 \frac{d\omega}{\pi} \overset{t\to\infty}{\longrightarrow} \frac{1}{M}\langle p^2\rangle, \tag{2.110}$$

which in the asymptotic limit of large times give the exact equilibrium dispersions for the displacement and momentum, respectively. A detailed discussion of the exact dispersions are given in Ref. [140], for which we state the relevant expressions in Appendix E. The frequency integrals above can be formulated as double-time integrals to match with the expressions in

Ref. [111].[22]

In the asymptotic limit, one may write $D_q = \frac{2}{M}(E_{\rm pot} - E_{\rm kin})$, which is the difference of the potential energy $E_{\rm pot} \equiv \langle \frac{M\gamma_q}{2} q^2 \rangle$ and kinetic energy $E_{\rm kin} \equiv \langle \frac{p^2}{2M} \rangle$ in thermal equilibrium.

The connection to the Redfield parameters follows in a rigorous perturbative expansion, which we carry out in Appendix E. As a result of this thesis, we find

$$\gamma_q \simeq \Omega^2 + \gamma_q^{(2)}, \tag{2.111}$$

$$\gamma_p \simeq \gamma_p^{(2)}, \tag{2.112}$$

$$D_q \simeq D_q^{(2)}, \tag{2.113}$$

$$D_p \simeq D_p^{(2)}, \tag{2.114}$$

which shows that for the damped harmonic oscillator the Redfield equation follows rigorously from the exact master equation only under the condition of weak coupling.

For consistency, in the zero-coupling limit one finds $\gamma_q = \Omega^2$ and $\gamma_p = 0$. With this, the exact dispersions reduce to the expectation values in the canonical Gibbs state, i.e., $\frac{1}{M}\langle p^2 \rangle = M\Omega^2 \langle q^2 \rangle = \frac{\Omega}{2} \coth(\beta\Omega/2)$, which is the mean energy of the oscillator in canonical equilibrium. This is known as the equipartition theorem and one obtains $D_q = 0$.

[22] By reordering the integrals, it is $K_q(t) = \frac{1}{M} \int_0^t \mathrm{d}s \int_0^t \mathrm{d}u \ \mathrm{Re}\left[\int_0^\infty J(\omega) \coth(\beta\omega/2) e^{-\mathrm{i}\omega(s-u)} \frac{d\omega}{\pi}\right] \chi(s)\chi(u)$, where one identifies the real part of the bath correlation, $K_q(t) = \frac{1}{M} \int_0^t \mathrm{d}s \int_0^t \mathrm{d}u \ \mathrm{Re}\left[C(s-u)\right] \chi(s)\chi(u)$, which agrees with the expression in [111]. Analogously, one finds $K_p(t) = \frac{1}{M} \int_0^t \mathrm{d}s \int_0^t \mathrm{d}u \ \mathrm{Re}\left[C(s-u)\right] \dot{\chi}(s)\dot{\chi}(u)$.

3 Pseudo-Lindblad equation

The Redfield equation presented in Section 2.4 is a master equation for the reduced density matrix of the system, which preserves the trace and the hermiticity of the density operator. However, it is well-known that the Redfield equation may lead to negatively populated states and is often less preferred than a GKSL master equation, which guarantees positivity by its algebraic structure. Furthermore, the dynamics of a GKSL master equation can be solved efficiently by means of quantum jump trajectories [51–55, 19, 57].

In this chapter, we construct pseudo-Lindblad representations of the Redfield equation that are of GKSL form, except the fact that some of the dissipators have negative weights. This is achieved by analysing the algebraic structure of the Redfield equation, where different operators act non-diagonally on the density matrix. We find equivalent pseudo-Lindblad representations by diagonalizing the algebraic form. It turns out that the diagonalization scheme is not unique, and we distinguish between a unitary diagonalization in Section 3.1 and different non-unitary diagonalizations in Section 3.2.

The latter approach gives rise to different diagonal pseudo-Lindblad representations of the Redfield equation with varying negative relaxation weight. We propose the *truncated GKSL master equation* by truncating the negative contribution. For this purpose, we first find the optimal representation that minimizes the negative weight. We provide numerical simulations and analytical considerations to demonstrate that this GKSL master equation is applicable in a large parameter regime beyond the limitations of the quantum-optical master equation.

The idea for this project has been initiated by Daniel Vorberg and André Eckardt, who found an ad-hoc pseudo-Lindblad formulation of the Redfield equation, which is however different from the approach outlined here. This initial idea was also the starting point for the author's master's thesis, in which a truncation method was developed that is similar to the unitary diagonalization in Section 3.1, however, restricted to pure Ohmic baths. In collaboration with Ling-Na Wu, an earlier stage of this project, where the diagonalization of the Redfield superoperator has been accomplished by an educated guess, has been published in Ref. [141]. More recently, we submitted a preprint [142], in which we rederive the same class of pseudo-Lindblad equations, however, in a rigorous manner by studying all possible symmetries. In this chapter, we follow the latter approach for the construction and the optimization of the pseudo-Lindblad equation.

3.1 Unitary diagonalization of the Redfield equation in the system's eigenbasis

Considering the Redfield equation represented in the eigenbasis of the system in Eq. (2.51), it resembles the GKSL structure, except that it is not diagonal in the jump operators $L_{qk} = |q\rangle\langle k|$. In this section, we derive a pseudo-Lindblad form for the Redfield equation in energy representation using a unitary transformation. In the energy basis, the Redfield dissipator takes the form [see Section 3.1]

$$\mathcal{D}^{\mathrm{Red}}[\varrho(t)] = \sum_{qk,q'k'} S_{qk} S_{k'q'} M_{(qk),(q'k')} \Big[L_{qk} \varrho(t) L^\dagger_{q'k'} - \frac{1}{2} \Big\{ L^\dagger_{q'k'} L_{qk}, \varrho(t) \Big\} \Big], \tag{3.1}$$

with the Hermitian Kossakowski matrix M,

$$M_{(qk),(q'k')} = G(\Delta_{qk}) + G(\Delta_{q'k'})^*, \tag{3.2}$$

where $G(\Delta)$ is again the complex coupling density and where (qk) is a double index labelling the D^2-dimensional space of operators in energy representation. In Eq. (3.1) the matrix elements S_{qk} and $S_{q'k'}$ are amplitudes for the jump operators L_{qk} and $L_{q'k'}$, respectively. We obtain a diagonal representation by solving the eigenvalue problem of the D^2-dimensional, Hermitian coefficient matrix M. Its eigenvalue problem reads

$$\sum_{q'k'} \big(G(\Delta_{qk}) + G(\Delta_{q'k'})^* \big)\, v^\sigma_{q'k'} = g_\sigma\, v^\sigma_{qk}, \tag{3.3}$$

with real eigenvalues g_σ and eigenvectors $v^\sigma = (v^\sigma_{qk})$.

A numerical diagonalization for large systems is very demanding and does not provide insights for the general problem. Therefore, as a novel result, we analytically solve the eigenvalue problem using simple algebraic methods. First, we find a closed quadratic equation for the non-zero eigenvalues g_σ, and secondly we use this to construct the eigenvectors v^σ.

For that purpose, it is useful to introduce averages of the form

$$\overline{x} \equiv \frac{1}{D^2} \sum_{qk} x_{qk}, \tag{3.4}$$

such as $\overline{v^\sigma} \equiv \frac{1}{D^2} \sum_{qk} v^\sigma_{qk}$, $\overline{G^* v^\sigma} \equiv \frac{1}{D^2} \sum_{qk} G(\Delta_{qk})^* v^\sigma_{qk}$, etc., and variances $V[x] \equiv \overline{x^2} - \overline{x}^2$. As starting point, we formally solve the eigenvalue problem for v^σ_{qk}, assuming $g_\sigma \neq 0$,

$$v^\sigma_{qk} = \frac{D^2}{g_\sigma} \left(G(\Delta_{qk})\, \overline{v^\sigma} + \overline{G^* v^\sigma} \right). \tag{3.5}$$

In the following, on the right-hand side, the explicit dependence on the eigenvector v^σ is

removed by taking appropriate averages.

By taking the average of Eq. (3.5) we find the relation $\overline{v^\sigma} = \frac{D^2}{g_\sigma}\left(\overline{G}\,\overline{v^\sigma} + \overline{G^* v^\sigma}\right)$ or, equivalently, $\overline{v^\sigma} = \overline{G^* v^\sigma}/(\frac{g_\sigma}{D^2} - \overline{G})$ which we plug into the eigenvalue problem (3.5) to arrive at

$$v^\sigma_{qk} = \frac{D^2}{g_\sigma}\overline{G^* v^\sigma}\left(\frac{G(\Delta_{qk})}{\frac{g_\sigma}{D^2} - \overline{G}} + 1\right). \tag{3.6}$$

Here, in order to cancel $\overline{G^* v^\sigma}$ we multiply by $G(\Delta_{qk})^*$ and, yet again, take the average. It follows $1 = \frac{D^2}{g_\sigma}\left(\frac{\overline{|G|^2}}{\frac{g_\sigma}{D^2} - \overline{G}} + \overline{G^*}\right)$, which is a quadratic equation for the eigenvalue g_σ. It is explicitly solved by[1]

$$\frac{g_\sigma}{D^2} = \overline{G'}\left(1 + \sigma\sqrt{1 + \frac{V[G'] + V[G'']}{\overline{G'}^2}}\right), \tag{3.7}$$

with $\sigma = \pm 1$, where we split $G(\Delta)$, $G(\Delta) \equiv G'(\Delta) + \mathrm{i}G''(\Delta)$, into its real and imaginary part.

Secondly, for the eigenvectors v^σ, we start again from Eq. (3.5) and substitute $\overline{G^* v^\sigma} = \overline{v^\sigma}(\frac{g_\sigma}{D^2} - \overline{G})$ to obtain

$$v^\sigma_{qk} = \frac{D^2}{g_\sigma}\overline{v^\sigma}\left(G(\Delta_{qk}) + \sigma\sqrt{\overline{|G|^2}}e^{-\mathrm{i}\sigma\varphi}\right). \tag{3.8}$$

Here, the second term is given by the complex quantity

$$\begin{aligned}\frac{g_\sigma}{D^2} - \overline{G} &= \sigma\sqrt{\overline{G'}^2 + V[G'] + V[G'']} - \mathrm{i}\overline{G''},\\ &= \sigma\sqrt{\overline{|G|^2} - \overline{G''}^2} - \mathrm{i}\overline{G''},\\ &\equiv \sigma\sqrt{\overline{|G|^2}}e^{-\mathrm{i}\sigma\varphi},\end{aligned} \tag{3.9}$$

for which, in the last line, φ defines the complex phase, which can be interpreted geometrically as shown in Fig. 3.1. For the complex phase, we find $\tan\varphi = \frac{\overline{G''}}{\sqrt{\overline{|G|^2} - \overline{G''}^2}}$, $\sin\varphi = \frac{\overline{G''}}{\sqrt{\overline{|G|^2}}}$, and $\cos\varphi = \frac{\sqrt{\overline{|G|^2} - \overline{G''}^2}}{\sqrt{\overline{|G|^2}}}$, with $\varphi \in [0, \frac{\pi}{2})$.

As a final step, with the norm $\sum_{q'k'}|v^\sigma_{q'k'}|^2 = |\overline{v^\sigma}|^2\sqrt{\overline{|G|^2}}\frac{D^2}{|g_\sigma|}2\cos\varphi$,[2] we arrive at the normal-

[1] The quadratic equation for g_σ is $0 = (\frac{g_\sigma}{D^2} - \overline{G^*})(\frac{g_\sigma}{D^2} - \overline{G}) - \overline{|G|^2}$, which has the solution $\frac{g_\sigma}{D^2} = \overline{G} + \overline{G^*} \pm \sqrt{(\overline{G} + \overline{G^*})^2 + \overline{|G|^2} - |\overline{G}|^2}$. With real and imaginary part, i.e., $G = G' + \mathrm{i}G''$, it follows $\frac{g_\sigma}{D^2} = \overline{G'} \pm \sqrt{\overline{G'}^2 + \overline{G'^2} - \overline{G'}^2 + \overline{G''^2} - \overline{G''}^2}$.

[2] The norm of the eigenvector is given by $\sum_{q'k'}|v^\sigma_{q'k'}|^2 = \frac{D^4}{g_\sigma^2}|\overline{v}^\sigma|^2\sqrt{\overline{|G|^2}}2(\sqrt{\overline{|G|^2}} + \sigma\mathrm{Re}[e^{\mathrm{i}\sigma\varphi}\overline{G}]) = \frac{D^4}{g_\sigma^2}|\overline{v}^\sigma|^2\sqrt{\overline{|G|^2}}2\cos\varphi\,(\frac{\sqrt{\overline{|G|^2}}}{\cos\varphi} + \sigma\overline{G'} - \tan\varphi\,\overline{G''})$. Now by using the expressions for the complex phase [see Fig. 3.1] the latter term evaluates to $\frac{\sqrt{\overline{|G|^2}}}{\cos\varphi} + \sigma\overline{G'} - \tan\varphi\,\overline{G''} = \sqrt{\overline{G'^2} + V[G'] + V[G'']} + \sigma\overline{G'} = \frac{\sigma g_\sigma}{D^2} = \frac{|g_\sigma|}{D^2}$.

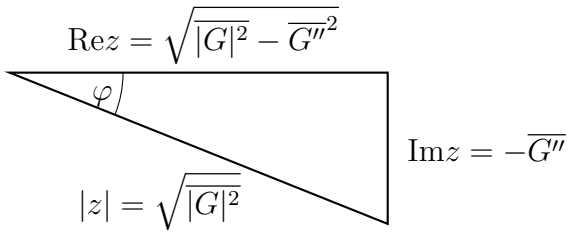

Figure 3.1: Complex quantity $z = \frac{g_\sigma}{D^2} - \overline{G}$ visualized in the complex plane.

ized eigenvector,

$$\frac{v^\sigma_{qk}}{\sqrt{\sum_{q'k'} |v^\sigma_{q'k'}|^2}} = \frac{1}{\sqrt{2|g_\sigma| \cos\varphi}} \left(\frac{1}{\lambda} e^{\mathrm{i}\sigma\frac{\varphi}{2}} G(\Delta_{qk}) + \sigma\lambda e^{-\mathrm{i}\sigma\frac{\varphi}{2}} \right), \tag{3.10}$$

for which we neglected the global phase factor $\frac{\overline{v^\sigma}}{|\overline{v^\sigma}|} e^{-\mathrm{i}\frac{\varphi}{2}}$ and introduced the rescaling parameter $\lambda^2 \equiv \sqrt{\overline{|G|^2}}$ to match with the notation of Eq. (3.42) below.

In summary, by diagonalization of the coefficient matrix

$$G(\Delta_{qk}) + G(\Delta_{q'k'})^* = \sum_\sigma g_\sigma \frac{v^\sigma_{qk}}{|v^\sigma|} \frac{(v^\sigma_{q'k'})^*}{|v^\sigma|}, \tag{3.11}$$

the dissipative part of the Redfield superoperator (2.51), with coupling operator S and convoluted operator $\mathbb{S} = \sum_{qk} S_{qk} G(\Delta_{qk}) \, |q\rangle\langle k|$, takes a pseudo-Lindblad form with dissipator

$$\mathcal{D}^{\mathrm{Red}}[\varrho] = \sum_{\sigma=+1,-1} \sigma \Big[A_\sigma \varrho A_\sigma^\dagger - \frac{1}{2} \Big\{ A_\sigma^\dagger A_\sigma, \varrho \Big\} \Big]. \tag{3.12}$$

It contains only two jump operators

$$A_\sigma = \sum_{qk} \sqrt{|g_\sigma|} \frac{v^\sigma_{qk}}{|v^\sigma|} S_{qk} \, |q\rangle\langle k| = \frac{1}{\sqrt{2\cos\varphi}} \left(\frac{1}{\lambda} e^{\mathrm{i}\sigma\frac{\varphi}{2}} \mathbb{S} + \sigma\lambda e^{-\mathrm{i}\sigma\frac{\varphi}{2}} S \right). \tag{3.13}$$

For a discussion of the eigenvalues g_σ and jump operators A_σ, we refer to Section 3.2 below. In the following section, it is shown that, surprisingly, the Redfield dissipator as a whole remains invariant, when λ and φ are varied as arbitrary real parameters.

3.2 Non-unitary, basis-independent diagonalization of the Redfield dissipator

In the previous section, we obtained a pseudo-Lindblad representation of the Redfield equation by solving the eigenvalue problem of the Kossakowski matrix. For that purpose, we

started from the eigenbasis representation. In the following, we find a two-parameter family of pseudo-Lindblad representations without involving a basis. The basis-free procedure is simpler, more general, and gives rise to different representations that are related by symmetry transformations.

Starting from the basis independent form of the Redfield Eq. (2.42), first, one completes the latter terms to a commutator and anti-commutator $-S\mathbb{S}\varrho(t) - \varrho(t)\mathbb{S}^\dagger S = -\mathrm{i}[(S\mathbb{S} - \mathbb{S}^\dagger S)/(2\mathrm{i}), \varrho(t)] - (1/2)\{S\mathbb{S} + \mathbb{S}^\dagger S, \varrho(t)\}$, to arrive at

$$\mathcal{R}^{(2)}[\varrho(t)] = -\mathrm{i}[H_{\mathrm{LS}}, \varrho(t)] + \mathcal{D}^{\mathrm{Red}}[\varrho(t)], \tag{3.14}$$

with Lamb-shift Hamiltonian

$$H_{\mathrm{LS}} = \frac{S\mathbb{S} - \mathbb{S}^\dagger S}{2\mathrm{i}}. \tag{3.15}$$

Moreover, the dissipative part has the familiar form

$$\mathcal{D}^{\mathrm{Red}}[\varrho(t)] = \sum_{i,j=1}^{2} \sigma^x_{ij} \left[S_i \varrho(t) S_j^\dagger - \frac{1}{2}\Big\{ S_j^\dagger S_i, \varrho(t) \Big\} \right], \tag{3.16}$$

with the Kossakowski matrix given by the Pauli-x matrix,

$$\sigma^x = \begin{pmatrix} 0 & 1 \\ 1 & 0 \end{pmatrix}, \tag{3.17}$$

and the jump operators $S_1 \equiv S$ and $S_2 \equiv \mathbb{S}$. This form of the Redfield equation can also be found, e.g., in Refs. [36, 44].

Note that H_{LS} and $\mathcal{D}^{\mathrm{Red}}$ are not uniquely defined, but that they may be transformed according to $S_i \to S_i' = S_i - \alpha_i$ and $H_{\mathrm{LS}} \to H_{\mathrm{LS}}' = H_{\mathrm{LS}} + \sum_{i,j} \sigma^x_{ij} \frac{\alpha_i^* S_j^\dagger - \alpha_j^* S_i}{2\mathrm{i}}$ with complex constants α_i, which have matching physical dimension with S_i. This freedom was used in Ref. [116] to minimize the weight of the dissipator to arrive at a unique Lamb-shift Hamiltonian, which is then employed to define thermodynamic properties such as heat, work, and entropy production. In the following we explore a different freedom, which allows to transform the dissipator alone.[3] This approach allows us to minimize the term with the negative weight in the pseudo-Lindblad representation.

Essentially, the algebraic structure of the dissipative part is a bilinear-form of the Pauli matrix σ^x with the row vector $(S, \mathbb{S})$ of the operators S and $\mathbb{S}$. By diagonalizing the Kossakowski matrix, one obtains a representation of the Redfield equation with new jump operators that act symmetrically on the state. For instance, the terms $S\varrho(t)\mathbb{S}^\dagger$ are transformed to $A_+\varrho(t)A_+^\dagger$ and $A_-\varrho(t)A_-^\dagger$, with appropriate operators A_+ and A_-. To this end, note that the Kossakowski

[3] This transformation is mentioned in Ref. [116] but not further exploited.

matrix σ^x is diagonalized via the unitary transformation

$$U = \frac{1}{\sqrt{2}} \begin{pmatrix} 1 & -1 \\ 1 & 1 \end{pmatrix}. \tag{3.18}$$

to

$$\sigma^z = \begin{pmatrix} 1 & 0 \\ 0 & -1 \end{pmatrix} = U^\dagger \sigma^x U. \tag{3.19}$$

With this, the entries of the Kossakowski matrix $\sigma^x_{ij} = (U\sigma^z U^\dagger)_{ij}$ are expressed as

$$\sigma^x_{ij} = \sum_{\sigma=+1,-1} \sigma\, U_{i\sigma} U^*_{j\sigma}. \tag{3.20}$$

This is inserted in the Redfield dissipator and one identifies the new jump operators $(A_+, A_-) = (S, \mathbb{S})\, U$,

$$A_\sigma = \sum_i S_i U_{i\sigma}, \tag{3.21}$$

with $\sigma = +1, -1$. Thus, the unitary U defines a transformation of the Redfield equation, where the Kossakowski matrix is transformed as $\sigma^x \xrightarrow{U} \sigma^z = U\sigma^x U^\dagger$ and the jump operators are transformed as $(S, \mathbb{S}) \xrightarrow{U} (A_+, A_-) = (S, \mathbb{S})\, U$. The transformed Redfield equation has the form

$$\mathcal{D}^{\mathrm{Red}}[\varrho(t)] = \sum_{\sigma=+1,-1} \sigma \Big[A_\sigma \varrho(t) A^\dagger_\sigma - \frac{1}{2} \Big\{ A^\dagger_\sigma A_\sigma, \varrho(t) \Big\} \Big], \tag{3.22}$$

which is similar to a GKSL equation with two jump operators A_+ and A_-, however, with corresponding relaxation weights $\sigma = 1$ and $\sigma = -1$. The negative relaxation weight is the reason why the Redfield equation cannot be referred to as GKSL equation. Instead we refer to it as *pseudo-Lindblad* equation. As in the unitary diagonalization procedure, which yields the pseudo-Lindblad representation (3.12), we again find two jump operators; one with a positive weight and the other with a negative weight. Further below, it is also shown that the detailed form of the jump operators A_σ can be written with parameters λ and φ as in Eq. (3.13).

In comparison to the quantum-optical master equation, the pseudo-Lindblad equation is obtained without diagonalizing the system's Hamiltonian. Also, whereas for the quantum-optical master equation the number of jump operators grows quadratically with the Hilbert space dimension, the pseudo-Lindblad dissipator (3.22) only has two jump operators. In contrast to the diagonalization derived in Section 3.1, here, we do not start from the eigenbasis representation.

Apart from our work [141, 142], a similar decomposition of the Redfield equation has re-

cently been used in Ref. [143], however, for a specific choice of symmetry that does not correspond to the optimization carried out below. Dissipators of this form are also used for time-convolutionless description of non-Markovian processes [69, 71, 89]. An intriguing similar master equation for the noise-averaged density matrix has been found in Ref. [144], which is, however, derived from a stochastic Hamiltonian with non-Markovian noise.

Above, the new jump operators $A_\sigma = \frac{1}{\sqrt{2}}(\sigma S + \mathbb{S})$, would be linear combinations of S and $\mathbb{S}$. However, the physical dimension of S and $\mathbb{S}$ do not match, i.e., S and $\mathbb{S}$ differ by the unit of the spectral density in Eq. (2.15). Therefore, it is required to rescale the operators

$$S \to \lambda S, \qquad \mathbb{S} \to \frac{1}{\lambda}\mathbb{S}, \tag{3.23}$$

with λ^2 being a rate to match the physical dimensions of S and $\mathbb{S}$. By writing the Redfield equation as in Eq. (2.42) the additional parameter simply cancels out showing that the Redfield equation is invariant under the transformation above. In the following, symmetries of the Redfield equation are analyzed systematically and it is shown that this can be used to minimize the negative weight.

3.3 Symmetry transformation of the Redfield equation

As is shown at the end of the last section, the Redfield equation is invariant under transformations

$$(S, \mathbb{S}) \to (\lambda S, \mathbb{S}/\lambda), \tag{3.24}$$

which rescale the operators S and $\mathbb{S}$ with a parameter λ. The rescaling λ is a free parameter of the Redfield equation, which can be used to minimize the weight of the negative contribution. This is carried out in the section below. This opens the question, whether there are further transformations that leave the dissipator invariant, but vary the individual jump operators. Therefore, before we turn to the optimization procedure, in this section, the invariant transformations of the Redfield equation are studied rigorously. We find that such transformations are characterized by two free parameters.

We are interested in transformations characterized by 2×2 matrices Λ that leave the Kossakowski matrix invariant

$$\sigma^x = \Lambda \sigma^x \Lambda^\dagger. \tag{3.25}$$

Using this transformation for the entries of the Kossakowski matrix in the Redfield dissipator in Eq. (3.16), i.e., $\sigma^x_{ij} = \sum_{nm} \sigma^x_{nm} \Lambda_{in} \Lambda^*_{jm}$, the operators transform as $(S, \mathbb{S}) \xrightarrow{\Lambda} (S, \mathbb{S})\,\Lambda$.

Subsequently, we can obtain a diagonal representation by diagonalization with the unitary

U, as discussed in Section 3.2 above. In total, we are interested in transformations ΛU of the Redfield dissipator

$$\begin{pmatrix} \sigma^x \\ (S,\mathbb{S}) \end{pmatrix} \xrightarrow{\Lambda} \begin{pmatrix} \Lambda\sigma^x\Lambda^\dagger \\ (S,\mathbb{S})\,\Lambda \end{pmatrix} \xrightarrow{U} \begin{pmatrix} \sigma^z \\ (S,\mathbb{S})\,\Lambda U \end{pmatrix}, \tag{3.26}$$

by which the Redfield equation takes pseudo-Lindblad form as in Eq. (3.22), with the new jump operators

$$(A^\Lambda_+, A^\Lambda_-) = (S,\mathbb{S})\,\Lambda U. \tag{3.27}$$

Note that $\sigma^z = (\Lambda^\dagger U)^\dagger\sigma^x(\Lambda^\dagger U)$ defines a general diagonalization of σ^x, however, with a non-unitary matrix $\Lambda^\dagger U$, i.e., generally $(\Lambda^\dagger U)(\Lambda^\dagger U)^\dagger = \Lambda^\dagger\Lambda \neq \mathbb{1}$. Instead, it is

$$\begin{pmatrix} 1 & 0 \\ 0 & -1 \end{pmatrix} = (U^\dagger\Lambda U)\begin{pmatrix} 1 & 0 \\ 0 & -1 \end{pmatrix}(U^\dagger\Lambda U)^\dagger, \tag{3.28}$$

which defines generalized unitary matrices $U^\dagger\Lambda U \in \mathbb{C}^{2,2}$. Generalized unitary transformations are also relevant for the Minkowski metric in special relativity or in Bogoliubov theory of quadratic Hamiltonians [145].

Here, the transformation ΛU is relevant because it changes the weight $\|A^\Lambda_\sigma\|^2$ of the jump operators A^Λ_σ. To find the optimal transformation that minimizes the weight of the negative contribution, in the following, the most general transformation is constructed.

3.3.1 Symmetry parameters of the Redfield equation

The transformation ΛU for the Redfield equation is not unique. Instead there are different representations of the pseudo-Lindblad jump operators A^Λ_σ, which are related by symmetry transformations $\sigma^x = \Lambda\sigma^x\Lambda^\dagger$ of the Kossakowski matrix σ^x. In this section, starting from arbitrary complex entries Λ_{ij} in

$$\Lambda = \begin{pmatrix} \Lambda_{11} & \Lambda_{12} \\ \Lambda_{21} & \Lambda_{22} \end{pmatrix}, \tag{3.29}$$

corresponding to eight real parameters, the most general representation for the jump operators A^Λ_σ is constructed. It is shown that this gives rise to two relevant symmetry parameters λ and φ.

To begin with, the symmetry condition $\sigma^x = \Lambda\sigma^x\Lambda^\dagger$ reads

$$\begin{aligned}\begin{pmatrix} 0 & 1 \\ 1 & 0 \end{pmatrix} &= \begin{pmatrix} \Lambda_{11} & \Lambda_{12} \\ \Lambda_{21} & \Lambda_{22} \end{pmatrix}\begin{pmatrix} 0 & 1 \\ 1 & 0 \end{pmatrix}\begin{pmatrix} \Lambda_{11}^* & \Lambda_{21}^* \\ \Lambda_{12}^* & \Lambda_{22}^* \end{pmatrix}, \\ &= \begin{pmatrix} \Lambda_{11}\Lambda_{12}^* + \Lambda_{12}\Lambda_{11}^* & \Lambda_{11}\Lambda_{22}^* + \Lambda_{12}\Lambda_{21}^* \\ \Lambda_{11}^*\Lambda_{22} + \Lambda_{12}^*\Lambda_{21} & \Lambda_{21}\Lambda_{22}^* + \Lambda_{22}\Lambda_{21}^* \end{pmatrix},\end{aligned} \tag{3.30}$$

for which the entries on the off-diagonal are related by complex conjugation. The symmetry condition reduces to the three coupled equations

$$0 = 2\mathrm{Re}[\Lambda_{11}\Lambda_{12}^*] = 2|\Lambda_{11}||\Lambda_{12}|\cos(\arg(\Lambda_{11}) - \arg(\Lambda_{12})), \tag{3.31}$$

$$0 = 2\mathrm{Re}[\Lambda_{22}\Lambda_{21}^*] = 2|\Lambda_{22}||\Lambda_{21}|\cos(\arg(\Lambda_{22}) - \arg(\Lambda_{21})), \tag{3.32}$$

$$1 = \Lambda_{11}\Lambda_{22}^* + \Lambda_{12}\Lambda_{21}^*, \tag{3.33}$$

The conditions above fix four out of eight parameters in Λ, since the first two are real and only the third is complex.

Assuming $\Lambda_{ij} \neq 0$, Eqs. (3.31) and (3.32) yield the phase relations

$$e^{\mathrm{i}\arg(\Lambda_{11})}e^{-\mathrm{i}\arg(\Lambda_{12})} = \pm\mathrm{i}, \tag{3.34}$$

$$e^{-\mathrm{i}\arg(\Lambda_{22})}e^{\mathrm{i}\arg(\Lambda_{21})} = \pm\mathrm{i}, \tag{3.35}$$

and thus, apart from a global phase $e^{\mathrm{i}\alpha}$, one deduces the diagonal entries to be real and the off-diagonals to be purely imaginary. Thus, using Eqs. (3.31) and (3.32) the symmetry transformation reduces to

$$\Lambda = e^{\mathrm{i}\alpha}\begin{pmatrix} \lambda_{11} & \mathrm{i}\lambda_{12} \\ \mathrm{i}\lambda_{21} & \lambda_{22} \end{pmatrix}, \tag{3.36}$$

with real parameters λ_{ij}. With this, the third condition in Eq. (3.33) reduces to

$$1 = \lambda_{11}\lambda_{22} + (\mathrm{i}\lambda_{12})(-\mathrm{i}\lambda_{21}) = |\det\Lambda|, \tag{3.37}$$

the absolute value of the determinant of Λ being equal to one. This reduces the four parameters λ_{ij} to three. In the following, we find a suitable parametrization of α and three further parameters. To this end, note that the invariance under rescaling the operators in Eq. (3.24),

$$(\lambda S, \mathbb{S}/\lambda) = (S, \mathbb{S})\begin{pmatrix} \lambda & 0 \\ 0 & 1/\lambda \end{pmatrix}, \tag{3.38}$$

is obtained for the particular choice of the parameters, i.e., $\alpha = 0$, $\lambda = \lambda_{11} = 1/\lambda_{22}$ and

$0 = \lambda_{12} = \lambda_{21}$. The most general transformation can now be parametrized as

$$\Lambda = \frac{e^{\mathrm{i}\alpha}}{\sqrt{\cos\varphi}} \begin{pmatrix} \lambda\cos(\frac{\varphi+\beta}{2}) & \mathrm{i}\lambda\sin(\frac{\varphi+\beta}{2}) \\ -\mathrm{i}\frac{1}{\lambda}\sin(\frac{\varphi-\beta}{2}) & \frac{1}{\lambda}\cos(\frac{\varphi-\beta}{2}) \end{pmatrix}. \tag{3.39}$$

It possesses also also non-zero off-diagonal entries and one verifies easily $|\det\Lambda| = 1$. The parametrization above has four symmetry parameters $(\lambda, \varphi, \alpha, \beta)$ and, therefore, defines a general parametrisation.

Together with the unitary transformation U the jump operators A^{Λ}_{σ} for the pseudo-Lindblad representation follow from the transformation

$$\Lambda U = \frac{e^{\mathrm{i}\alpha}}{\sqrt{2\cos\varphi}} \begin{pmatrix} \lambda e^{\mathrm{i}\frac{\varphi+\beta}{2}} & -\lambda e^{-\mathrm{i}\frac{\varphi+\beta}{2}} \\ \frac{1}{\lambda}e^{-\mathrm{i}\frac{\varphi-\beta}{2}} & \frac{1}{\lambda}e^{\mathrm{i}\frac{\varphi-\beta}{2}} \end{pmatrix}, \tag{3.40}$$

and are given by

$$(A^{\Lambda}_{+}, A^{\Lambda}_{-}) = (S, \mathbb{S})\,\Lambda U, \tag{3.41}$$

which yields

$$A^{\Lambda}_{\sigma} = \frac{e^{\mathrm{i}(\alpha+\sigma\frac{\beta}{2})}}{\sqrt{2\cos\varphi}}\Big[\sigma\lambda e^{\mathrm{i}\sigma\frac{\varphi}{2}}\ S + \frac{1}{\lambda}e^{-\mathrm{i}\sigma\frac{\varphi}{2}}\ \mathbb{S}\Big], \tag{3.42}$$

with $\sigma = +1, -1$, where the parameters α and β occur as global phase factor. The jump operators in Eq. (3.42) mark the central result of this chapter. Because in the pseudo-Lindblad equation (3.22) the jump operators always occur in Hermitian conjugated pairs, the global phases cancel out for each GKSL channel. Because there are two GKSL channels the effective number of free parameter reduces from four to two and are given by a rescaling parameter λ and a complex phase φ. The most general form of A^{Λ}_{σ} also count for the jump operators in Eq. (3.13), which are found previously, in Section 3.1, within a unitary diagonalization scheme.

In summary, the Redfield equation is brought to pseudo-Lindblad form with an equivalent class of two jump operators A^{Λ}_{+} and A^{Λ}_{-}. The equivalent representations are related by symmetry transformations of the Kossakowski matrix, which is parametrized by two free parameters λ and φ.

The symmetry parameters change the norm of the jump operators. In the next section, we find the optimal values for λ and φ that minimize the negative weight.

3.4 Minimization of the negative relaxation weight

In Section 3.3.1, we find a two-parameter family of jump operators that are characterized by the symmetry parameters λ and φ. Even though, the Redfield dissipator is invariant under

variation of the symmetry parameters, the jump operators change. In particular, the weight, i.e., the norm of the jump operators is modified. In this section, we find the optimal parameters that minimize the negative relaxation weight. Here, the Frobenius norm

$$\|A\|^2 = \mathrm{tr}(AA^\dagger), \tag{3.43}$$

for arbitrary operators A is used. Independent of the particular basis, it can be calculated as the sum over the absolute squared matrix elements, $\|A\|^2 = \sum_{nm} |\langle n|A|m\rangle|^2$. Furthermore, the Frobenius norm satisfies the addition identity[4]

$$\|A+B\|^2 = \|A\|^2 + 2\mathrm{Re}\,\mathrm{tr}(AB^\dagger) + \|B\|^2, \tag{3.44}$$

for any bounded operators A and B. As a central result of this chapter, using this identity we obtain the relaxation weights for the jump operators,

$$\|A^\Lambda_\sigma\|^2 = \sigma\mathrm{Re}\,\mathrm{tr}(\mathbb{S}S) + \underbrace{\frac{\lambda^2}{2\cos(\varphi)}\|S\|^2 - \tan(\varphi)\mathrm{Im}\,\mathrm{tr}(\mathbb{S}S) + \frac{1/\lambda^2}{2\cos(\varphi)}\|\mathbb{S}\|^2}_{\equiv f(\lambda,\varphi)}. \tag{3.45}$$

The difference of the relaxation weights is invariant under the symmetry,

$$\|A^\Lambda_+\|^2 - \|A^\Lambda_-\|^2 = 2\mathrm{Re}\,\mathrm{tr}(\mathbb{S}S), \tag{3.46}$$

and in Eq. (3.53) is shown to be positive. The weights $\|A^\Lambda_\sigma\|^2$ are schematically depicted in Fig. 3.2(a).

Remarkably, even though the Redfield equation is invariant under the symmetry transformation the relaxation weights are affected by the rescaling λ and the phase φ and one may find optimal values that minimize $\|A^\Lambda_-\|$ and, thanks to Eq. (3.46), also $\|A^\Lambda_-\|/\|A^\Lambda_+\|$ as well as $\|A^\Lambda_+\|$ and $\|A^\Lambda_-\| + \|A^\Lambda_+\|$. The optimal values that minimize $f(\lambda,\varphi) = \lambda^2/(2\cos(\varphi))\|S\|^2 - \tan(\varphi)\mathrm{Im}\,\mathrm{tr}(\mathbb{S}S) + \|\mathbb{S}\|^2/(2\cos(\varphi)\lambda^2)$, also minimize both the positive and negative relaxation weights, respectively.

In Fig. 3.2(b), $f(\lambda,\varphi)$ is schematically depicted as a function of λ, for arbitrarily chosen fixed φ, $\mathrm{Im}\,\mathrm{tr}(\mathbb{S}S)$, $\|\mathbb{S}\|^2$ and $\|S\|^2$. As pointed out, the rescaling parameter λ is necessary to account for the dimensional mismatch of $\mathbb{S}$ and S, such that λ^2 defines a rate. For large λ, the jump operators are dominated by the coupling operator S, whereas for small λ the convoluted operator $\mathbb{S}$ is dominant [Eq. (3.42)]. The optimal rescaling is balancing both terms and is

[4] Using $\mathrm{tr}(B^\dagger A) = \mathrm{tr}(A^\dagger B)^*$ and $\|A+B\|^2 = \mathrm{tr}(A^\dagger A + A^\dagger B + B^\dagger A + B^\dagger B)$ one easily shows the identity in Eq. (3.44)

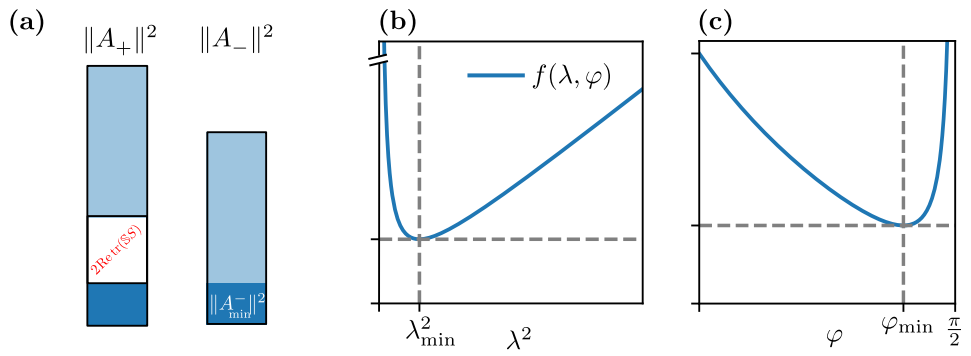

Figure 3.2: In (a) schematic for positive and negative relaxation weights. The negative weight is smaller than the positive one. The difference $\|A_+\|^2 - \|A_-\|^2 = 2\mathrm{Re}\,\mathrm{tr}(\mathbb{S}S) > 0$ is indicated by the white region in the right bar. Both weights can be varied indicated by the light blue region. The dark blue region marks the optimum with a minimal negative weight. In (b) and (c) $f(\lambda,\varphi) = (\|A_+\|^2 + \|A_-\|^2)/2$ (solid blue) as a function of the rescaling and complex phase, respectively. The minimum $(\lambda_{\mathrm{min}}, \varphi_{\mathrm{min}})$ minimizes both $\|A_-\|^2$ and $\|A_+\|^2$.

found to be

$$\lambda^2_{\mathrm{min}} = \frac{\|\mathbb{S}\|}{\|S\|}, \tag{3.47}$$

for which it is $f(\lambda_{\mathrm{min}}, \varphi) = \|\mathbb{S}\|\|S\|/\cos(\varphi) - \tan(\varphi)\mathrm{Im}\,\mathrm{tr}(\mathbb{S}S)$. Thus, the optimal rescaling is found by identifying λ^{-2} with the typical timescale that is related to the amplitude of the bath correlation function. In general, the optimization is crucial for the validity of the truncation and is further illustrated in Section 3.8, where we point out the relevance of the optimization.

The complex phase is yet another free parameter. In particular, by neglecting the complex phase, $\varphi = 0$, it follows that $f(\lambda_{\mathrm{min}}, 0) = \|\mathbb{S}\|\|S\|$, which is no global minimum, see Fig. 3.2(c). Rather, the optimal choice is

$$\sin(\varphi_{\mathrm{min}}) = \frac{\mathrm{Im}\,\mathrm{tr}(\mathbb{S}S)}{\|S\|\|\mathbb{S}\|}, \tag{3.48}$$

and it follows that

$$f(\lambda_{\mathrm{min}}, \varphi_{\mathrm{min}}) = \sqrt{\|S\|^2\|\mathbb{S}\|^2 - [\mathrm{Im}\,\mathrm{tr}(\mathbb{S}S)]^2}. \tag{3.49}$$

In the following, in order to keep the notation simple, the jump operators with optimal parameters are denoted as

$$A_\sigma \equiv A^\Lambda_\sigma\big|_{\lambda_{\mathrm{min}},\varphi_{\mathrm{min}}} = \frac{1}{\sqrt{2\cos\varphi_{\mathrm{min}}}}\left[\sigma\sqrt{\frac{\|\mathbb{S}\|}{\|S\|}}e^{\mathrm{i}\sigma\frac{\varphi_{\mathrm{min}}}{2}}\ S + \sqrt{\frac{\|S\|}{\|\mathbb{S}\|}}e^{-\mathrm{i}\sigma\frac{\varphi_{\mathrm{min}}}{2}}\ \mathbb{S}\right]. \tag{3.50}$$

Altogether, the optimization leads to minimal relaxation weights for the jump operators,

$$\|A_\sigma\|^2 = \sqrt{\|S\|^2\|\mathbb{S}\|^2 - [\mathrm{Im}\,\mathrm{tr}(\mathbb{S}S)]^2} + \sigma \mathrm{Re}\,\mathrm{tr}(\mathbb{S}S). \tag{3.51}$$

Note, if the matrix elements of $\mathbb{S}$ and S are real, which is the case for a purely Ohmic bath discussed in the next section, it follows that $\|A_\sigma\|^2 = \|S\|\|\mathbb{S}\| + \sigma\,\mathrm{tr}(\mathbb{S}S)$.

3.5 The truncated GKSL master equation

The Redfield equation is a pseudo-Lindblad equation with dissipator (3.22) and differs from a GKSL equation by the existence of a negative relaxation weight. In this section, we propose a new master equation of GKSL form with dissipator

$$\mathcal{D}^{\mathrm{Red}}[\varrho(t)] \simeq \mathcal{D}^{\mathrm{trunc}}[\varrho(t)] = A_+\varrho(t)A_+^\dagger - \frac{1}{2}\Big\{A_+^\dagger A_+, \varrho(t)\Big\}, \tag{3.52}$$

which is obtained from the Redfield equation by neglecting the negative contribution. We justify this approximation by minimizing the negative relaxation weight absolutely and relative compared to the positive weight in Section 3.4. Furthermore, we estimate the validity of this approximation by analyzing the weight of the truncated negative term. To this end, we represent the operators in the energy eigenbasis and obtain analytical expressions, which we discuss as a function of the bath temperature and the spectral density of the bath.

To begin with, it is shown that the negative relaxation weight is smaller than the positive one as stated above in Eq. (3.46). To evaluate the difference $\|A_+\|^2 - \|A_-\|^2 = 2\mathrm{Re}\,\mathrm{tr}(\mathbb{S}S)$, we now calculate the trace in the eigenbasis of the system. Using $\langle q|S|k\rangle = S_{qk}$ and $\langle q|\mathbb{S}|k\rangle = G(\Delta_{qk})S_{qk}$, where $G(\Delta)$ is the complex valued coupling density with the real part given by $G'(\Delta) = J(\Delta)n_\beta(\Delta)$ [Eq. (2.19)], we obtain

$$\|A_+\|^2 - \|A_-\|^2 = 2\mathrm{Re}\,\mathrm{tr}(\mathbb{S}S) = \sum_{mn} R_{mn} > 0, \tag{3.53}$$

which is a sum over the positive rates $R_{mn} = 2G'(\Delta_{nm})|S_{nm}|^2$ of the quantum-optical master equation [Eq. (2.52)]. It may be interpreted as net relaxation weight of the Redfield dissipator that is invariant under the symmetry transformation.

For the truncation, we aim for $\|A_-\|^2/\|A_+\|^2 \ll 1$. Ideally, if $\mathbb{S}$ and S are linear dependent, i.e., $\mathbb{S} = G'S$ with some constant G', the symmetry parameters can be chosen, such that the negative weight vanishes. In this particular case, the jump operators in Eq. (3.42) reduce to $A_\sigma^\Lambda = \frac{1}{\sqrt{2}}(\sigma\lambda S + \frac{G'}{\lambda}\mathbb{S})$, with phases fixed to $\alpha = \beta = \varphi = 0$. An obvious choice for the rescaling parameter would be $\lambda = \sqrt{G'}$, such that the optimal jump operators are $A_+ = \sqrt{2G'}S$ and $A_- = 0$. This is also known as the singular coupling limit [146]: For instance, in case of infinitesimally short-lived correlations, i.e., $C(t) = G'\delta(t)$, the convoluted operator reduces to

$\mathbb{S} = G'S$ and the Redfield superoperator in Eq. (2.42) takes the GKSL form [146]

$$\mathcal{R}^{(2)}_{\text{sing}}[\varrho(t)] = 2G' \left(S\varrho(t)S - \frac{1}{2}\{SS, \varrho(t)\} \right), \tag{3.54}$$

with jump operator S and relaxation weight $2G'$.

However, in general the weight (3.51) of the negative contribution is finite. In contrast to the ideal case stated above, in general $\mathbb{S} = \sum_{qk} G(\Delta_{qk}) S_{qk} \, |q\rangle\langle k| \neq G'S$ with a certain distribution of the coupling density.

To explicitly calculate the weights of the pseudo-Lindblad jump operators, the traces are evaluated in the eigenbasis of the system. Note that $G(\Delta)$ might also be explicitly time-dependent and, therefore, all the analysis also applies to the time-dependent Redfield equation. However, for the sake of simplicity in this section, we restrict ourselves to the time-independent case, where

$$\operatorname{tr}(\mathbb{S}S) = \sum_{nm} |S_{nm}|^2 \big(G'(\Delta_{nm}) + \mathrm{i} G''_0(\Delta_{nm}) \big) + \mathrm{i} \underbrace{\sum_{nm} |S_{nm}|^2 G''_{\text{th}}(\Delta_{nm})}_{=0}, \tag{3.55}$$

$$\|\mathbb{S}\|^2 = \sum_{nm} |S_{nm}|^2 \big(G'(\Delta_{nm})^2 + [G''_0(\Delta_{nm}) + G''_{\text{th}}(\Delta_{nm})]^2 \big), \tag{3.56}$$

and

$$\|S\|^2 = \sum_{nm} |S_{nm}|^2. \tag{3.57}$$

Here, in the first line, the sum over the thermal noise cancels because of the antisymmetry $G''_{\text{th}}(\Delta_{nm}) = -G''_{\text{th}}(\Delta_{mn})$, see Eqs. (2.22) and (A.8).

For the expressions above, it is handy to introduce the average

$$\overline{x} \equiv \frac{1}{\|S\|^2} \sum_{qk} |S_{nm}|^2 x(\Delta_{nm}), \tag{3.58}$$

such that $\operatorname{tr}(\mathbb{S}S) = \|S\|^2 \overline{G}$ and $\|\mathbb{S}\|^2 = \|S\|^2 \overline{|G|^2}$. In this way, the coupling matrix elements divided by the squared norm of S, i.e., $|S_{nm}|^2 / \|S\|^2$ define a probability distribution. A typical distribution for the real part and imaginary part of the coupling density is depicted in Fig. 3.3(a), Fig. 3.3(d) and Fig. 3.3(b), Fig. 3.3(e), respectively. Here, because the level splittings are degenerate, for instance, it is $\Delta_{nn} = 0$ for all n, we define the probability distribution as

$$S(\Delta) \equiv \sum_{\substack{nm \\ \Delta_{nm} = \Delta}} S_{nm}, \tag{3.59}$$

where the sum is performed over all matrix elements that belong to the same level splitting $\Delta_{nm} = \Delta$. The maxima in the distributions originate from the degenerate zero frequency transition $\Delta = 0$ with $S(\Delta = 0) = \sum_n |S_{nn}|^2$. For a Drude bath, one easily verifies $G'(\Delta = 0) = \gamma T$ [Eq. (2.19)] and $G''(\Delta = 0) = 0$ [Eqs. (2.7) and (2.24)].

The optimal parameters in Eqs. (3.47) and (3.48) are now expressed as

$$\lambda_{\min}^2 = \frac{\|\mathbb{S}\|}{\|S\|} = \sqrt{\overline{|G|^2}}, \tag{3.60}$$

$$\sin\varphi_{\min} = \frac{\operatorname{Im}\operatorname{tr}(\mathbb{S}S)}{\|S\|\|\mathbb{S}\|} = \frac{\overline{G''}}{\sqrt{\overline{|G|^2}}}. \tag{3.61}$$

With this, the minimal weights (3.51) of the pseudo-Lindblad jump operators can be written as

$$\|A_\sigma\|^2 = \|S\|^2\overline{G'}\Big(\sigma 1 + \sqrt{1 + \frac{V[G'] + V[G'']}{\overline{G'}^2}}\Big), \tag{3.62}$$

where the prefactor $\|S\|^2\overline{G'}$, with only the real part of the coupling density, defines the overall magnitude. The form of the weights in Eq. (3.62) matches with the eigenvalues g_σ (3.7) of the Kossakowski matrix in the unitary diagonalization scheme presented previously in Section 3.1. In contrast, here, we use a different average (3.58) that takes into account the coupling operator

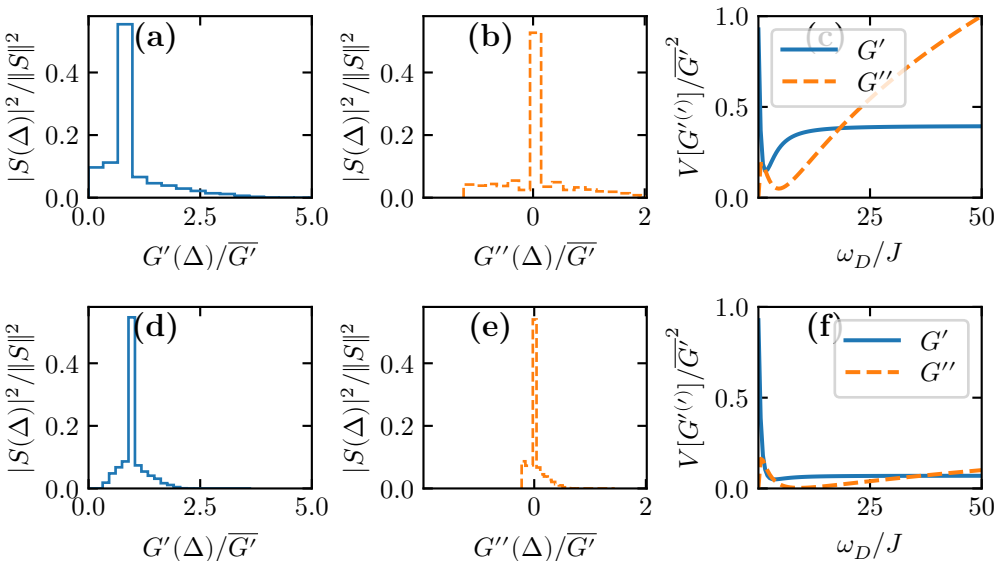

Figure 3.3: Weight-distribution of the coupling density for the real part $G'(\Delta)$ in (a) and imaginary part $G''(\Delta)$ in (b) normalized to the average $\overline{G'}$ for $\omega_D = 17J$. In (c) variance $V[G']$ as a function of cutoff ω_D/J in solid blue ($V[G'']$ in dashed orange). We consider an extended Hubbard model in Section 3.7 with tunneling J, $M = 8$, $N = 4$, $V = 1J$ coupled to a bath at temperature $T = 0.8J$ with $\gamma = 1$ and $S = a_1^\dagger a_1$. Panels (d)-(f) analogous, except for a higher temperature $T = 2J$.

S, whereas previously the eigenvalues g_σ are based upon the bare average (3.4).

Here, we introduce the second moment of the probability distribution,

$$V[x] \equiv \overline{x^2} - \overline{x}^2, \tag{3.63}$$

wich defines the squared deviation from the mean $\overline{x}$, i.e., the variance of the coupling density. Interestingly, the imaginary part $G''(\Delta)$ of the coupling density only contributes via its variance $V[G'']$. Equation (3.62) above shows that the negative weight depends on the deviation of the coupling density $G(\Delta)$ from its mean value. We observe, that if the second term under the root is zero, which is the case for vanishing variances, there would be no negative relaxation weight. Also, this can be vaguely related to the decay time of the bath correlation function. Using the relation $G(\Delta) = \int e^{-\mathrm{i}\Delta\tau} C(\tau) d\tau$ from Section 2.2.3, the shorter the decay time of the bath correlation, the more peaked $G(\Delta)$. From this argument, it is evident that the truncation approximation is accurate for extreme Markovian environments with a short bath correlation time.

For two different temperatures, $T = 0.8J$ and $T = 2J$, we plot the variances as function of the Drude cutoff ω_D/J in Fig. 3.3(c) and Fig. 3.3(f). The variance of the real part saturates for cutoff frequencies exceeding the largest energy level splitting of the system. For low temperatures, in Fig. 3.3(c), the variance of the imaginary part diverges with the cutoff frequency, because the imaginary part of the coupling density is dominated by logarithmically diverging zero-point fluctuation, see Eq. (2.24). For a higher temperature, in Fig. 3.3(f), the variance $V[G'']$ remains smaller because the divergence is compensated by thermal-noise. This is further illustrated by comparing Fig. 3.3(b) for low temperatures with Fig. 3.3(e) for high temperatures. For low temperatures, the distribution of the coupling density in Fig. 3.3(b) is rather symmetric, because it is dominated by the zero-point fluctuation, for which it is $G''_0(\Delta) = G''_0(-\Delta)$. In contrast, for high temperatures, the distribution in Fig. 3.3(e) is less symmetric, since thermal noise $G''_{\mathrm{th}}(\Delta) \neq G''_{\mathrm{th}}(-\Delta)$ dominates.

In the special case of only one transition frequency Ω, which is the case for the harmonic oscillator or for a two-level system with zeros on the diagonals of the coupling matrix $S_{qq} = 0$,[5] the averages and variances simplify to $\overline{x} = \frac{x(\Omega)+x(-\Omega)}{2}$ and $V[x] = \left(\frac{x(\Omega)-x(-\Omega)}{2}\right)^2$, respectively, so that with the expressions from Section 2.2.3 for the coupling density, it follows that

$$\overline{G'} = J(\Omega)\frac{\coth(\beta\Omega/2)}{2}, \tag{3.64}$$

$$V[G'] = J(\Omega)^2\frac{1}{4}, \tag{3.65}$$

$$V[G''] = \left(G''_{\mathrm{th}}(\Omega) - J(\Omega)\frac{1}{\pi}\ln\left[\frac{\Omega}{\omega_D}\right]\right)^2 \simeq J(\Omega)^2\left(-\frac{1}{\beta\omega_D} - \frac{1}{\pi}\ln\left[\frac{\Omega}{\omega_D}\right]\right)^2. \tag{3.66}$$

[5] For a generic two level system with $S_{qq} \neq 0$, $\|S\|^2 = |S_{00}|^2 + 2|S_{01}|^2 + |S_{11}|^2$ and for some quantity $x(\Delta)$ the average is given by $\overline{x} = \frac{|S_{00}|^2+|S_{11}|^2}{\|S\|^2}x(0) + \frac{|S_{01}|^2}{\|S\|^2}(x(\Omega)+x(-\Omega))$.

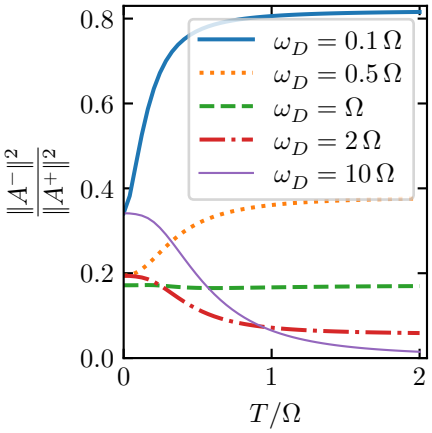

Figure 3.4: Relative negative relaxation weight $\frac{\|A_-\|^2}{\|A_+\|^2}$ for a system with a single transition frequency Ω as a function of temperature T/Ω and for different values of Drude cutoff $\omega_D = 0.1, 0.5, 1, 2, 10\,\Omega$ from top to bottom.

In summary, the relative negative relaxation weight $\|A_-\|^2/\|A_+\|^2$ only depends on the variance of the complex coupling density $G(\Delta)/\overline{G'}$, normalized to the average $\overline{G'}$. The weights for the average are determined by the squared matrix elements of the coupling operator $|S_{nm}|^2|/\|S\|^2$. If there is just one transition frequency, the relative negative relaxation weight only depends on the temperature and the cutoff, and is plotted in Fig. 3.4. For high temperature and large cutoff, the negative relaxation weight vanishes. In contrast, for low temperatures a small cutoff is favoured. In the following two sections, we discuss the regimes of low and high temperature in more detail and find the optimal regime for the truncation.

3.5.1 Limit of zero temperature

At zero temperature the Bose function becomes a step-wise function

$$n_\beta(\Delta) \overset{T\to 0}{=} -\Theta(-\Delta). \tag{3.67}$$

As a reminder, the Bose function and the spectral density $J(\Delta)$ (2.11) is continued to negative frequencies in order to define the coupling density (2.19). The equation above states $n_\beta(|\Delta|) \overset{T\to 0}{=} 0$ and $n_\beta(-|\Delta|) \overset{T\to 0}{=} -1$, which is found from $n_\beta(\Delta) = 1/(e^{\Delta/T} - 1)$. For the real part of the coupling density $G(\Delta)$ in the limit of zero temperature, one obtains $G'(\Delta) = J(|\Delta|)\Theta(-\Delta)$ and the thermal noise vanishes $G''_{\text{th}}(\Delta) = 0$ (2.25). The weights at zero temperature become

$$\|A_\sigma\|^2 \overset{T\to 0}{=} \frac{1}{2}\|S\|^2\overline{J(|\Delta|)}\Big(\sigma 1 + \sqrt{2 + \frac{\frac{1}{2}V[J(|\Delta|)] + V[G''_0]}{\frac{1}{4}\overline{J(|\Delta|)}^2}}\Big), \tag{3.68}$$

with the variance of the zero-point fluctuations given by

$$V[G_0''] = \frac{1}{4\omega_D^2}\left(\overline{J(\Delta)^2\Delta^2} - \overline{J(\Delta)\Delta}^2\right) + \frac{1}{\pi^2}\overline{J(\Delta)^2 \ln\left(\frac{|\Delta|}{\omega_D}\right)^2}. \tag{3.69}$$

Thus, the optimal weights at zero temperature read

$$\|A_\pm\|^2 \overset{T\to 0}{=} \frac{1}{2}\|S\|^2\overline{J(|\Delta|)}(\pm + \sqrt{2}) \simeq \|S\|^2\overline{J(|\Delta|)} \begin{cases} 1.21 \\ 0.21 \end{cases}, \tag{3.70}$$

assuming the second term under the root in Eq. (3.68) becomes zero. The latter is the case for ultra-peaked spectral densities and vacuum fluctuations, i.e., $V[J(|\Delta|)] = V[G_0''] = 0$.

In the special case that there is only one transition with frequency $\Omega > 0$, as is discussed in the previous section, we have $\overline{J(|\Delta|)} = J(\Omega)$, $V[J(|\Delta|)] = 0$, $V[G_0''] = (1/\pi^2)J(\Omega)^2 \ln(\Omega/\omega_D)^2$ and the weights simplify to,

$$\|A_\sigma\|^2 \overset{T\to 0}{=} \frac{1}{2}\|S\|^2 J(\Omega)\left(\sigma 1 + \sqrt{2 + \frac{4}{\pi^2}\ln\left(\frac{\Omega}{\omega_D}\right)^2}\right), \tag{3.71}$$

for which the cutoff $\omega_D = \Omega$ leads to the optimal weights.

3.5.2 Pure Ohmic bath and high temperature limit

In the literature, very often zero-point fluctuations and thermal noise are neglected. For the Drude bath, we refer to this limit as pure Ohmic with spectral density $J(\Delta) = \gamma\Delta$, where the cutoff frequency is pushed to infinity. Technically, this leads to divergent zero-point fluctuations and thermal noise, see Eqs. (2.24) and (2.25). However, in the high-temperature limit, one has $G_0''(\Delta) + G_{\text{th}}''(\Delta) \simeq J(\Delta)\left(\frac{1}{2}\frac{\Delta}{\omega_D} - \frac{1}{\beta\omega_D}\right)$, which tends to zero for $\omega_D \to \infty$. This is the deep Markovian regime with a short decay time of the bath correlation, $\tau_{\text{B}} = \max\{1/\omega_D,\ \beta/2\pi\}$ see Eq. (2.17).

For a pure Ohmic bath, the weights of the jump operators reduce to,

$$\|A_\sigma\|^2 = \|S\|^2\overline{G'}\left(\sigma 1 + \sqrt{1 + \frac{V[G']}{\overline{G'}^2}}\right). \tag{3.72}$$

In the special case that there is only one transition with frequency Ω, as discussed above, one has

$$\begin{aligned} \|A_\sigma\|^2 &= \frac{1}{2}\|S\|^2 J(\Omega)\coth(\beta\Omega/2)\left(\sigma 1 + \sqrt{1 + \tanh(\beta\Omega/2)^2}\right), \\ &\simeq \|S\|^2\frac{J(\Omega)}{\beta\Omega}\left(\pm 1 + 1 + \frac{\beta^2\Omega^2}{8}\right). \end{aligned} \tag{3.73}$$

For a generic system in the high temperature limit, we use $G'(\Delta) \simeq \frac{J(\Delta)}{\beta\Delta}$ and find

$$\|A_\sigma\|^2 \simeq \|S\|^2 \frac{\overline{J(\Delta)}}{\beta\Delta}\left(\sigma 1 + \sqrt{1 + \frac{V\left[\frac{J(\Delta)}{\Delta}\right]}{\overline{\frac{J(\Delta)}{\Delta}}^2}}\right), \tag{3.74}$$

with $V[\frac{J(\Delta)}{\Delta}] = V[\gamma] = 0$ for a pure Ohmic bath. In Appendix F, we complete this analysis by taking into account the zero-point fluctuation and thermal noise at high temperature.

Altogether for high temperatures the relative weight of the negative contribution scales as $\|A_-\|^2/\|A_+\|^2 = O(\beta^2)$. Thus, the negative term in the pseudo-Lindblad dissipator tends to zero at high temperatures and can be neglected. As can be seen from Eq. (3.42) with $\mathbb{S} \simeq \gamma/\beta\ S$ and $\lambda_{\min} \simeq \sqrt{\gamma/\beta}$, in the limit of $\beta \to 0$ the Redfield equation approaches a GKSL master equation with a single jump operator $A_+ \simeq \sqrt{2\gamma/\beta}S$.

In summary, we derive an alternative GKSL approximation to the Redfield equation that does not rely on ultraweak system-bath coupling. In the next section, by applying it to an extended Hubbard model, we show that away from equilibrium it provides a good approximation in a large parameter regime, where the quantum-optical master equation fails.

3.6 Multiple baths and non Hermitian coupling

So far, in order to keep the notation simple, we restrict ourselves to open systems that are coupled via one coupling operator to a single heat bath. In the following, we generalize the concepts developed in this chapter to open systems that are coupled to multiple baths. This is relevant for nonequilibrium setups where the system is driven to nonequilibrium steady states. We consider the case where the total Hamiltonian of the system-bath compound reads

$$H_{\text{tot}} = H_{\text{S}} + \sum_\alpha (S_\alpha \otimes B_\alpha + H_{\text{B}\alpha}), \tag{3.75}$$

where α labels independent baths.

Because the total Hamiltonian does not contain any cross terms the baths are uncorrelated, so that $\langle \boldsymbol{B}_\alpha(t) B_{\alpha'}\rangle = \delta_{\alpha,\alpha'} C_\alpha(t)$ and the Redfield equation is obtained by linear combination of the dissipator for each individual α. Consequently the Kossakowski matrix of the Redfield equation can be block-diagonalized for the individual coupling channels α. As a consequence, for the pseudo-Lindblad equation, the jump operators are found for each channel separately,

$$A^\sigma_\alpha = \frac{1}{\sqrt{2\cos\varphi_\alpha}}\left[\sigma\lambda_\alpha e^{-\mathrm{i}\sigma\frac{\varphi_\alpha}{2}}\ S_\alpha + \frac{1}{\lambda_\alpha} e^{\mathrm{i}\sigma\frac{\varphi_\alpha}{2}}\ \mathbb{S}_\alpha\right], \tag{3.76}$$

where $\lambda_\alpha^2 = \|\mathbb{S}_\alpha\|/\|S_\alpha\|$ and $\sin\varphi_\alpha = \operatorname{Im}\operatorname{tr}_{\text{S}}(\mathbb{S}_\alpha S_\alpha)/\|S_\alpha\|\|\mathbb{S}_\alpha\|$ follow from optimization procedure. The optimal parameters minimize the negative relaxation weight for each coupling

operator individually. Finally, in the truncated master equation all negative contributions are neglected.

Such a decomposition also holds for non-hermitian coupling operators $S \neq S^\dagger$ in the system-bath Hamiltonian $H_{\mathrm{SB}} = S \otimes B^\dagger + S^\dagger \otimes B$, with Redfield equation given in (2.41). Essentially one obtains two channels $S_1 = S$ and $S_2 = S^\dagger$ with the distinct convoluted operators,

$$\mathbb{S}_1(t) = \int_0^t \mathrm{d}\tau \left\langle \boldsymbol{B}^\dagger(\tau) B \right\rangle \boldsymbol{S}^\dagger(-\tau), \tag{3.77}$$

$$\mathbb{S}_2(t) = \int_0^t \mathrm{d}\tau \left\langle \boldsymbol{B}(\tau) B^\dagger \right\rangle \boldsymbol{S}(-\tau). \tag{3.78}$$

3.7 Truncated master equation for the extended Hubbard model coupled to a thermal bath

The truncation approach reduces the Redfield equation to GKSL form, for which the dynamics can be solved efficiently by simulating quantum trajectories. This is particularly important for simulating open many-body systems, for which the numerical complexity grows exponentially with the system size. In this section, we test this approach by applying it to an extended Hubbard chain, and find that the truncated master equation provides a better approximation to the Redfield equation than the secular approximation in a large parameter regime, especially in non-equilibrium scenarios. Moreover, combining our approach with quantum-trajectory simulations, we can treat system sizes that we cannot solve by integrating the Redfield equation. The majority of results in this section are published in Ref. [141].

A system of N spinless fermions in a tight-binding chain of length M with nearest-neighbor interaction is described by the extended Hubbard Hamiltonian

$$H_{\mathrm{S}} = -J \sum_{\ell=1}^{M-1} \left(a_\ell^\dagger a_{\ell+1} + a_{\ell+1}^\dagger a_\ell \right) + V \sum_{\ell=1}^{M-1} a_\ell^\dagger a_\ell a_{\ell+1}^\dagger a_{\ell+1}, \tag{3.79}$$

with fermionic creation and annihilation operators $a_\ell^\dagger$ and a_ℓ, respectively, with $a_\ell^\dagger a_{\ell'} + a_{\ell'} a_\ell^\dagger = \delta_{\ell,\ell'}$ and $a_\ell^\dagger a_{\ell'}^\dagger + a_{\ell'}^\dagger a_\ell^\dagger = a_\ell a_{\ell'} + a_{\ell'} a_\ell = 0$. The tunneling parameter J quantifies the kinetic energy of the particles and V is the interaction energy of particles occupying adjacent sites.

$\frac{M!}{(M-N)!\,N!}$	$M=2$	$M=6$	$M=9$	$M=12$	$M=15$	$M=18$	$M=21$
$N=1$	2	6	9	12	15	18	21
$N=\lfloor \frac{M}{3} \rfloor$	2	15	84	495	3 003	18 564	116 280
$N=\lfloor \frac{M}{2} \rfloor$	2	20	126	924	6 435	48 620	352 716

Table 3.1: Hilbert space dimension for a one-dimensional lattice of length M filled with N spinless fermions.

The corresponding Hilbert space is spanned by

$$\dim(\mathcal{H}_{\text{Ferm,1D}}) = \frac{M!}{(M-N)!\,N!} \tag{3.80}$$

Fock states with fixed particle number N. Examples for the Hilbert space dimension for fillings $N/M = 1/3$ and $N/M = 1/2$ are given in Table 3.1.

Despite the vast scaling of the Hilbert space dimension with the system size, a numerical exact diagonalization of the many-body Hamiltonian is still possible for small systems. Assuming each real coefficient in the Hamiltonian as a double precision float requires 4 B (bytes) in memory, a system of length $M = 18$ at half filling allocates ≈ 10 GB of memory and is no limitation for modern desktop computers. For comparison, a chain of length $M = 21$ would need approximately 500 GB, showing that exact diagonalization schemes for larger systems become challenging.[6]

3.7.1 Equilibrium steady state

The system shall be coupled to a local heat bath at temperature T via the density $S = a_1^\dagger a_1$ in the system-bath Hamiltonian $H_{\text{SB}} = \sqrt{\gamma} a_1^\dagger a_1 \otimes B$ schematically depicted in Fig. 3.5. Here, the coupling strength γ is dimensionless and comprises the system-bath coupling strength relative to the energy scales in the system given by the tunneling parameter J in Eq. (3.79). The interaction is modelled with the Drude spectral density $J(\Delta) = \gamma\Delta/(1 + \Delta^2/\omega_D^2)$. For a bath that couples globally to all sites, similar results are found as outlined in the section below. In order to quantify the deviation of the quantum-optical master equation and the truncated master equation from the Redfield result, we introduce the trace distance as error measure

[6] Since the interaction in the many-body Hamiltonian is short ranged, the number of Fock states to which each Fock state is coupled scales polynomial in the system size. Therefore, the matrix representation in the Fock basis is a sparse matrix, for which the memory allocation is moderate [147]. Saving H requires $\sim \dim(\mathcal{H}_{\text{Ferm,1D}})\, M$ numbers. However, density operators represented in the Fock basis are typically not sparse.

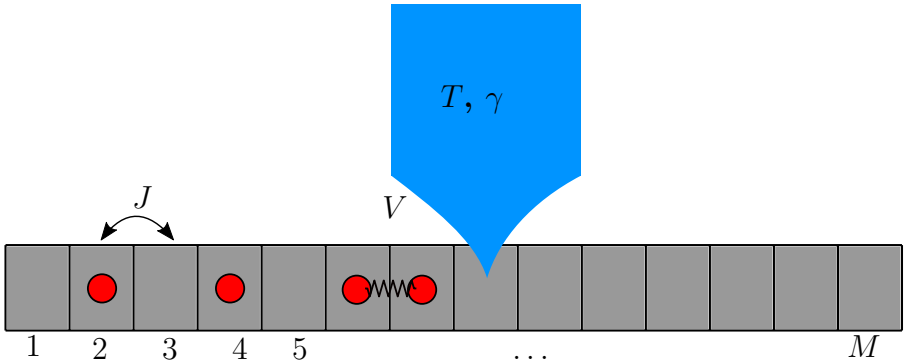

Figure 3.5: Illustration of extended Hubbard model in one dimension with M lattice sites, tunnelling J and nearest neighbour interaction V. A thermal bath of temperature T is couples locally with coupling strength γ to a single site of the chain.

[148, 149],

$$\mathrm{dist}(\varrho^{\mathrm{X}}, \varrho^{\mathrm{Red}}) = \frac{1}{2}\,\mathrm{tr_S}\,\sqrt{(\varrho^{\mathrm{X}} - \varrho^{\mathrm{Red}})^2} \in [0, 1], \tag{3.81}$$

which is bounded from above by one and where ϱ^{X} with $X = \mathrm{Lind}$ or $X = \mathrm{trunc}$ is the steady-state of either the quantum-optical master equation or the truncated master equation, respectively. To keep the notation simple the term *Lindblad* in the figures refers to the quantum-optical master equation. The steady state is found by spectral decomposition of the master equation and is identified with the eigenvector corresponding to the eigenvalue zero. For the simulations, routines of the QuTiP library [150] are used.

In Fig. 3.6, we plot the equilibrium (i.e. steady-state) error measures as a function of coupling strength γ and temperature T/J. For fixed temperature $T/J = 5.43$ and in the weak coupling regime, the error of the quantum-optical master equation scales linear with γ [Fig. 3.6(ii)], whereas the error of the truncation is smaller and of higher order [Fig. 3.6(iii)]. Also, the result of the truncated master equation shows good agreement for large temperatures. For fixed coupling strength $\gamma = 0.19$, in Fig. 3.6(i), we can see that $\mathrm{dist}(\varrho^{\mathrm{trunc}}, \varrho^{\mathrm{Red}})$ (solid red line)

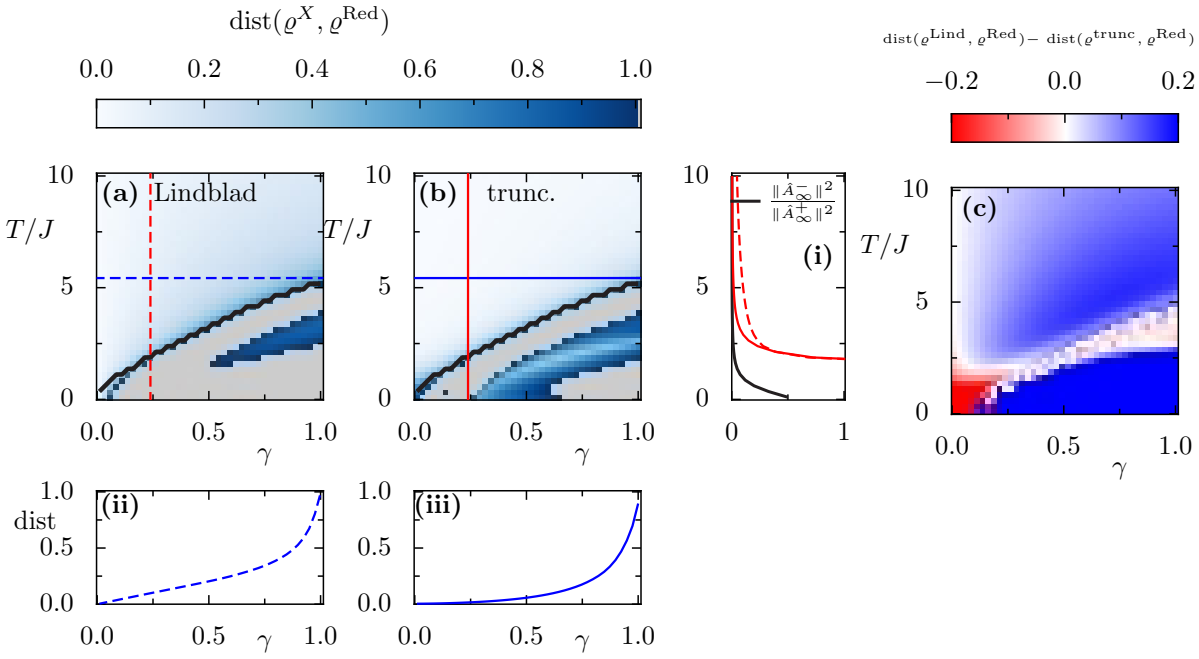

Figure 3.6: Equilibrium error, $\mathrm{dist}(\varrho^{X}, \varrho^{\mathrm{Red}})$, of the quantum optical (a) and of the truncated master equation (b) as a function of the coupling strength γ and bath temperature T/J for the steady state. The smaller panels (i)-(iii) show cuts for fixed $\gamma = 0.19$ [(ii), (iii), along the vertical blue lines in (a) and (b)] and fixed $T/J = 5.43$ [(i) along the horizontal red lines in (a) and (b)]. To the right of the wiggly black line in (a) and (b) the Redfield steady state acquires negative populations and yields errors larger than 1 [grey]. In (c) we plot the difference $\mathrm{dist}(\varrho^{\mathrm{Lind}}, \varrho^{\mathrm{Red}}) - \mathrm{dist}(\varrho^{\mathrm{trunc}}, \varrho^{\mathrm{Red}})$. The parameters are $l = 8$, $N = 4$, $V = 2\,J$, $\omega_D = 17\,J$.

decays rapidly with temperature, like $\|A_-\|^2\|A_+\|^2$ (black solid line), whereas $\mathrm{dist}(\varrho^{\mathrm{trunc}}, \varrho^{\mathrm{Red}})$ decays much slower. From the difference $\mathrm{dist}(\varrho^{\mathrm{Lind}}, \varrho^{\mathrm{Red}}) - \mathrm{dist}(\varrho^{\mathrm{trunc}}, \varrho^{\mathrm{Red}})$, in Fig. 3.6(c), it is evident that the steady-state solution of the truncated master equation is in better agreement with the Redfield result than the quantum-optical master equation for all parameters, except for very weak coupling and low temperatures.

Note that this is also the regime in which the Redfield steady state acquires unphysical negative probabilities as marked by the grey colour in Fig. 3.6(a) and Fig. 3.6(b). This is a known problem of the Redfield formalism [38, 45, 46, 39]. Namely, for low temperatures the bath correlation time becomes large compared to the coupling strength for which the Born-Markov approximation no longer holds [151]. This is in accordance with our analysis that for low temperatures the weight of the negative contribution in the pseudo-Lindblad dissipator grows significantly causing the Redfield steady-state to have negative populations. This is corroborated by our previous discussion about the positivity condition of the damped harmonic oscillator in Section 2.6.1

3.7.2 Transient dynamics

Let us now study the relaxation dynamics of the open quantum system initialized in $\varrho(t = 0) = |\psi\rangle\langle\psi|$ with $|\psi\rangle = \frac{|0\rangle+|1\rangle}{\sqrt{2}}$ being the coherent superposition of the ground state $|0\rangle$ and first excited state $|1\rangle$, with $H_{\mathrm{S}}|k\rangle = E_k|k\rangle$. For coupling strength $\gamma = 0.2$ and temperature $T = 5J$ in Fig. 3.7, we plot the dynamics for the real part of $\langle 0|\varrho(t)|1\rangle$ under the Redfield, truncated, and quantum-optical (Lindblad) master equations. For a complete parameter scan, we eva-

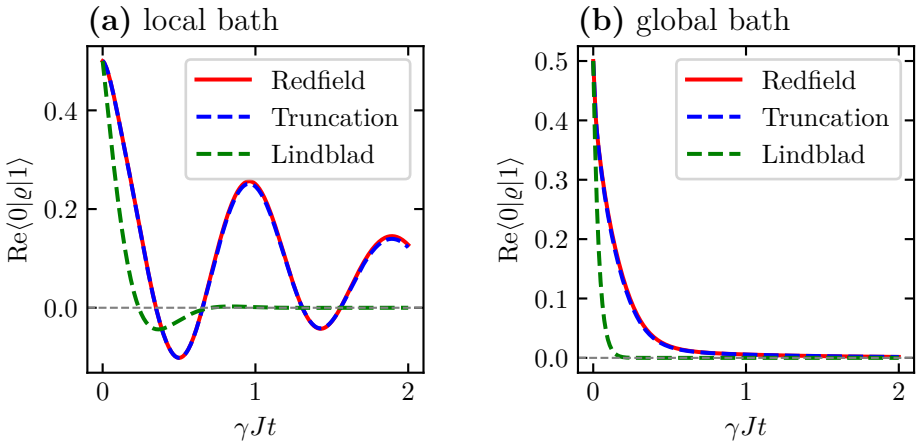

Figure 3.7: Transient dynamics for the density matrix element $\langle 0|\varrho(t)|1\rangle$ under the Redfield, truncated, and quantum-optical master equations in solid red, dashed blue, and dashed green, respectively. The initial state is $\varrho(t = 0) = |\psi\rangle\langle\psi|$ with $\psi = (|0\rangle + |1\rangle)/\sqrt{2}$. The parameters are $\gamma = 0.2$ and $T = 5J$. In (a) for a local bath with coupling operator $S = a_1^\dagger a_1$ and Drude cutoff $\omega_D = 17J$. In (b) for a global bath with multiple coupling operators $S_\ell = a_\ell^\dagger a_\ell$ with $\ell = 1, \ldots, M$ and Drude cutoff $\omega_D = 40J$.

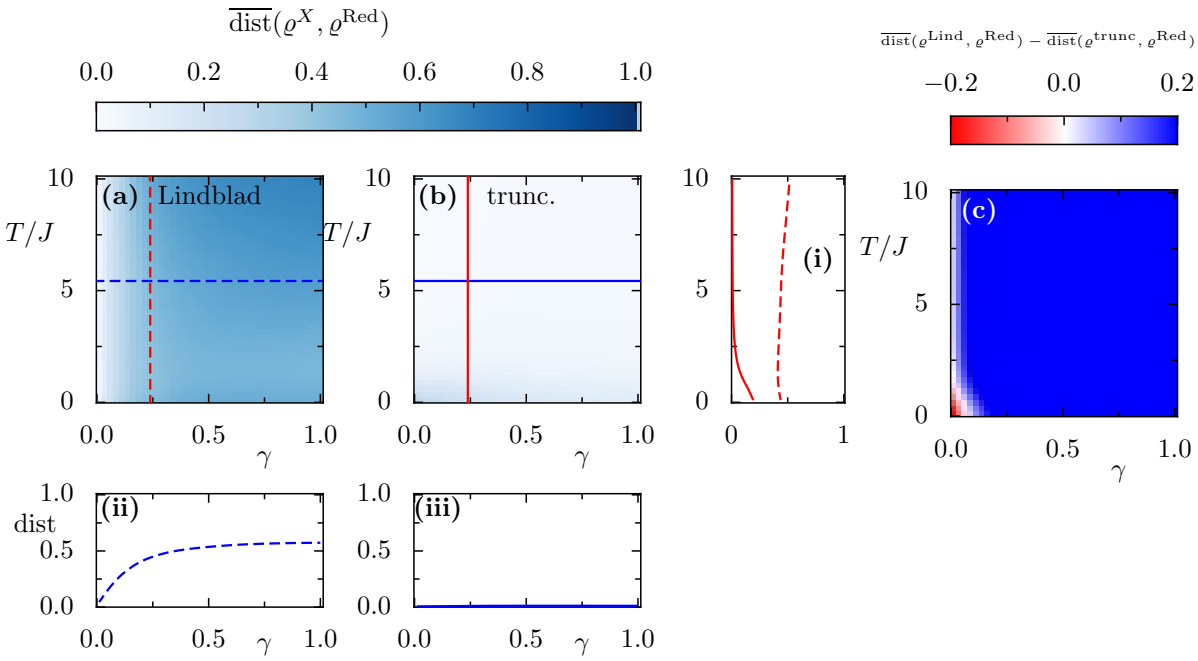

Figure 3.8: Same as Fig. 3.6 for dynamics, where distance measure is averaged over the transient with averaging time $\tau_{\text{R}} = (2/\gamma)J$.

luate the error for the transient dynamics by introducing the time averaged distance measure $\overline{\text{dist}}(\varrho^X, \varrho^{\text{Red}}) = (1/\tau_{\text{R}}) \int_0^{\tau_{\text{R}}} \text{dist}(\varrho^X(t), \varrho^{\text{Red}}(t))dt$, where we obtain the time-dependent solutions by direct integration of the particular master equation. We aim at choosing the time window $[0, \tau_{\text{R}}]$ big enough to cover the transient regime but small enough not to capture the steady-state properties. Since under the quantum-optical master equation the state thermalizes on an exponentially short time scale with respect to the coupling strength, as is also depicted in Fig. 3.7(a), here, we choose $\tau_{\text{R}} = (2/\gamma)J$.

The quantum-optical master equation provides a poor prediction of the transient dynamics [Fig. 3.8(a)]. A large error of 0.5 is reached already for very small coupling $\gamma \simeq 0.3$ [Fig. 3.8(ii)]. For short times, neglecting non-resonant terms with $\Delta_{qk} \neq \Delta_{q'k'}$ in the rotating-wave approximation overestimates the relaxation [152]. Here the truncation method [Fig. 3.8(b)] clearly outperforms the quantum-optical master equation. For all parameters, except a small regime for $T/J \leq 1$ and $\gamma \leq 0.07$, the time averaged error for the truncated master equation is not only smaller than the one in the quantum-optical master equation [Fig. 3.6(c)], but also very close to zero [Fig. 3.8(iii), Fig. 3.8(i) solid red].

3.7.3 Globally coupled bath

The coupling operator S of the system-bath interaction H_{SB} defines the way in which the bath is coupled to the system. Local coupling operators are most relevant for transport properties, where the baths couple to the edges of a system. In this section, we briefly discuss the case

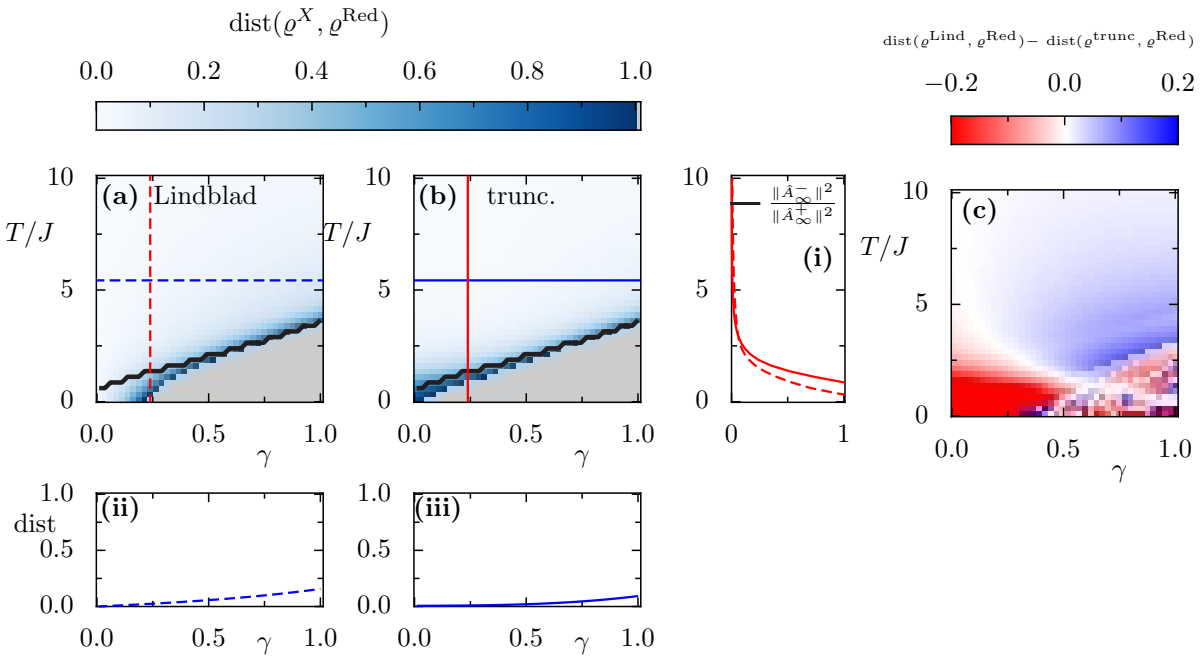

Figure 3.9: Equilibrium error of the quantum optical (Lindblad) and truncated master equation analogous to Fig. 3.6, except for bath that couples globally to the system. The parameters are $l = 8$, $N = 4$, $V = 2\,J$, $\omega_D = 40\,J$.

when the system couples globally to its environment.

For models, where the coupling operator itself is a global quantity, e.g., for the damped harmonic oscillator, all the previous expressions hold. However, in particular, for the extended Hubbard model the coupling operator $S = \sum_{\ell=1}^{M} n_\ell = N\mathbb{1}$, is not a sensible choice because it yields the conserved total particle number. Instead, one has to consider a system-bath interaction Hamiltonian that consists of several coupling terms. We choose $S_\alpha = n_\alpha$ where the index α labels independent baths of the same temperature. In Fig. 3.9, we repeat the analysis of the local bath in Fig. 3.6 but for a bath that couples globally to the system rather than to a single site only. We choose the cutoff $\omega_D = 40J$, as compared to $\omega_D = 17J$ for the local bath. For high temperatures, this does not affect the results since the variances in Fig. 3.3(f) are very small. However, the variances in the low temperature regime are much larger, see Fig. 3.3(c), so that we obtain a more profound difference between low and high temperature regime.

Here the trace distance to the full Redfield result in Eq. (3.81) again serves as an error measure for the quantum-optical master equation and the truncated master equation, respectively. As compared to a bath that only couples locally, here the damping dominates the coherent dynamics. The relaxation time becomes shorter as shown in Fig. 3.7(b) and, therefore, we compute the time averaged distance measure in Fig. 3.10 for $\tau_{\mathrm{R}} = (1/\gamma)J$ (as compared to $\tau_{\mathrm{R}} = (2/\gamma)J$, which was used for the local bath). The initial state is a coherent superposition of the ground state and first the excited state.

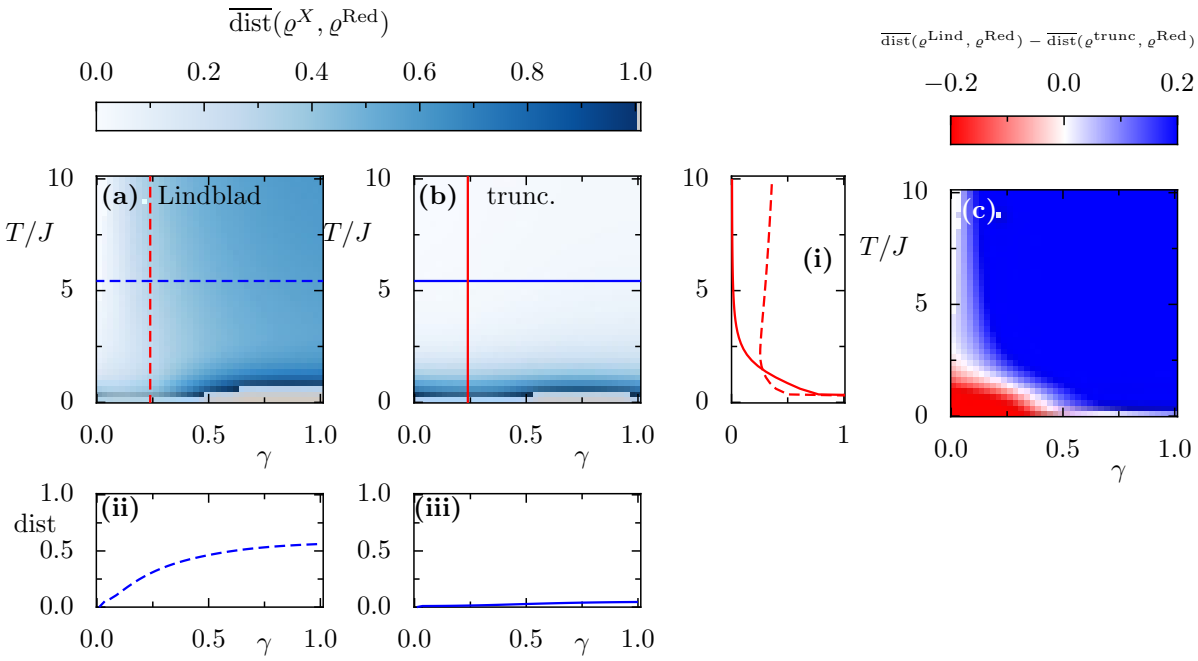

Figure 3.10: Same as Fig. 3.9 except for dynamics, where distance measure is averaged over the transient with averaging time $\tau_{\mathrm{R}} = (1/\gamma)J$.

By looking at the relative errors in Figs. 3.9 and 3.10(c), it is evident that for weak coupling and low temperature the quantum-optical master equation performs better, whereas for finite coupling and higher bath temperature the truncated master equation is favourable. In summary, the case of a global bath is qualitatively similar to the case of a local bath.

3.8 Importance of the minimization procedure

Above, in Section 3.4, we find the parameters $\lambda^2_{\mathrm{min}} = \|\mathbb{S}\|/\|S\|$ and $\sin\varphi_{\mathrm{min}} = \mathrm{Im}\,\mathrm{tr}_{\mathrm{S}}(\mathbb{S}S)/(\|\mathbb{S}\|\|S\|)$ that minimize the negative weight of the pseudo-Lindblad dissipator, which are optimal for truncating the negative contribution. In general, for a different choice of parameters, truncating the negative contribution is a much worse approximation. In this section, we compare the optimal truncated master equation with the different choice $\varphi = 0$ and $\lambda^2 = J$, where J is the tunneling amplitude between adjacent sites of the chain.

To begin with, we motivate the different choice of the parameters. For the optimal phase, note that $\sin\varphi_{\mathrm{min}} \propto \mathrm{Im}\,\mathrm{tr}(\mathbb{S}S) \propto \overline{G_0''}$ [Eq. (3.55)], with $G_0''(\Delta)$ being the zero-point fluctuation. For a large cutoff, the average of the zero-point fluctuation vanishes [Eq. (2.24)] and, thus, the optimal phase reduces to $\varphi_{\mathrm{min}} = 0$.

The rescaling parameter λ, for which λ^{-2} carries the dimension of time, defines a new timescale of the master equation. The optimization procedure shows that the timescale is related to the average of the coupling density. On the contrary, the alternative choice $\lambda^2 = J$ relates it to

the typical time scale of the system, which turns out not to be a good choice.

In Fig. 3.11, we depict the dynamics of the truncated master equation with optimized $\lambda^2_{\text{min}} = \|\mathbb{S}\|/\|S\|$ in blue and for $\lambda^2 = J$ in thin grey. The result of the truncated master equation is in very good agreement with the Redfield result in red, since the relative weight of the negative contribution is small. This holds both for the populations in Fig. 3.11(a) and for the coherence in Fig. 3.11(b) and also the error measure is particularly small, see Fig. 3.11(c). In contrast, the choice of $\lambda_t^2 = J$ leads to significant deviations especially for the populations in (a) but also for the coherences in (b). Interestingly, the error is still of the same order as that for the quantum-optical master equation [Fig. 3.11(c)].

We can explain our observation further by evaluating the weight of the negative contribution for the choice of $\lambda^2 = J$. It follows from Eq. (3.45) that

$$\|A_-\|^2 = \frac{\|S\|^2}{2}\left[J - 2\overline{G'} + \frac{\overline{G'^2} + \overline{G''^2}}{J^2}\right], \tag{3.82}$$

which for ultraweak coupling, by letting $G' = G'' = 0$, reduces to the finite value of $\|A_-\|^2 = \|S\|^2 J/2$ independent of the bath parameters. Since J is the typical energy scale of the system, this does not correspond to a small value. This explains the bad performance of the new choice.

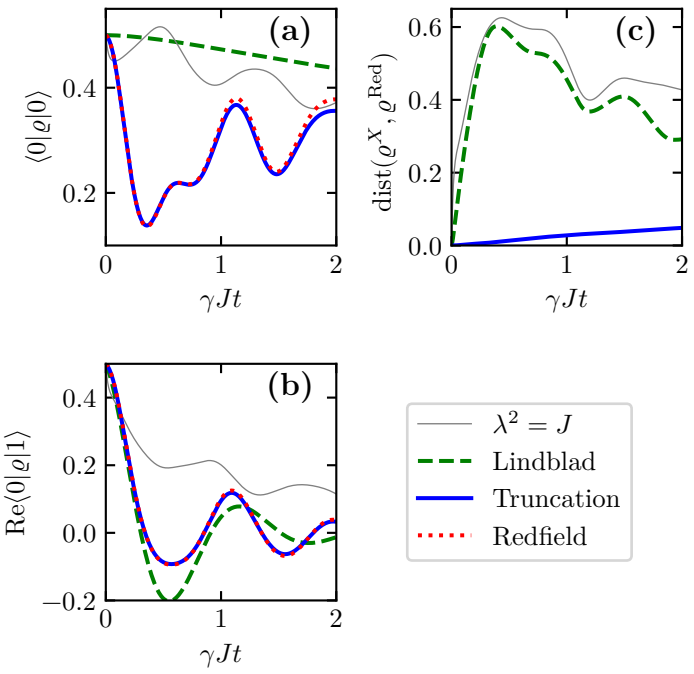

Figure 3.11: Relevance of the optimization. Dynamics for the different master equations, i.e., populations in (a), coherences in (b) and trace distance to the Redfield result in (c). The bath couples to the first site of the chain and the parameters are $l = 5$, $N = 2$, $V = 2J$, $\omega_D = 17J$, $\gamma = 0.2$ and $T = 2J$.

Thus, a reasonable choice for the parameter λ^2 is generally not given by the typical timescale of the system. The optimal value of λ is instead determined by the timescale that is related to the amplitude of the bath correlation function.

3.9 Application to a boundary driven system

By coupling a system to several heat baths of different temperature it becomes driven dissipative and approaches a nonequilibrium steady state. The understanding and control of such driven-dissipative systems is of fundamental interest for many applications, such as the description of transport beyond linear response or the controlled preparation of nonequilibrium steady states [1–3, 5–7]. Beyond ultraweak coupling the theoretical description becomes extremely challenging. In this section, we examine properties of the nonequilibrium steady-state of the driven-dissipative system, focusing on parameters, where the quantum-optical master equation is known to be an inadequate description [61].

The system is driven by two local baths at different temperatures $T_L < T_R$ that couple to the occupations $S_1 = a_1^\dagger a_1$ (left) and $S_2 = a_M^\dagger a_M$ (right) of the outermost sites of the chain, respectively [Fig. 3.12].

In Fig. 3.13, the particle imbalance

$$\Delta N = N_L - N_R, \tag{3.83}$$

in the nonequilibrium steady-state is shown, where $N_L = \sum_{\ell<M/2} \langle n_\ell \rangle$ and $N_R = \sum_{\ell>M/2} \langle n_\ell \rangle$ count the particles on the left and right half of the chain, respectively.

According to the thermoelectric effect [153] a larger particle mobility near to the hotter, right reservoir is expected, increasing the particle density on the left side of the chain, i.e., $\Delta N > 0$. However, this behavior is not captured correctly by the quantum-optical master equation. Just as in equilibrium, the off-diagonal elements of the density matrix decay and the steady-state is diagonal in the eigenbasis of H_S. Since the eigenstates reflect the symmetry of the system, which has no preferred orientation, the nonequilibrium steady-state of the quantum-optical master equation localizes evenly among the left and right half of the chain [Fig. 3.13(a) dashed

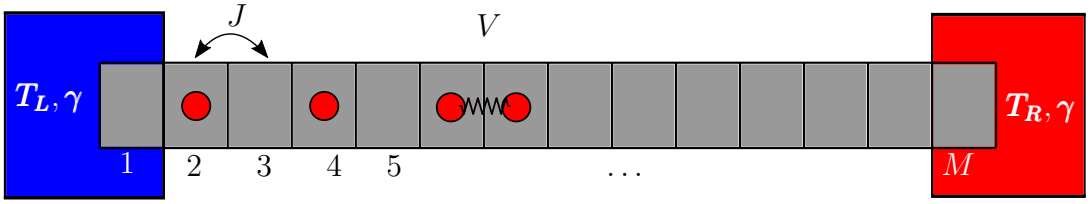

Figure 3.12: Illustration of extended Hubbard model in one dimension with M lattice sites, tunnelling J and nearest neighbour interaction V. Two thermal baths of different temperature couple to the edges of the system, i.e., on the leftmost and the rightmost lattice site, respectively.

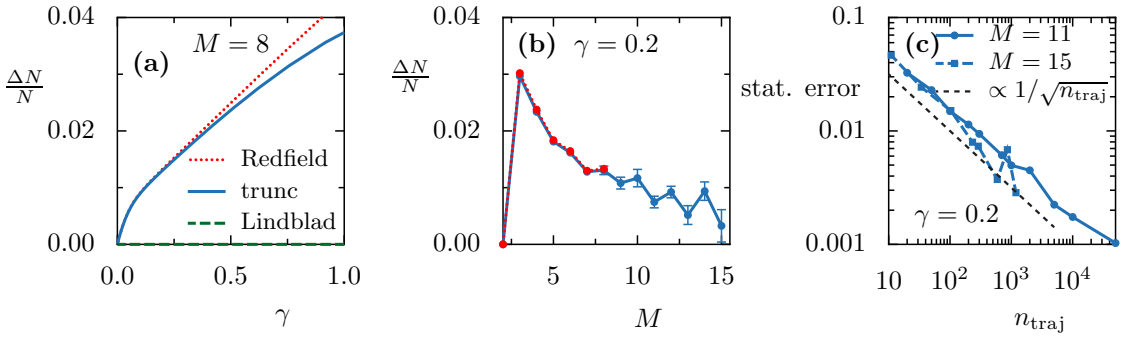

Figure 3.13: Particle imbalance Eq. (3.83) for nonequilibrium steady-state for $N = \lfloor M/2 \rfloor$ $V = 2J$, $\omega_D = 17J$, $T_L = 7J$, $T_R = 13J$. In (a) as a function of coupling strength γ for fixed $M = 8$ and in (b) as a function of M for fixed $\gamma = 0.2$. For system sizes $M \leq 8$, the steady state is calculated as eigenvector to eigenvalue zero (Redfield in dotted red, truncated master equation in solid blue, quantum-optical master equation (Lindblad) (in dashed green). For $M \geq 8$, the truncated master equation is solved by quantum-trajectory simulations. Averages taken over $5 \cdot 10^4$, 10^4, $6 \cdot 10^3$ and 10^3 trajectories for $M = 8 - 11$, $M = 12, 13$, $M = 14$ and $M = 15$, respectively. Panel (c) shows the statistical error as a function of the number of trajectories for $M = 11$ and $M = 15$ at fixed $\gamma = 0.2$. Lines are guides to the eye.

green].

For finite coupling, this parity is broken and finite off-diagonal matrix elements of the nonequilibrium steady-state give rise to a non-zero particle imbalance. This effect is captured by the truncated master equation [Fig. 3.13(a)]. Furthermore, its GKSL-form allows the use of quantum-trajectory simulations [51]. This is beneficial especially for many body systems, for which the Hilbert space dimension grows exponentially with the system size. Thus, the truncated master equation allows to study larger systems that are hardly accessible by direct integration of the Redfield equation [Fig. 3.13(b) dotted red] and the statistical error decays with one over the square root of the number of trajectories [Fig. 3.13(c)].

3.10 Dissipative flow in nonequilibrium steady states

Another interesting application of the truncated master equation is quantum thermodynamics, which has gained significant attention in recent years, e.g. Refs. [125, 124, 61, 154, 155, 88, 156, 157, 116, 158, 159]. For ultraweak system-bath coupling, thermodynamics is usually described in equilibrium using the concepts of statistical mechanics. However, far from equilibrium and beyond the regime of ultraweak coupling, the theoretical description of quantum thermodynamics is a controversial issue. One approach is to start from a thermal state of system and bath together and deduce a reduced Hamiltonian for the open system [124, 125]. This is briefly discussed in Appendix B. Other approaches define quantities such as heat and work from the perspective of the reduced system, e.g., in Ref. [61, 116] or by extending the system by bath degrees of freedom using the reaction-coordinate mapping [88, 159].

Motivated by the definition in Ref. [116], in this section, we study the expectation value

$$\langle H_{\mathrm{S}} + H_{\mathrm{LS}} \rangle = \mathrm{tr}_{\mathrm{S}} \left((H_{\mathrm{S}} + H_{\mathrm{LS}}) \varrho(t) \right) , \tag{3.84}$$

of the system Hamiltonian renormalized by the Lamb-shift Hamiltonian H_{LS} in Eq. (3.15) for the Redfield equation and in Eq. (2.53) for the quantum-optical master equation. As pointed out in Section 3.2 for master equations the Lamb-shift Hamiltonian H_{LS} is not uniquely defined. In Ref. [116], the authors study a similar quantity, however, with a different H_{LS} that minimizes the dissipation.

By taking the time-derivative, we define

$$I[\varrho(t)] \equiv \partial_t \langle H_{\mathrm{S}} + H_{\mathrm{LS}} \rangle , \tag{3.85}$$

which we refer to as *net dissipative flow*. To interpret the quantity, note that the general balance equation for energy in the total system-bath compound is given by $\partial_t \, \mathrm{tr}_{\mathrm{tot}}((H_{\mathrm{S}} + H_{\mathrm{SB}} + H_{\mathrm{B}}) \varrho_{\mathrm{tot}}(t)) = 0$. In the limit of ultraweak coupling, the interaction energy can be neglected and the net dissipative flow quantifies the energy that is exchanged between system and bath.

In this section, we study the net dissipative flow for the perturbative master equations in Sections 2.4, 2.5 and 3.5, which takes the form

$$I^{\mathrm{X}}[\varrho(t)] = \mathrm{tr}_{\mathrm{S}} \left((H_{\mathrm{S}} + H_{\mathrm{LS}}) \mathcal{D}^{\mathrm{X}}[\varrho(t)] \right) , \tag{3.86}$$

where the coherent contribution of the master equation $\mathrm{tr}_{\mathrm{S}}((H_{\mathrm{S}} + H_{\mathrm{LS}})[(H_{\mathrm{S}} + H_{\mathrm{LS}}), \varrho(t)]) = 0$ does not contribute. Here, it is $X = \mathrm{Redfield}, \mathrm{RWA}, \mathrm{trunc.}$, which stands for the dissipator of the Redfield, quantum optical (in RWA) or the truncated master equation, respectively. For

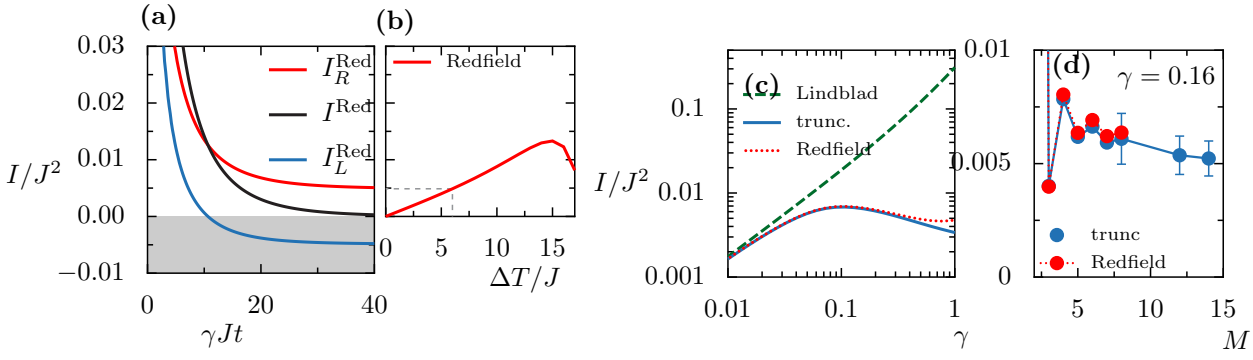

Figure 3.14: Dissipative flows I_L, I_R and net dissipative flow $I = I_L + I_R$. In (a) transient dynamics for initial ground state. In (b) dissipative flow in Redfield steady-state as a function of the temperature difference $\Delta T = T_R - T_L$ at fixed mean temperature $T_L + T_R = 20\,J$. In (c) and (d) steady-state dissipative flow as a function of coupling strength γ and system size M, respectively. Up to variation the parameters are $M = 8$, $N = 4$, $V = 2\,J$, $\gamma = 0.16$, $T_{L(R)} = 7(13)\,J$ and $\omega_D = 17\,J$. Lines to guide the eye.

the boundary driven setup, in Fig. 3.12, the dissipator is the sum $\mathcal{D}^{\mathrm{X}} = \mathcal{D}^{\mathrm{X}}_L + \mathcal{D}^{\mathrm{X}}_R$ for the left and right bath, respectively. Consequently

$$I[\varrho(t)] = I_L[\varrho(t)] + I_R[\varrho(t)] \tag{3.87}$$

is the net flow resulting from the dissipative flows of the individual baths.

For the Redfield equation, the dynamics for dissipative flows is plotted in Fig. 3.14(a) for the model depicted in Fig. 3.12. The physical dimension of the dissipative flow is energy over time, which is measured in units of J^2. In the nonequilibrium steady state, $\partial_t \varrho(t)\big|_{\varrho(t)=\varrho_{ss}} = 0$, it follows that $I_R = -I_L$ which describes a stationary flow through the system. If the temperature difference between the baths is low, this stationary flow grows linearly with the temperature bias ΔT [Fig. 3.14(b)].

Within the zero-coupling limit of the quantum-optical master equation the dissipative flow can be identified with the rate, under which quanta of energy Δ_{qk} are exchanged between system and bath, i.e., $I_L^{\mathrm{RWA}}[\varrho_{\mathrm{ss}}^{\mathrm{RWA}}] = \sum_{qk}(\Delta_{qk} + \omega_q^{\mathrm{LS}} - \omega_k^{\mathrm{LS}})R_{qk}p_k$, which is easily obtained from $\langle q|H_{\mathrm{S}} + H_{\mathrm{LS}}|n\rangle = (E_q + \omega_q^{\mathrm{LS}})\delta_{qn}$ and the Pauli rate equation $\langle q|\mathcal{D}^{\mathrm{RWA}}[\varrho_{\mathrm{ss}}^{\mathrm{RWA}}]|q\rangle$ for the populations $p_k = \langle k|\varrho_{\mathrm{ss}}^{\mathrm{RWA}}|k\rangle$ with rates R_{qk} [6, 160] [cf. Eqs. (2.52) and (2.63)]. The steady-state populations of the quantum-optical master equation are independent of the coupling strength. Thus, the dissipative flow scales linearly with the coupling strength γ as shown in Fig. 3.14(c). However, the Redfield result has a non-trivial dependence on the coupling strength γ and gives rise to a non-monotonic behaviour of the dissipative flow in Fig. 3.14(c). The truncated master equation accurately reproduces the Redfield result beyond ultraweak coupling [solid blue line in Fig. 3.14(c)]. Furthermore, since the truncated master equation is of GKSL form, we can unravel the dynamics efficiently by quantum trajectories. For the Redfield equation, we are not able to calculate the dissipative flow in the nonequilibrium steady state for system sizes of $M > 8$, whereas for the truncated master equation $M = 15$ was still possible. This is shown in Fig. 3.14(d), where the error bars indicate the statistical fluctuations for approximately 100 000 trajectories.

3.11 Truncation of the exact Hu-Paz-Zhang master equation

The damped harmonic oscillator is a paradigmatic example of an open quantum system as it is one of the few exactly solvable systems [86, 111, 113, 128]. In the high-temperature regime, it is described by Brownian motion, which is captured by a GKSL master equation [21]. However, there is no corresponding equation of motion for general systems.

In this section, we make the connection between the exact Hu-Paz-Zhang master equation discussed in Section 2.6 and the equation of Brownian motion by making use of the truncation

approach developed in the previous sections.

The Caldeira-Leggett master equation (2.77), with arbitrary coefficients $\gamma_q(t)$, $\gamma_p(t)$, $D_q(t)$, $D_p(t)$, is quadratic in the displacement q and momentum p. By identifying the Hermitian conjugated terms, it can be brought to Redfield form

$$\partial_t \varrho(t) = -\mathrm{i}\left[\frac{p^2}{2M} + \frac{M\gamma_q(t)}{2}q^2,\ \varrho(t)\right] + \left(\mathbb{S}^{\mathrm{HPZ}}\varrho(t)\, q - q\,\mathbb{S}^{\mathrm{HPZ}}\varrho(t) + \mathrm{H.c.}\right), \tag{3.88}$$

with $S = q$ and

$$\mathbb{S}^{\mathrm{HPZ}} \equiv M^2 D_p(t)\, q + \left(\mathrm{i}\frac{\gamma_p(t)}{2} - M D_q(t)\right) p, \tag{3.89}$$

playing the role of the convoluted operator as in the Redfield equation (2.42). In the form of (3.88), it is obvious that the Caldeira-Leggett master equation is hermiticity-preserving and trace-preserving.

Depending on the detailed choice of the coefficients $\gamma_p(t)$, $\gamma_q(t)$, $D_q(t)$, $D_p(t)$, the master equation (3.88) above might either be the second-order Redfield equation, the exact Hu-Paz-Zhang equation or some phenomenological master equation [131]. This shows that the algebraic structure of the Caldeira-Leggett master equation is equivalent to the Redfield equation. Therefore, it can equivalently be written as a pseudo-Lindblad equation with Lamb-shift Hamiltonian

$$H_{\mathrm{LS}}^{\mathrm{HPZ}} = \frac{q\mathbb{S}^{\mathrm{HPZ}} - \mathbb{S}^{\mathrm{HPZ}\dagger}q}{2\mathrm{i}} = \frac{\gamma_p(t)}{4}\{q,\, p\} - \frac{M D_q(t)}{2\mathrm{i}}[q,\, p], \tag{3.90}$$

where due to $[q, p] = \mathrm{i}\mathbb{1}$, the diffusive parameter $D_q(t)$ gives a constant off-set and might be absorbed in an overall energy shift. The jump operators are given by Eq. (3.42),

$$A_\sigma^{\mathrm{HPZ}} = \frac{1/\lambda}{\sqrt{2\cos\varphi}}\Big[\left(\sigma\lambda^2 e^{-\mathrm{i}\sigma\varphi} + M^2 D_p(t)\right) q + \left(\mathrm{i}\frac{\gamma_p(t)}{2} - M D_q(t)\right) p\Big], \tag{3.91}$$

where the irrelevant overall phase factor $e^{\mathrm{i}\sigma\frac{\varphi}{2}}$ is omitted. In Ref. [21], a GKSL generator for the Hu-Paz-Zhang master equation is found by addition of a term that is small in the high-temperature limit. Here, in the pseudo-Lindblad representation, we arrive at the same generator by truncating the negative contribution. To arrive at the result of Ref. [21] the choice for the free parameters would be

$$\varphi \to 0, \qquad \lambda^2 \to M^2 D_p(t), \tag{3.92}$$

for which the first term in the jump operator either adds up for A_+^{HPZ} or cancels for A_-^{HPZ}, respectively. This is already a generalization to the result of Ref. [21] for arbitrary (possibly exact), time-dependent coefficients $\gamma_p(t)$, $D_q(t)$ and $D_p(t)$. For the static limit, and high-

temperature, and weak coupling, and large cutoff frequency, one obtains

$$\begin{aligned} \gamma_q &\simeq \Omega^2, \\ \gamma_p &\simeq \gamma, \\ D_q &\simeq 0, \\ D_p &\simeq \frac{\gamma}{M\beta}, \end{aligned} \tag{3.93}$$

which can be derived from the second-order Redfield coefficients Eqs. (2.79) to (2.81), and which is often referred to as quantum Brownian motion or classical limit in Ref. [111]. Neglecting the principle-value integrals in the Redfield theory leads to the same expressions for $\gamma_q^{(2)} = D_q^{(2)} = 0$, which is usually referred to as the pure Ohmic approximation. With these coefficients one arrives at the result of Ref. [21][7]

$$A_+^{\mathrm{HPZ}} \simeq \sqrt{\frac{\gamma}{2}}\left[\sqrt{\frac{4M}{\beta}}q + \mathrm{i}\sqrt{\frac{\beta}{4M}}p\right]. \tag{3.94}$$

At small, but finite inverse temperatures β, the truncated negative jump operator reads

$$A_-^{\mathrm{HPZ}} \simeq \mathrm{i}\sqrt{\frac{\gamma}{2}}\sqrt{\frac{\beta}{4M}}p. \tag{3.95}$$

Using the results obtained above, we can now show that the parameters (3.92), which describe the result of Ref. [21], become optimal in the high-temperature limit of Brownian motion. Moreover, we can generalize (or improve) the result of Ref. [21] by minimizing $\|A_-^{\mathrm{HPZ}}\|$ also beyond this limit.

In principle, the Hilbert space of the harmonic oscillator is infinite dimensional, such that the norm of the displacement and momentum is not well-defined. However, the state space can be truncated at an energy that is large compared to both the initial energy of the system and the temperature of the environment. As a consequence of the truncation, one has a finite-dimensional state space, so that the commutator of two operators is always traceless. This breaks the commutation relations of bosonic operators for states close to the truncation. Namely, in a finite dimensional Hilbert space with cutoff D, the product of the bosonic

[7] The expression for the jump operator of quantum Brownian motion differs from the expressions in Ref. [21] by an overall factor of $\sqrt{1/2}$, which can be absorbed by redefining the coupling strength γ.

operators in the energy basis is,

$$(aa^\dagger)_{nm} = \begin{pmatrix} 1 & 0 & \cdots & 0 & 0 \\ 0 & 2 & \cdots & 0 & 0 \\ \vdots & \vdots & \ddots & \vdots & \vdots \\ 0 & 0 & \cdots & D-1 & 0 \\ 0 & 0 & \cdots & 0 & 0 \end{pmatrix}, \tag{3.96}$$

and

$$(a^\dagger a)_{nm} = \begin{pmatrix} 0 & 0 & \cdots & 0 & 0 \\ 0 & 1 & \cdots & 0 & 0 \\ \vdots & \vdots & \ddots & \vdots & \vdots \\ 0 & 0 & \cdots & D-2 & 0 \\ 0 & 0 & \cdots & 0 & D-1 \end{pmatrix}, \tag{3.97}$$

so that $[a, a^\dagger] \neq 1$, i.e.,

$$([a, a^\dagger])_{nm} = \begin{pmatrix} 1 & 0 & \cdots & 0 & 0 \\ 0 & 1 & \cdots & 0 & 0 \\ \vdots & \vdots & \ddots & \vdots & \vdots \\ 0 & 0 & \cdots & 1 & 0 \\ 0 & 0 & \cdots & 0 & 1-D \end{pmatrix} \neq \delta_{nm}, \tag{3.98}$$

giving $\operatorname{tr}[a, a^\dagger] = 0$.

A truncation of the state space is always required for numerical implementation of the system. Here, it allows us to apply the optimization procedure of Section 3.4. For the norm of the jump operators, one obtains

$$\begin{aligned} \|A_\sigma^{\mathrm{HPZ}}\|^2 = \frac{1/\lambda^2}{2\cos\varphi}\Big[&\left(\lambda^4 + \sigma\lambda^2 M^2 D_p(t) 2\cos\varphi + M^4 D_p(t)^2\right)\|q\|^2 \\ &+ \left(\frac{\gamma_p(t)^2}{4} + M^2 D_q(t)^2\right)\|p\|^2\Big], \end{aligned} \tag{3.99}$$

where the mixing term, involving $\operatorname{tr}(qp) = (\mathrm{i}/2)\operatorname{tr}[a, a^\dagger] = 0$, vanishes in a finite dimensional state space. The latter can be seen from the relations $q = \sqrt{1/2M\Omega}(a^\dagger + a)$ and $p = \mathrm{i}\sqrt{M\Omega/2}(a^\dagger - a)$, which also yield $\|p\|^2 = M^2\Omega^2\|q\|^2$.

The difference of the weights is given by Eq. (3.53)

$$\|A_+^{\mathrm{HPZ}}\|^2 - \|A_-^{\mathrm{HPZ}}\|^2 = 2M^2 D_p(t)\|q\|^2, \tag{3.100}$$

and is invariant under the variation of the symmetry parameters λ and φ. It can also be written as $\|A_+^{\mathrm{HPZ}}\|^2 - \|A_-^{\mathrm{HPZ}}\|^2 = 2\mathrm{Re}\,\mathrm{tr}(\mathbb{S}^{\mathrm{HPZ}}q)$ [Eq. (3.46)].

The optimal rescaling λ^{HPZ} and complex phase φ^{HPZ}, which minimize the negative contribution, are readily obtained from Eqs. (3.60) and (3.61),

$$\lambda^{\mathrm{HPZ}}(t)^2 = \frac{\|\mathbb{S}^{\mathrm{HPZ}}\|}{\|q\|} = M^2 D_p(t)\sqrt{1 + \frac{\Omega^2\gamma_p(t)^2}{4M^2 D_p(t)^2} + \Omega^2\frac{D_q(t)^2}{D_p(t)^2}}, \tag{3.101}$$

$$\sin\varphi^{\mathrm{HPZ}} \propto \mathrm{Im}\,\mathrm{tr}(\mathbb{S}^{\mathrm{HPZ}}S) = 0, \tag{3.102}$$

for which we obtain

$$\|A_\sigma^{\mathrm{HPZ}}\|^2 = M^2 D_p(t)\left(\sigma + \sqrt{1 + \frac{\Omega^2\gamma_p(t)^2}{4M^2 D_p(t)^2} + \Omega^2\frac{D_q(t)^2}{D_p(t)^2}}\right)\|q\|^2. \tag{3.103}$$

This is a generalization of the result in Ref. [21] to arbitrary $\gamma_p(t)$, $D_q(t)$, $D_p(t)$. It is consistent with the limit of Brownian motion, which is easily seen by considering the coefficients of Eq. (3.93) and Taylor expanding the root.

3.12 Ultraweak coupling limit - breakdown of detailed balance

In Section 3.7 above, for an extended Hubbard model coupled to thermal baths, it is shown in Figs. 3.6 and 3.8 to 3.10 that the truncated master equation deviates from the Redfield equation for low temperatures also for ultraweak coupling. Therefore, it is indeed different from a weak coupling approximation. In this section, we show that equilibrium steady state $\varrho^{(0),\mathrm{trunc}}$ of the truncated master equation in the ultraweak coupling limit is different from the canonical Gibbs state $e^{-\beta H_{\mathrm{S}}}/Z_{\mathrm{S}}$. In Fig. 3.15(a), for an extended Hubbard model coupled to one thermal baths, we find that the ground-state population of the truncated master equation underestimates the prediction of the Redfield and quantum-optical master equation. In the limit of ultraweak coupling, the Redfield and quantum-optical master equation yield the canonical Gibbs state, whereas the truncated master equation deviates from it [Fig. 3.15(b)]. One might find an exponential fit for the data of the truncated master equation in Fig. 3.15(b) and define an effective Gibbs state at a higher effective temperature.

The equilibrium populations $p_n^{(0)}$ in zeroth order of the coupling follow from the hierarchy in Eq. (2.63) and, together with $-\mathrm{i}\,\langle n|[H_{\mathrm{LS}},\ \varrho^{(0)}]|n\rangle = 0$, can be written as solution of the rate equation in the pseudo-Lindblad representation

$$0 = \sum_{\sigma=-1,1}\sigma\sum_m\Big(|\,\langle n|A_\sigma|m\rangle\,|^2 p_m^{(0)} - |\,\langle m|A_\sigma|n\rangle\,|^2 p_n^{(0)}\Big), \tag{3.104}$$

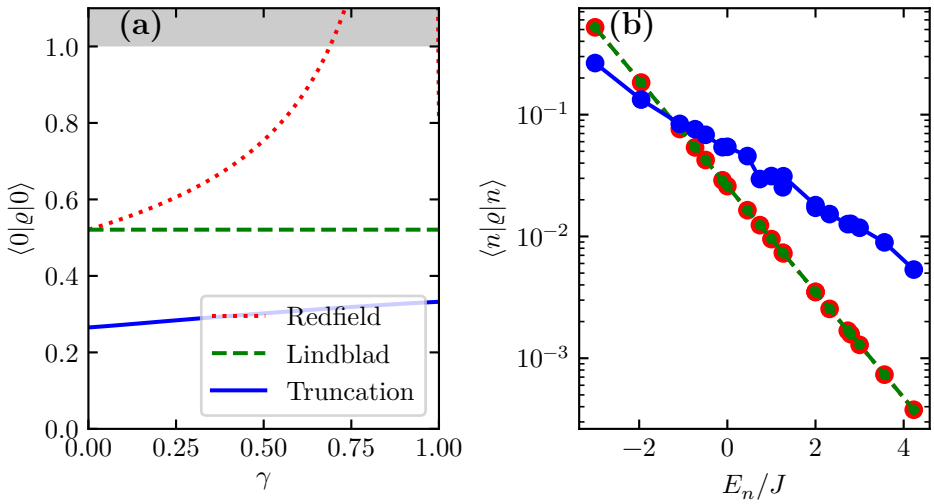

Figure 3.15: In (a) ground-state population of Redfield (in dotted red), quantum optical (Lindblad) (in dashed green) and truncated master equation (in solid blue) as a function of coupling strength. In (b) populations of the system's eigenstates as a function of eigenenergies E_n in a logarithmic scale for ultraweak coupling, $\gamma = 0.001$. The parameters are $l = 6$, $N = 3$, $V = 1\,J$, $\omega_D = 17\,J, T = 1\,J$.

with Pauli rates given by the matrix elements of the jump operators

$$\| \langle n|A_\sigma|m\rangle\|^2 = |S_{nm}|^2 \frac{1}{2\cos(\varphi)} \left[\lambda^2 + \sigma 2\mathrm{Re}(e^{\mathrm{i}\sigma\varphi} G(\Delta_{nm})) + \frac{1}{\lambda^2}|G(\Delta_{nm})|^2\right]. \tag{3.105}$$

Obviously, in the pseudo-Lindblad equation we obtain rates that are different from the ones known from the detailed balance condition. It is only in the combination of positive and negative channels that we obtain the familiar rates, $\| \langle n|A_+|m\rangle\|^2 - \| \langle n|A_-|m\rangle\|^2 = 2G'(\Delta_{nm})|S_{nm}|^2$.[8] The truncation of the negative weights breaks the detailed balance condition (2.21) and consequently the zeroth-order result differs from the canonical Gibbs state. In this approximation, the populations can be obtained by numerically solving $0 = \sum_m (| \langle n|A_+|m\rangle |^2 p_m^{(0),\mathrm{trunc.}} - | \langle m|A_+|n\rangle |^2 p_n^{(0),\mathrm{trunc.}})$. They are complicated functions of the coupling density $G(\Delta)$ and the coupling matrix S_{nm}. Furthermore, the steady state depends on the symmetry parameters λ and φ, which is unphysical. This aspect of the truncated master equation has been pointed out in Ref. [161].

We can conclude that the quantum-optical master equation is better suited for describing the equilibrium steady state in the limit of ultraweak coupling than the truncated master equation.

[8] The difference of the Pauli rates is closely related to the net rate of the Redfield equation $\|A_+\|^2 - \|A_-\|^2 = 2\mathrm{Re}\,\mathrm{tr}(\mathbb{S}S)$.

3.13 Excursion - Rate equations beyond GKSL regime

In an open quantum system, the coupling to the bath induces spontaneous transitions between the internal states of the system. On a phenomenological level, this can be described by a rate equation of the form, $\partial_t p_q(t) = \sum_n (R_{qn} p_n(t) - R_{nq} p_q(t))$, where $p_q(t)$ is the time dependent population of the internal state labelled by "q" and R_{qn} is the rate for transporting population from the n-th state to the q-th state, see sketch in Fig. 3.16 (a). We now show that by a specific choice of basis, any GKSL and pseudo-Lindblad equation, such as the Redfield equation, give rise to such a rate equation.

In order to describe populations, one has to introduce a basis representation for the reduced density matrix $\varrho(t)$ of the system. For ultraweak coupling, in regimes where the quantum-optical master equation (2.52) is valid, the system's eigenbasis is the preferred basis. Evaluating the matrix elements $\langle q|\partial_t \varrho(t)|k\rangle = -\mathrm{i}\,\langle q|[H, \varrho(t)|k\rangle + \langle q|\mathcal{R}^{\mathrm{RWA}}[\varrho(t)]|k\rangle$ leads to decoupled equations for the coherences and populations. For the coherences with $q \neq k$, one obtains complex oscillations with an exponential decay,

$$\partial_t \varrho_{qk}(t) = \left\{ -\mathrm{i}\left(\Delta_{qk} + \omega_q^{LS} - \omega_k^{LS}\right) - \sum_n \frac{R_{nq} + R_{nk}}{2} \right\} \varrho_{qk}(t), \tag{3.106}$$

where the energies are shifted by $\omega_q^{LS} = \sum_n G''(\Delta_{nq})\,|S_{nq}|^2$. The diagonal elements, i.e., the populations of the energy eigenstates, obey the rate equation

$$\partial_t \varrho_{qq}(t) = \sum_n \left(R_{qn}\ \varrho_{nn}(t) - R_{nq}\ \varrho_{qq}(t)\right), \tag{3.107}$$

with rates given by,

$$R_{qn} = 2G'(\Delta_{nq})\,|S_{nq}|^2\,. \tag{3.108}$$

For a double-well model $H_{\mathrm{S}} = -J/2(a_1^\dagger a_2 + a_2^\dagger a_1)$ with $N = 3$ bosons and four internal states, which is coupled via $S = a_1^\dagger a_1$ to a thermal bath of temperature $T/J = 2$, the dynamics of the populations and coherences is depicted in Fig. 3.16(b) and Fig. 3.16(c), respectively.

In order to find a rate equation for a generic GKSL or pseudo-Lindblad equation, we first solve the dynamics and diagonalize the state at every instance of time,

$$\varrho(t) = \sum_n p_n(t)\,|n(t)\rangle\langle n(t)|\,. \tag{3.109}$$

Thus, by construction there are no coherences in the instantaneous eigenbasis. However, the time-dependent states $\{|n(t)\rangle\}$ are in general coherent superpositions of different energy

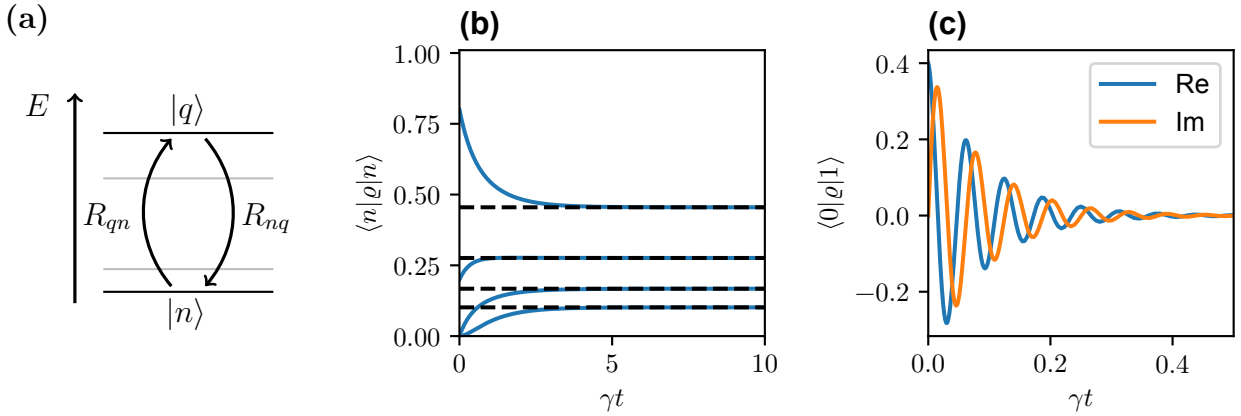

Figure 3.16: In the energy eigenbasis, the quantum-optical master equation gives rise to a rate equation for the populations, schematically depicted in (a). For a double-well model $H_\mathrm{S} = -J/2(a_1^\dagger a_2 + a_2^\dagger a_1)$ with $N = 3$ bosons and coupling $S = a_1^\dagger a_1$ to a thermal bath of temperature $T/J = 2$, we plot rotating-wave dynamics for populations in (b) and coherences in (c). The initial state is coherent superposition of ground state and first excited state $|\psi(0)\rangle = \frac{1}{\sqrt{2}}(|0\rangle + |1\rangle)$.

eigenstates. In this diagonal basis, we now calculate the change of the populations,

$$\begin{aligned}\langle n(t)|\partial_t \varrho|n(t)\rangle = \sum_m \Big(&\dot{p}_m \langle n(t)|m(t)\rangle \langle m(t)|n(t)\rangle + \\ &p_m[\langle n(t)|\dot{m}(t)\rangle \langle m(t)|n(t)\rangle + \langle m(t)|n(t)\rangle \langle \dot{m}(t)|n(t)\rangle]\Big), \\ = \dot{p}_n,&\end{aligned} \tag{3.110}$$

which holds due to orthogonality and because the derivative is anti hermitian, i.e., $\langle n|\dot{m}\rangle = -\langle \dot{m}|n\rangle$. To start with, consider a generic GKSL equation

$$\partial_t \varrho(t) = -\mathrm{i}[H, \varrho(t)] + L\varrho(t)L^\dagger - \frac{1}{2}\{L^\dagger L,\, \varrho(t)\}, \tag{3.111}$$

with Hamiltonian H and one jump operator L. Plugging this equation into (3.110), the coherent part drops out as it does not couples to the instantaneous populations,

$$\langle n(t)|[H, \sum_m p_m(t)\,|m(t)\rangle\langle m(t)|]|n(t)\rangle = 0, \tag{3.112}$$

and only the dissipative part remains,

$$\begin{aligned}\dot{p}_n &= \langle n(t)|\, L\varrho L^\dagger - \frac{1}{2}L^\dagger L\varrho - \frac{1}{2}\varrho L^\dagger L\,|n(t)\rangle\,,\\ &= \sum_m \Big(p_m \,\langle n(t)|L|m(t)\rangle\, \langle m(t)|L^\dagger|n(t)\rangle \\ &\qquad - \frac{1}{2}p_m\,\langle n(t)|L^\dagger L|m(t)\rangle\,\delta_{m,n} - \frac{1}{2}p_m\,\delta_{n,m}\,\langle m(t)|L^\dagger L|n(t)\rangle\Big),\\ &= \sum_m |L_{nm}(t)|^2\, p_m - p_n \sum_{m'} \langle n(t)|L^\dagger\,|m'(t)\rangle\langle m'(t)|\,L|n(t)\rangle\,,\\ &= \sum_m \Big(|L_{nm}(t)|^2\, p_m - |L_{mn}(t)|^2\, p_n\Big). \end{aligned} \tag{3.113}$$

This is the rate equation, for which the absolute squared matrix element $|L_{mn}(t)|^2$ is the positive rate for the transition of state n to state m and $|L_{nm}(t)|^2$ is the positive rate for the inverse process. Thus, a generic GKSL equation can be represented as a rate equation for the instantaneous eigenvalues of the density matrix. The associate rates are the squared matrix elements of the jump operator. Here, the basis is explicitly time dependent and encodes already the solution of the master equation. The rate equation above can only be written down explicitly, if the solution is already known. In other words, it is not useful for solving the dynamics.

For the Redfield equation (2.42), by following the same analysis as above, one arrives at

$$\dot{p}_n = \sum_m \left(R_{nm}(t)\, p_m - R_{mn}(t)\, p_n\right), \tag{3.114}$$

with $R_{nm}(t) = 2\mathrm{Re}[S_{nm}(t)\mathbb{S}^*_{mn}(t)]$. Even though it has the structure of a rate equation, the crucial difference is that the quantities $R_{nm}(t)$ occur as weights that are not necessarily positive.

Rate equations are often useful as they allow for efficient simulation by means of (classical) Monte Carlo sampling of random walks through the configuration space of internal states [162]. In Chapter 4 below, stochastic unravelings of master equation by means of quantum Monte Carlo sampling is discussed. In contrast to the random walk approach, it unravels the full density matrix including coherences.

3.14 Concluding remarks to the truncated master equation

In this chapter, the truncated master equation is proposed. It is a GKSL approximation to the Redfield equation alternative to the rotating-wave approximation. In a first step, by diagonalizing the Kossakowski matrix the Redfield equation is written in pseudo-Lindblad form. An two-parameter family of pseudo-Lindblad equations is found, which are related to

each other by symmetry transformations. The symmetry parameters control the weight of the jump operators and the optimal parameters are chosen such that it minimizes the negative weight in the pseudo-Lindblad representation absolutely and relatively to the positive weight. By truncating the negative contribution, the Redfield equation is reduced to GKSL form.

This approach is applicable especially for high temperatures beyond ultraweak coupling, also in regimes where the rotating-wave approximation breaks down. In particular, out of equilibrium, e.g., for transient dynamics [see Figs. 3.8 and 3.11] the truncated master equation is in excellent agreement with the full Redfield result. It also accurately captures the nonequilibrium steady state of the Redfield equation away from equilibrium, which is tested for the particle imbalance in Fig. 3.13, and the dissipative flow in Fig. 3.14. The truncated master equation is of GKSL form and, thus, allows for efficient quantum jump unraveling. This is beneficial as compared to the direct integration of the Redfield equation, which is only possible for moderate system sizes.

Nevertheless, for ultraweak coupling in equilibrium, the truncated master equation breaks the detailed balance condition. The resulting steady state, thus, does not agree with the canonical Gibbs state and spuriously depends also on the symmetry parameters. However, this also highlights the relevance of the negative contribution. Especially in ultraweak coupling the negative weights are necessary to guarantee a consistent equilibrium state.

Since the negative-weight terms in the pseudo-Lindblad representation of the Redfield equation do matter in some regimes, in Chapter 4 below, a novel quantum jump unraveling for quantum master equations of pseudo-Lindblad form is derived.

4 Stochastic unravelings of quantum master equations

Driven-dissipative quantum systems, which are often described by a quantum master equation of GKSL form, are gaining significant attention. However, as is discussed in Chapter 2, the standard microscopic derivation within the Born-Markov-Redfield formalism also requires the rotating-wave approximation, which is questionable beyond ultraweak coupling and is especially challenged for many-body systems, where the energy level splitting becomes small as a function of the system size. In Chapter 3, we propose an alternative approximation to reduced the Redfield equation to GKSL form, which provides an accurate description in a large parameter regime beyond ultraweak coupling, where the rotating-wave approximation fails. In particular, this is relevant for nonequilibrium scenarios like transient dynamics and the nonequilibrium steady state.

However, there are parameter regimes where the truncation approach leads to significant deviations from the Redfield equation, such that the negative-weight dissipator of the pseudo-Lindblad equation has to be considered. Apart from providing an accurate description, and equally important for large systems, the theoretical description should allow for efficient numerical simulations. Namely, a direct integration of the master equation is only possible for moderate system sizes, because the allocated memory for the density matrix scales with the Hilbert space dimension squared. This is especially problematic in many-body systems, for which the Hilbert space dimension D scales exponentially with the system size.

A powerful approach is to unravel the dynamics of the density matrix by quantum trajectories

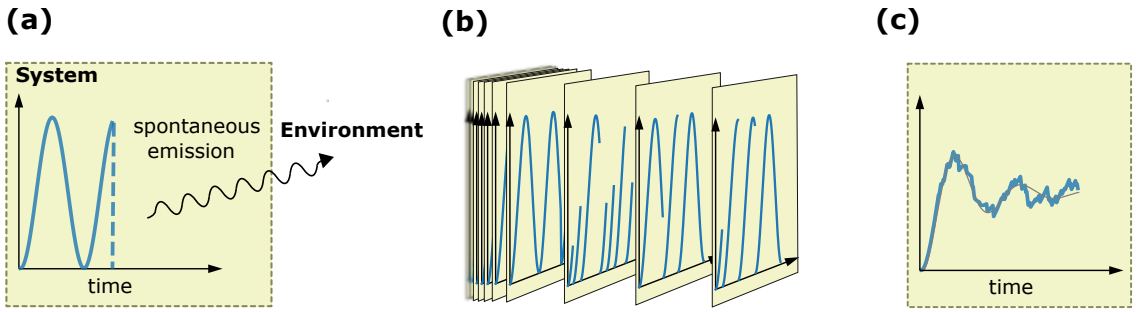

Figure 4.1: In (a) spontaneous emission of a system coupled to its environment. In (b) individual trajectories in a stochastic quantum jump unraveling. In (c) average over quantum jump trajectories.

that evolve stochastically. The basic idea is that for an open quantum system the coherent time evolution of a pure state is interrupted by spontaneous occurring quantum jumps as depicted schematically in Fig. 4.1(a). By continuously monitoring the environment within a time interval, the system undergoes stochastic dynamics: Either it follows coherent oscillations, or it performs a sudden quantum jump, as illustrated Fig. 4.1(b). In an ensemble average for a large number of such "trajectories" of time dependent pure states, the discontinuities are smoothed out, as depicted schematically in Fig. 4.1(c). The resulting dynamics then corresponds to the deterministic evolution of the density matrix. In other words, individual trajectories are single realisations of the same stochastic process, which on average yield an unraveling for the stochastic operator

$$\varrho(t) \equiv \lim_{N\to\infty} \frac{1}{N} \sum_{n=1}^{N} |\psi_n(t)\rangle\langle\psi_n(t)| \,, \tag{4.1}$$

or $\varrho(t) \simeq \frac{1}{N} \sum_{n=1}^{N} |\psi_n(t)\rangle\langle\psi_n(t)|$ for sufficiently large N.

Compared to the evolution of the full density operator, with D^2 matrix elements, the simulation of a quantum trajectory, with D entries, requires less memory. Moreover, such unravelings can also directly describe stochastic processes, which have been observed in atomic and photonic systems [163–165].

In the Markovian regime, when the dynamics is described by a GKSL master equation, there is the well-known Monte Carlo wave function approach (MCWF) [51], which is revisited in Section 4.1. However, it solely works for positive relaxation strengths, which define the rates under which spontaneous quantum jumps are performed.

In the following, we propose a novel scheme to deal with negative relaxation rates in a quantum jump unraveling that works also for static negative rates and for which the trajectories are equipped with one additional sign bit only. The approach closes the gap of the truncation approach to efficiently solve the Redfield dynamics in regimes, where the negative relaxation strength cannot be truncated.

The idea for the approach has been the result of Ché Netzer's Bachelor thesis, which I co-supervised. I refined the ideas and developed numerical implementations, which has been jointly published in Ref. [166]. In parts, the results and texts in Sections 4.3 to 4.10 are taken from Ref. [166].

As a proof of principle, we implement our method for the master equation of eternally non-Markovian dynamics for a single qubit as well as for a chain of interacting spinless fermions coupled to a thermal bath. For the latter, we make the connection to the truncation approach developed in Chapter 3 and minimize the negative relaxation rate to obtain good statistical convergence.

4.1 Monte Carlo wave function approach

The simulation of quantum trajectories is straightforward in the ultraweak-coupling limit, where the system-bath coupling is weak compared to the (quasi)energy level splitting in the system. In this case, the system is described by the quantum-optical master equation [see Eq. (2.52) in Section 2.5], which is of GKSL (Gorini-Kossakowski-Sudarshan-Lindblad) form [49, 50] ($\hbar = 1$),

$$\partial_t \varrho(t) = -\mathrm{i}[H, \varrho(t)] + \sum_i \gamma_i \left(L_i \varrho(t) L_i^\dagger - \frac{1}{2}\{L_i^\dagger L_i, \varrho(t)\} \right), \tag{4.2}$$

with the coherent evolution captured by some Hamiltonian H and dissipation described by jump operators L_i with associated non-negative strengths γ_i. Here, H, γ_i, and L_i can be time dependent.

One can rewrite Eq. (4.2) as

$$\partial_t \varrho(t) = -\mathrm{i}[H_{\mathrm{eff}} \varrho(t) - \varrho(t) H_{\mathrm{eff}}^\dagger] + \sum_i \gamma_i L_i \varrho(t) L_i^\dagger. \tag{4.3}$$

The first term is a generalized von-Neumann equation with non-Hermitian, effective Hamiltonian

$$H_{\mathrm{eff}} = H - \frac{\mathrm{i}}{2} \sum_i \gamma_i L_i^\dagger L_i. \tag{4.4}$$

The terms $\gamma_i L_i \varrho L_i^\dagger$ describe transitions between different states.

From this equation, we can immediately obtain a stochastic process for the evolution of pure states known as Monte Carlo wave function (MCWF) approach [51–56, 19, 57]. In each time step δt, the state either evolves coherently according to

$$|\psi(t+\delta t)\rangle = \frac{(1 - \mathrm{i}\delta t H_{\mathrm{eff}})\,|\psi(t)\rangle}{\|(1 - \mathrm{i}\delta t H_{\mathrm{eff}})\,|\psi(t)\rangle\|}, \tag{4.5}$$

with probability $1 - \sum_i r_i(t)\delta t$ or a quantum jump occurs,

$$|\psi(t+\delta t)\rangle = \frac{L_i\,|\psi(t)\rangle}{\|L_i\,|\psi(t)\rangle\|}, \tag{4.6}$$

with probability $r_i(t)\delta t$ and jump rates $r_i(t) = \gamma_i \langle\psi(t)|L_i^\dagger L_i|\psi(t)\rangle$. The state of the system is then given (or, for finite N, approximated) by the ensemble average $\varrho(t) = \overline{|\psi(t)\rangle\langle\psi(t)|}$ over an infinitely (or sufficiently) large number N of trajectories $|\psi_n(t)\rangle$, where $\overline{X} \equiv \frac{1}{N}\sum_{n=1}^N X_n$.

However, the assumption of ultraweak coupling, leading to the GKSL master equation, is questionable in various situations, for instance, in large systems, with small finite-size gaps

and tiny avoided crossings between many-body states, as well as in Floquet systems with driving frequency ω, where the average quasi energy level spacing is ω/D [65], where D is the Hilbert-space dimension.

Beyond ultraweak coupling, in the previous Chapter 3, it is shown that the Redfield equation can be written in pseudo-Lindblad form (3.22), which looks like a GKSL master equation (4.2) except for the fact that the coefficients γ_i also take negative values. Within the MCWF approach, quantum jumps with $\gamma_i < 0$ would happen with negative jump rate $r_i(t) < 0$ and, thus, cannot be performed.

4.2 Existing unravelings for negative relaxation strengths

A stochastic unraveling of pseudo-Lindblad equations is relevant, for instance, for the Redfield equation, which can be brought to pseudo-Lindblad form [see Chapter 3]. Generally, negative relaxation strengths are relevant for non-Markovian dynamics [167], stochastic Hamiltonians with non-Markovian noise [144], gauge transformed Lindbladians [168], and exact master equations [111, 93, 89]. To overcome the problem of negative jump rates, different quantum-jump unravelings have been formulated, which, however, require significantly more computational resources [67–69, 77, 71–73, 67, 169].

In some cases, negative relaxation strengths are interpreted as back flow of information from the environment into the system. In the non-Markovian quantum jump method [70–73], this is realised by reverting jump processes that occurred earlier in the dynamics, whenever the rate becomes negative. This method has been implemented for phenomenological master equations of single- or few coupled qubits, when the relaxation strengths oscillate between positive and negative values. However, pseudo-Lindblad equations also appear in time independent forms with non-oscillatory but static negative rates, such as the Redfield equation in Chapter 3. Furthermore, the non-Markovian quantum jump method does not admit independent (parallel) evaluation of trajectories. The numerical implementation of the non-Markovian quantum jump method is very challenging, since the probability to revert a jump depends on the occupation of the target state, for which the whole ensemble is required [71]. In Ref. [73], the diffusive limit of the non-Markovian quantum jump method has been derived, which would extent the regime where the method is applicable. A generalization of the non-Markovian jump method to many-body systems has been proposed in Ref. [170], which is used to study measurement-induced phase transitions. For non-oscillatory relaxation weights, the rate-operator quantum-jump approach has been developed [169]; however, it requires a rather costly diagonalization of a state-dependent operator in every time step of the evolution.

Alternatively, it has been shown that non-Markovian processes can be embedded in Markovian ones that would be described by a GKSL master equation. However, this requires an extended Hilbert space, for which the dimension at least triples [69, 171]. Thus, in principle, the

conventional MCWF approach also applies to the non-Markovian dynamics by mapping the Redfield equation to an equivalent GKSL equation, but yet by tripling the memory allocation per trajectory. For a stochastic unraveling, it is actually sufficient only to consider a doubling of the Hilbert space [67, 68]. Here, the idea is to use an asymmetric unraveling $\varrho \equiv \overline{\varrho_n} = \overline{|\psi\rangle\langle\Phi|} + \text{H.c}$, with pairs $\{|\psi_n\rangle, |\Phi_n\rangle\}$ of quantum trajectories. However, this approach is crucially different from the MCWF, since by disregarding the third auxiliary degree of freedom in the Markovian embedding, which works as a sink and source in Ref. [69], the quantum trajectories are not normalized. An improved algorithm, which preserves the norm, has been realized in Ref. [68] by a particular choice of the jump rates. A detailed discussion for numerical stability form norm preserving algorithms can be found in Ref. [172].

In the following, a new quantum-trajectory approach is presented, the starting point of which is the pseudo-Lindblad representation. It works for arbitrary pseudo-Lindblad weights γ_i. The trajectories evolve independently allowing for parallelized simulations, and it does not require the doubling of state space. This is realized by extending the system's state space in a minimal (and for the memory requirement of simulations, practically irrelevant) fashion by a single classical bit $s \in \{-1, +1\}$, $|\psi(t)\rangle \to \{|\psi(t)\rangle, s(t)\}$.

4.3 Pseudo-Lindblad quantum trajectories

To unravel the dynamics of a pseudo-Lindblad quantum master equation (4.2), with the γ_i allowed to be negative, by quantum trajectories $\{|\psi(t)\rangle, s(t)\}$, first choose a time step δt that is sufficiently short for the first-order time integration, and jump rates $r_i(t) > 0$ for each jump operator L_i to be specified below. Within one time step, a quantum jump occurs described by

$$\begin{aligned} |\psi^{(i)}(t+\delta t)\rangle &= \frac{\sqrt{|\gamma_i|}L_i\,|\psi(t)\rangle}{\sqrt{r_i(t)}}, \\ s^{(i)}(t+\delta t) &= \frac{\gamma_i}{|\gamma_i|}\,s(t), \end{aligned} \tag{4.7}$$

with probability $r_i(t)\delta t$ or, alternatively, with the remaining probability $1 - \sum_i r_i(t)\delta t$, the state evolves under the effective Hamiltonian H_{eff} given by Eq. (4.4)[1]

$$\begin{aligned} |\psi^{(0)}(t+\delta t)\rangle &= \frac{(1 - \mathrm{i}\delta t H_{\text{eff}}(t))\,|\psi(t)\rangle}{\sqrt{1 - \delta t \sum_i r_i(t)}}, \\ s^{(0)}(t+\delta t) &= s(t). \end{aligned} \tag{4.8}$$

This approach is schematically depicted in Fig. 4.2. Essentially, the trajectories evolve similarly to the conventional MCWF approach. In particular, for the quantum jumps the rates are

[1] By Taylor expanding the denominator in Eq. (4.8) to first order in the small time step δt, $1/\sqrt{1 - \delta t \sum_i r_i(t)} \simeq 1 + \frac{1}{2}\delta t \sum_i r_i(t)$, the deterministic evolution can equivalently be formulated as a first order differential equation $\partial_t |\psi^{(0)}(t)\rangle = \left(\frac{1}{2}\sum_i r_i(t) - \mathrm{i}H_{\text{eff}}\right) |\psi^{(0)}(t)\rangle$.

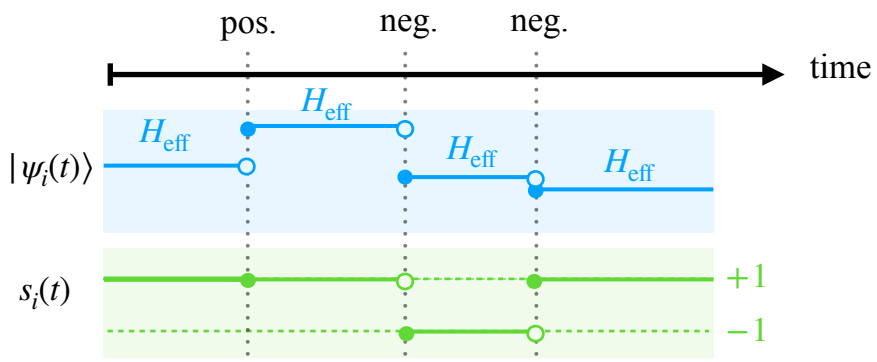

Figure 4.2: Sketch for the pseudo-Lindblad quantum jump (PLQT) unraveling approach. A trajectory evolves under the effective Hamiltonian indicated by the blue horizontal lines. A quantum jump is indicated by a discontinuity in the line. In the lower part of the sketch, depending on whether the relaxation weight is positive or negative the sign does not change or changes, respectively.

explicitly positive. As a new aspect, the sign of the trajectory is encoded in one auxiliary classical bit.

We now show that the ensemble of pure states obtained by this PLQT approach converges to the correct density operator solving Eq. (4.2) according to

$$\varrho(t) = \overline{s(t)\,|\psi(t)\rangle\langle\psi(t)|}. \tag{4.9}$$

For a pure initial state $\sigma(t) = s(t)\,|\psi(t)\rangle\langle\psi(t)|$, on average the update scheme is the weighted sum of the processes described above:

$$\overline{\sigma(t+\delta t)} = \sum_i r_i(t)\delta t\ \sigma^{(i)}(t+\delta t) + \left(1 - \sum_i r_i(t)\delta t\right)\sigma^{(0)}(t+\delta t), \tag{4.10}$$

with $\sigma^{(i)} = s^{(i)}\,|\psi^{(i)}\rangle\langle\psi^{(i)}|$ and $\sigma^{(0)} = s^{(0)}\,|\psi^{(0)}\rangle\langle\psi^{(0)}|$. By inserting Eqs. (4.7) and (4.8), the jump rates $r_i(t)$ cancel out and one arrives at

$$\overline{\sigma(t+\delta t)} = \sigma(t) + \delta t\left(\sum_i \gamma_i L_i \sigma(t) L_i^\dagger - \mathrm{i}H_{\text{eff}}\sigma(t) + \mathrm{i}\sigma(t)H_{\text{eff}}^\dagger\right), \tag{4.11}$$

almost corresponding to the action of the master Eq. (4.2). The final step to arrive at Eq. (4.2) is to average Eq. (4.11) also over an ensemble of pure states at initial time t, so that $\overline{\sigma(t+\delta t)} \to \varrho(t+\delta t)$ and $\sigma(t) \to \varrho(t)$.

As is discussed below, one consequence of the presence of negative weights $\gamma_i < 0$ is that individual wave functions ψ_n are not normalized. As a result, the ensemble-averaged trace is preserved only in the limit $N \to \infty$ of an infinite ensemble. The fluctuations of the trace and their dependence on N are shown in Fig. 4.5 for an explicit example. Therefore, in a finite

ensemble, one obtains better convergence by explicit normalization

$$\varrho_N = \frac{1}{\mathcal{N}} \sum_n^N s_n \, |\psi_n\rangle\langle\psi_n| \,, \tag{4.12}$$

with

$$\mathcal{N} = \sum_n^N s_n \, \langle\psi_n|\psi_n\rangle \,, \tag{4.13}$$

at every time t. A rigorous proof of our algorithm using the Ito formalism is outlined in the section below. In case that all γ_i are positive, the sign bits do not change, and the algorithm corresponds to the conventional MCWF approach.

The additional sign bit is a scalar stochastic process that is conditioned on the trajectory $|\psi_n\rangle$. Note that recently, another unraveling of non-Lindblad master equations was also proposed in Ref. [173]. It is different from our approach, but also involves an effective classical degree of freedom given by a real number of constant average, rather than our single bit, whose average is time dependent, as will be seen below.

For the PLQT approach, as for other unraveling schemes [68], the jump rates $r_i(t) > 0$ can, in principle, be chosen arbitrarily. In practice, there is, however, a trade-off. Whereas for too small rates r_i, large ensembles of trajectories are required to sample each jump process i sufficiently, we also have to require that the probability $1 - \sum_i r_i \delta t$ remains positive and large enough for the given time step δt. A typical choice known from conventional MCWF simulations is [57]

$$r_i(t) = |\gamma_i| \frac{\| L_i \, |\psi(t)\rangle \|^2}{\| |\psi(t)\rangle \|^2}, \tag{4.14}$$

for which the quantum jump does not alter the norm $\| |\psi\rangle \| \equiv \sqrt{\langle\psi|\psi\rangle}$ of the state, i.e., $\| \left|\psi^{(i)}(t+\delta t)\right\rangle \| = \| |\psi(t+\delta t)\rangle \|$. Note, however, that for $\gamma_i < 0$ this choice implies that the norm increases during the coherent time evolution with H_{eff}, $\| \left|\psi^{(0)}(t+\delta t)\right\rangle \| = (1 + \delta t \sum_{\gamma_i<0} r_i(t)) \| |\psi(t)\rangle \|$.[2] This is not the case for the conventional MCWF approach, where $\gamma_i \geq 0$.

In this section, we use a heuristic argument for the average process of the PLQT approach and show that it leads to the pseudo-Lindblad master equation. In the next section, we give a rigorous analytical proof by making use of the Ito formalism of stochastic processes.

[2] The norm after the coherent time step follows from $\langle\psi^{(0)}(t)|\psi^{(0)}(t)\rangle = \langle\psi(t)| \frac{1-\mathrm{i}\delta t(H_{\text{eff}} - H_{\text{eff}}^\dagger)}{1-\delta t \sum_i r_i(t)} |\psi(t)\rangle = \frac{1-\delta t \sum_i r_i(t) \mathrm{sgn}(\gamma_i)}{1-\delta t \sum_i r_i(t)} \langle\psi(t)|\psi(t)\rangle$ and Taylor expansion to first order in the small time step δt.

4.4 PLQT unraveling in Ito formalism

The starting point is the pseudo-Lindblad master equation Eq. (4.2) with jump operators L_i and relaxation strength γ_i, which we explicitly allow to be negative. For convenience, in the following, we absorb the magnitude of relaxation strength into the jump operator $L_i \propto \sqrt{|\gamma_i|}$ and denote the sign by $\sigma_i = \gamma_i/|\gamma_i| = \pm 1$,

$$\partial_t \varrho(t) = -\mathrm{i}[H, \varrho(t)] + \sum_i \sigma_i \left(L_i \varrho(t) L_i^\dagger - \frac{1}{2}\{L_i^\dagger L_i, \varrho(t)\} \right). \tag{4.15}$$

Each channel i gives rise to a stochastic process, which we can unravel with pseudo-Lindblad quantum trajectories (PLQT). In the Ito formalism, the change of the trajectory is described as follows:

$$|d\psi\rangle = \sum_i dN_i \Big(\frac{\sigma_i L_i}{\sqrt{r_i(t)}} |\psi\rangle - |\psi\rangle \Big) + dt \Big(\sum_i \frac{r_i(t)}{2} - \mathrm{i}H_{\text{eff}} \Big) |\psi\rangle \,, \tag{4.16}$$

with dN_i describing independent jump processes. For quantum jumps, dN_i take the values 1 or 0, depending on whether a jump takes place or not. The average value

$$\overline{dN_i} = r_i(t) dt, \tag{4.17}$$

defines the jump rate $r_i(t) > 0$, which is a free parameter because it later cancels out in the ensemble average. The second term in Eq. (4.16) describes deterministic evolution,

$$\partial_t |\psi^{(1)}(t)\rangle = \Big(\sum_i \frac{r_i(t)}{2} - \mathrm{i}H_{\text{eff}} \Big) |\psi^{(1)}(t)\rangle \,, \tag{4.18}$$

with effective Hamiltonian Eq. (4.4).

For the deterministic time evolution, the sign is directly encoded in the effective Hamiltonian, whereas for the quantum jump one cannot differentiate between positive and negative relaxation strengths. This can be seen from the fact that $-L_i |\psi\rangle \simeq L_i |\psi\rangle$ differ by a global phase factor only and, thus, are equivalent. In other words, for a pure state $|\psi\rangle\langle\psi|$ the relative sign in the jumps $(-L_i) |\psi\rangle\langle\psi| (-L_i)^\dagger$ would simply cancel. In order to recover the relative sign, the idea is to create an asymmetric ensemble $|\psi\rangle\langle\tilde{\psi}| = s |\psi\rangle\langle\psi|$ where $|\tilde{\psi}\rangle$ is a copy of the trajectory $|\psi\rangle$, except that the sign after a quantum jump is not changed,

$$|d\tilde{\psi}\rangle = \sum_i dN_i \Big(\frac{L_i}{\sqrt{r_i(t)}} |\tilde{\psi}\rangle - |\tilde{\psi}\rangle \Big) + dt \Big(\sum_i \frac{r_i(t)}{2} - \mathrm{i}H_{\text{eff}} \Big) |\tilde{\psi}\rangle \,. \tag{4.19}$$

This is the same asymmetric unraveling proposed by Breuer and coworkers in reference [67] for the special case of a pseudo-Lindblad master equation so that the trajectories only differ

by a relative sign. That is why it is not necessary to simulate $|\tilde{\psi}\rangle$ but that it is sufficient to store the information about the additional sign bit.

The rest of the proof follows the standard arguments of any quantum jump unraveling. A nice overview is given by I. Kondov and coworkers in reference [68]. To show that the unraveling yields on average the pseudo-Lindblad equation (4.15), we calculate an infinitesimal change of one signed trajectory,

$$d(s\,|\psi\rangle\langle\psi|) = d\,|\psi\rangle\langle\tilde{\psi}| = |d\psi\rangle\langle\tilde{\psi}| + |\psi\rangle\langle d\tilde{\psi}| + |d\psi\rangle\langle d\tilde{\psi}|\,. \tag{4.20}$$

Note that, for stochastic processes, the quadratic term also contributes to lowest order. The first two terms give

$$\begin{aligned} |d\psi\rangle\langle\tilde{\psi}| + |\psi\rangle\langle d\tilde{\psi}| = \sum_i dN_i \Big(\frac{\sigma_i L_i\,|\psi\rangle\langle\tilde{\psi}|}{\sqrt{r_i(t)}} + \frac{|\psi\rangle\langle\tilde{\psi}|\,L_i^\dagger}{\sqrt{r_i(t)}} - |\psi\rangle\langle\tilde{\psi}| \Big) \\ - \sum_i dN_i\,|\psi\rangle\langle\tilde{\psi}| + dt \Bigg(\sum_i r_i(t)\,|\psi\rangle\langle\tilde{\psi}| - \mathrm{i}H_{\text{eff}}\,|\psi\rangle\langle\tilde{\psi}| + |\psi\rangle\langle\tilde{\psi}|\,\mathrm{i}H_{\text{eff}}^\dagger \Bigg), \end{aligned} \tag{4.21}$$

and essentially contribute to the effective Hamiltonian. Note that on average the first two terms in the second line cancel each other, since $\overline{dN_i} = r_i dt$.

For the quadratic term $|d\psi\rangle\langle d\tilde{\psi}|$, only stochastic processes dN_i contribute. Since the processes are independent and for single realizations one has $dN_i = 0, 1$, it follows that $dN_i dN_j = \delta_{ij} dN_i$. We then get

$$\begin{aligned} |d\psi\rangle\langle d\tilde{\psi}| &= \sum_i dN_i^2 \Big(\frac{\sigma_i L_i\,|\psi\rangle}{\sqrt{r_i(t)}} - |\psi\rangle \Big) \Big(\frac{\langle\tilde{\psi}|\,L_i^\dagger}{\sqrt{r_i(t)}} - \langle\tilde{\psi}| \Big), \\ &= \sum_i dN_i\ \sigma_i \frac{L_i\,|\psi\rangle\langle\tilde{\psi}|\,L_i^\dagger}{r_i(t)} - \sum_i dN_i \Big(\frac{\sigma_i L_i\,|\psi\rangle\langle\tilde{\psi}|}{\sqrt{r_i(t)}} + \frac{|\psi\rangle\langle\tilde{\psi}|\,L_i^\dagger}{\sqrt{r_i(t)}} - |\psi\rangle\langle\tilde{\psi}| \Big), \end{aligned} \tag{4.22}$$

where the latter terms cancel the first line in Eq. (4.21), and we arrive at

$$d(\,|\psi\rangle\langle\tilde{\psi}|) = dt \Big[-\mathrm{i}H_{\text{eff}}\,|\psi\rangle\langle\tilde{\psi}| + |\psi\rangle\langle\tilde{\psi}|\,\mathrm{i}H_{\text{eff}}^\dagger \Big] + \sum_i \frac{dN_i}{r_i(t)} \sigma_i L_i\,|\psi\rangle\langle\tilde{\psi}|\,L_i^\dagger. \tag{4.23}$$

By taking the ensemble average, we replace $\overline{dN_i} = r_i(t)dt$ and arrive at the pseudo-Lindblad equation (4.15) for the density matrix $\varrho \equiv \overline{|\psi\rangle\langle\tilde{\psi}|}$.

4.5 Non-Markovian dephasing for a single qubit

As a proof of principle, we implement the PLQT algorithm for a qubit subjected to purely dissipative dynamics,

$$\partial_t \varrho(t) = \frac{1}{2}\Big(\mathcal{D}(\sigma^x) + \mathcal{D}(\sigma^y) - \tanh(t)\mathcal{D}(\sigma^z)\Big)[\varrho(t)], \tag{4.24}$$

with GKSL channels $\mathcal{D}(\sigma^i)[\varrho] = \sigma^i \varrho \sigma^i - \varrho$, where σ^i are Pauli operators, with ${\sigma^i}^\dagger \sigma^i = {\sigma^i}^2 = \mathbb{1}$. This equation is known as the master equation for the eternal non-Markovian dynamics [174, 167]. The existence of a negative weight makes it inaccessible to the standard MCWF, while also the non-Markovian quantum jump method [71] fails, since $-\tanh(t) < 0$ for all t.

In Appendix G, the analytical solution, with detailed discussion found in Ref. [167], is ob-

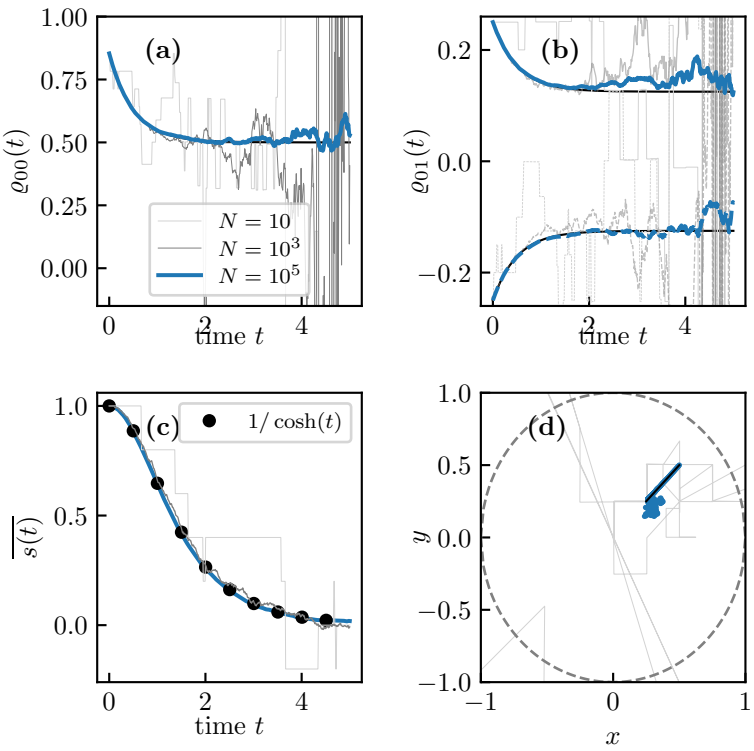

Figure 4.3: Non-Markovian dynamics [Eq. (4.24)] for density matrix elements ϱ_{00} (a), $\mathrm{Re}\varrho_{01}$ (solid), $\mathrm{Im}\varrho_{01}$ (dashed) (b), and the Bloch vector in the x-y plane (d). Analytical solution (black) and unraveling with $N = 10^5$ PLQTs with time step $\delta t = 0.01$ in blue ($N = 10, 10^3$ in thin and intermediate gray lines) for an initial Bloch state with $\phi = \Theta = \pi/4$. (c) shows the averaged sign bit.

tained in the Bloch-vector representation,

$$\varrho(t) = \frac{1}{2}\left(\mathbb{1} + x(t)\,\sigma^x + y(t)\,\sigma^y + z(t)\,\sigma^z\right), \tag{4.25}$$

$$x(t) = \frac{1}{2}(1+e^{-2t})x(0), \tag{4.26}$$

$$y(t) = \frac{1}{2}(1+e^{-2t})y(0), \tag{4.27}$$

$$z(t) = e^{-2t}z(0), \tag{4.28}$$

for which the stationary state $\varrho(t) \overset{t\to\infty}{\longrightarrow} (1/2)(\mathbb{1} + (x(0)/2)\,\sigma^x + (y(0)/2)\,\sigma^y)$ is the projection of the initial Bloch-vector onto the x-y plane with half of its initial length. Thus, for all times the dynamics depends on the initial state. For the classification, of whether the dynamics is Markovian or non-Markovian, we refer to Ref. [167], where it is shown to be a completely positive evolution albeit without being completely-positive divisible. For completeness, we remark that the dynamics of the time-independent generator, $\varrho(t) = (1/2)(\mathbb{1} + x(0)\,\sigma^x + y(0)\,\sigma^y + e^{-2t}z(0)\,\sigma^z$, which is obtained by replacing the negative weight with its asymptotic value, i.e., $-\tanh(t) \to -1$, differs significantly from the full time-dependent result. In particular, states that are polarized in the x-y plane do not dissipate.

For this model, the PLQT approach is easily implemented and, because the jump operators are unitary, the jump rates are state independent; i.e. $\|\sigma^i\,|\psi(t)\rangle\|^2 = \||\psi(t)\rangle\|^2$. This leads to a simplification of the rates in Eq. (4.14), and one has $r_x = r_y = 1/2$, $r_z(t) = \tanh(t)/2$. Also the action of effective Hamiltonian $H_{\text{eff}} = -(\mathrm{i}/2)(1 - \tanh(t)/2)$, entering Eq. (4.8), is not state dependent, because it is proportional to the identity.

The averaged sign follows the rate equation $\partial_t \overline{s}(t) = -2r_z(t)\overline{s}(t)$, which we derive in Section 4.8 and which is solved by $\overline{s}(t) = 1/\cosh(t)$, as shown in Fig. 4.3(c). Quantum jumps $|\psi\rangle \to \sigma^i\,|\psi\rangle$ are realized in the Bloch-vector representation. In general, the components of the Bloch vector are given by the expectation values of the Pauli operators $x = \langle\psi|\sigma^x|\psi\rangle$, $y = \langle\psi|\sigma^y|\psi\rangle$, and $z = \langle\psi|\sigma^z|\psi\rangle$. Using $\langle\sigma^i\sigma^j\sigma^i\rangle = (2\delta_{ij} - 1)\,\langle\sigma^j\rangle$, the components of the Bloch vector after a quantum jump are given by

$$\begin{bmatrix} x \\ y \\ z \end{bmatrix} \overset{\sigma^x}{\to} \begin{bmatrix} x \\ -y \\ -z \end{bmatrix}, \qquad \begin{bmatrix} x \\ y \\ z \end{bmatrix} \overset{\sigma^y}{\to} \begin{bmatrix} -x \\ y \\ -z \end{bmatrix}, \qquad \begin{bmatrix} x \\ y \\ z \end{bmatrix} \overset{\sigma^z}{\to} \begin{bmatrix} -x \\ -y \\ z \end{bmatrix}, \tag{4.29}$$

for a quantum jump with σ^x, σ^y and σ^z, respectively.

By simulating $N = 10^5$ trajectories in Fig. 4.3(a) and 4.3(b), we obtain accurate results for the transient dynamics until, at $t_{\text{R}} \sim 2$, the system reaches the steady state regime. Besides this physical relaxation time, we also find an *algorithmic* relaxation time $t_A \sim 4$, at which the number of negative and positive trajectories become equal, and the averaged sign decays to zero [Fig. 4.3(c)]. Beyond this algorithmic relaxation time, fluctuations are typically increased

[Fig. 4.3(a) and (4.3)(b)], requiring larger ensemble sizes N. This effect can be understood by noting that a stochastic process of a real variable x_n with positive mean $\overline{x}$ will have bounded fluctuations $\Delta x = \overline{(x-\overline{x})^2}^{-1/2} \leq \overline{x}$ as long as $x_n > 0$, whereas Δx is not bounded by $\overline{x}$, when x_n can also take negative values. Thus, ideally, t_A should be large compared to the time span of the simulation. The algorithmic relaxation time is determined by the inverse sign-flip rate $r_{\mathrm{SF}} = \sum_{i,\gamma_i<0} r_i$, e.g., $t_A = r_{\mathrm{SF}}^{-1}$ for time-independent r_{SF}. Thus, we can increase t_A simply by lowering the strengths for negative processes with weights $\gamma_i < 0$ relative to positive ones with $\gamma_i > 0$. However, this will also increase the number of trajectories needed for properly sampling those negative-weight processes. Thus, before doing this, one should first attempt to rewrite the master equation, so that the relative weight of negative processes is reduced. This can be done for pseudo-Lindblad equations derived from the Redfield equation as shown in Chapter 3 with results published in Refs. [141, 142], as we will recapitulate now.

4.6 State-dependent optimization of the pseudo-Lindblad equation

For a microscopic model, a master equation is often derived within the Born-Markov-Redfield formalism [37, 94]. We consider a system-bath Hamiltonian of the form $H_{\mathrm{tot}} = H + \sum_i S_i \otimes B_i + H_i$ with system Hamiltonian H that couples to individual baths H_i, where S_i and B_i denote the system and bath coupling operators, respectively. The Redfield equation can then be written in pseudo-Lindblad form [141]

$$\partial_t \varrho(t) = -\mathrm{i}[H + H^{\mathrm{LS}}, \varrho(t)] + \sum_{i,\sigma=\pm} \sigma \left(L_{i\sigma} \varrho(t) L_{i\sigma}^\dagger - \frac{1}{2}\{L_{i\sigma}^\dagger L_{i\sigma}, \varrho(t)\} \right), \tag{4.30}$$

with Lamb-shift Hamiltonian $H^{\mathrm{LS}} = (1/2\mathrm{i}) \sum_i S_i \mathbb{S}_i + \mathrm{H.c.}$, convoluted operators $\mathbb{S}_i$ from Eq. (2.42) and Lindblad-like jump operators

$$L_{i\sigma} = \frac{1}{\sqrt{2}} \left[\lambda_i(t) S_i + \sigma \frac{1}{\lambda_i(t)} \mathbb{S}_i \right], \tag{4.31}$$

with arbitrary, time-dependent real parameters $\lambda_i(t)$. We see that due to the negative relaxation rates with $\sigma = -1$, the Redfield equation is generally not of GKSL form, unless further approximations are employed in the limit of ultraweak coupling [21, 94, 37] or for high bath temperatures [61]. In Chapter 3, we propose the truncated master equation in Section 3.5, where we minimize the norm of the jump operator that belongs to the negative weight. For a

purely Ohmic bath, the choice in Eq. (3.47) reads

$$\lambda_{i,\mathrm{glob}}(t)^2 = \sqrt{\frac{\mathrm{tr}\ \mathbb{S}_i^\dagger \mathbb{S}_i}{\mathrm{tr}\ S_i S_i}}, \tag{4.32}$$

and minimizes the norm of the negative channels in the pseudo-Lindblad equation globally, i.e., on average for all states. A further reduction of negative processes can be achieved by state-dependent optimization. Namely, according to Eq. (4.14), where (assuming, without loss of generality, a normalized state) the rates for negative quantum jumps with L_{i-} are given by $r_{i-}(t) = \frac{1}{2}\Big(\lambda_i(t)^2 \|S_i\,|\psi(t)\rangle\|^2 + \frac{1}{\lambda_i(t)^2}\|\mathbb{S}_i\,|\psi(t)\rangle\|^2 - 2\mathrm{Re}\,\langle\psi(t)|S_i\mathbb{S}_i|\psi(t)\rangle\Big)$. Thus, the choice

$$\lambda_{i,\mathrm{loc}}(t)^2 = \frac{\|\mathbb{S}_i\,|\psi(t)\rangle\|}{\|S_i\,|\psi(t)\rangle\|}, \tag{4.33}$$

minimizes the rates for negative quantum jumps in the unraveling of the Redfield equation. Since the states in the numerator and the denominator of Eq. (4.33) have to be evaluated for evolving the state anyway, this local optimization can be implemented efficiently.

We test our method using state-dependent optimization according to Eq. (4.33) for the extended Hubbard chain of spinless fermions as in Section 3.7 with system Hamiltonian given by Eq. (3.79). For the dissipator, we have

$$\langle n|\mathbb{S}_\ell|m\rangle = \frac{J(\Delta_{nm})}{e^{\Delta_{nm}/T}-1}\,\langle n|S_\ell|m\rangle\,, \tag{4.34}$$

with system operator $S_\ell = a_\ell^\dagger a_\ell$, level splitting $\Delta_{nm} = E_n - E_m$, and bath temperature T. We

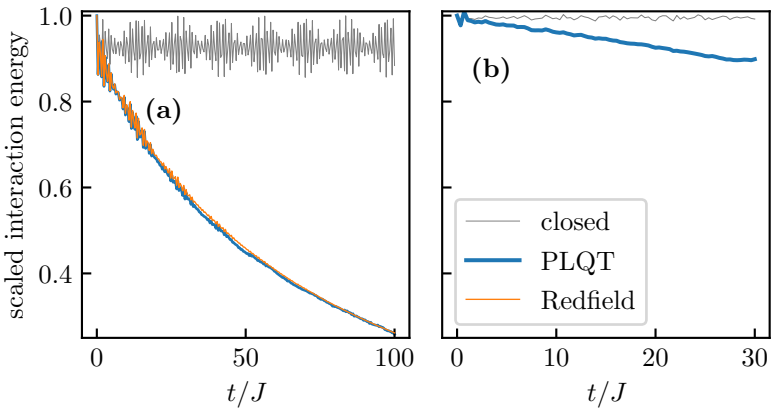

Figure 4.4: Dynamics of scaled interaction energy of extended Hubbard chain of two (eight) particles on four (13) sites (a) [(b)] with $V/J = 7$. We compare the dynamics of the isolated (gray line) and open system with $\gamma/J = 0.02$ and $T/J = 1$ (blue line for PLQT, thin orange for Redfield equation). The decrease of interactions is related to bath-induced doublon-breaking processes.

consider a purely Ohmic bath, with spectral density $J(E) = \gamma E$ and coupling strength γ.

In Fig. 4.4, we depict the decay of the interaction energy for an initial state in which pairs of adjacent sites are occupied $|\psi(0)\rangle = |011011\ldots\rangle$. The quench dynamics for such a charge density wave in a spin polarized Fermi-Hubbard model has been recently observed experimentally by Bakr and co-workers [175]. We assume strong interactions, $V/J = 7$, for which the doublon pairs can only be broken when the system exchanges energy with the bath. This leads to a decay of the energy of the open system as depicted in Fig. 4.4(a), where the transient oscillations are well reproduced.

4.7 Norm conservation and choice of jump rates

As shown above, the jump rates $r_i(t)$ are free parameters of the unraveling because they cancel out in the ensemble average [68]. This is similar to the relaxation strengths in the master equation (4.2), which can always be redefined by rescaling the jump operators. For instance, this rescaling is adopted in Eq. (4.15). However, the jump rates influence the dynamics on the level of single trajectories and typically one chooses state-dependent jump rates such as in Eq. (4.14), which yield quantum jumps that do not change the norm of the state,

$$|\psi(t)\rangle \to \frac{L_i\,|\psi(t)\rangle}{\sqrt{r_i(t)}} = \frac{L_i\,|\psi(t)\rangle}{\|L_i\psi(t)\|}\|\psi(t)\|. \tag{4.35}$$

For state-dependent jump rates, the deterministic evolution in Eq. (4.18) is non-linear in the state $|\psi^{(1)}(t)\rangle$. For the conventional MCWF approach this non-linear term compensates for the loss of the norm during the time evolution under the non-Hermitian effective Hamiltonian [57, 68]. In turn, for master equations with negative relaxation strengths, the norm increases according to

$$\begin{aligned}
\partial_t\|\psi^{(1)}\|^2 &= \langle\psi^{(1)}|\partial_t\psi^{(1)}\rangle + \langle\partial_t\psi^{(1)}|\psi^{(1)}\rangle\,, \\
&= \underbrace{\langle\psi^{(1)}|{-\mathrm{i}H}|\psi^{(1)}\rangle + \langle\psi^{(1)}|\mathrm{i}H|\psi^{(1)}\rangle}_{=0} + \sum_i \langle\psi^{(1)}|(r_i(t) - \sigma_i L_i^\dagger L_i)|\psi^{(1)}\rangle\,, \\
&= 2\sum_{i,\sigma_i=-1} \langle\psi^{(1)}|L_i^\dagger L_i|\psi^{(1)}\rangle\,,
\end{aligned} \tag{4.36}$$

where the sum is taken over all channels with negative relaxation rate. Alternatively, one may choose different jump rates $r_i(t) > 0$ such that the deterministic time evolution is norm preserving. The condition for this choice follows from Eq. (4.36) and reads

$$\sum_i r_i(t) = \sum_i \sigma_i \frac{\|L_i\psi\|^2}{\|\psi\|^2}. \tag{4.37}$$

For unitary jump operators, the rates can be chosen independently of the state.

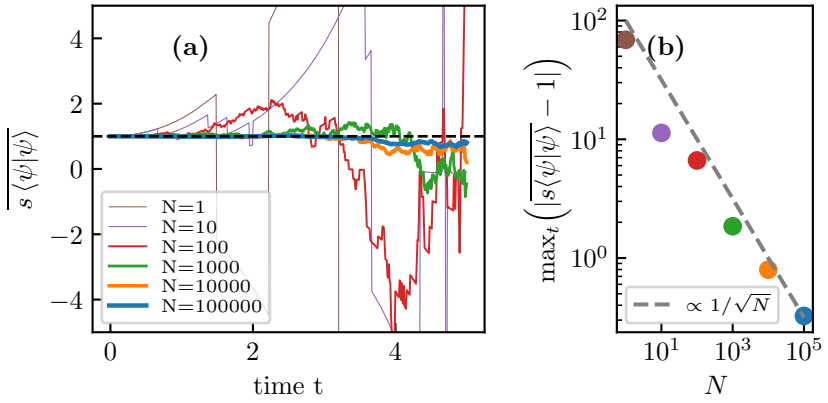

Figure 4.5: We simulate PLQTs for the eternal non-Markovian master equation in Section 4.5. (a) Dynamics of ensemble average $\overline{s\,\langle\psi|\psi\rangle}$ for increasing number N of trajectories (thicker lines). (b) Maximal deviation of the average from the value 1 during the time evolution as a function of ensemble size N.

Considering the eternal non-Markovian master equation, discussed in Section 4.5, the condition reads $\sum_i r_i(t) = 1 - \tanh(t)/2$. One possible choice for positive jump rates that do not change the norm in the deterministic time step is

$$r_x = r_y = \frac{1}{4}, \qquad r_z = \frac{1-\tanh(t)}{2}, \tag{4.38}$$

which is different to the choice in Section 4.5 [$r_x = r_y = 1/2$, $r_z = \tanh(t)/2$]. Again, the rates for σ^x and σ^y-jumps are taken to be equal. The σ^z jump, which corresponds to the negative relaxation strength $\gamma_z < 0$, happens more often in the beginning but vanishes in the static limit. Note that, if the deterministic time evolution is norm conserving, in turn the quantum jumps are not. For the qubit in Eq. (4.24), this would give quantum jumps $|\psi\rangle \to 2\sigma^x|\psi\rangle$, $|\psi\rangle \to 2\sigma^y|\psi\rangle$ and $|\psi\rangle \to \sqrt{2}\sigma^z|\psi\rangle/\sqrt{1-\tanh(t)}$. Hence, for negative relaxation strengths, there is no choice for jump rates $r_i(t) > 0$ for which the trajectories remain normalized.

The increase of the norm, however, is cancelled by trajectories with opposing sign, such that on average the trace is preserved. This is shown in Fig. 4.5(a), where we plot the dynamics of the ensemble average $\frac{1}{N}\sum_n^N s_n\langle\psi_n|\psi_n\rangle$ for increasing number N of trajectories. This holds true because on average the ensemble of trajectories evolves according to the master equation, which is trace-preserving, i.e., $\mathrm{tr}(\overline{s\,|\psi\rangle\langle\psi|}) = \overline{s\,\langle\psi|\psi\rangle} = 1$. For finite N, the fluctuations are on the order of $1/\sqrt{N}$ [Fig. 4.5(b)]. They can be removed by explicitly normalizing the ensemble as mentioned Section 4.3.

4.8 Dynamics of the averaged sign bit

Following the arguments of the PLQT approach proposed in Section 4.3, a trajectory $\{|\psi(t)\rangle, s(t)\}$ probabilistically changes its sign with the rate

$$R(t) \equiv \sum_{i,\gamma_i<0} r_i(t), \tag{4.39}$$

where the sum runs over all jump rates $r_i(t)$ that correspond to a negative $\gamma_i < 0$. The dynamics of the sign then follows the update scheme

$$s(t+\delta t) = \begin{cases} -s(t) & \text{with probability } R(t)\delta t, \\ s(t) & \text{with probability } 1 - R(t)\delta t. \end{cases} \tag{4.40}$$

For the averaged sign $\overline{s}(t)$, one takes the weighted average

$$\overline{s}(t+\delta t) = -R(t)\delta t\, \overline{s}(t) + (1 - R(t)\delta t)\ \overline{s}(t), \tag{4.41}$$

from which we can deduce the first order differential equation[3]

$$\partial_t \overline{s}(t) = -2R(t)\ \overline{s}(t), \tag{4.44}$$

where we have used the limit $\partial_t \overline{s}(t) = \lim_{\delta t\to 0}(s(t+\delta t) - s(t))/\delta t$. Provided $R(t)$ is a known,

[3] Alternatively, the averaged sign can be retrieved from the relative numbers $s_+(t) = N_+(t)/N$ and $s_-(t) = N_-(t)/N$ of positive and negative trajectories, respectively, $\overline{s}(t) = s_+(t) - s_-(t)$. The dynamics can be formulated by means of the rate equation depicted in Fig. 4.6,

$$\partial_t s_+(t) = -R(t)\,(s_+(t) - s_-(t)) \tag{4.42}$$
$$\partial_t s_-(t) = -R(t)\,(s_-(t) - s_+(t)) = -\dot{s}_+(t). \tag{4.43}$$

By summing up both equations, one obtains the first order differential equation for the averaged sign, $\partial_t \overline{s}(t) = \partial_t s_+(t) - \partial_t s_-(t) = -2R(t)\overline{s}(t)$.

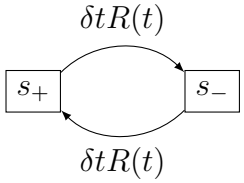

Figure 4.6: Scheme for change of sign. Within a short time interval δt the process of trajectories to change the sign form positive to negative, i.e., $s_+ \to s_-$, and vice-versa the inverse process $s_+ \leftarrow s_-$, both happen with the same rate $R(t)$.

smooth, and state-independent function, the averaged sign follows an exponential decay

$$\bar{s}(t) = \exp\Big[-2\int_0^t R(\tau)d\tau\Big]. \tag{4.45}$$

This is the case, e.g., for the master equation of the eternal non-Markovian dynamics discussed in Section 4.5. However, even if the decay rate depends on the particular state, qualitatively the net sign decays exponentially on a time scale that is given by the negative relaxation rate. Therefore, for sufficiently long times, the number of positive and negative trajectories is balanced (up to statistical fluctuations). As a result, $\bar{s}(t)$ generally vanishes for times that are long compared to an *algorithmic* relaxation time.

4.9 Efficiency for sparse objects

For the numerical implementation, we obtain the trajectories to first order in a small time step δt. The optimal choice of δt is found empirically and is a tradeoff between numerical accuracy and a limited computation time. In the interaction picture, for weak coupling, the dynamics happens on a slower timescale than in the Schrödinger picture. Thus, the time step can be chosen larger without loss of numerical accuracy.

For the dynamics of a particular observable A, it is not reasonable to store the full time-

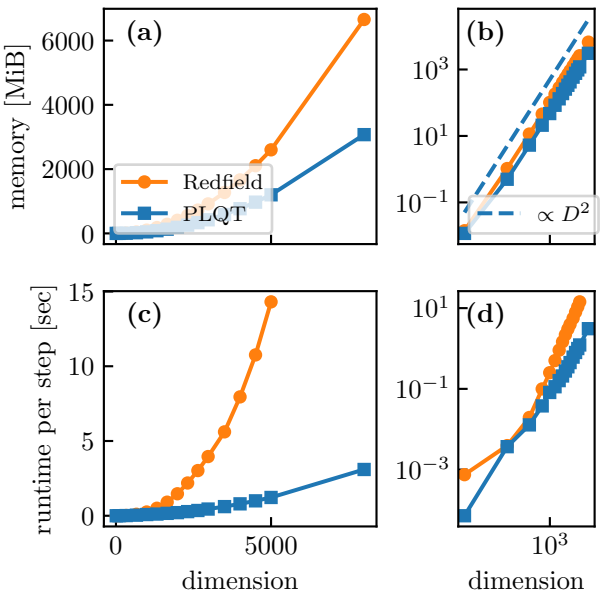

Figure 4.7: Required memory [(a) linear scale, (b) logarithmic scale] versus Hilbert-space dimension in logarithmic scale and single-time-step run-time [(c) linear scale, (d) logarithmic scale] versus Hilbert-space dimension in logarithmic scale for both a single trajectory (blue) and the Redfield master equation (red). The data were obtained for an Intel Core i9-10900 processor with up to 5.2 GHz.

dependent state as a large vector with complex entries. Instead, for an observable A, one stores the expectation value $\langle\psi_n(t)|A|\psi_n(t)\rangle$ together with the norm $\|\psi_n(t)\|$ and the sign $s_n(t)$. While the storage of the trajectory data boils down to a few real numbers, the time evolution requires the full state vector. If not only the Hamiltonian, but also the jump operators, are sparse, the memory needed for integrating a quantum trajectory is linear in the state-space dimension D. The latter is the case, however, mainly in phenomenological master equations with local jump operators and not for the Redfield equation, so that the memory needed usually scales like D^2. The memory needed for integrating the Redfield equation scales equally like D^2 (since it is sufficient to store and apply the jump operators rather than the full superoperator). Nevertheless, we find that the memory requirement for quantum trajectories is still lower than that for integrating the master equation. For the Redfield equation and a single PLQT, we compare the required memory and the single-time-step run time in [Fig. 4.7(a) and 4.7(b)] and [Fig. 4.7(c) and 4.7(d)], respectively. We find that the required memory is noticeably reduced for the quantum-trajectory simulation, even though, as discussed above, it still scales like D^2. The latter is not specific to our approach, but generally the case also for other quantum-trajectory simulations. For the run time, the relative reduction is even stronger and shows different scaling with D. The difference is, that two matrix-matrix products are needed for the Redfield integration, and one matrix-vector product for the PLQT approach.

Recently, in Ref. [176], a novel representation Redfield equation has been derived, in which the convoluted operator (2.43) is represented as a series expansion in orders of nested commutators of the coupling operator S with the system Hamiltonian H_S. By truncating the series at a finite order, one obtains a local approximation of the Redfield equation involving sparse matrices only. This gives a promising perspective to apply the PLQT approach to larger systems. Furthermore, for sparse matrices, the unraveling can also be combined with matrix-product states (e.g. [177, 178]). It is interesting to see how far such an approach would compare to a representation of the density operator by matrix-product operators, e.g., in Refs. [179, 180].

4.10 Concluding remarks to the pseudo-Lindblad quantum trajectory unraveling

We have developed an efficient unraveling of master equations of pseudo-Lindblad form, which includes the Redfield equation as an important case [141]. Different from previous approaches, which at least require an effective doubling of the state space, it requires a minimal extension of the state space by one classical sign bit only. It is applicable also for dissipation strengths that are always negative, it does not require matrix diagonalization during the time integration, and it allows for a parallel implementation, since all trajectories are independent of each other. We believe that it will be a useful tool for the simulation of open many-body systems beyond ultraweak system-bath coupling. The addition of the sign bit is a minor modification of

the standard MCWF algorithm and can be implemented efficiently. Efficient implementation schemes may be straightforwardly realized in software libraries such as QUTIP [150].

In future work, it will be interesting to systematically investigate the impact of negative dissipation strengths γ_i on the required ensemble size and the optimal choice of the corresponding rates for efficient simulation. Finally, the combination of PLQT simulations with the recently derived local quantum master equation [176] opens a promising route for the efficient simulation of open many-body quantum systems.

5 Canonically consistent quantum master equation

In Chapter 2, we review the inconsistency of second-order master equations that lead to inaccurate stationary states beyond ultraweak coupling. For instance, for the Redfield equation, this inconsistency causes the stationary state not to be positive in certain parameter regimes. In general, positivity violation of master equations, which are not of GKSL form, is a long-standing issue in the theory of open quantum systems. For the Redfield equation, this problem is resolved, in Chapter 3, by reducing the Redfield equation to GKSL form by minimizing and truncating the negative contributions in the dissipator. Nevertheless, there are regimes beyond ultraweak coupling and low bath temperatures, where the negative contributions are crucial for the dynamics and cannot be neglected. For this case, in Chapter 4, we develop an efficient stochastic unraveling for master equations of pseudo-Lindblad form that include dissipators with negative weight.

However, these approaches do not yield a more accurate stationary state. For a consistent state up to leading second order in the coupling, a fourth-order master equation would have to be considered, as is discussed in Sections 2.5.2 and 2.6.2. Furthermore, this would also resolve the positivity violation of the stationary state. In particular, a master equation does not need to be of GKSL form in order to guarantee positive dynamics [46, 93] [Section 2.6.1].

In this chapter, we introduce a new *canonically consistent quantum master equation* (CC-QME), in which correlations between the system and reservoir build over time and correctly

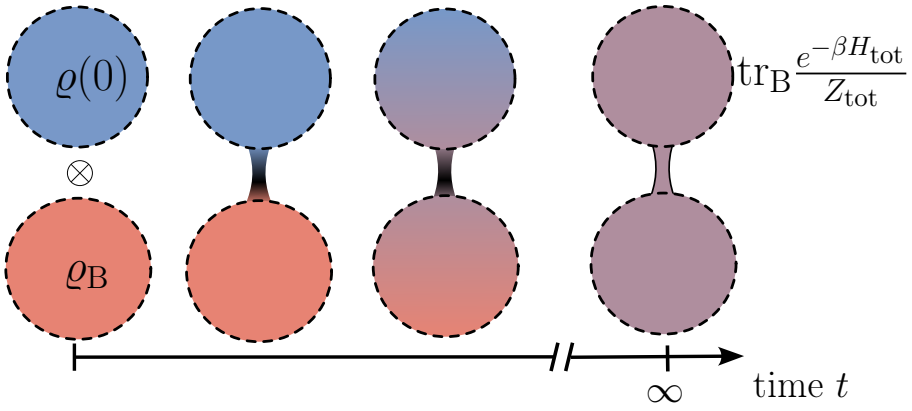

Figure 5.1: In open quantum systems correlations build up dynamically between system and environment.

account for the long-time correlations as dictated by statistical mechanics [Fig. 5.1].

Our method is based on incorporating the exact reduced Gibbs state into the generator of the dynamics. With this, we avoid a rigorous but cumbersome fourth-order perturbation theory. We obtain a correction to the second-order Redfield equation that does not only steer the reduced system towards a correct steady state, but also improves the accuracy of the dynamics. The CCQME solves the long-standing issue of unphysical negative probabilities, a common occurrence in the Redfield formalism [86, 61, 40, 47, 132, 141, 181] and leads to an accurate steady state in second-order of the coupling.

Our CCQME opens a new perspective in the theory of open quantum systems leading to a reduced density matrix that is accurate beyond the commonly used Redfield and GKSL equations, while retaining the same conceptual and numerical complexity.

This project has been realized in collaboration with Alexander Schnell and Juzar Thingna. In joint discussions, we formulated the idea to provide a dynamical theory for the analytical continuation approach of the steady state, for which Ref. [41] has been the starting point. Throughout the project both, Alexander Schnell and Juzar Thingna equally provided excellent guidance, for which I refined the ideas and realized explicit expressions and numerical implementations. Especially, but not exclusively, for the application to the many-body Hamiltonian, in Section 5.8, the contributions of Alexander Schnell are highly acknowledged.

5.1 Analytical continuation from second to fourth order

Before we turn to a dynamical description, we consider the stationary state. As revisited in Section 2.5.2, the stationary solution of a second-order master equation is consistent only in zeroth order because for finite coupling it would require corrections from the fourth-order master equation. This inconsistency has been resolved in Refs. [41, 42] by taking the limit $\lim_{m\to n} \varrho^{(2)}_{nm}$ in Eq. (2.66). At first glance, it is not guaranteed to obtain populations from coherences as a formal limit; however, as is shown in Refs. [41, 42], this analytical continuation yields the populations of the exact reduced Gibbs state in second-order perturbation theory.

To some extent, the method shows that for finite coupling the stationary state can be obtained consistently in second order: In detail, the state is obtained by the tensor elements of the Redfield equation, i.e., the coupling density $G(\Delta_{nm})$, and, due to the analytical continuation, also its derivative $\partial_\Delta G(\Delta)\big|_{\Delta=\Delta_{nm}}$. Therefore, the tensor elements of the second-order Redfield equation are sufficient to capture finite coupling effects consistently.

In this section, this is illustrated for the reduced Gibbs state of the damped harmonic oscillator. For this model, the exact stationary state is obtained analytically as a Gaussian state with equilibrium dispersions $\langle q^2\rangle$ and $\langle p^2\rangle$, respectively. In Section 2.6.2, it is shown that for weak coupling the perturbative expansion up to second order involves the fourth-order master equation. Equivalently, one may start from the exact analytical expressions for $\langle q^2\rangle$ and

$\langle p^2\rangle$ and obtain the second-order contributions explicitly, which leads to the expressions in Eqs. (E.1) and (E.2). The second-order contributions can be written as

$$M\left\langle q^2\right\rangle^{(2)} = \frac{1}{2\Omega}\frac{\partial}{\partial\Omega}\frac{1}{\beta}\sum_{l=-\infty}^{\infty}\frac{|\nu_l|\bar{\kappa}(|\nu_l|)}{\Omega^2+\nu_l^2}, \tag{5.1}$$

$$\frac{1}{M}\left\langle p^2\right\rangle^{(2)} = \Big[1+\frac{\Omega}{2}\frac{\partial}{\partial\Omega}\Big]\frac{1}{\beta}\sum_{l=-\infty}^{\infty}\frac{|\nu_l|\bar{\kappa}(|\nu_l|)}{\Omega^2+\nu_l^2}, \tag{5.2}$$

where a formal derivative with respect to the central oscillator frequency is introduced. The Laplace series can, equivalently, be written in the form of frequency integrals [Appendix E],

$$\frac{M}{\beta}\sum_{l=-\infty}^{\infty}\frac{|\nu_l|\bar{\kappa}(|\nu_l|)}{\Omega^2+\nu_l^2} = \Omega\coth(\beta\Omega/2)\mathcal{P}\int_0^\infty\frac{J(\omega)/\omega}{\Omega^2-\omega^2}\frac{d\omega}{\pi} - \mathcal{P}\int_0^\infty\frac{J(\omega)}{\Omega^2-\omega^2}\coth(\beta\Omega/2)\frac{d\omega}{\pi}, \tag{5.3}$$

which are well-known from the Redfield theory [Eq. (2.22)]. They may be expressed in terms of the imaginary part of the coupling density, where the first integral is related to the frequency shift $\mathcal{P}\int_0^\infty \frac{J(\omega)/\omega}{\Omega^2-\omega^2}\frac{d\omega}{\pi} = \frac{M}{2\Omega^2}\gamma_q^{(2)}$ [Eq. (2.78)] and the second integral yields the diffusion coefficient $\mathcal{P}\int_0^\infty \frac{J(\omega)}{\Omega^2-\omega^2}\coth(\beta\Omega/2)\frac{d\omega}{\pi} = M^2D_q^{(2)}$ [Eq. (2.81)].

Thus, for this concrete example of equilibrium dispersions, it is shown that a rigorous fourth-order expansion of the exact master equation can be omitted by taking formal derivatives of the Redfield coefficients. The main result of Ref. [41, 42], is that this holds in general for the steady state of the Redfield equation. There, the equilibrium coherences are analytically continued to the populations. In the remaining part of this chapter, we generalize this concept to a dynamical description.

5.2 Dyson-series expansion of the dynamical map - Linear divergence with time

Up to second order, the reduced dynamical map for an initial state of the system is identified in Eq. (2.35),

$$\begin{aligned} e^{\mathrm{i}H_\mathrm{S}t}\varrho(t)e^{-\mathrm{i}H_\mathrm{S}t} &\simeq \varrho(0) \\ &- \int_0^t d\tau_1\int_0^{\tau_1}d\tau_2\,\mathrm{tr}_B\, e^{\mathrm{i}H_\mathrm{S}\tau_1}[H_\mathrm{SB},[\boldsymbol{H}_\mathrm{SB}(-\tau_2),e^{-\mathrm{i}H_\mathrm{S}\tau_1}\varrho(0)e^{\mathrm{i}H_\mathrm{S}\tau_1}\otimes\varrho_\mathrm{B}]]e^{-\mathrm{i}H_\mathrm{S}\tau_1}, \end{aligned} \tag{5.4}$$

where the variable transformation $\tau_2\to\tau_1-\tau_2$, is used to make the dependence on τ_1 explicit. Here, the initial state of the total system-bath compound is a product state, $\varrho_\mathrm{tot}(0)=\varrho(0)\otimes\varrho_\mathrm{B}$, where ϱ_B is the equilibrium state of the bath. By identifying the time-dependent Redfield

superoperator on the right-hand side, and using the superoperator notation $e^{\mathrm{i}[H_\mathrm{S},\cdot]\tau_1}$, which acts on a generic state ϱ as $e^{\mathrm{i}[H_\mathrm{S},\cdot]\tau_1}[\varrho] = e^{\mathrm{i}H_\mathrm{S}\tau_1}\varrho e^{-\mathrm{i}H_\mathrm{S}\tau_1}$, one obtains the integrated representation of Eq. (2.36),

$$e^{\mathrm{i}H_\mathrm{S}t}\varrho(t)e^{-\mathrm{i}H_\mathrm{S}t} \simeq \left(\mathbb{1} + \int_0^t e^{\mathrm{i}[H_\mathrm{S},\cdot]\tau_1}\mathcal{R}^{(2)}_{\tau_1}e^{-\mathrm{i}[H_\mathrm{S},\cdot]\tau_1}d\tau_1\right)[\varrho(0)], \tag{5.5}$$

which is the starting point for the derivation of the time-local second-order Redfield equation [Section 2.4].

Truncating the series expansion of the reduced dynamical map to second order in the coupling is ill-defined for long times and, thus, is inadequate in describing the long-time dynamics: This can be seen from the tensor elements of the second-order map in the eigenbasis of the system,

$$\langle n|\int_0^t e^{\mathrm{i}[H_\mathrm{S},\cdot]\tau_1}\mathcal{R}^{(2)}_{\tau_1}e^{-\mathrm{i}[H_\mathrm{S},\cdot]\tau_1}[|q\rangle\langle k|]|m\rangle\, d\tau_1 = \int_0^t e^{\mathrm{i}(\Delta_{nm}-\Delta_{qk})\tau_1}\,\langle n|\mathcal{R}^{(2)}_{\tau_1}[|q\rangle\langle k|]|m\rangle\, d\tau_1, \tag{5.6}$$

which map the initial matrix elements $\varrho_{qk}(0)$ to the second-order matrix elements of the time-evolved state $\varrho^{(2)}_{nm}(t)$. For asymptotic times $t \to \infty$, the tensor elements of the dynamical map are the half-sided Fourier transform of the Redfield tensor elements. For $\Delta_{nm} = \Delta_{qk}$ and asymptotic, time-independent Redfield tensor, it is shown, in Ref. [40], that the integral diverges linearly with time. In detail, only those tensor elements diverge that map populations to populations, i.e., for $q = k$ and $n = m$, and that map coherences with frequency Δ_{nm} to coherences with the same frequency $\Delta_{nm} = \Delta_{qk}$ [115, 182]. This explains why the coherences in second-order perturbation theory are obtained consistently, whereas for the populations a second-order theory is insufficient.

As a theoretical concept, if all orders of the coupling would be considered, the divergences in the dynamical map would cancel out, such that the asymptotic limit is well-defined. With this exact asymptotic dynamical map, a weak coupling expansion would yield a finite second-order result.

This shows that it is crucial in which order the two limits of asymptotic time and weak coupling are taken. This shall be further motivated by a heuristic argument for the exponential decay $e^{-\gamma t}$ with positive coupling strength γ: On the one hand, first taking the long-time limit $\lim_{t\to\infty} e^{-\gamma t} = 0$ is convergent for arbitrary strength γ. This is also the basic idea in equilibrium statistical mechanics, which works in the limit of $t \to \infty$. On the other hand, in a dynamical theory, such as quantum mechanics, one might approach the problem from weak-coupling approximations. In a dynamical approach, the weak-coupling limit precedes the long-time limit giving $e^{-\gamma t} \simeq \sum_{n=0}^{N} \frac{(-1)^n\gamma^n t^n}{n!}$, which truncated at some order N is divergent for long times, except in lowest order for ultraweak coupling [183]. In other words, the order of limits is crucial to ensure convergence at all orders leading to a convergent perturbation truncation. In problems such as those tackled in this work, a guiding principle for the correct order of the

limits is the consistence with statistical mechanics.

In the following sections, we construct a dynamical theory that includes a second-order contribution of the the dynamical map

$$\varrho(t) \simeq \left(\mathbb{1} + \mathcal{Q}_t^{(2)}\right)[e^{-\mathrm{i}H_\mathrm{S}t}\varrho(0)e^{\mathrm{i}H_\mathrm{S}t}]. \tag{5.7}$$

In doing so, it is assumed that in zeroth order, the map is given by the coherent evolution under the system Hamiltonian. The second-order contribution is given by the superoperator $\mathcal{Q}_t^{(2)}$, which acts on the coherently evolved initial state. This is inspired by the the Dyson-series expansion (5.5). For asymptotic times, the superoperator $\mathcal{Q}_t^{(2)}$ shall converge to $\mathcal{Q}^{(2)} = \lim_{t\to\infty}\mathcal{Q}_t^{(2)}$.

5.3 Time-local master equation with inspiration drawn from statistical mechanics

In the standard open quantum systems framework, one avoids the dynamical map and its divergence, by taking the time derivative of Eq. (5.5) to obtain a first-order differential equation, $\partial_t\varrho(t) \simeq -\mathrm{i}[H_\mathrm{S}, \varrho(t)] + \mathcal{R}_t^{(2)}[e^{-\mathrm{i}H_\mathrm{S}t}\varrho(0)e^{\mathrm{i}H_\mathrm{S}t}]$ [Eq. (2.36)]. There, the generator becomes non-local in time as the right-hand side depends on the initial condition $\varrho(0)$.

In the following, we formulate a time-local master equation using the second-order contribution of the dynamical map in Eq. (5.7). To this end, we take the formal inverse[1] $(\mathbb{1} + \mathcal{Q}_t^{(2)})^{-1} \simeq \mathbb{1} - \mathcal{Q}_t^{(2)}$ and use this relation to solve for the freely evolving state, $e^{-\mathrm{i}H_\mathrm{S}t}\varrho(0)e^{\mathrm{i}H_\mathrm{S}t} \simeq (\mathbb{1} - \mathcal{Q}_t^{(2)})[\varrho(t)]$. By plugging this relation into the first-order differential equation above, we obtain the main result of this chapter, which is the time-local quantum master equation

$$\partial_t\varrho(t) = -\mathrm{i}\left[H_\mathrm{S}, \varrho(t)\right] + \mathcal{R}_t^{(2)}\left[(\mathbb{1} - \mathcal{Q}_t^{(2)})[\varrho(t)]\right], \tag{5.8}$$

which involves a fourth-order correction to the Redfield equation (2.38). In the following, we obtain $\mathcal{Q}_t^{(2)}$ in the asymptotic limit for large times from canonical perturbation theory of statistical mechanics and refer to Eq. (5.8) as *canonically consistent quantum master equation* (CCQME).

As compared to the standard approximation in Born-Markov formalism, $e^{-\mathrm{i}H_\mathrm{S}t}\varrho(0)e^{\mathrm{i}H_\mathrm{S}t} \simeq \varrho(t)$ [Section 2.4], the approach presented here is more consistent, as it also takes into account second-order corrections of the dynamical map. In fact, as we demonstrate below, this *consistency* is the reason, why the dynamics leads to the correct asymptote in second order.

Instead of following pathological perturbative expansions for the dynamical map, which in-

[1] For a generic state ϱ, it is $(\mathbb{1} - \mathcal{Q}_t^{(2)})(\mathbb{1} + \mathcal{Q}_t^{(2)})[\varrho] = \varrho - \mathcal{Q}_t^{(2)}[\mathcal{Q}_t^{(2)}[\varrho]]$, for which on second order we neglect the fourth-order contribution.

volve divergences in each order separately, we propose to combine notions of quantum mechanics and statistical mechanics in a holistic way. For finite coupling, we assume that the system eventually relaxes to the reduced Gibbs state

$$\lim_{t\to\infty}\varrho(t)=\frac{\mathrm{tr}_{\mathrm{B}}\,e^{-\beta(H_{\mathrm{S}}+H_{\mathrm{B}}+H_{\mathrm{SB}})}}{Z_{\mathrm{tot}}}\simeq\varrho^{(0)}+\mathcal{Q}^{(2)}[\varrho^{(0)}]-\varrho^{(0)}\,\mathrm{tr}_{\mathrm{S}}\,\mathcal{Q}^{(2)}[\varrho^{(0)}],\tag{5.9}$$

with $\varrho^{(0)}=e^{-\beta H_{\mathrm{S}}}/Z_{\mathrm{S}}$ being the canonical Gibbs state obtained for ultraweak coupling in the long-time limit. The details of the expansion above are carried out in Appendix B. In particular, for finite coupling, the reduced Gibbs state deviates from the canonical Gibbs state and the lowest-order correction $\mathcal{Q}^{(2)}[\varrho^{(0)}]$ is of second order in system-bath coupling. Here, $\mathcal{Q}^{(2)}$ is a hermiticity-preserving superoperator that acts on the canonical Gibbs state $\varrho^{(0)}$ and generates the second-order contribution $\varrho^{(2)}$ for both coherences and populations, respectively. The last term in Eq. (5.9), which is quadratic in the canonical Gibbs state, is a consequence of normalization. By construction the canonically consistent quantum master equation (5.8) is trace preserving and, therefore, this non-linear term is omitted.[2] Since $\mathcal{Q}^{(2)}$ is defined only by its action on one particular state, it is not unique. However, in Appendix B, a reasonable choice that is related to the dynamical Redfield theory is worked out,

$$\mathcal{Q}^{(2)}[\varrho]=\Pi\frac{1}{\mathrm{i}\Delta}\mathcal{R}^{(2)}[\varrho]+\Pi^{c}\left(\sum_{nl}|S_{nl}|^{2}\big[V''(\Delta_{nl})\mathcal{D}(|n\rangle\langle l|)[\varrho]+G''(\Delta_{ln})\,|n\rangle\,\partial_{E_n}\varrho_{nn}\,\langle n|\,\big]\right).\tag{5.10}$$

Here, the first term is directly related to the Redfield theory and describes the action on the coherent subspace $\Pi=\sum_{n\neq m}|n\rangle\langle n|\cdot|m\rangle\langle m|$, where the commutator $\mathrm{i}\Delta=\mathrm{i}[H_{\mathrm{S}},\cdot]$ is invertible. In the complementary subspace, with projector $\Pi^{c}=\sum_{n}|n\rangle\langle n|\cdot|n\rangle\langle n|$, the action on the populations can be understood in an analytical continuation approach, which involves the derivatives of the Redfield tensor, $V(\Delta)=\partial_{\Delta}G(\Delta)$ [41]. In detail, the superoperator is written as pseudo-Lindbladian $\mathcal{D}(|n\rangle\langle l|)$ with the jump operators $|n\rangle\langle l|$ and weights $|S_{nl}|^{2}V''(\Delta_{nl})$. Additionally, a superoperator arises that is formally derived from the derivative of the canonical Gibbs state in Eq. (B.20).

In the following, we include the superoperator $\mathcal{Q}^{(2)}$ into the dynamical theory. We require the asymptotic state to be consistent with statistical mechanics and, for that purpose, we make the conjecture

$$\lim_{t\to\infty}\mathcal{Q}_{t}^{(2)}\to\mathcal{Q}^{(2)},\tag{5.11}$$

[2] The CCQME is trace preserving for any superoperator $\mathcal{Q}^{(2)}$ because it is further contracted with the Redfield superoperator. This can be seen from the time-evolved state, $\varrho(t+\delta t)=\varrho(t)+\delta t\left(\mathrm{i}[H_{\mathrm{S}},\varrho(t)]+\mathcal{R}^{(2)}[\varrho(t)]-\mathcal{R}^{(2)}[\mathcal{Q}^{(2)}[\varrho(t)]]\right)$, where by taking the trace all terms proportional to δt drop out, i.e., $\mathrm{tr}_{\mathrm{S}}\,\varrho(t+\delta t)=\mathrm{tr}_{\mathrm{S}}\,\varrho(t)$.

and identify the asymptotic dynamical map with the superoperator obtained from the exact reduced Gibbs state. We do not intend to rigorously proof the conjecture above, for which both $\mathcal{Q}_t^{(2)}$ and $\mathcal{Q}^{(2)}$ would have to be well defined. In the following, four striking arguments are given that justify the assumption above:

Firstly, in the coherent subspace the asymptotic dynamical map is rigorously obtained from the Dyson-series expansion in Eq. (5.5). Carrying out the time-integral leads to the convergent result $\lim_{t\to\infty} \Pi\mathcal{Q}_t^{(2)} = \Pi_{\frac{1}{\mathrm{i}\Delta}}\mathcal{R}^{(2)}$, and agrees with the conjecture above. Thus, in the coherent subspace, the conjecture (5.11) becomes an identity. For the orthogonal subspace, in which the superoperator acts on the populations, the form of $\mathcal{Q}^{(2)}$ is inspired by the analytical continuation procedure of Ref. [41] and reviewed in Section 5.1.

Secondly, if we consider the canonical Gibbs state as initial state, i.e., $\varrho(0) = \varrho^{(0)}$, the time evolved state reads according to Eq. (5.7) $\varrho(t) \simeq (\mathbb{1} + \mathcal{Q}_t^{(2)})[\varrho^{(0)}]$. This is compared to the reduced Gibbs state $\varrho \simeq (\mathbb{1} + \mathcal{Q}^{(2)})[\varrho^{(0)}]$. Now, if we use the conjecture (5.11), the asymptotic state for large times approaches the reduced Gibbs state.[3]

Thirdly, as is shown below in Eq. (5.15), the stationary state of the resulting master equation Eq. (5.8) is given by the reduced Gibbs state.

Fourthly, by identifying the superoperator $\mathcal{Q}^{(2)}$ in the fourth-order expansion of the steady state in Eq. (2.57)

$$0 = -\mathrm{i}[H_\mathrm{S}, \varrho^{(4)}] + (\mathcal{R}^{(2)}\mathcal{Q}^{(2)} + \mathcal{R}^{(4)})[\varrho^{(0)}], \tag{5.12}$$

we obtain a necessary condition for $\mathcal{R}^{(4)}$ as a function of $\mathcal{R}^{(2)}\mathcal{Q}^{(2)}$. In detail, by projecting onto the populations, for which $\langle n|[H_\mathrm{S}, \varrho^{(4)}]|n\rangle = 0$, it follows that

$$\langle n|\mathcal{R}^{(4)}[\varrho^{(0)}]|n\rangle = -\langle n|\mathcal{R}^{(2)}\mathcal{Q}^{(2)}[\varrho^{(0)}]|n\rangle\,. \tag{5.13}$$

This necessary condition for the fourth-order superoperator is fulfilled by setting $\mathcal{R}^{(4)} \equiv -\mathcal{R}^{(2)}\mathcal{Q}^{(2)}$, which is identified as the new fourth-order contribution in the canonically consistent quantum master equation (5.8).

By construction, it is straightforward to prove that the steady-state solution of the CCQME is given by the reduced Gibbs state. Inserting the reduced Gibbs state into the CCQME yields

$$\partial_t(\mathbb{1} + \mathcal{Q}^{(2)})[\varrho^{(0)}] = -\mathrm{i}\left[H_\mathrm{S}, (\mathbb{1} + \mathcal{Q}^{(2)})[\varrho^{(0)}]\right] + \mathcal{R}^{(2)}\Big[(\mathbb{1} - \mathcal{Q}^{(2)})(\mathbb{1} + \mathcal{Q}^{(2)})[\varrho^{(0)}]\Big]. \tag{5.14}$$

Using $[H_\mathrm{S}, \varrho^{(0)}] = 0$ and neglecting fourth-order terms in $(\mathbb{1} - \mathcal{Q}^{(2)})(\mathbb{1} + \mathcal{Q}^{(2)}) \simeq \mathbb{1}$, we arrive

[3] Here we neglect the normalization term, which can be dropped in a dynamical theory, since the time-local master equation Eq. (5.8) is trace preserving.

at

$$\partial_t(\mathbb{1}+\mathcal{Q}^{(2)})[\varrho^{(0)}] \simeq -\mathrm{i}[H_\mathrm{S},\varrho^{(2)}]+\mathcal{R}^{(2)}[\varrho^{(0)}]=0. \tag{5.15}$$

Here, by noting that $0=-\mathrm{i}[H_\mathrm{S},\varrho^{(2)}]+\mathcal{R}^{(2)}[\varrho^{(0)}]$ is the second hierarchy (2.56) of the exact equilibrium state, the right-hand side equates to zero, showing that $(\mathbb{1}+\mathcal{Q}^{(2)})[\varrho^{(0)}]$ is indeed the stationary state correct up to second order in the coupling.

The spirit of the CCQME, to steer the dynamics towards the correct asymptotic state, corresponds to a universal concept. Exemplary, it is seen in the Hu-Paz-Zhang master equation of the damped harmonic oscillator. Namely, the Hu-Paz-Zhang master equation is derived, such that it is consistent with the exact dynamics. In particular, in the asymptotic limit there is a one-to-one correspondence of the coefficients in the master equation and the exact equilibrium state. In the next section, we demonstrate that the CCQME also improves the dynamical accuracy, thereby refining the archetypal second-order Redfield and quantum-optical master equation.

5.4 Benchmark with exact dynamics - Guaranteeing positive evolution

We corroborate our method by comparing it to the exactly solvable dynamics for the damped harmonic oscillator [Section 2.6]. For this model, we focus on the time-independent CCQME with asymptotic generator using the approximations

$$\mathcal{Q}_t^{(2)} \simeq \mathcal{Q}^{(2)}, \tag{5.16}$$

and $\mathcal{R}_t^{(2)} \simeq \mathcal{R}^{(2)}$, and prove that the CCQME resolves the long-standing issue of positivity violation, albeit without being of GKSL form. Below, in Section 5.7, we also use the time-dependent generator $\partial_t\varrho(t)=-\mathrm{i}\,[H_\mathrm{S},\varrho(t)]+\mathcal{R}_t^{(2)}\left[(\mathbb{1}-\mathcal{Q}^{(2)})[\varrho(t)]\right]$ with asymptotic $\mathcal{Q}^{(2)}$ but time-dependent Redfield superoperator. Here, in this section, we compare the dynamics of the exact Hu-Paz-Zhang master equation, the CCQME, the Redfield equation, and the quantum-optical master equation. To keep the notation simple, the quantum-optical master equation is referred to as Lindblad equation. We find that our approach, despite not being a GKSL master equation, avoids unphysical negative populations for finite coupling strengths and ensures, by construction, that the equilibrium state is the reduced Gibbs state up to second order.

In Fig. 5.2, for weak coupling $\gamma=0.2\,\Omega$ and low temperature $T=0.3\,\Omega$, we benchmark the dynamics for the initial state $\varrho(0)=\exp[-H_\mathrm{S}/\Omega]/Z_\mathrm{S}$ [(a) and (c)] and the steady state [(b) and (d)] with the exact solution. We quantify the deviation from the exact result again by using the trace distance $\mathrm{dist}(\varrho,\varrho_\mathrm{ex})=(1/2)\,\mathrm{tr_S}\sqrt{(\varrho(t)-\varrho_\mathrm{ex}(t))^2}\in[0,1]$, which is the same

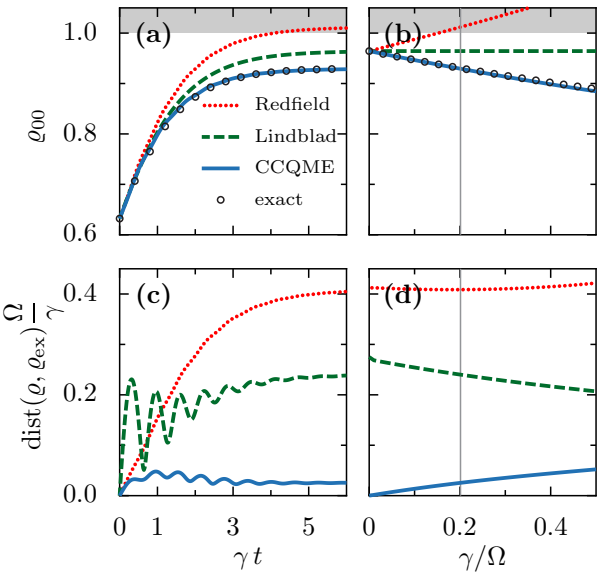

Figure 5.2: Comparison between the Redfield (dotted red), Lindblad (dashed green), CCQME (solid blue), and the non-perturbative exact solution (open circles) for a harmonic oscillator system with frequency Ω coupled to a thermal bath with strength γ. The ground-state population dynamics are shown in (a), while (b) depicts ground-state population in equilibrium. The gray regions in (a) and (b) indicate unphysical regimes where the ground state populations exceed 1. Deviation of the density matrix to the exact result characterized by the trace distance $\mathrm{dist}(\varrho, \varrho_{\mathrm{ex}})$ is shown for the dynamics in (c) and steady state in (d). The system is initiated in $\varrho(0) = \exp[-H_{\mathrm{S}}/\Omega]/Z_{\mathrm{S}}$, and we truncate to the $N = 60$ lowest levels. The bath temperature is $T/\Omega = 0.3$ and has an Ohmic Lorentz-Drude spectral density, $J(\omega) = \gamma\omega/(1 + \omega^2/\omega_{\mathrm{D}}^2)$ with cutoff $\omega_{\mathrm{D}}/\Omega = 5$ and strength $\gamma/\Omega = 0.2$ [(a) and (c)] marked by a gray vertical line in (b) and (d).

quantity studied already for the truncation approach in Section 3.7. Moreover, we plot the corresponding population ϱ_{00} of the ground state for the different approximations.

For the Redfield equation, errors build up over time such that the steady state shows finite errors in second order in H_{SB} [see Fig. 5.2(d)]. In general, at small temperatures as studied here, the trace distance is nearly equivalent to the percentage error in the ground-state population. Therefore, the maximum trace distance of ≈ 0.08 (for $\gamma = 0.2\,\Omega$) for the Redfield case in Fig. 5.2(c) represents a maximum error of $\approx 8\%$. The Lindblad equation shows large oscillations in the trace distance ($\approx 5\%$) but does not suffer from unphysical solutions. The CCQME accurately reproduces the ground state population for all times in Fig. 5.2(a) and shows only small deviations ($< 1\%$ for all times) from the exact solution in Fig. 5.2(c). This is a noticeable improvement to both the Redfield and the Lindblad solutions especially in the regime beyond ultraweak coupling.

In equilibrium increasing the coupling, the ground-state population decreases. In Fig. 5.2(b), the CCQME accurately reproduces this trend and also perfectly matches with the exact curve in the strong coupling regime. On the one hand, the solution of the quantum-optical master equation remains independent of the system-bath coupling γ. On the other hand, the Redfield

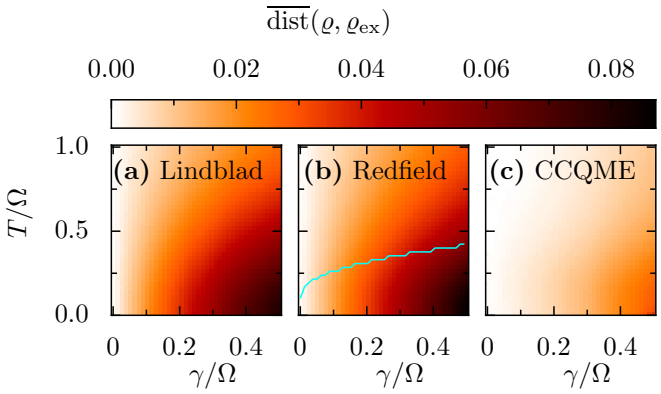

Figure 5.3: Time averaged trace distance ($\overline{\mathrm{dist}}(\varrho, \varrho_{\mathrm{ex}}) = \tau_{\mathrm{R}}^{-1} \int_0^{\tau_{\mathrm{R}}} \mathrm{d}t\, \mathrm{dist}(\varrho, \varrho_{\mathrm{ex}})$) over relaxation time $\tau_{\mathrm{R}} = 2/\gamma$ as a function of temperature and coupling strength for the Lindblad equation (a), Redfield equation (b), and CCQME (c). The Redfield steady-state solution in (b) violates positivity in the parameter regime below the solid teal line. Other parameters are the same as in Fig. 5.2

not only gives an incorrect ground-state population but also erroneously predicts that with increasing coupling strength the the ground-state population increases. At moderate values of the coupling strength, the ground-state population exceeds the value of one, which due to trace preservation, $\mathrm{tr}_{\mathrm{S}}(\varrho) = 1$, implies that the excited states have unphysical negative populations.

We quantify the deviations in second order of the coupling. To this end, we divide the trace distance by the coupling strength and numerically approach the limit of coupling to zero [Fig. 5.2(d)].[4] If the approximate solution matches the exact solution up to second order, this measure approaches zero. In equilibrium, this is the case for the CCQME [solid blue line in Fig. 5.2(d)]. For the Redfield and Lindblad solutions, however, we yield a finite deviation, which shows discrepancies in second-order.

To get a complete overview of the deviations, in Fig. 5.3, we calculate the time-averaged trace distance to the exact result for the entire relaxation process as a function of temperature and coupling strength, when initiating the system in an out-of-equilibrium state. Beyond ultraweak coupling, the Lindblad and Redfield equations are only valid for high bath temperatures, a regime, which is often referred to as classical limit. In contrast, the CCQME leads to a more accurate result in the full parameter regime. Importantly, the CCQME solution yields a positive density matrix in the entire parameter range. This is in sharp contrast to the Redfield dynamics, which fails at low temperatures [below solid teal line in Fig. 5.3(b)].

Here, beyond the results we have published in Ref. [184], it is now shown rigorously that for the particular example of the damped harmonic oscillator the CCQME guarantees a positive evolution up to second order in the coupling. Here, we make use of the fact that the reduced

[4] Let ϱ denote the exact equilibrium state and ϱ^X denote the steady state of the Redfield, Lindblad, or canonically consistent master equation. We expand the difference up to second order in the coupling strength, $\varrho - \varrho^X \simeq \varrho^{(0)} - \varrho^{X(0)} + \varrho^{(2)} - \varrho^{X(2)}$. In zeroth order, the approximate master equations are adequate and the difference vanishes, i.e., $\varrho^{X(0)} = \varrho^{(0)}$. Since $\varrho^{(2)}, \varrho^{X(2)} \propto \gamma$, we obtain the second-order deviations by dividing by γ and approaching the limit of $\gamma \to 0$.

Gibbs state is a Gaussian state and find a superoperator $\mathcal{Q}^{(2)}$, which is of pseudo-Lindblad form. With this, we can connect the CCQME to the Hu-Paz-Zhang master equation, which takes into account the exact equilibrium dispersions $\langle q^2\rangle$ and $\langle p^2\rangle$ up to second order. As discussed in Section 2.6.2, a consistent treatment of displacement and momentum guarantees positivity of the equilibrium state.

In order to address the question of positivity, let us represent the CCQME in real space with center of mass coordinate r and relative coordinate x [Section 2.6.2],

$$\partial_t \varrho(t,x,r) = \mathrm{i}\left(\frac{1}{M}\partial_x\partial_r - M\Omega^2 rx\right)\varrho(t,x,r) + \mathcal{L}^{(2)}(x,r)\left[1-\mathcal{Q}^{(2)}(x,r)\right]\varrho(t,x,r), \tag{5.17}$$

where the first term describes the free, coherent evolution of harmonic oscillator and $\mathcal{L}^{(2)}(x,r) = -\mathrm{i}M\gamma_q^{(2)}rx - \gamma_p^{(2)}x\partial_x - \mathrm{i}MD_q^{(2)}x\partial_r - M^2D_p^{(2)}x^2$ is the positional representation of the Redfield superoperator[5] as can be derived from Section 2.6.2 and Ref. [111].

In Appendix B, we derive a general representation for the superoperator $\mathcal{Q}^{(2)}$, which applies to arbitrary models. For the damped harmonic oscillator, for which the reduced Gibbs state is a Gaussian state with exact equilibrium dispersions $\langle q^2\rangle$ and $\langle p^2\rangle$, in the following, we derive an explicit representation for the superoperator $\mathcal{Q}^{(2)}$. To this end, we perform a Taylor-expansion for the exponential in Eq. (2.84) around the zeroth-order dispersions $\langle q^2\rangle \simeq \langle q^2\rangle^{(0)} + \langle q^2\rangle^{(2)}$ and $\langle p^2\rangle \simeq \langle p^2\rangle^{(0)} + \langle p^2\rangle^{(2)}$, respectively. With this, one finds for the reduced Gibbs state

$$\varrho(x,r) \simeq \left(1 + \frac{1}{2}\frac{\langle q^2\rangle^{(2)}}{\left(\langle q^2\rangle^{(0)}\right)^2}r^2 - \frac{1}{2}\left\langle p^{(2)}\right\rangle^{(2)}x^2\right)\varrho^{(0)}(x,r), \tag{5.18}$$

where one immediately identifies the action of the superoperator

$$\mathcal{Q}^{(2)}(x,r) = \frac{1}{2}\frac{\langle q^2\rangle^{(2)}}{\left(\langle q^2\rangle^{(0)}\right)^2}r^2 - \frac{1}{2}\left\langle p^{(2)}\right\rangle^{(2)}x^2. \tag{5.19}$$

With this, the fourth-order term in the CCQME acts on the state as

$$\mathcal{L}^{(2)}(x,r)\mathcal{Q}^{(2)}(x,r)\varrho(t,x,r) = \Big(-\mathrm{i}MD_q^{(2)}\frac{\langle q^2\rangle^{(2)}}{(\langle q^2\rangle^{(0)})^2}rx + \gamma_p^{(2)}\left\langle p^2\right\rangle^{(2)}x^2 + \mathcal{Q}^{(2)}(x,r)\mathcal{L}^{(2)}(x,r)\Big)\varrho(t,x,r), \tag{5.20}$$

where the first two terms follow from the product rule of the derivatives. They can be captured

[5] It is $\langle q|\mathcal{R}^{(2)}[\varrho(t)]|q'\rangle = \mathcal{L}^{(2)}(x,r)\varrho(t,x,r)$, with $\varrho(t,x,r) = \langle q|\varrho(t)|q'\rangle$ and $r = (q+q')/2$ and $x = q - q'$, respectively.

by redefining

$$\gamma_q^{(2)} \to \gamma_q^{(2)} - D_q^{(2)} \frac{\langle q^2 \rangle^{(2)}}{(\langle q^2 \rangle^{(0)})^2}, \tag{5.21}$$

$$M^2 D_p^{(2)} \to M^2 D_p^{(2)} + \gamma_p^{(2)} \langle p^2 \rangle^{(2)} = \gamma_p^{(2)} (\langle p^2 \rangle^{(0)} + \langle p^2 \rangle^{(2)}), \tag{5.22}$$

which effectively give contributions in fourth order of the coupling. The other coefficients $\gamma_p^{(2)}$ and $D_q^{(2)}$ remain unchanged. The shift of $\gamma_q^{(2)}$ changes the squared frequency and modifies the coherent dynamics. Since it is a fourth-order contribution, it shifts the equilibrium dispersion $\langle q^2 \rangle$ in Eq. (2.88) also in fourth-order, which can be neglected for a consistent second-order theory. Very importantly, the shift of the dissipative coefficient $D_p^{(2)}$, which is related to the momentum dispersion of the stationary state, is corrected in a consistent way. In Section 2.6.2, the inconsistency of $\langle q^2 \rangle$ and $\langle p^2 \rangle$ in the steady state solution of the Redfield equation is found to be the reason, why positivity is violated beyond ultraweak coupling. Fortunately, the CCQME corrects this mismatch in a consistent way and leads to a positive evolution. Note, in this argument we neglect the latter term $\mathcal{Q}^{(2)}(x,r)\mathcal{L}^{(2)}(x,r)$, which is of fourth order in the variables x and r and also contributes to the dynamics. For the damped harmonic oscillator, for which only the momentum dispersion needs to be corrected for a consistent stationary state in second order, this additional term may be dropped. It is an open question what influence this term has on the dynamics. The CCQME and our discussion of positivity only holds for weak coupling in second-order perturbation theory. For stronger coupling, e.g., for $\gamma \gtrsim \Omega$ as discussed in Section 5.5, we observe large deviations between the exact solution and the solution of the CCQME, which eventually also violates positivity.

To end this section, we address the question whether the CCQME can be written in GKSL form. A GKSL master equation might be favourable as it guarantees positivity by the algebraic structure and not depending on the very details of the dissipator. However, for the damped harmonic oscillator, the CCQME resembles the Hu-Paz-Zhang master equation, which is shown to be a pseudo-Lindblad equation as it also includes negative relaxation weights [Section 3.11]. As discussed throughout the previous chapters, a GKSL form is not a necessity for positive evolution, and instead positivity rather depends on the consistency of the master equation. Nevertheless, for the damped harmonic oscillator, the superoperator $\mathcal{Q}^{(2)}$ can be written very compact form as a pseudo-Lindbladian:

To this end, we study the translation of superoperators to differential operators in real space in more detail. Generally, in real space superoperators translate to differential operators

according to the relations [111]

$$x \longleftrightarrow [q, \cdot], \tag{5.23}$$

$$r \longleftrightarrow \frac{1}{2}\{q, \cdot\}, \tag{5.24}$$

$$\partial_x \longleftrightarrow \frac{\mathrm{i}}{2}\{p, \cdot\}, \tag{5.25}$$

$$\partial_r \longleftrightarrow \mathrm{i}[p, \cdot]. \tag{5.26}$$

For instance, we obtain the real-space representation of the Redfield superoperator

$$\mathcal{L}^{(2)}(x, r) \longleftrightarrow \mathcal{R}^{(2)}, \tag{5.27}$$

and the superoperator (5.19)

$$\mathcal{Q}^{(2)}(x, r) \longleftrightarrow \mathcal{Q}^{(2)}. \tag{5.28}$$

A rigorous identification follows by calculating the matrix elements in real space, i.e., $\langle q|\mathcal{R}^{(2)}|q'\rangle$ with $r = (q + q')/2$, $x = q - q'$ and properly inserting identities according to $\mathbb{1} = \int dq\, |q\rangle\langle q|$. The result of this procedure leads to the relations in Eqs. (5.23) to (5.26). Using these relations for $\mathcal{Q}^{(2)}(x, r)$, which is a function of x^2 and r^2, the superoperator $\mathcal{Q}^{(2)}$ would be written with a double commutator $[q, [q, \cdot]]$ and a double anti-commutator $\{q, \{q, \cdot\}\}$.[6] However, as mentioned above, the superoperator $\mathcal{Q}^{(2)}$ is not unique. Here, because $\mathcal{Q}^{(2)}(x, r)$ acts on the Gaussian state

$$\varrho^{(0)}(x, r) = \frac{1}{\sqrt{2\pi \langle q^2\rangle^{(0)}}} e^{-\frac{1}{2}\left(\frac{r^2}{\langle q^2\rangle^{(0)}} + \langle p^2\rangle^{(0)} x^2\right)}, \tag{5.29}$$

a multiplication with r^2 corresponds to a second derivative with respect to r up to multiplication with $(\langle q^2\rangle^{(0)})^2$. We use the explicit relation

$$r^2 \varrho^{(0)}(x, r) = \left(\langle q^2\rangle^{(0)}\right)^2 \partial_r{}^2 \varrho^{(0)}(x, r) \longleftrightarrow -\left(\langle q^2\rangle^{(0)}\right)^2 [p, [p, \varrho^{(0)}]], \tag{5.30}$$

and, thus, find the alternative choice of the superoperator

$$\mathcal{Q}^{(2)}(x, r)\varrho^{(0)}(x, r) = -\frac{1}{2}\left(-\frac{\langle q^2\rangle^{(2)}}{\left(\langle q^2\rangle^{(0)}\right)^2} r^2 + \langle p^{(2)}\rangle^{(2)} x^2\right) \varrho^{(0)}(x, r), \tag{5.31}$$

$$\longleftrightarrow -\frac{1}{2}\left(\langle q^2\rangle^{(2)} [p, [p, \cdot]] + \langle p^2\rangle^{(2)} [q, [q, \cdot]]\right) \varrho^{(0)}, \tag{5.32}$$

[6] The operator structure would be $\mathcal{Q}^{(2)}(x, r) = \frac{1}{2}\frac{\langle q^2\rangle^{(2)}}{(\langle q^2\rangle^{(0)})^2} r^2 - \frac{1}{2}\langle p^{(2)}\rangle^{(2)} x^2 \longleftrightarrow \frac{1}{8}\frac{\langle q^2\rangle^{(2)}}{(\langle q^2\rangle^{(0)})^2}\{q, \{q, \cdot\}\} - \frac{1}{2}\langle p^{(2)}\rangle^{(2)} [q, [q, \cdot]]$.

which acts as a pseudo-Lindbladian with jump operators p and q with weights $\langle q^2\rangle^{(2)} < 0$ and $\langle p^2\rangle^{(2)} > 0$, respectively.

In the CCQME, the superoperator $\mathcal{Q}^{(2)}$ occurs in the contraction with the Redfield superoperator. As shown in Section 5.4.1 below, this leads to a pseudo-Lindbladian with jump operators that are quadratic in q and p.

5.4.1 Contraction of GKSL superoperators

The proposal of the CCQME involves the concatenation (i.e., the product) of two superoperators. This raises the question what the algebraic structure of the resulting superoperator is. In this section, the product of general GKSL superoperators is considered and it is shown that it leads to pseudo-Lindblad superoperators. To start with, consider a GKSL superoperator

$$\mathcal{D}(a)[\varrho] = a\varrho a^\dagger - \{a^\dagger a, \varrho\}, \tag{5.33}$$

e.g., for the purely dissipative dynamics $\partial_t \varrho(t) = \mathcal{D}(a)[\varrho(t)]$. It is solved by $\varrho(t) = e^{\mathcal{D}(a)t}[\varrho(0)]$, which includes all products, i.e., concatenations of GKSL superoperators. In the simplest scenario of a two-level system, e.g., when $a = \sigma_i$ is a Pauli operator, the algebraic structure is reproduced, except for an overall negative weight. Namely $\mathcal{D}(\sigma_i)^2 = -2\mathcal{D}(\sigma_i)$, with an overall negative sign, which is not of GKSL form but instead a pseudo-Lindbladian. For the dynamics, the negative sign is very important as it follows that $\varrho(t) = e^{-2t}\mathcal{D}(\sigma_i)[\varrho(0)]$.

Generally, for squaring a GKSL superoperator one finds the identity

$$\mathcal{D}(a)\mathcal{D}(a) = \mathcal{D}(aa) + \frac{1}{2}\mathcal{D}(a^\dagger a) - \Big(\mathbb{S}[.]a^\dagger - \frac{1}{2}\{a^\dagger\mathbb{S}, [.]\} + a[.]\mathbb{S}^\dagger - \frac{1}{2}\{\mathbb{S}^\dagger a, [.]\}\Big), \tag{5.34}$$

which follows for arbitrary jump operator a after reordering the terms. The first two terms are GKSL superoperators with jump operators given by the products a^2 and $a^\dagger a$, respectively. However, the latter terms break the GKSL form, where the operators a and

$$\mathbb{S} = \frac{1}{2}\Big(aa^\dagger a + a^\dagger aa\Big), \tag{5.35}$$

act non-diagonally on the density matrix. Note that in the previous example the products $a^2 = a^\dagger a = \sigma_i^2 = \mathbb{1}$ yield the identity for which the first two GKSL contributions vanish.

The non-GKSL terms in Eq. (5.34) are crucial and, in fact, have the same algebraic structure as the Redfield dissipator in Eq. (3.16), with $\mathbb{S}$ taking the role of the convoluted operator. Following the diagonalization procedure of Chapter 3, we thus find a pseudo-Lindblad representation for squaring a generic GKSL superoperator,

$$\mathcal{D}(a)\mathcal{D}(a) = \mathcal{D}(a^2) + \frac{1}{2}\mathcal{D}(a^\dagger a) - \Big(\mathcal{D}(A^+) - \mathcal{D}(A^-)\Big), \tag{5.36}$$

with two additional jump operators

$$A^{\pm} = \frac{1}{\sqrt{2}}(\pm a + \mathbb{S}), \tag{5.37}$$

for either positive and negative relaxation weight, respectively. Altogether, the squared GKSL superoperator gives rise to four channels; three with positive weight and one with negative weight. The number of channels and the magnitude of the relaxation weights can be numerically obtained using the test proposed in Ref. [185].

Analogously, by using simple algebraic tools one can find identities for the product of dissipators with different jump operators and for the concatenation of a GKSL superoperator and a coherent contribution, such as $-\mathrm{i}[H, \cdot]$.

5.5 Validity regime of the CCQME

For weak but finite coupling, i.e., $\gamma/\Omega \leq 0.5$, the CCQME very accurately agrees with the exact dynamics. That is because the CCQME is a second-order-consistent master equation, whose coupling strength γ is a perturbative (control) parameter, that governs the precision of the simulated dynamics. Similarly to previous discussion, we calculate the ground-state population in Fig. 5.4(a), (b) and in Fig. 5.4(c), (d) the trace distance to the exact result.

Here, we consider a larger bath temperature $T/\Omega = 1$ for which quantum effects are less relevant. Compared to the system's time scale, given by $1/\Omega$, in this regime the bath correlation function decays much faster and the Markov approximation is well justified. In this high-temperature regime, the Redfield and quantum optical master equations are usually expected to be valid approximations. This is shown in Fig. 5.4, where the results are close together and in

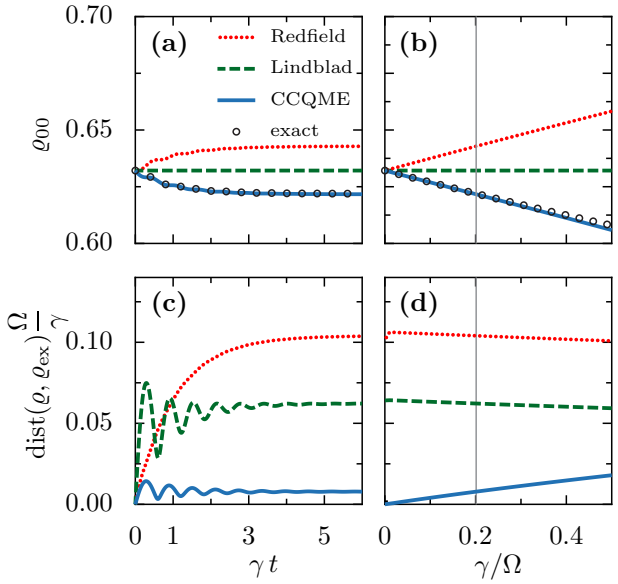

Figure 5.4: Analogous to Fig. 5.2 above; except for a higher bath temperature $T/\Omega = 1$.

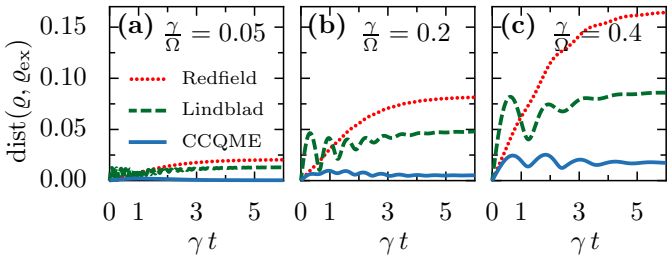

Figure 5.5: Error for Redfield (dotted red), quantum optical master equation (referred to as Lindblad) (dashed green), and CCQME (solid blue) calculated as trace distance to exact result as a function of scaled time for different values of the coupling strength (a) $\gamma/\Omega = 0.05$, (b) $\gamma/\Omega = 0.2$, and (c) $\gamma/\Omega = 0.4$. The initial state is $\varrho(0) = \exp[-H_{\mathrm{S}}/\Omega]/Z_{\mathrm{S}}$ and the bath temperature is $T/\Omega = 0.3$. For the simulation we take the Markovian master equations with Drude cutoff $\omega_{\mathrm{D}}/\Omega = 5$.

particular the Redfield solution remains positive. However, strictly speaking also here both the results of the Redfield and quantum optical master equations only remain valid for ultraweak coupling, whereas the CCQME accurately captures the ground state population also for finite coupling in Fig. 5.4 and overall has the smallest trace distance to the exact result [Figs. 5.4 and 5.5]. In contrast, the steady-state solutions of the quantum optical master equation are independent of the coupling strength and the Redfield result increases with coupling strength, as seen in Fig. 5.4(b) and Fig. 5.2(b). As described in the main text, for stronger coupling the effective temperature should increase and the higher lying states should get populated, a property only captured by the CCQME.

In Fig. 5.5 we plot the trace distance for different values of the system-bath coupling strength γ. By construction, the steady state of the CCQME accurately captures finite coupling effects but it is not obvious that it also leads to accurate dynamics. In the main text, we analyze the

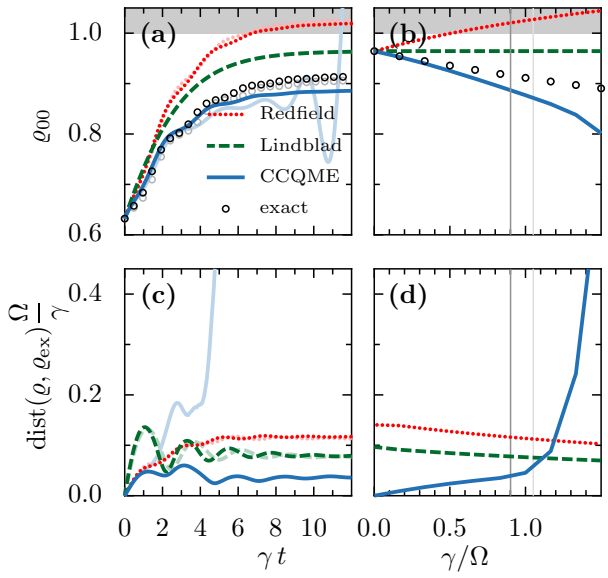

Figure 5.6: Analogous to Fig. 5.2; except for $\gamma/\Omega = 0.9$ (dark lines and symbols), $\gamma/\Omega = 1.01$ (light lines and symbols), and $\omega_{\mathrm{D}}/\Omega = 1$.

time averaged trace distance as a function of bath temperature and coupling strength. Here, we give an overview for the dynamics of the trace distance for different values of the coupling strength. All panels show qualitatively similar results, with the CCQME outperforming the other quantum master equations. Moreover, the trace distance between the results of the CCQME and exact master equation decreases monotonically with smaller values of the coupling not only in the steady-state regime but also throughout the evolution.

If we increase γ beyond the second-order coupling regime, i.e., $\gamma/\Omega \approx 1$, the CCQME steady state starts to deviate significantly from the exact result but the solution is still positive [see dark lines and symbols in Fig. 5.6]. For strong coupling $\gamma/\Omega > 1$, the approximations leading to the CCQME are no longer valid and the solution may violate positivity [see light lines and symbols in Fig. 5.6]. On the other hand, for weak-coupling approaches like the Redfield equation, positivity is already violated for $\gamma/\Omega \approx 0.5$.

5.6 CCQME for systems coupled to multiple baths

We now consider nonequilibrium setups, as, e.g., in Refs. [186–190], where the system is driven by several independent baths, $H_\mathrm{B} = \sum_\alpha H_{\mathrm{B}\alpha}$, which couple to the system via the interaction Hamiltonian $H_\mathrm{SB} = \sum_\alpha S_\alpha \otimes (B_\alpha + B_\alpha^\dagger)$. In second order of the coupling, the Redfield and quantum-optical master equations are obtained by adding the dissipative superoperators for the individual baths as discussed in Sections 3.7.3 and 3.9 for the boundary driven Hubbard chain.

In contrast to equilibrium, e.g., where all baths have the same temperature, in nonequilibrium the stationary state is not dictated by statistical mechanics. Thus, in principle, we cannot steer the dynamics towards a known stationary state. However, the basic concept underlying the CCQME, i.e., connecting the asymptotic dynamical map with the stationary state, is still applicable. Furthermore, for the stationary state, the superoperators $\mathcal{Q}_\alpha^{(2)}$ can still be obtained for each bath individually, following rigorously from the Redfield superoperators $\mathcal{R}_\alpha^{(2)}$ according to Eq. (5.10).

We propose the CCQME for boundary driven systems as

$$\partial_t \varrho(t) = -\mathrm{i}[H_\mathrm{S}, \varrho(t)] + \sum_\alpha \mathcal{R}_{t,\alpha}^{(2)} \left[\left(\mathbb{1} - \sum_\beta \mathcal{Q}_{t,\beta}^{(2)} \right) [\varrho(t)] \right], \tag{5.38}$$

which contains products of superoperators for different baths, as they naturally occur beyond second order [126, 127].

Let us test this ansatz by studying a boundary-driven harmonic oscillator. We apply the CCQME to a minimal transport setup, where the harmonic oscillator is driven by two independent thermal baths as depicted schematically in Fig. 5.7(a).

For uncorrelated baths, the damping kernels $\bar{\kappa}_\alpha(z)$ (2.97) are added, such as the temporal

correlations $C_\alpha(t)$ (2.10). Consequently, the autocorrelation function $\bar{\chi}(z)$ (2.101) and the influence kernels $K_q(t)$ (D.20) and $K_p(t)$ (D.21) are altered to

$$\bar{\chi}(z) = \frac{1}{z^2 + z\sum_\alpha \bar{\kappa}_\alpha(z) + \Omega^2}, \tag{5.39}$$

$$K_q(t) = \int_0^t \mathrm{d}s \int_0^t \mathrm{d}u \sum_\alpha \mathrm{Re}[C_\alpha(|s-u|)]\, G(s)\, G(u), \tag{5.40}$$

$$K_p(t) = \int_0^t \mathrm{d}s \int_0^t \mathrm{d}u \sum_\alpha \mathrm{Re}[C_\alpha(|s-u|)]\, \dot{G}(s)\, \dot{G}(u). \tag{5.41}$$

The remaining structure of the coefficients $\gamma_q(t)$, $\gamma_p(t)$, $D_q(t)$ and $D_p(t)$ is the same as in equilibrium allowing us to obtain and solve the exact Hu-Paz-Zhang master equation for the nonequilibrium scenario.

For the CCQME, we start from the time-nonlocal equation of motion

$$\partial_t \varrho(t) = -\mathrm{i}[H_\mathrm{S}, \varrho(t)] + (\mathcal{R}_l^{(2)} + \mathcal{R}_r^{(2)})[e^{-\mathrm{i}[H_\mathrm{S},\cdot]t}[\varrho(0)]], \tag{5.42}$$

where the Redfield operators for the left and right bath, respectively, act on the freely evolving initial state. We now replace the initial state according to the inverse map

$$e^{-\mathrm{i}[H_\mathrm{S},\cdot]t}[\varrho(0)] \simeq (\mathbb{1} - \mathcal{Q}_l^{(2)} - \mathcal{Q}_r^{(2)})[\varrho(t)], \tag{5.43}$$

where the superoperators are obtained from Eqs. (5.10) and (B.20). We arrive at the boundary

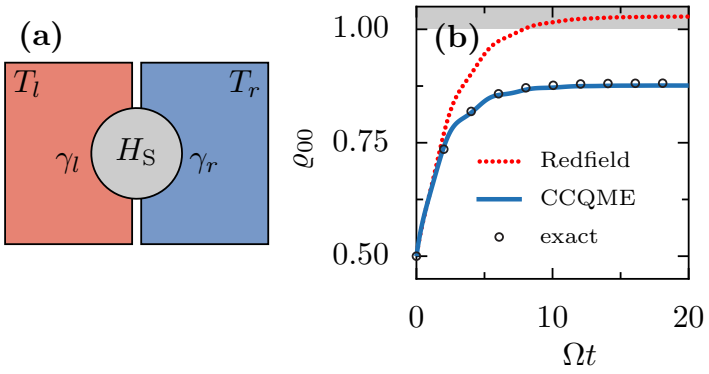

Figure 5.7: Harmonic oscillator coupled to two independent baths illustrated in panel (a). Dynamics for the ground state population when the system is initiated in a superposition of the ground and first excited state $|\psi(0)\rangle = (1/\sqrt{2})\,(|0\rangle + |1\rangle)$ under the Redfield equation (dotted red), boundary driven CCQME (solid blue), and the exact solution (open black circles) in panel (b). For the simulation $N = 20$ first levels are taken. The bath parameters are $\gamma_l/\Omega = \gamma_r/\Omega = 0.2$, $T_l/\Omega = 0.3$, $T_r/\Omega = 0.5$, and $\omega_\mathrm{D}/\Omega = 5$.

driven CCQME,

$$\partial_t \varrho(t) = -\mathrm{i}\,[H_\mathrm{S}, \varrho(t)] + (\mathcal{R}_l^{(2)} + \mathcal{R}_r^{(2)})[(\mathbb{1} - \mathcal{Q}_l^{(2)} - \mathcal{Q}_r^{(2)})[\varrho(t)]]. \tag{5.44}$$

For Ohmic baths with a Drude cutoff, the dynamics for the ground state population is depicted in Fig. 5.7(b). As expected, for low temperatures and finite coupling, the Redfield theory shows unphysical behaviour with the ground-state population exceeding unity. On the contrary, the CCQME shows good agreement with the exact solution, corroborating our claim that Eq. (5.38) is suitable for studying the dynamics of quantum systems coupled to multiple baths.

5.7 Numerical complexity of the CCQME and comparison to the hierarchical equations of motion approach

The CCQME involves the product of two second-order superoperators and is, therefore, effectively a fourth-order master equation that is constructed to correctly capture the state in second order. A rigorous derivation of the fourth-order master equation is cumbersome: Not only does it involve multiple time integrals [191, 126] and four-point bath correlations [192], but also involves quadratic divergences in time, which cannot be cured by simply taking the time-derivative as in the second-order Redfield formalism [127].

On the contrary, the conceptual complexity of the CCQME is the same as for the second-order Redfield equation. The engineered $\mathcal{Q}^{(2)}$ superoperator only involves the coupling density and its derivatives and does not require more resources than the Redfield superoperator.

The CCQME is explicitly implemented in the eigenbasis of the system, for which we use exact diagonalization of the system Hamiltonian H_S. The contraction of the superoperators $\mathcal{R}^{(2)}\mathcal{Q}^{(2)}$ is a product of two tensors $\sum_{ij} \mathcal{R}_{nm}^{(2)\,ij} \mathcal{Q}_{ij}^{(2)\,qk}$, each with rank four and with $\mathcal{R}_{nm}^{(2)\,ij} = \langle n|\mathcal{R}^{(2)}[|i\rangle\langle j|]|m\rangle$ being the matrix elements $\langle n|\cdot|m\rangle$ of the state that follows from applying the Redfield superoperator onto $|i\rangle\langle j|$. The tensor elements $\mathcal{Q}_{ij}^{(2)\,qk}$ are defined analogously. In a numerical implementation of the time-independent CCQME, the product is carried out only once and is stored as tensor in the memory.

The dynamics under a generic master equation $\partial_t \varrho(t) = \mathcal{R}[\varrho(t)]$ with time-independent generator $\mathcal{R}$, is obtained by consecutive application of the generator[7]

$$\varrho(t) = \sum_{n=0}^{\infty} \frac{t^n}{n!} \underbrace{\mathcal{R}[\mathcal{R}[\ldots}_{n\text{-fold}}[\varrho(0)]\ldots]]. \tag{5.45}$$

[7] Software libraries, such as QUTIP [150], use integration schemes which adapt the time step, which is also extended to time-dependent generators. Other routines use a spectral decomposition of the generator. The latter is also a way to obtain the stationary state as eigenvector to the eigenvalue zero.

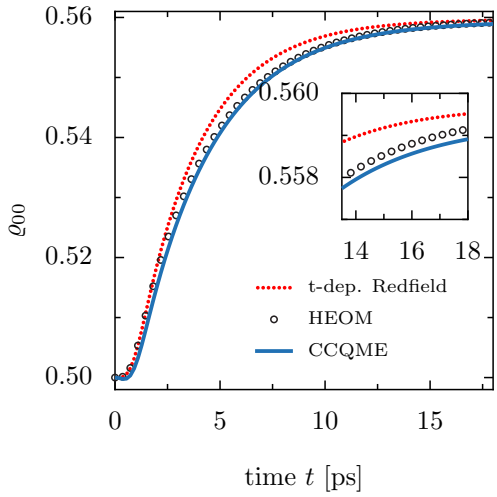

Figure 5.8: Comparison of the spin-boson ground-state dynamics with the hierarchical-equations-of-motion data taken from Ref. [75] [open circles], time-dependent Redfield [dotted red], and the CCQME result [solid blue]. The parameters are chosen as $\varepsilon = \pi/2\,\mathrm{ps}^{-1}$, $T = 50\,K$, $\lambda = 0.01485\,\mathrm{ps}^{-1}$, and $\omega_c = 2.2\,\mathrm{ps}^{-1}$.

As an alternative to perturbative master equations, the reduced dynamics can also be described by numerically exact *hierarchical equations of motion* [74–76]. There, the idea is to express the equation of motion with functional derivatives that are interpreted as auxiliary states, the hierarchies, to which the reduced state couples. The dynamics is the simulated via a stochastic unraveling and by truncating the hierarchies at a certain order. In the deep quantum regime, i.e., for low bath temperatures, the number of hierarchies growths exponentially and is often not feasible for larger systems. This is in particular the regime in which the CCQME is beneficial, since it does not require more computational resources than the Redfield equation, but yields accurate dynamics.

In this section, we compare the CCQME with hierarchical equations of motion for the spin-boson model. Note that the spin-boson model can also be solved using the reaction-coordinate approach, which is less computationally expensive than the hierarchical equations of motion, but still more expensive than the CCQME [88, 37, 193]. The total system-bath Hamiltonian reads

$$H_{\mathrm{tot}} = \frac{\varepsilon}{2}\sigma_x + \sigma_z \sum_k g_k(a_k^\dagger + a_k) + \sum_k \omega_k a_k^\dagger a_k, \tag{5.46}$$

and we consider an Ohmic spectral density with exponential cutoff

$$J(\omega) = \sum_k g_k^2 \delta(\omega - \omega_k) = \lambda(\omega/\omega_c)e^{-\omega^2/\omega_c^2}. \tag{5.47}$$

For the Redfield dynamics, we take the time-dependent coupling density $G_t(\Delta)$ (2.18) with bath correlation function $C(t)$ (2.10). For ultraweak coupling and high bath temperatures, the

Redfield equation guarantees positivity as shown explicitly for the ground state population in Fig. 5.8. However, it does not match the numerically exact hierarchical-equations-of-motion dynamics. For the CCQME, we combine the time-dependent Redfield equation with the static $\mathcal{Q}^{(2)}$ superoperator and obtain accurate dynamics without the computational complexity of the hierarchical equations of motion.

5.8 CCQME for a many-body Hamiltonian

Having benchmarked the performance for a single-spin-boson model, here, we demonstrate the performance of the CCQME for a genuine many-body system. For the results presented in this section, we gratefully acknowledge the contribution of Alexander Schnell.

As the model we choose an Ising chain of length L with open boundary conditions and external fields in x- and z-direction coupled to a bosonic Drude bath. The corresponding total system-bath Hamiltonian reads,

$$H_{\mathrm{tot}} = -J\sum_{i=1}^{L-1}\sigma_z^i\sigma_z^{i+1} + \sum_{i=1}^{L}\left(h_x^i\sigma_x^i + h_z^i\sigma_z^i\right) + \sigma_z^{L/2}\sum_k g_k(a_k^\dagger + a_k) + \sum_k \omega_k a_k^\dagger a_k, \tag{5.48}$$

where the bath is coupled locally via $\sigma_z^{L/2}$ to the central site. In order to avoid near degeneracies

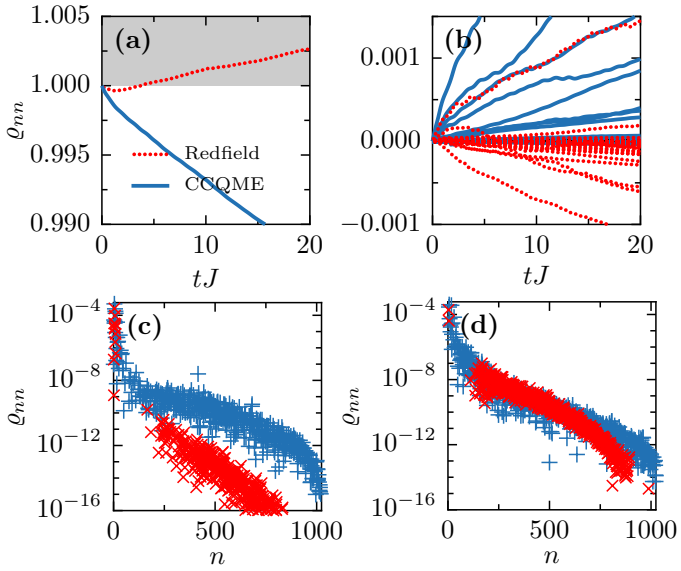

Figure 5.9: Many-body populations of a spin chain of length $L = 10$ coupled locally to a Lorentz-Drude bath for (a) the many-body ground state and (b) all excited states as a function of time t. Snapshot of the populations at (c) $t = 1/J$ and (d) $t = 20/J$, red (blue) crosses depict Redfield (CCQME). On the logarithmic scale, only positive populations can be shown. Redfield eventually predicts negative populations that are of the order of the coupling strength, while the CCQME remains mostly positive at long times. The parameters are chosen as $\gamma = 0.04J$, $T = 0.9J$, and $\omega_{\mathrm{D}} = 5J$.

in the many-body spectrum, we choose slowly twisting fields according to

$$h_x^i = 0.8J + \frac{i-1}{L-1}0.2J, \tag{5.49}$$

$$h_z^i = 0.7J - \frac{i-1}{L-1}0.2J, \tag{5.50}$$

that break the underlying symmetries and lift degeneracies.

We consider a Drude spectral density $J(\omega) = \sum_k g_k^2 \delta(\omega - \omega_k) = \gamma\omega/(1 + (\omega/\omega_\mathrm{D})^2)$, with coupling strength γ and cutoff ω_D. Such a spectral density is not easy to treat via hierarchical equations of motion [75] or reaction coordinate mapping to residual baths [82–84, 37]. In the latter case, the residual coupling is proportional to the width of the Drude spetral density. Hence, the relatively large system size of $L = 10$ (and Hilbert space dimension $2^{10} = 1024$) is inaccessible for those methods using a machine with 64GB RAM as we use it, while we are still able to solve the CCQME.

In Fig. 5.9, we plot the dynamics of the populations ϱ_{nn} of the many-body eigenstates for a chain of length $L = 10$ both for the Redfield master equation as well as for the CCQME, starting in the pure many-body ground state $\varrho(0) = |\psi_0\rangle\langle\psi_0|$. Remarkably, even though the Redfield solution is unphysical, with many negative populations of the excited states [Fig. 5.9(b)] and a ground-state population above unity [Fig. 5.9(a)], the ground-state population for the CCQME solution remains physical at all times, and positivity violation of the excited state populations is rare and of small magnitude. At $t = 20/J$ the negative populations in Redfield sum up to $\sum_{n,\varrho_{nn}<0} \varrho_{nn}(t) \approx -4.3 \cdot 10^{-2}$ which is of the order of the coupling strength $\gamma/J = 4 \cdot 10^{-2}$. For the CCQME, the negative populations only appear in second order of the coupling strength, $\sum_{n,\varrho_{nn}<0} \varrho_{nn} \approx -6.7 \cdot 10^{-5}$, which is three orders of magnitude lower compared to Redfield.

5.9 Concluding remarks to the canonically consistent quantum master equation

In this chapter, we propose a quantum master equation, which corrects the standard Born-Markov equations (Redfield or quantum optical) incorporating effects of higher order in system-bath coupling, so that also the populations are accurately captured in second order. The CCQME draws inspiration from the statistical reduced Gibbs state and correctly steers the dynamics of a quantum system coupled with finite strength to a reservoir. By construction, it yields the exact equilibrium state and significantly improves the dynamics as compared to the Redfield or Lindblad equation. Despite not being being of GKSL form our approach does not suffer from negative solutions, which we prove explicitly for the damped harmonic oscillator. The CCQME is not only accurate but also easy to implement since it requires no additional

information as compared to the Redfield equation.

Moreover, it is model-independent and could shed light onto finding leading order correction due to the presence of system-bath coupling in the emerging field of strong-coupling quantum thermodynamics [194–197, 125] or in dissipative quantum many-body systems as demonstrated for an Ising chain. The CCQME could also be extended to study transport through systems strongly connected to multiple reservoirs aiding the field of strong-coupling quantum transport [198, 193, 199, 200].

We mainly focus on time-independent master equations using the approximation $\mathcal{Q}_t^{(2)} \simeq \mathcal{Q}^{(2)}$ for asymptotic large times. This is, however, easily combined with the time-dependent Redfield superoperator $\mathcal{R}_t^{(2)}$. In future work, one might use a hybrid approach using a fully time-dependent CCQME. To this end, one may combine the Dyson-series expansion of the reduced dynamical map, in Eq. (5.5), which yields

$$\mathcal{Q}_t^{(2)} = \int_0^t e^{\mathrm{i}[H_\mathrm{S},\cdot](\tau_1 - t)} \mathcal{R}_{\tau_1}^{(2)} e^{-\mathrm{i}[H_\mathrm{S},\cdot](\tau_1 - t)} d\tau_1, \tag{5.51}$$

and use it for the CCQME on short times t, where $\mathcal{Q}_t^{(2)} \ll \mathbb{1}$ is guaranteed. For asymptotic times, where the integral diverges linearly with time, replace $\mathcal{Q}_t^{(2)} \simeq \mathcal{Q}^{(2)}$ from Eq. (5.10).

6 Prelude to Future Directions

In the previous chapters, autonomous open quantum systems with a time-independent total Hamiltonian are considered that couple weakly to baths at equilibrium. In this chapter, we extend the view into two different directions:

In Section 6.1, the ultrastrong coupling regime is considered, for which we focus on the reduced equilibrium state proposed in Ref. [135]. Despite being conceptually very different, it is shown that ultrastrong coupling shares common aspects with ultraweak coupling.

Furthermore, in Section 6.2, we consider driven-dissipative open quantum systems that are periodically driven. It is shown that the methods developed in Chapters 3 and 4, which rely on a basis-free formulation of the Redfield equation, can directly be applied also to this case. Introducing a basis, however, is in contrast to autonomous systems. Here, another basis, spanned by the Floquet modes, is the preferred basis to express the Redfield equation. The differences to autonomous systems are pointed out and the idea for a consistent asymptotic state for finite coupling is formulated.

6.1 Ultrastrong coupling

Ultrastrong coupling between system and bath is conceptually very different from weak coupling, because system and bath are not well separated, but instead get strongly correlated. One may approach the ultrastrong coupling regime by doing a perturbative expansion for small inverse coupling. In this way, concepts of the ultraweak-coupling approach might be adapted. First of all, as seen for ultraweak coupling, a certain basis, i.e., the energy eigenbasis of the system Hamiltonian, is distinguished. In fact, the rotating-wave approximation for the quantum-optical master equation is closely related to the eigenbasis representation of the unperturbed problem. It leads to a dynamical decoupling of coherences and populations, where the coherences decay exponentially with time and the populations obey a rate equation. The steady state is diagonal in the energy eigenbasis and independent of the coupling strength and, thus, can be accurate only in the limit of coupling approaching zero.

Very recently, in Refs. [91, 135], it has been shown that for ultrastrong coupling the equilibrium state is diagonal with respect to the eigenstates $|s_n\rangle$ of the coupling operator S in $H_{\mathrm{SB}} = S \otimes (B^\dagger + B)$, which now defines the unperturbed problem. By starting from the exact equilibrium state of the total system-bath compound and tracing out the bath, the reduced

Gibbs state can be obtained [Appendix B]. In the limit of ultrastrong coupling, the reduced Gibbs state is given by [135]

$$\varrho = \frac{\mathrm{tr_B}\, e^{-\beta(H_\mathrm{S}+H_\mathrm{SB}+H_\mathrm{B})}}{Z_\mathrm{tot}} \overset{\|H_\mathrm{SB}\|\to\infty}{\longrightarrow} \frac{e^{-\beta\sum_n P_n H_\mathrm{S} P_n}}{\mathrm{tr_S}\, e^{-\beta\sum_n P_n H_\mathrm{S} P_n}}, \tag{6.1}$$

which agrees with the canonical Gibbs state, except for the fact that the effective Hamiltonian H_eff that for the equilibrium state is defined as, $\varrho = \frac{e^{-\beta H_\mathrm{eff}}}{\mathrm{tr_S}\, e^{-\beta H_\mathrm{eff}}}$ [Appendix B], is the projection $P_n = |s_n\rangle\langle s_n|$ onto the pointer basis. This stationary state is in agreement with a dynamical theory proposed in Ref. [91] for ultrastrong coupling. There, it is found that the coherences decay rapidly and decouple from the population dynamics, which obey a rate equation. We may conclude that the ultrastrong coupling limit is analogous to the ultraweak coupling limit described by the quantum-optical master equation.

To bridge the gap between a consistent second-order theory for weak, but finite coupling, which is the focus of this thesis, and the ultrastrong coupling limit, several questions arise: What is the second-order theory for strong, but finite coupling? Or, more specifically, what is the analog of the second-order Redfield equation for strong coupling? Does it obey (complete) positivity and would it be of GKSL or pseudo-Lindblad form. In the latter case, what would be the symmetry transformations? Can it be efficiently unravelled by pseudo-Lindblad quantum trajectories [Chapter 4]? Can we formulate a more consistent ultrastrong master equation by steering the dynamics towards the correct asymptote [Chapter 5]? The answers to these questions would go beyond the scope of this thesis. Nevertheless, the evident similarities between ultraweak coupling and ultrastrong coupling suggest that all the questions can be answered in one or the other way.

In the following, the proposal of the ultrastrong equilibrium state of Ref. [135] is confirmed for the spin-boson model and the damped harmonic oscillator. Here, we also address whether the limit of ultrastrong coupling is approached on an exponential or power-law scale with respect to the coupling strength. Firstly, the exact equilibrium state of the spin-boson model is considered and it is found that the ultrastrong coupling limit is approached exponentially. Secondly, for the damped harmonic oscillator we observe a power-law dependence.

6.1.1 Equilibrium state of spin-boson model for ultrastrong coupling

In this section, Eq. (6.1), which has been the result of Ref. [135], is tested for the spin-boson model with total system-bath Hamiltonian[1]

$$H_\mathrm{tot} = \Delta\sigma^z + \gamma S \otimes B + H_\mathrm{RN} + H_\mathrm{B}, \tag{6.2}$$

[1] In this section, the definition of the coupling strength, i.e., $H_\mathrm{SB} \propto \gamma$, does not agree with the rest of this work, where $H_\mathrm{SB} \propto \sqrt{\gamma}$ is taken.

with the coupling operator $S = \cos(\theta)\sigma^z + \sin(\theta)\sigma^x$ and the renormalization Hamiltonian $H_{\mathrm{RN}} = -G''_{\mathrm{RN}}S^2$, which is introduced in Sections 2.4.3 and 2.6. For this model, the effective Hamiltonian that yields the exact reduced Gibbs state, is derived in Ref. [201]. There, the authors perform a unitary polaron transformation that acts on the system and the bath to arrive at the low-temperature approximation

$$H_{\mathrm{eff}}(\gamma) = \frac{\Delta}{2}\left[(1+e^{-\frac{2\gamma^2}{\Omega^2}}) + (1-e^{-2\frac{\gamma^2}{\Omega^2}})\cos(2\theta)\right]\sigma^z + \frac{\Delta}{2}(1-e^{-2\frac{\gamma^2}{\Omega^2}})\sin(2\theta)\sigma^x, \tag{6.3}$$

which is valid for a Brownian spectral density with peak at frequency Ω and dimensionless width parameter ξ,

$$J(\omega) = \gamma^2\omega\frac{4\xi\Omega^2}{(\omega^2-\Omega^2)^2 + (2\pi\xi\Omega\omega)^2}. \tag{6.4}$$

By noting the pointer basis states, i.e., the two eigenstates $|s_+\rangle = \cos(\theta/2)\,|0\rangle + \sin(\theta/2)\,|1\rangle$ and $|s_-\rangle = \sin(\theta/2)\,|0\rangle - \cos(\theta/2)\,|1\rangle$ of the coupling operator S, with $|0\rangle$ and $|1\rangle$ being eigenstates of σ^z, one easily shows that in the limit of ultrastrong coupling the effective Hamiltonian coincides with the proposal of [135],

$$\begin{aligned} H_{\mathrm{eff}}(\gamma\to\infty) &= \frac{\Delta}{2}\left([1+\cos(2\theta)]\sigma^z + \sin(2\theta)\sigma^x\right), \\ &= \langle s_-|H_{\mathrm{S}}|s_-\rangle\,|s_-\rangle\langle s_-| + \langle s_+|H_{\mathrm{S}}|s_+\rangle\,|s_+\rangle\langle s_+|\,. \end{aligned} \tag{6.5}$$

In addition, for this particular model, the ultrastrong limit is a fair approximation already for moderate values of γ/Ω because of the exponential dependence of $H_{\mathrm{eff}}(\gamma)$ on γ.

6.1.2 Equilibrium state of the damped harmonic oscillator for ultrastrong coupling

For the damped harmonic oscillator, a detailed discussion of an effective Hamiltonian is found in Ref. [128]. In contrast to the Hamiltonian of mean force in Ref. [125], the effective Hamiltonian is not unique but might differ by a constant energy shift. However, the reduced equilibrium state is still unique, since this constant drops out. As discussed in Section 2.6.2, the exact equilibrium state is a Gaussian state, which is only described by the dispersions of displacement and momentum, $\langle q^2\rangle$ and $\langle p^2\rangle$, respectively. The real-space representation Eq. (2.84)

$$\langle q|\varrho_G|q'\rangle = \frac{1}{\sqrt{2\pi\,\langle q^2\rangle}}e^{-\frac{1}{2}\left(\frac{(q+q')^2}{4\langle q^2\rangle} + \langle p^2\rangle(q-q')^2\right)}, \tag{6.6}$$

is a suitable starting point for the comparison with the ultrastrong-coupling state of Ref. [17], as the coupling operator $S = q$ is given by the displacement operator.

For ultrastrong coupling, the leading order terms for $|\nu_l|\bar{\kappa}(\nu_l|) \gg \Omega^2$ in the Matsubara series in Eqs. (D.17) and (D.18) yield

$$M\left\langle q^2\right\rangle \simeq \frac{1}{\beta}\sum_{l=-\infty}^{\infty}\frac{1}{|\nu_l|\bar{\kappa}(|\nu_l|)}, \tag{6.7}$$

$$\frac{1}{M}\left\langle p^2\right\rangle \simeq \frac{1}{\beta}\sum_{l=-\infty}^{\infty}1 \to \infty, \tag{6.8}$$

for which the momentum dispersion is found to diverge. Therefore, the matrix elements for $q \neq q'$ vanish and the reduced equilibrium state is diagonal in the pointer basis, i.e., $\langle q|\varrho_G|q'\rangle = \delta_{q,q'}(2\pi\left\langle q^2\right\rangle)^{-1/2}e^{-q^2/2\left\langle q^2\right\rangle}$, which is already in agreement with the result of Ref. [17].

Quantitatively, since the damping kernel $\kappa(|\nu_l|)$ is of second order in the coupling strength, for infinite coupling the exact reduced equilibrium state approaches an infinitely localized state in real space $\langle q|\varrho_G|q\rangle \to \delta(q)$. Thus, when the coupling dominates all energy scales, the stationary state is temperature independent and also scale invariant with respect to the system energy scale Ω. The direct comparison with the prediction of Ref. [17] is not very obvious, as one would have to project the kinetic energy operator to the diagonals in real space, i.e., $\int \langle q|p^2|q\rangle\,|q\rangle\langle q|\,dq$. Furthermore, how the ultrastrong-coupling limit is approached as a function of the coupling strength depends on the detailed form of the damping kernel and with this on the spectral density. In particular, the analysis of the exact and time-dependent coefficients in the Hu-Paz-Zhang master equation in Fig. D.1 shows that the limit of ultrastrong coupling is not always well-defined for a Drude spectral density. Whether other bath models give finite results should be considered in more detail.

6.2 Time-periodically driven open quantum systems

The previous chapters, deal with open quantum systems that are coupled to equilibrium baths and in detail with a dynamical theory for the reduced state of the system. It is motivated by the experimental progress of driven-dissipative quantum many-body systems, where, for instance, a system can be driven out of equilibrium by coupling it to multiple reservoirs. Alternatively, the system can also be driven time-periodically. In the presence of a bath, time-periodically-driven systems are usually treated using Floquet-Born-Markov theory [63, 5, 64, 202, 11].

However, for time-periodically driven systems the quantum-optical master equation, which requires the rotating-wave approximation, is even more questionable than for undriven systems, since the system's timescale is crucially influenced by the drive. In particular, the quasienergies are not unique but only defined up to multiples of the drive quanta, which is reviewed in detail in Ref. [203]. As a result, the average level splitting is given by ω/D with driving frequency ω and state-space dimension D. It thus decreases exponentially with the system size, challenging the RWA. Thus, the same issues known for autonomous open quantum systems apply even

more to time-periodically driven open quantum systems. In this section, it is briefly mentioned that the formalisms developed in Chapters 3 and 4 for the Redfield equation can directly be applied also to this case. Here, we also pave the way for a consistent modification of the Redfield theory [Chapter 5] in the spirit of an analytical continuation for the asymptotic state that provides the correct populations in second order.

6.2.1 Floquet-Born-Markov theory

In a perturbative expansion for weak system-bath coupling, presented in Section 2.4, a second-order master equation is obtained. In particular, all arguments also apply to time-periodically-driven systems. Analogously to Eq. (2.42), one obtains the Redfield equation $\partial_t \varrho(t) = -\mathrm{i}[H_\mathrm{S}(t), \varrho(t)] + (\mathbb{S}_t \varrho(t) S - S\mathbb{S}_t \varrho(t) + \mathrm{H.c})$, for a system-bath interaction $H_\mathrm{SB} = S \otimes (B^\dagger + B)$ and time-periodic system Hamiltonian,

$$H_\mathrm{S}(t) = H_\mathrm{S}(t+T), \tag{6.9}$$

with time-period $T = 2\pi/\omega$. Thus, analogously we find the pseudo-Lindblad representation with symmetry parameters, which can be tuned to minimize the negative relaxation weight, in order to truncate the negative contribution [Chapter 3]. Furthermore, the pseudo-Lindblad quantum trajectory (PLQT) unraveling can also be applied directly [Chapter 4].

For the convoluted operator of the time-periodically driven systems, $\mathbb{S}_t = \int_0^t C(\tau)\boldsymbol{S}(-\tau)d\tau$, the interaction-picture operator is given by

$$\boldsymbol{S}(-t) = U^\dagger(-t,0) S U(-t,0), \tag{6.10}$$

with the time-evolution operator

$$U(t,0) = T_< e^{-\mathrm{i}\int_0^t H_\mathrm{S}(\tau)d\tau}, \tag{6.11}$$

with time-ordering operator $T_<$.[2] In contrast to the energy eigenbasis for autonomous systems, here, the distinguished basis is given by the time-periodic Floquet modes $|u_q(t)\rangle = |u_q(t+T)\rangle$ and associated quasienergies ε_q satisfying [65, 204]

$$U(t,0)\,|u_q(0)\rangle = e^{-\mathrm{i}\varepsilon_q t}\,|u_q(t)\rangle\,. \tag{6.12}$$

The Floquet modes are eigenstates of the one-cycle time-evolution operator, $U(T,0)\,|u_q(0)\rangle = e^{-\mathrm{i}\frac{2\pi}{\omega}\varepsilon_q}\,|u_q(0)\rangle$, where the eigenvalues define the quasienergies up to multiples of the driving quanta ω. Thereby, two quasienergies ε_q, ε_q' differing only by integer multiples of ω are equivalent. The dynamics within one period of the drive is referred to as the micromotion [203].

[2] Here the time-ordering operator is denoted by $T_<$, not to confuse it with the period T of the drive.

The matrix elements of the static coupling operator are time periodic and can be represented as Fourier series

$$\langle u_q(t)|S|u_k(t)\rangle = \sum_n S_{qk}(n)e^{\mathrm{i}n\omega t}, \tag{6.13}$$

with $S_{qk}(n) = \frac{1}{T}\int_0^T \langle u_q(\tau)|S|u_k(\tau)\rangle\, e^{-\mathrm{i}n\omega\tau}d\tau$. For the interaction-picture operator, one finds [204, 63]

$$\langle u_q(t)|\boldsymbol{S}(-\tau)|u_k(t)\rangle = \sum_n e^{\mathrm{i}n\omega t}S_{qk}(n)e^{-\mathrm{i}(\Delta_{qk}+n\omega)\tau}, \tag{6.14}$$

for the matrix elements, with $\Delta_{qk} = \varepsilon_q - \varepsilon_k$ being the difference of quasienergies. Here, in order to define a unique choice of the quasienergies $\varepsilon_{q\nu} = \varepsilon_k + \nu\omega$ and corresponding Floquet modes $|u_{k\nu}(t)\rangle$, we assume appropriate integer ν, such that the quasienergies lie in the interval

$$\varepsilon_{q\nu} \in (-\omega/2, \omega/2], \tag{6.15}$$

which is known as the first Floquet-Brillouin zone. This way of folding back the quasienergies onto the first Brillouin zone might imply rapid oscillations in the micromotion caused by phase factors given by $e^{-\mathrm{i}\nu\omega t}$, which is, however, not studied in further detail. In the following, for the sake of simplicity only, we drop the subscript ν.

Using the matrix elements above, the convoluted operator for periodically-driven open quantum systems is explicitly obtained from the time-dependent matrix elements

$$\langle u_q(t)|\mathbb{S}_t|u_k(t)\rangle = \sum_n e^{\mathrm{i}n\omega t}S_{qk}(n)G_t(\Delta_{qk}+n\omega), \tag{6.16}$$

with the coupling density $G_t(\Delta)$ [Eq. (2.19)] evaluated at $\Delta_{qk}+n\omega$. Note that the autonomous case is recovered by taking only one Fourier component, $n = 0$.

In the Floquet basis $\varrho_{ij}(t) = \langle u_i(t)|\varrho(t)|u_j(t)\rangle$, the Redfield equation takes the bulky form [63, 64]

$$\begin{aligned}\partial_t\varrho_{ij}(t) = -\mathrm{i}\Delta_{ij}\varrho_{ij}(t) + \sum_{n,n'}\sum_{q,k} e^{\mathrm{i}(n+n')\Omega t} \\ \Big[G_t(\Delta_{ik}+n\omega)S_{ik}(n)S_{qj}(n')\varrho_{kq}(t) + G_t^*(-(\Delta_{qj}+n\omega))S_{qj}(n)S_{ik}(n')\varrho_{kq}(t) \\ - G_t(\Delta_{qk}+n\omega)S_{qk}(n)S_{iq}(n')\varrho_{kj}(t) - G_t^*(-(\Delta_{qk}+n\omega))S_{qk}(n)S_{kj}(n')\varrho_{iq}(t)\Big],\end{aligned} \tag{6.17}$$

where, again, the autonomous case is recovered by taking only one Fourier component $n' = n = 0$. Often, the rotating-wave approximation is performed to obtain the quantum-optical master

equation, which leads to a dynamical decoupling of coherences, which decay exponentially, and the populations, which obey a rate equation. As in autonomous case, it is argued in the interaction-picture representation, where all rapidly oscillating terms are neglected. This is more restrictive for time-periodically driven systems because the coupling needs to be small compared to the quasienergy differences and also compared to the driving frequency ω [63, 64]. However, for high-periodic driving the quasienergies lie in a narrow band of width ω, for which the rotating-wave approximation is challenged by the tiny quasi-energy level splitting.

Below, we consider the full Floquet-Redfield equation (6.17) (i.e. without any RWA), which is valid for weak coupling and arbitrary driving frequency. In the basis-free formulation, i.e., without invoking the Floquet basis, it is emphasized that the algebraic form agrees with the Redfield equation for autonomous systems. For asymptotic times, the generator is time periodic and, therefore, the state does not approach a steady-state regime; but rather becomes asymptotically time-periodic. This asymptotic state is studied in the next section.

6.2.2 Prelude to an analytical continuation for the asymptotic state of periodically-driven open quantum systems

Applying the concepts of equilibrium statistical mechanics to periodically-driven quantum systems, for which there is no conservation of energy, we expect a state of maximal entropy without the constraint of energy conservation, which is given by the maximally mixed state [205–208]. Since the maximally mixed state reflects a state of infinite temperature, generically, periodically driven systems are subjected to so-called Floquet heating [206, 208–210]. As a result, it was conjectured [206, 208–210] that, in the sense of eigenstate thermalization, individual Floquet states of periodically driven many-body systems, are superpositions of eigenstates of the instantaneous Hamiltonian with very different energy. One interesting motivation for considering open quantum Floquet systems is, thus, to engineer the coupling to a bath in order to prevent heating and to stabilize non-trivial nonequilibrium quantum states.

In this section, the asymptotic state of the Floquet-Redfield equation is studied. It is shown that one can still infer matrix elements of the asymptotic state by following a perturbative expansion in the system-bath coupling strength. In zeroth order, the asymptotic state is the stationary solution of the quantum-optical master equation with static rates. In contrast to the autonomous case, the rates do not obey the detailed-balance condition, and do not give rise to a state of Gibbs form [63, 5, 64]. Including only second-order terms in the perturbative expansion, like in the autonomous case, the Floquet-Redfield equation leads to an asymptotic state, for which only the coherences are correct in second order. A prelude to future directions is given in the spirit of the analytical continuation for autonomous open quantum systems in Ref. [41], which has led to a consistent description also for finite coupling.

In general, a driven-dissipative system described by Eq. (6.17) does not approach a steady state. Instead, the matrix elements $\varrho_{ij}(t) = \langle u_i(t)|\varrho(t)|u_j(t)\rangle$ asymptotically approach a time-

periodic regime

$$\varrho_{ij}(t) \to \sum_{n''} \varrho_{ij}(n'') e^{in''\omega t}, \tag{6.18}$$

since the right hand side of Eq. (6.17) is time-periodic and linear [63, 64].

For high-driving frequencies, e.g., in the regime of the quantum-optical master equation, the fast oscillations in the asymptotic state average out, so that, $\varrho_{ij}(n'') \simeq \delta_{n'',0}\varrho_{ij}$. The time-averaged asymptotic state $\varrho_{ij}(0)$ is then the steady state solution to the static Floquet-Redfield equation, where one replaces the time-periodic rates on the right-hand side of Eq. (6.17) with their averaged quantities, i.e., by setting $n = -n'$ [63]. Note that the asymptotic matrix elements $\varrho_{ij}(0)$ are only stationary in the time-periodic Floquet basis, whereas they might still be oscillating in any other computational basis. Consequently, observables in the asymptotic limit generically still oscillate with the driving frequency ω.

In the following, it is shown that in lowest order of the system-bath coupling, the asymptotic state obeys a Pauli rate equation and that the off-diagonal contributions decay. This coincides with the solution of the quantum-optical master equation. Off-diagonal contributions turn out to be higher-order corrections that can be systematically inferred from the Pauli solution. In contrast to the derivation for instance in Ref. [63, 5], here, no RWA is performed.

By inserting the asymptotic state of Eq. (6.18) into the Floquet-Redfield Eq. (6.17) and relabelling the Fourier indices, one obtains an infinite series with oscillating terms, which have to vanish for all times. This only holds, if each term vanishes separately for all indices n'',

$$\begin{aligned} 0 = -\mathrm{i}(\Delta_{ij} + n''\omega)\varrho_{ij}(n'') + \sum_{n,n'}\sum_{l,m}\Big[& G(\Delta_{im} + n\omega)S_{im}(n)S_{lj}(n'' - n - n')\varrho_{ml}(n') \\ & + G^*(-(\Delta_{lj} + n\omega))S_{lj}(n)S_{im}(n'' - n - n')\varrho_{ml}(n') \\ & - G(\Delta_{lm} + n\omega)S_{lm}(n)S_{il}(n'' - n - n')\varrho_{mj}(n') \\ & - G^*(-(\Delta_{lm} + n\omega))S_{lm}(n)S_{mj}(n'' - n - n')\varrho_{il}(n')\Big]. \end{aligned} \tag{6.19}$$

Analogously, to the procedure for autonomous systems in Section 2.5.2, this equation is perturbatively solved order by order in the system-bath coupling strength. The asymptotic coupling density $G(\Delta)$ is of second order in the coupling strength and for the Fourier coefficients one writes $\varrho_{ij}(n) \simeq \varrho_{ij}^{(0)}(n) + \varrho_{ij}^{(2)}(n)$. Since the Redfield equation is only valid in the weak coupling regime, neglecting higher-order contributions is well justified. In zeroth order, one obtains

$$0 = -\mathrm{i}(\Delta_{ij} + n\omega)\varrho_{ij}^{(0)}(n), \tag{6.20}$$

which implies vanishing Fourier coefficients if the drive is not resonant with the quasienergy splittings, i.e., $\varrho_{ij}^{(0)}(n) = 0$ for $\Delta_{ij} + n\omega \neq 0$. In the static case, this leads to a zeroth-order contribution that is diagonal in the eigenbasis of the system. As stated above in Eq. (6.15),

without loss of generality, we assume the quasienergies ε_i to lie in the first Floquet-Brillouin zone. Consequently, the difference of two quasienergies can never be compensated by drive quanta and the sum $\Delta_{ij} + n\omega$ only vanishes, if, and only if, both terms vanish separately. In other words, the only non-zero contributions of the zeroth-order contribution is diagonal in the Floquet basis ($i = j$) and is not oscillating ($n = 0$),

$$\varrho_{ij}^{(0)}(n) = \delta_{i,j}\delta_{n,0}\varrho_{ii}^{(0)}(0). \tag{6.21}$$

Alternatively, one can express the zeroth-order result in the Floquet basis as

$$\varrho_{ij}^{(0)} = \sum_{n=} \varrho_{ij}(n)^{(0)} e^{\mathrm{i}n\omega t} = \delta_{i,j}\varrho_{ii}^{(0)}(0), \tag{6.22}$$

where the series reduces to the time-independent term.

In second order there are two contributions. Firstly, there is the term that involves the coherent part applied to $\varrho_{ij}^{(2)}(n'')$, which we bring to the left-hand side. Secondly, there is the dissipator applied to the zeroth-order $\varrho_{ij}^{(0)}(n'')$,

$$\begin{aligned}\mathrm{i}(\Delta_{ij} + n''\omega)\varrho_{ij}^{(2)}(n'') = \sum_n \sum_l \Big[& G(\Delta_{il} + n\omega)S_{il}(n)S_{lj}(n'' - n)\varrho_{ll}^{(0)}(0) \\ & + G^*(-(\Delta_{lj} + n\omega))S_{lj}(n)S_{il}(n'' - n)\varrho_{ll}^{(0)}(0) \\ & - G(\Delta_{lj} + n\omega)S_{lj}(n)S_{il}(n'' - n)\varrho_{jj}^{(0)}(0) \\ & - G^*(-(\Delta_{il} + n\omega))S_{il}(n)S_{lj}(n'' - n)\varrho_{ii}^{(0)}(0)\Big],\end{aligned} \tag{6.23}$$

where the constraints for the zeroth order of Eq. (6.21) have been used on the right-hand side. This equation holds for any triplet (i, j, n''). In particular, for $i = j$ and $n'' = 0$ the left-hand side cancels and one obtains the stationary solution of a rate equation for the populations in zeroth order,

$$0 = \sum_l \Big[R_{il}\varrho_{ii}^{(0)} - R_{li}\varrho_{ll}^{(0)}\Big]. \tag{6.24}$$

The quantity $R_{ij} = \sum_n 2\mathrm{Re}[G(\Delta_{il}+n\omega)]S_{il}(n)S_{li}(-n)$ is identified as the rate for the transition of population from Floquet state $|u_l(t)\rangle$ to Floquet state $|u_i(t)\rangle$. Altogether, for ultraweak coupling, in zeroth-order perturbation theory, the asymptotic state is obtained from the rate equation of the quantum-optical master equation [63].

For finite coupling, special care has to be taken by solving for $\varrho_{ij}^{(2)}(n'')$ in Eq. (6.23). For off-resonant triplets (i, j, n''), the second-order result follows by simply dividing by $\Delta_{ij} + n''\omega \neq 0$. However, on resonance, i.e., for $\Delta_{ij} + n''\omega = 0$, this is not directly possible. Consequently, the Floquet-Redfield equation leads to an inconsistent asymptote for finite coupling. This is same problem as for autonomous systems, as discussed in Section 2.5.2.

Inspired by the idea of obtaining the correct populations from analytical continuation for autonomous systems (see Ref. [41] and Section 5.1), in the following we seek for an analogous approach for open quantum Floquet systems: To be more precise, we formally infer the resonant matrix elements in the limit $\lim_{\Delta_{ij}+n''\omega\to 0}$ from the off-resonant ones. The limit approaches an indeterminate form ("0/0") and requires the application of l'Hospital's theorem. Furthermore, the limit depends on the derivatives of the coupling density $G(\Delta)$ and the zeroth-order results $\varrho_{ii}^{(0)}$. Such an analytical continuation for autonomous systems is the central result of Ref. [41] and is the basis of the canonically consistent master equation proposed in Chapter 5. The generalization for periodically-driven systems seems straightforward.

Certainly, as in the autonomous case it is by no means guaranteed that this formal limit is physically reasonable. Additionally, the analytical continuation approach could not be benchmarked with statistical mechanics since the asymptotic state of driven-dissipative systems is an out-of-equilibrium state. However, if the driving Hamiltonian fulfils certain conditions, such as a small driving frequency and commuting drives $[H_{\text{ext}}(t_1), H_{\text{ext}}(t_2)] = 0$ and $[H_{\text{ext}}(t), H_{\text{SB}}] = 0$, the asymptotic state is described a by an effective Floquet-Gibbs state [64, 211]. Furthermore, the analytical continuation procedure could be benchmarked against the exact solution of the driven harmonic oscillator represented, e.g., in Ref. [212].

To summarize, driven quantum systems with strong dissipation are a promising platform to drive quantum many-body system out of equilibrium. However, for strong dissipation the rotating-wave approximation of the quantum-optical master equation breaks down and a theoretical description is more challenging. By noting the algebraic form of the Floquet-Redfield master equation, the methods for the pseudo-Lindblad equation proposed in Chapters 3 and 4 can directly be applied. Regarding future work, a consistent description beyond ultraweak system-bath coupling in the spirit of the canonically consistent master equation proposed in Chapter 5, an analytical continuation approach, for which we paved the way in this section, seems straightforwardly possible.

7 Summary and outlook

The progress for the experimental control of open quantum systems that are coupled to heat baths challenges the theoretical description to be both accurate and efficient. It is challenging because the effective dynamics of the reduced system, which is obtained by averaging over the bath's degrees of freedom, does not obey a universal equation of motion, but rather requires to derive a suitable effective description. In this thesis, the formulation via time-local quantum master equations for the reduced density matrix of the system is considered.

For modelling open quantum systems, in the literature master equations of GKSL form (2.31) are widely used. The action of a GKSL master equation is easily understood for pure quantum states. The first terms of a GKSL master equation act as an effective Hamiltonian with an anti-Hermitian contribution. This alone models dissipation as the probability for measuring the quantum state, i.e., the norm of the quantum state, decays during the time evolution. However, the GKSL master equation, as such, is norm preserving. Thus, the remaining term of the GKSL master equation can be understood a jump process, which recycles the lost probability to other quantum states. In this way, a GKSL master equation allows for an efficient quantum jump unraveling, known as Monte Carlo wave function approach. Furthermore, a GKSL master equation guarantees completely positive dynamics

The problem is that the standard approach of deriving a master equation of GKSL form requires ultraweak coupling, which is often not valid especially for large systems. The intention of this thesis is to find a master equation formulation, which is consistent with the microscopic details of system, bath and the interaction.

To this end, Chapter 2 is the basis and introduces the well-known concepts of open quantum system dynamics. With the main focus on bosonic baths, first, the correlations in thermal equilibrium are introduced. These play a crucial role for the effective dynamics of the system and determine the temperature dependent coupling density, which is the central quantity for all master equations considered. The real part of the coupling density is well-known from golden-rule type expressions of perturbation theory. The imaginary part that is often neglected turns out to be crucial, e.g., for a consistent equilibrium state beyond ultraweak coupling [Section 2.5.2].

Throughout the thesis, weak coupling between system and bath is assumed and, thus, master equations are obtained perturbatively in orders of the coupling.[1] To lowest (second) order, in

[1] With the exception of Section 6.1, where the regime of ultrastrong coupling is discussed.

Section 2.4, the Redfield master equation is obtained. It is emphasized that the derivation presented here does not neglect time non-local integral kernels nor does it rely on a factorization for the states of system and bath. The Redfield equation follows rigorously in second-order perturbation theory, which is further explained for the exact master equation of a damped harmonic oscillator in Section 2.6.

Compared to other master equations, the Redfield equation leads to accurate dynamics beyond ultraweak system bath coupling. Nevertheless, the Redfield equation is not free of problems and, e.g., known to potentially yield negatively populated states. This is shown for several examples throughout the thesis and typically occurs in regimes beyond ultraweak coupling and low bath temperatures. The inconsistency of generic perturbative master equations is discussed in Section 2.5.2. As a new result, we relate the violation of positivity to a known problem of the Redfield equation, namely that, despite being derived systematically in second-order, it does not accurately capture the state in that order. We prove this analytically for a damped harmonic oscillator in Section 2.6.2. Namely, beyond ultraweak coupling the state becomes more localized in real space and broader in momentum space. However, the latter is not captured by the Redfield equation, which might be seen as a violation of the uncertainty principle and, in Sections 2.6.1 and 2.6.2, it is shown to be the reason why positivity is violated.

To circumvent the problems of the Redfield equation, it is often reduced to GKSL form. For that purpose, one typically performs a rotating-wave approximation (RWA) in the eigenbasis of the system to arrive at the quantum-optical master equation (2.52), which is of GKSL form. The RWA relies on ultraweak coupling, where the oscillation frequencies given by the pairwise differences of the eigenenergies, are fast compared to slow dynamics of the state determined by the coupling strength. However, the RWA is not justified beyond ultraweak coupling.

To overcome the limitations of RWA, in Chapter 3, an alternative approximation is proposed, for reducing the Redfield equation to GKSL form. To this end, the Redfield equation is first written in pseudo-Lindblad form, which is very similar to the GKSL form apart from negative relaxation weights. As a second step, the negative weight is minimized and truncated. Here, a two-parameter family of pseudo-Lindblad representations of the Redfield equation is found. Different representations are related by symmetry transformation of the Kossakowski matrix and are classified with two symmetry parameters. Effectively, the new jump operators, which depend on the symmetry parameters, follow from the transformation via a pseudo-unitary diagonalization of the Kossakowski matrix. In particular, the symmetry parameters change the weight of the pseudo-Lindblad jump operators. In this way, the symmetry parameters yield unprecedented control of pseudo-Lindblad equations and we find the optimal values that minimize the negative contribution. It is found that for not too small bath temperatures also beyond the ultraweak coupling regime, the negative weight is very small. Therefore, in a large parameter regime, beyond the limitations of the rotating-wave approximation the truncation of the negative weight can be justified and, thus, the Redfield equation is reduced to GKSL

form.

As an outlook, one might obtain even smaller negative weights by using a more general transformation that shifts the weight of the dissipator to the Lamb-shift Hamiltonian. Such an approach has already been applied to define thermodynamic quantities such as heat and work beyond ultraweak coupling.

In Chapter 4, a new quantum-trajectory unraveling for pseudo-Lindblad equations is presented. For GKSL master equations acting in a Hilbert space of dimension D, a stochastic unraveling by state vectors, with D entries, is always favoured as compared to the direct integration of the density matrix, with D^2 entries. This is very important for many-body systems, for which the dimension scales exponentially with the system size and for which a direct integration of the density matrix is often not possible. However, the conventional approach cannot be applied for pseudo-Lindblad equations, such as the Redfield equation, because quantum jumps for negative relaxation weight would occur with negative probability. Existing quantum-jump approaches for pseudo-Lindblad equations are numerically challenging. For instance, the state space is effectively doubled, or the approach does not allow for parallel simulation of quantum trajectories, because the evolution of each trajectory depends on the whole ensemble. In Sections 4.3 and 4.4, a surprisingly simple generalization of the conventional approach for pseudo-Lindblad equations is found, where the quantum state is augmented by one auxiliary classical sign bit only. In the simulation, the sign is dynamically changed whenever a quantum jump with a negative relaxation weight occurs. The density matrix is then given by an ensemble average over the stochastic trajectories, which are weighted with the corresponding sign bits. The algorithm bridges the gap and enables the efficient unraveling of Redfield dynamics in regimes where the negative weight is small but cannot be truncated. Especially for the transient dynamics, before the number of negative trajectories equals the number of positive ones, good statistical convergence is observed for the examples studied in Sections 4.5 and 4.6. To this end, the algorithm is combined with a similar optimization procedure, where the negative weight is minimized locally for each trajectory. Also, if the stationary state is reached before the algorithm saturates, large statistical fluctuations are avoided. Furthermore, because trajectories can be simulated in parallel on a cluster of computer nodes, the simulation of a large number of trajectories is often not a problem.

In future work, the pseudo-Lindblad quantum-trajectory approach can be combined with the local approximation of the Redfield equation, in which all operators are sparsely filled, to efficiently solve the dynamics of dissipative many-body systems. To this end, an implementation scheme using dynamical adjustment of the time step and with a spontaneous interruption of the integration is preferred rather than the implementation being of first order in a small time step.

In Chapter 5, a new master equation beyond the limitations of the Redfield theory is proposed, which modifies the Redfield equation with contributions of higher order in the coupling. In a

rigorous perturbative expansion, these higher order contributions would depend on the inverse of the dynamical map. However, it is a known result that the series expansion of the dynamical map diverges in each order separately. Truncated at second order, in Section 5.2, it is shown that the divergence is linear with time, which leads to an inconsistent steady state. Here, in order to solve the inconsistencies, the dynamical theory is augmented with arguments of statistical mechanics. Namely, based on the exact equilibrium state of the total system-bath compound, in Section 5.3, a superoperator is found that yields the lowest-order correction to the ultraweak coupling limit. The proposal of the canonically consistent quantum master equation (CCQME) (5.8) is to identify this superoperator with the asymptotic dynamical map, which is a novel way to combine a dynamical description with statistical mechanics. In this way, the Redfield equation is modified consistently in second-order perturbation theory, for which the higher-order contributions steer the dynamics towards the correct asymptote. This is corroborated by numerical simulations for various models in Sections 5.4 to 5.8. By benchmarking the CCQME against exact solutions, it is shown to significantly improve upon the dynamics of the Redfield equation, while retaining the same conceptual and numerical complexity. As an unpublished result, in Section 5.4, for the equilibrium state of the damped harmonic oscillator it is proven that the CCQME circumvents the long-standing problem of positivity violation, albeit without being of GKSL form.

Surprisingly, the generic formulation for the superoperator is also applicable to nonequilibrium scenarios of driven-dissipative quantum systems that are coupled to several independent baths. As a proof of principle, this is tested for a quantum dot coupled to two baths of different temperature in Section 5.6. Altogether, the CCQME opens a new perspective in the theory of open quantum systems leading to a reduced density matrix accurate beyond the ultraweak coupling regime of Redfield and GKSL equations.

It is an open question, whether the CCQME with the superoperator (5.10) can, in general, be written in pseudo-Lindblad form or GKSL form, respectively. Refining the canonically consistent superoperator in a model independent form (5.10), might be challenging, especially because of the contribution that effectively acts as a derivative onto the state. First steps in this direction have been done for the damped harmonic oscillator in Sections 5.4 and 5.4.1 by making use of Gaussian states. A simpler formulation, e.g., one that only includes GKSL superoperators is beneficial, and for instance, would allow to directly simulate pseudo-Lindblad quantum trajectories. Furthermore, here, the numerical simulations focus on the time-independent CCQME and a combination with the time-dependent Redfield superoperator. In principle, a hybrid approach would be possible, where the time-dependent dynamical map is dynamically continued by the asymptotic superoperator (5.10), which is briefly mentioned in the concluding remarks (5.9).

The thesis finishes with a prelude to future directions in Chapter 6. To this end, in Section 6.1, the ultrastrong coupling regime is considered, for which recently the stationary state and a

dynamical theory have been proposed. Such as this thesis aims to describe open-quantum-system dynamics beyond ultraweak coupling, in future work it is interesting to bridge the gap to strong but finite coupling. This could be done by doing a perturbative expansion for small inverse coupling. Furthermore, in Section 6.2, time-periodically driven open quantum systems are discussed. As in the autonomous case, the theoretical description often relies on the RWA. However, this is restricted to ultraweak coupling and high-frequency driving and, thus, is more restrictive than in the autonomous case. It is shown, that for time-periodically driven systems the algebraic structure of the Redfield equation does not change and, thus, the concepts developed in Chapters 3 and 4 directly apply. It is an open question, whether a canonically consistent quantum master equation for time-periodically driven systems can be formulated.

Appendix

A Zero-point fluctuation and thermal noise for Drude bath

In this section, the expressions in Eqs. (2.24) and (2.25) for the zero-point fluctuation and thermal noise for a Drude bath with spectral density

$$J(\omega) = \frac{\gamma\omega}{1+\omega^2/\omega_D^2}, \tag{A.1}$$

are derived. The zero-point fluctuation is defined as

$$G_0''(\Delta) = \mathcal{P}\int_0^\infty \frac{J(\omega)}{\omega^2-\Delta^2}\left[\Delta - \frac{\Delta^2}{\omega}\right]\frac{d\omega}{\pi}, \tag{A.2}$$

where the Cauchy principal values are found by using the indefinite integrals

$$\int \frac{\omega}{(1+\omega/\omega_D^2)(\omega^2-\Delta^2)}\frac{d\omega}{\pi} = \frac{1}{2(1+\Delta^2/\omega_D^2)}\frac{1}{\pi}\ln\left[\frac{\omega^2-\Delta^2}{\omega^2+\omega_D^2}\right], \tag{A.3}$$

for the first term and

$$\int \frac{1}{(1+\omega^2/\omega_D^2)(\omega^2-\Delta^2)}\frac{d\omega}{\pi} = -\frac{1}{1+\Delta^2/\omega_D^2}\left(\frac{1}{\omega_D}\arctan(\omega/\omega_D) + \frac{1}{2\Delta}\ln\left[\frac{\omega/\Delta+1}{\omega/\Delta-1}\right]\right), \tag{A.4}$$

for the second. With the evaluation at the limits, $\ln\left[\frac{\omega^2-\Delta^2}{\omega^2+\omega_D^2}\right]\Big|_0^\infty = -2\ln\left[\frac{|\Delta|}{\omega_D}\right]$, $\arctan(\omega/\omega_D)\Big|_0^\infty = \pi/2$ and $\ln\left[\frac{\omega/\Delta+1}{\omega/\Delta-1}\right]\Big|_0^\infty = 0$, it follows that

$$G_0''(\Delta) = \frac{\gamma\Delta}{1+\Delta^2/\omega_D^2}\left(-\frac{1}{\pi}\ln\left[\frac{|\Delta|}{\omega_D}\right] + \frac{1}{2}\frac{\Delta}{\omega_D}\right). \tag{A.5}$$

For evaluating the thermal noise

$$G_{\rm th}''(\Delta) = 2\Delta\mathcal{P}\int_0^\infty \frac{J(\omega)n_\beta(\omega)}{\omega^2-\Delta^2}\frac{d\omega}{\pi}, \tag{A.6}$$

first write the Bose function as $n_\beta(\omega) = 1/2(-1 + \coth(\beta\omega/2))$ and reuse the result above to arrive at

$$G_{\mathrm{th}}(\Delta) = \frac{\gamma\Delta}{1+\Delta^2/\omega_D^2}\frac{1}{\pi}\ln\left[\frac{|\Delta|}{\omega_D}\right] + \Delta\mathcal{P}\int_0^\infty \frac{J(\omega)\coth(\beta\omega/2)}{\omega^2-\Delta^2}\frac{d\omega}{\pi}. \tag{A.7}$$

Next, expand the hyperbolic cotangent, $\coth(\beta\omega/2) = 1/(\beta\omega/2)\sum_{n=-\infty}^{\infty} 1/(1+\nu_n^2/\omega^2)$ with $\nu_n = 2\pi n/\beta$ and solve the integral for each term. Using the analytical form of the indefinite integral, the Cauchy-principle integral can be carried out to give

$$\begin{aligned}&\frac{\gamma\Delta}{\beta/2}\sum_{n=-\infty}^{\infty}\mathcal{P}\int_0^\infty \frac{1}{(1+\omega^2/\omega_D^2)(1+\nu_n^2/\omega^2)(\omega^2-\Delta^2)}\frac{d\omega}{\pi}\\ &\quad= -\frac{\gamma\Delta}{2(1+\Delta^2/\omega_D^2)}\underbrace{\frac{1}{\beta\omega_D/2}\sum_{n=-\infty}^{\infty}\frac{1}{1-\nu_n^2/\omega_D^2}}_{\coth(\beta\omega_D/2)} + \frac{\gamma}{\beta\Delta}\sum_{n=-\infty}^{\infty}\frac{|\nu_n|}{(1-\nu_n^2/\omega_D^2)(1+\nu_n^2/\Delta^2)}.\end{aligned} \tag{A.8}$$

The series can be given explicitly in terms of the cotangent for the first term and in terms of the Digamma-function ψ for the second term.[2] By further employing the reflection formula $\psi(1-x) = \pi\cot(\pi x) + \psi(x)$ and the recurrence relation $\psi(x) + \psi(1+x) = 1/x + 2\psi(x)$, the cotangent cancels and one arrives at[3]

$$G''_{\mathrm{th}}(\Delta) = \frac{\gamma\Delta}{1+\Delta^2/\omega_D^2}\frac{1}{\pi}\left(\ln\left[\frac{|\Delta|}{\omega_D}\right] + \frac{1}{\beta\omega_D/\pi} + \psi(\beta\omega_D/2\pi) - \mathrm{Re}\,\psi(\mathrm{i}\beta|\Delta|/2\pi)\right). \tag{A.9}$$

B Perturbative expansion of the exact equilibrium state - Identification of a canonically consistent superoperator $\mathcal{Q}^{(2)}$

For the exact equilibrium state of the reduced system, it is assumed that the total system-bath compound relaxes to a thermal equilibrium state with inverse temperature β, which is determined by the mean energy. By tracing over the bath degrees of freedom, the exact equilibrium state of the reduced system is

$$\varrho = \mathrm{tr}_{\mathrm{B}}\frac{e^{-\beta(H_0+H_{\mathrm{SB}})}}{Z_{\mathrm{tot}}}, \tag{B.1}$$

[2] $\sum_{n=1}^{\infty}\frac{n}{(n^2-a^2)(n^2-b^2)} = \frac{1}{2(a^2+b^2)}\big(-\psi(1+a) - \psi(1-a) + 2\mathrm{Re}\psi(1+\mathrm{i}b)\big)$

[3] For the complex valued digamma-function, one finds $\psi(z) = \int_0^\infty (e^{-t}/t - e^{-zt}/(1-e^{-t})dt$, provided the real part of z is positive from which follows $\psi(-\mathrm{i}x) = \psi(\mathrm{i}x)^*$.

with $H_0 = H_\mathrm{S} + H_\mathrm{B}$. The total partition function $Z_\mathrm{tot} = \mathrm{tr_S}\,\mathrm{tr}_B\, e^{-\beta(H_0+H_\mathrm{SB})}$ is obtained by tracing over the system and the bath. For ultraweak coupling and in zeroth-order perturbation theory, one obtains the canonical Gibbs state, $\varrho \overset{H_\mathrm{SB}\to 0}{\longrightarrow} \varrho^{(0)} = \frac{e^{-\beta H_\mathrm{S}}}{Z_\mathrm{S}}$. For finite coupling, the equilibrium state is a correlated state of the system and the bath.

Recently, the reduced Gibbs state in Eq. (B.1) is referred to as mean force Gibbs state, e.g., in Refs. [135, 184]. The name is inherited from the Hamiltonian of mean force [124, 125],

$$e^{-\beta H^*} \equiv \frac{1}{Z_\mathrm{B}}\,\mathrm{tr_B}\, e^{-\beta(H_0+H_\mathrm{SB})}, \tag{B.2}$$

which is the basis for thermodynamics beyond ultraweak coupling in which the free energy of the open system is defined as the difference of the free energy of the total system-bath compound and the bath.

However, starting from the exact equilibrium state, one might construct different effective Hamiltonians, $\varrho = \frac{e^{-\beta H_\mathrm{eff}}}{\mathrm{tr_S}\, e^{-\beta H_\mathrm{eff}}}$, by multiplying numerator and denominator with an arbitrary positive valued function of temperature and coupling strength. The resulting effective Hamiltonian differs from the Hamiltonian of mean force and would yield incorrect thermodynamic potentials for the strongly coupled reduced canonical thermodynamic systems. Since the exact reduced equilibrium state does not depend on the particular choice of the effective Hamiltonian, the term *mean force Gibbs state* might be misleading. This aspect has been emphasized by Hänggi and coworkers, e.g., in Refs. [124, 125] and in private communications as reaction to our publication in Ref. [184]. We acknowledge these concerns, and use the term *reduced Gibbs state*. In the following we provide a perturbative expansion of the reduced Gibbs state in orders of the system-bath coupling.

Analogous to the time-ordered series of the dynamical map in the interaction picture in Eq. (2.33), one obtains a representation for the exact reduced equilibrium state[4]

$$e^{-\beta(H_\mathrm{S}+H_\mathrm{B}+H_\mathrm{SB})} = e^{-\beta H_\mathrm{S}} e^{-\beta H_\mathrm{B}} \underbrace{T\exp\Big[-\mathrm{i}\int_0^{-\mathrm{i}\beta} \boldsymbol{H}_\mathrm{SB}(\tau)d\tau\Big]}_{\equiv D}, \tag{B.3}$$

which is, generated by $\boldsymbol{H}_\mathrm{SB}(\tau) = e^{\mathrm{i}(H_\mathrm{S}+H_\mathrm{B})\tau} H_\mathrm{SB} e^{-\mathrm{i}(H_\mathrm{S}+H_\mathrm{B})\tau}$ in imaginary time. Here, the right-hand side is Hermitian, which is seen from $D^\dagger = e^{\beta(H_\mathrm{S}+H_\mathrm{B})} D e^{-\beta(H_\mathrm{S}+H_\mathrm{B})}$.

With the representation above, it is straightforward to identify the corrections in orders of the system-bath coupling. Similar to the derivation of the master equation in Section 2.4, in the following, the partial trace is taken over the bath degrees of freedom. Furthermore, the

[4] The equation of motion for the operator $U(t) \equiv e^{\mathrm{i}H_0 t} e^{-\mathrm{i}(H_0+H_\mathrm{SB})t}$ is generated solely by the interaction, i.e., $\partial_t U(t) = -\mathrm{i}\boldsymbol{H}_\mathrm{SB}(t)U(t)$, with $\boldsymbol{H}_\mathrm{SB}(t) = e^{\mathrm{i}H_0 t} H_\mathrm{SB} e^{-\mathrm{i}H_0 t}$. This is solved by the time-ordered exponential $U(t) = T\exp\big[-\mathrm{i}\int_0^t \boldsymbol{H}_\mathrm{SB}(\tau)d\tau\big]$ [see Eq. (2.33)]. Now, by multiplying from the left with $e^{-\mathrm{i}H_0 t}$ and introducing the inverse temperature as complex time, i.e., replacing $t \to -\mathrm{i}\beta$, one obtains $e^{-\beta(H_0+H_\mathrm{SB})} = e^{-\beta H_0} T\exp\big[-\mathrm{i}\int_0^{-\mathrm{i}\beta} \boldsymbol{H}_\mathrm{SB}(\tau)d\tau\big]$.

series expansion involves bath correlation functions $\mathrm{tr}_B[\boldsymbol{B}^\dagger(\tau_1)\boldsymbol{B}(\tau_2)\dots e^{-\beta H_\mathrm{B}}]$, where only even orders contribute. Thus, the reduced Gibbs state up to second order is given by [41, 44]

$$\varrho \simeq \frac{\varrho^{(0)} + \varrho^{(0)}\,\mathrm{tr}_\mathrm{B}[\varrho_B D^{(2)}]}{1 + \mathrm{tr}_\mathrm{S}\,\mathrm{tr}_\mathrm{B}[\varrho_B D^{(2)}]} \simeq \varrho^{(0)} + \varrho^{(0)}\,\mathrm{tr}_\mathrm{B}[\varrho_B D^{(2)}] - \varrho^{(0)}\,\mathrm{tr}_\mathrm{S}\,\mathrm{tr}_\mathrm{B}[\varrho_B D^{(2)}], \tag{B.4}$$

where the last term ensures normalization, i.e., $\mathrm{tr}\,\varrho = 1$. Here,

$$D^{(2)} = -\int_0^{-\mathrm{i}\beta}\int_0^{\tau_1} \boldsymbol{H}_\mathrm{SB}(\tau_1)\boldsymbol{H}_\mathrm{SB}(\tau_2)d\tau_1 d\tau_2, \tag{B.5}$$

is the second-order contribution of the Dyson series above and $\varrho_\mathrm{B} = \frac{e^{-\beta H_\mathrm{B}}}{Z_B}$ and $\varrho^{(0)} = \frac{e^{-\beta H_\mathrm{S}}}{Z_S}$ denote the equilibrium states for ultraweak coupling of bath and system, respectively. In this work, we focus on the second-order theory. However, the extension to higher orders is straightforward. Thus, it is valid also in the strong coupling regime, i.e. beyond second order, by considering more terms in the Dyson series expansion of Eq. (B.3).

In order to make the connection to the dynamical theory in Chapter 5, here, we aim to identify a superoperator $\mathcal{Q}^{(2)}$, which acts on the canonical Gibbs state $\varrho^{(0)}$ and generates the second order contribution,

$$\mathcal{Q}^{(2)}[\varrho^{(0)}] \equiv \varrho^{(0)}\,\mathrm{tr}_\mathrm{B}[\varrho_B D^{(2)}] = -\varrho^{(0)}\int_0^{-\mathrm{i}\beta} d\tau_1 \int_0^{\tau_1} d\tau_2\,\mathrm{tr}_\mathrm{B}[\varrho_B \boldsymbol{H}_\mathrm{SB}(\tau_1)\boldsymbol{H}_\mathrm{SB}(\tau_2)]. \tag{B.6}$$

It turns out that the superoperator $\mathcal{Q}[\cdot]$ can be represented by the Redfield superoperator. The connection between the stationary state of the Redfield equation and the reduced Gibbs state up to second order has been made in Ref. [41]. We repeat the derivation with the motivation of identifying the superoperator $\mathcal{Q}^{(2)}$.

For a system-bath-coupling Hamiltonian $H_\mathrm{SB} = S \otimes (B + B^\dagger)$, the second-order contribution is explicitly given by,

$$\mathcal{Q}^{(2)}[\varrho^{(0)}] = -\varrho^{(0)}\int_0^{-\mathrm{i}\beta} d\tau_1 \int_0^{\tau_1} d\tau_2\, C(\tau_1 - \tau_2)\boldsymbol{S}(\tau_1)\boldsymbol{S}(\tau_2), \tag{B.7}$$

with the bath correlation[5] $C(\tau_1 - \tau_2) = \mathrm{tr}_\mathrm{B}[(\boldsymbol{B}^\dagger(\tau_1)\boldsymbol{B}(\tau_2) + \boldsymbol{B}(\tau_1)\boldsymbol{B}^\dagger(\tau_2))\varrho_\mathrm{B}]$ discussed in Section 2.2. Note that the bath correlation is shifted for models with reorganization Hamiltonian, as discussed in Section 2.4.3.

In the following, the integration is performed in a rotated frame by introducing the new

[5] In this derivation, the integrals are performed in real time, such that the operators in the interaction picture are compatible with Hermitian conjugation, i.e., $\boldsymbol{B}^\dagger(\tau) = e^{\mathrm{i}H_\mathrm{B}\tau}B^\dagger e^{-\mathrm{i}H_\mathrm{B}\tau}$. In Ref. [41], the integrals are calculated in complex time, which leads to a modified interaction-picture operator $\boldsymbol{B}(-\mathrm{i}\lambda) = e^{\lambda H_\mathrm{B}}Be^{-\lambda H_\mathrm{B}}$, which is not compatible with Hermitian conjugation, $\boldsymbol{B}(-\mathrm{i}\lambda)^\dagger = e^{-\lambda H_\mathrm{B}}B^\dagger e^{\lambda H_\mathrm{B}} \neq e^{\lambda H_\mathrm{B}}B^\dagger e^{-\lambda H_\mathrm{B}}$.

integration variables $s = \tau_1 + \tau_2$ and $u = \tau_1 - \tau_2$,[6]

$$Q^{(2)}[\varrho^{(0)}] = -\varrho^{(0)} \int_0^{-\mathrm{i}\beta} du\, C(u) \int_{u/2}^{-\mathrm{i}\beta-u/2} ds\, e^{\mathrm{i}H_{\mathrm{S}}s} \boldsymbol{S}(u/2)\boldsymbol{S}(-u/2) e^{-\mathrm{i}H_{\mathrm{S}}s}. \tag{B.8}$$

Now the s-integration can be carried out explicitly. The integral is qualitatively different for either coherences (off-diagonal elements in the energy basis) and populations (diagonal elements in the energy basis). For the coherences, one finds

$$\langle n|Q^{(2)}[\varrho^{(0)}]|m\rangle \overset{n\neq m}{=} -\frac{1}{\mathrm{i}\Delta_{nm}} \int_0^{-\mathrm{i}\beta} du C(u) \langle n| \left(\varrho^{(0)} \boldsymbol{S}(-\mathrm{i}\beta)\boldsymbol{S}(\mathrm{i}\beta - u) - \varrho^{(0)}\boldsymbol{S}(u) S \right) |m\rangle \,. \tag{B.9}$$

Using $\varrho^{(0)}\boldsymbol{S}(-\mathrm{i}\beta)\boldsymbol{S}(\mathrm{i}\beta - u) = S\boldsymbol{S}(-u)\varrho^{(0)}$ and identifying the convoluted operator as $\mathbb{S}_{-\mathrm{i}\beta} = \int_0^{-\mathrm{i}\beta} C(u)\boldsymbol{S}(-u)du$, which is evaluated in imaginary time, it follows that

$$\langle n|Q^{(2)}[\varrho^{(0)}]|m\rangle \overset{n\neq m}{=} -\frac{1}{\mathrm{i}\Delta_{nm}} \langle n| \left(S\mathbb{S}_{-\mathrm{i}\beta}\varrho^{(0)} - \varrho^{(0)}\mathbb{S}^{\dagger}_{-\mathrm{i}\beta} S \right) |m\rangle \,, \tag{B.10}$$

$$= \langle n| \frac{\mathcal{R}^{(2)}[\varrho^{(0)}]}{\mathrm{i}\Delta_{nm}} |m\rangle \,, \tag{B.11}$$

which is related to the action of the asymptotic time-independent Redfield superoperator in Eq. (2.64).[7]

For the populations, the integrand in Eq. (B.8) is independent of the integration variable s and one has

$$\langle n|Q^{(2)}[\varrho^{(0)}]|n\rangle = \int_0^{-\mathrm{i}\beta} du\, C(u)(\mathrm{i}\beta + u) \langle n|\varrho^{(0)}\boldsymbol{S}(u/2)\boldsymbol{S}(-u/2)|n\rangle \,, \tag{B.12}$$

$$= \langle n|\varrho^{(0)} \left(\int_0^{-\mathrm{i}\beta} du\, C(u)(\mathrm{i}\beta + u)\boldsymbol{S}(u) \right) S|n\rangle \,. \tag{B.13}$$

Here, another convoluted coupling operator appears, which is related to $\mathbb{S}_{-\mathrm{i}\beta}$ by introducing a formal derivative with respect to energy differences. To this end, we shift the region of integration by $-\mathrm{i}\beta$, for which the symmetry of the bath correlation $C(u - \mathrm{i}\beta) = C(-u)$ is used. Moreover, we employ $\varrho^{(0)}\boldsymbol{S}(-\mathrm{i}\beta + u) = \boldsymbol{S}(\tau)\varrho^{(0)}$, and perform a variable transformation $u \to -u$ to arrive at

$$\langle n|Q^{(2)}[\varrho^{(0)}]|n\rangle = -\langle n| \left(\int_0^{-\mathrm{i}\beta} du\, C(u) u \boldsymbol{S}(-u) \right) \varrho^{(0)} S|n\rangle \,. \tag{B.14}$$

[6] For the rotated frame, we make use of the integral identity $\int_0^{-\mathrm{i}\beta} d\tau_1 \int_0^{\tau_1} d\tau_2 f(\tau_1 + \tau_2, \tau_1 - \tau_2) = \int_0^{-\mathrm{i}\beta} du \int_{u/2}^{\beta - u/2} ds f(2s, u)$, which is valid for arbitrary function $(\tau_1, \tau_2) \mapsto f$.

[7] For the convoluted operator at imaginary time $-\mathrm{i}\beta$, we make use of the identity from Ref. [41], $-\int_0^{\beta} du\, C(-iu)e^{-uE} = G''(E) + e^{-\beta E}G''(-E)$, with $G''(E)$ being the imaginary part of the coupling density and arrive at the second order coherences as in Eq. (2.66), which is equivalent to Eq. (2.64).

Using $\boldsymbol{S}(-u) = e^{-\mathrm{i}[H_\mathrm{S},\cdot]}S$, the integral can now be rewritten as a formal derivative with respect to the commutator $\Delta \equiv [H_\mathrm{S},\cdot]$

$$\int_0^{-\mathrm{i}\beta} du\, C(u) u \boldsymbol{S}(-u) = -\frac{\partial}{\partial \mathrm{i}\Delta}\mathbb{S}_{-\mathrm{i}\beta}. \tag{B.15}$$

This is a formal expression is defined by its matrix elements

$$\langle n|\frac{\partial}{\partial \mathrm{i}\Delta}\mathbb{S}_{-\mathrm{i}\beta}|l\rangle \equiv \frac{\partial}{\partial \mathrm{i}\Delta_{nl}}\langle n|\mathbb{S}_{-\mathrm{i}\beta}|l\rangle\,, \tag{B.16}$$

with $\langle n|\mathbb{S}_{-\mathrm{i}\beta}|l\rangle = \mathrm{i}[G''(\Delta_{nl}) + e^{-\beta\Delta_{nl}}G''(-\Delta_{nl})]S_{nl}$ [41]. Inserted in Eq. (B.14), one arrives at

$$\langle n|Q^{(2)}[\varrho^{(0)}]|n\rangle = \sum_l \frac{e^{-\beta E_l}}{Z_\mathrm{S}} S_{ln}\frac{\partial}{\partial\Delta_{nl}}[G''(\Delta_{nl}) + e^{-\beta\Delta_{nl}}G''(-\Delta_{nl})]S_{nl}. \tag{B.17}$$

In contrast to the coherences, the populations are not obtained within the Redfield theory, as discussed in Sections 2.5.2 and 2.6.2. Thus, for the populations the structure of the superoperator $\mathcal{Q}^{(2)}$ is not obvious. However, by carrying out the derivatives one finds [41]

$$\begin{aligned}\langle n|Q^{(2)}[\varrho^{(0)}]|n\rangle = &\sum_l |S_{nl}|^2\left[V''(\Delta_{nl})\frac{e^{-\beta E_l}}{Z_\mathrm{S}} - V''(\Delta_{ln})\frac{e^{-\beta E_n}}{Z_\mathrm{S}}\right]\\ &+\sum_l |S_{nl}|^2 G''(\Delta_{ln})\frac{\partial}{\partial E_n}\frac{e^{-\beta E_n}}{Z_\mathrm{S}},\end{aligned} \tag{B.18}$$

with $V''(\Delta) \equiv \partial_\Delta G''(\Delta)$, and where the first two terms act as a rate equation for the canonical Gibbs state $\varrho^{(0)}$. The rate equation can be written as a pseudo-Lindblad equation with jump operators $S_{nl}\,|n\rangle\langle l|$ and weight $V''(\Delta_{nl})$, which might also be negative.

The last term in Eq. (B.18) describes a contribution that acts as a derivative onto the state itself. Instead of writing the derivative for the equilibrium state as $\partial_{E_n}e^{-\beta E_n}/Z_\mathrm{S} = -\beta e^{-\beta E_n}/Z_\mathrm{S}$, we infer the derivative superoperator defined in Ref. [41]. To this end, we formally solve the rate equation for the zeroth-order steady-state populations $\varrho^{(0)}_{nn} = e^{-\beta E_n}/Z_\mathrm{S}$ [see e.g., Eq. (2.63)]

$$\varrho^{(0)}_{nn} = \frac{\sum_{l\neq n}|S_{nl}|^2\, G'(\Delta_{nl})\;\varrho^{(0)}_{ll}}{\sum_{l\neq n}|S_{ln}|^2\, G'(\Delta_{ln})}. \tag{B.19}$$

Taking the derivative with respect to the energy E_n on both sides, we find the derivative superoperator

$$\partial_{E_n}\varrho^{(0)}_{nn} = \frac{\sum_{l\neq n}|S_{nl}|^2\,[V'(\Delta_{nl})\,\varrho^{(0)}_{ll} + V'(\Delta_{ln})\,\varrho^{(0)}_{nn}]}{\sum_{l\neq n}|S_{ln}|^2\, W'(\Delta_{ln})}, \tag{B.20}$$

with $V'(\Delta) = \partial_\Delta G'(\Delta)$. Using this derivative superoperator, we find a much better perfor-

mance of the canonically consistent master equation in Chapter 5, as compared to taking simply the multiplication with $-\beta$.

To conclude this section, we identify the superoperator $\mathcal{Q}^{(2)}$ from the reduced Gibbs state, which is obtained from the coupling density $G(\Delta)$ of the Redfield tensor and the derivatives $V(\Delta)$. This is essential for the canonically consistent quantum master equation proposed in Chapter 5. We introduce the projection superoperators

$$\Pi = \sum_{n \neq m} |n\rangle\langle n| \cdot |m\rangle\langle m| \,, \tag{B.21}$$

which projects to the off-diagonal subspace, where $\Delta = [H_\mathrm{S}, \cdot]$ is invertible, i.e., the inverse of Δ is defined via the matrix elements $\langle n|\Delta^{-1}|m\rangle \overset{n\neq m}{=} 1/\Delta_{nm}$, and the complementary diagonal subspace

$$\Pi^c = \sum_{n} |n\rangle\langle n| \cdot |n\rangle\langle n| \,, \tag{B.22}$$

for the populations. With this we can write the superoperator as

$$\mathcal{Q}^{(2)}[\varrho] = \Pi \frac{1}{\mathrm{i}\Delta} \mathcal{R}^{(2)}[\varrho] + \Pi^c \left(\sum_{nl} |S_{nl}|^2 \big[V''(\Delta_{nl}) \mathcal{D}(|n\rangle\langle l|)[\varrho] + G''(\Delta_{ln}) \, |n\rangle \, \partial_{E_n} \varrho_{nn} \, \langle n| \, \big] \right), \tag{B.23}$$

with GKSL superoperator $\mathcal{D}(L) = L \cdot L^\dagger - \frac{1}{2}\{L^\dagger L, \cdot\}$ and the formal derivative Eq. (B.20) for the populations.

C Exact Hu-Paz-Zhang master equation for the Drude spectral density

In Section 2.6, we discuss the exact master equation for the damped harmonic oscillator with Drude spectral density $J(\omega) = M\gamma\omega/(1 + \omega^2/\omega_D^2)$. There, the Green's function is found to be related to the roots λ_i of the cubic equation $0 = z^3 - z^2\omega_D + z(\Omega^2 + \gamma\omega_D) - \omega_D\Omega^2$.[8] The cubic polynomial may be factorized,

$$0 = (z - \lambda_1)(z - \lambda_2)(z - \lambda_3) = z^3 - z^2\omega_D + z(\Omega^2 + \gamma\omega_D) - \omega_D\Omega^2, \tag{C.1}$$

[8] Equivalently one obtains the same roots for $0 = z^3 + z^2\omega_D + z(\Omega^2 + \gamma\omega_D) + \omega_D\Omega^2$, where the sign of the even orders is changed.

such that by equating the coefficients one obtains the Vieta relations [111]

$$\lambda_1 + \lambda_2 + \lambda_3 = 2\alpha + \delta \qquad = \omega_D, \tag{C.2}$$

$$\lambda_1\lambda_2 + \lambda_1\lambda_3 + \lambda_2\lambda_3 = \alpha^2 + \eta^2 + 2\alpha\delta = \Omega^2 + \gamma\omega_D, \tag{C.3}$$

$$\lambda_1\lambda_2\lambda_3 = (\alpha^2 + \eta^2)\delta \qquad = \omega_D\Omega^2, \tag{C.4}$$

where we have utilized that the roots occur in complex conjugate pairs, i.e., $\lambda_1 = \lambda_2^* = \alpha + \mathrm{i}\eta$ and $\lambda_3 = \delta$. Here, $\alpha, \delta > 0$ are inverse relaxation times and η the oscillatory frequency of the Green's function $\chi(t)$. In Ref. [111], for weak coupling, i.e., to first order in $\gamma/\omega_D \ll 1$, approximate solutions are given,

$$\alpha \simeq \frac{\gamma}{2}\frac{1}{1+\Omega^2/\omega_D^2}, \tag{C.5}$$

$$\eta \simeq \Omega\sqrt{1 + 2\frac{\alpha}{\omega_D} - \frac{\alpha^2}{\Omega^2}}, \tag{C.6}$$

$$\delta = \omega_D - 2\alpha. \tag{C.7}$$

From these one can deduce the approximate asymptotic parameters $\gamma_q = \alpha^2 + \eta^2 \simeq \Omega^2 + \frac{J(\Omega)\Omega}{M\omega_D}$ and $\gamma_p = 2\alpha \simeq \frac{J(\Omega)}{M\Omega}$, which are the Redfield results in Eqs. (2.78) and (2.80).

In this section, the expressions for strong coupling are derived by doing a perturbative expansion in $1/\gamma$. To start with, insert Eq. (C.4) in Eq. (C.3) to arrive at the quadratic equation $0 = \delta^2 - \delta\frac{1}{2\alpha}(\Omega^2 + \gamma\omega_D) + \frac{\omega_D\Omega^2}{2\alpha}$, which by claiming α to be a positive and real quantity (such that $\chi(t)$ decays exponentially with time), has the unique solution

$$\delta = \frac{\Omega^2 + \gamma\omega_D}{4\alpha}\left(1 - \sqrt{1 - 8\alpha\frac{\omega_D\Omega^2}{(\Omega^2+\gamma\omega_D)^2}}\right), \tag{C.8}$$

$$\simeq \frac{\omega_D\Omega^2}{\Omega^2 + \gamma\omega_D}. \tag{C.9}$$

Here, the second line follows by Taylor expanding the root. By inserting this into Eq. (C.2), one finds $\alpha = \frac{1}{2}(\omega_D - \delta)$ and finally η follows from Eq. (C.3), $\eta^2 = \Omega^2 + \gamma\omega_D - \frac{\omega_D^2}{4} - \frac{\delta}{2}(\omega_D - \frac{3}{2}\delta)$. For strong coupling, to leading order in $\gamma\omega_D/\Omega^2 \gg 1$, one finally arrives at

$$\alpha \simeq \frac{\omega_D}{2} - \frac{\Omega^2}{2\gamma}, \tag{C.10}$$

$$\eta \simeq \Omega\sqrt{1 + \frac{\gamma\omega_D}{\Omega^2} - \frac{\omega_D^2}{4\Omega^2}}, \tag{C.11}$$

$$\delta \simeq \frac{\Omega^2}{\gamma}. \tag{C.12}$$

D Asymptotic limit of exact Hu-Paz-Zhang master equation

Often, time-dependent master equations are replaced with their time-independent approximation by taking the asymptotic limit $t \to \infty$. In doing so, it is expected that the time-dependent coefficients in the master equation relax fast relative to the time-scale of the open system's dynamics. Typically, this only leads to small modifications for the transient dynamics, however, the steady state is accurately described by the time-independent master equation.[9] For the Hu-Paz-Zhang master equation, the time-independent version with the asymptotic coefficients $\gamma_q \equiv \lim_{t\to\infty} \gamma_q(t)$ and analogously defined γ_p, D_q and D_p, respectively, allow for an intuitive understanding and can be expressed by the equilibrium dispersions $\langle q^2\rangle$ and $\langle p^2\rangle$. It is also the basis for perturbative expansion in the coupling strength, used to make the connection to the second-order Redfield master equation.

We start with the temperature-independent parameters, which are the renormalized squared frequency $\gamma_q(t)$ and the damping coefficient $\gamma_p(t)$ in Eqs. (2.105) and (2.106),

$$\gamma_q(t) = \frac{-4\sum_i |\lambda_i|^2\,|c_i|^2[\mathrm{Im}\lambda_i]^2 e^{-2\mathrm{Re}\lambda_i t} + \sum_{i<j,\lambda_i\neq\lambda_i^*} \lambda_i\lambda_j\, c_i c_j \big[\lambda_i-\lambda_j\big]^2 e^{-(\lambda_i+\lambda_j)t}}{-4\sum_i |c_i|^2[\mathrm{Im}\lambda_i]^2 e^{-2\mathrm{Re}\lambda_i t} + \sum_{i<j,\lambda_j\neq\lambda_i^*} c_i c_j \big[\lambda_i-\lambda_j\big]^2 e^{-(\lambda_i+\lambda_j)t}}, \tag{D.1}$$

$$\gamma_p(t) = \frac{-4\sum_i 2\mathrm{Re}\lambda_i\,|c_i|^2[\mathrm{Im}\lambda_i]^2 e^{-2\mathrm{Re}\lambda_i t} + \sum_{i<j,\lambda_j\neq\lambda_i^*} (\lambda_i+\lambda_j)\, c_i c_j \big[\lambda_i-\lambda_j\big]^2 e^{-(\lambda_i+\lambda_j)t}}{-4\sum_i |c_i|^2[\mathrm{Im}\lambda_i]^2 e^{-2\mathrm{Re}\lambda_i t} + \sum_{i<j,\lambda_j\neq\lambda_i^*} c_i c_j \big[\lambda_i-\lambda_j\big]^2 e^{-(\lambda_i+\lambda_j)t}}. \tag{D.2}$$

Here, we explicitly distinguish the terms with complex conjugated pairs, $\lambda_j = \lambda_i^*$, $c_j = c_i^*$ and the remaining terms with $\lambda_j \neq \lambda_i^*$, $c_j \neq c_i^*$, respectively. For a Drude bath with cutoff $\omega_D/\Omega = 2$, the dynamics is plotted in Fig. D.1(a) and (c) for $\gamma/\Omega = 1$ and $\gamma/\Omega = 2$, respectively. Since all terms in the nominators and denominators are exponentially decaying, in the asymptotic limit, only the slowest decaying terms remain. Let the roots and residues be denoted by $(\lambda_i) = (\alpha + \mathrm{i}\eta, \alpha - \mathrm{i}\eta, \delta, \dots)$ and $(c_i) = (c_1, c_1^*, c_3, \dots)$, respectively, where we do not consider terms with $i > 3$, which belong to a faster decay. We now study different scenarios:

In the first case, let

$$\alpha < \delta, \tag{D.3}$$

[9] There are counter examples for master equations, where the stationary state of the time-dependent master equation and the approximation with the asymptotic master equation differ. An example is the eternal non-Markovian master equation for a qubit in Appendix G. However, this example is rather exceptional and typically the assumption holds.

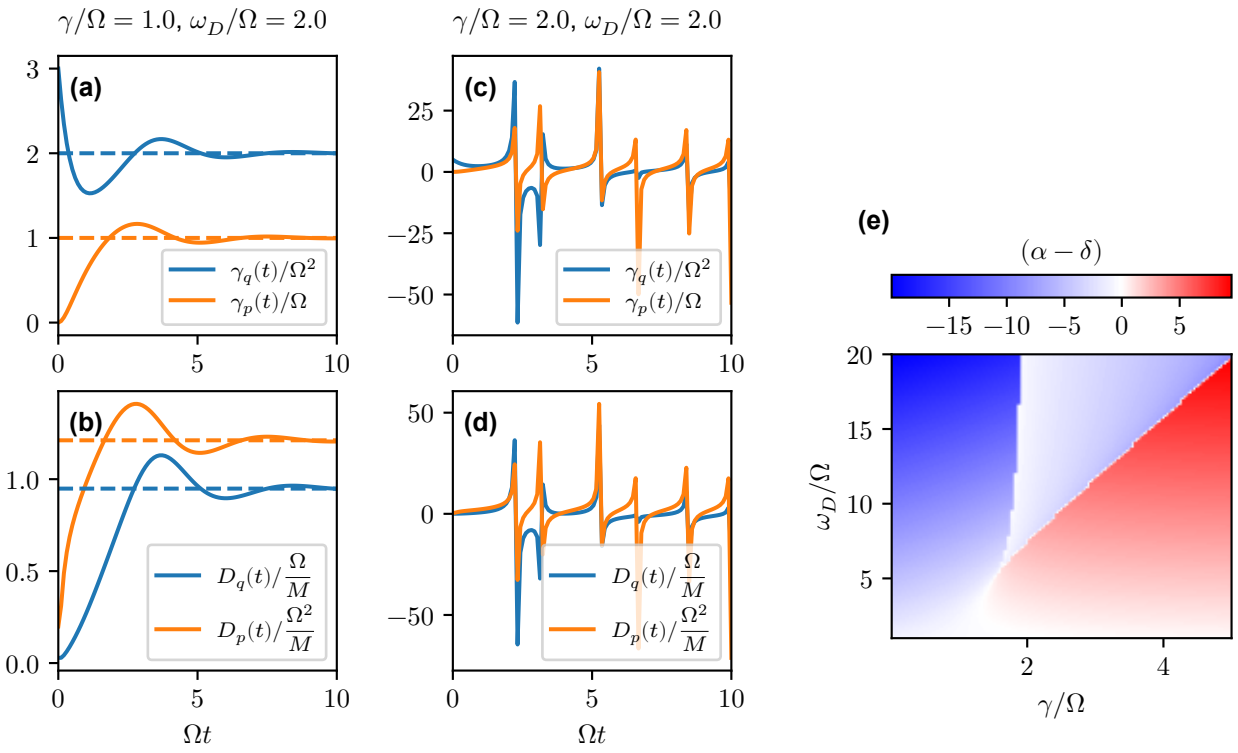

Figure D.1: Time dependent coefficients $\gamma_p(t)$, $\gamma_q(t)$ in (a) and $D_q(t)$, $D_p(t)$ in (b), respectively, for $\gamma/\Omega = 1$, $\omega_D/\Omega = 2$, $T/\Omega = 1$. The dashed lines show the asymptotes. Analogously in (c) and (d), except for stronger coupling $\gamma\Omega = 2$ without asymptotic regime. Asymptotic regime for $\alpha - \delta < 0$ highlighted blue in (e) as a function of γ and ω_D

corresponding to blue colors in Fig. D.1(e) and is used in panels (a) and (b). In this regime, the slowest decay is given by $e^{-2\alpha t}$ and the asymptotic coefficients read,

$$\gamma_q = \alpha^2 + \eta^2, \tag{D.4}$$

$$\gamma_p = 2\alpha, \tag{D.5}$$

which are the results of Eqs. (2.105) and (2.106) in the main text. In the second case, let

$$\lambda_3 = \delta < \alpha, \tag{D.6}$$

corresponding to red colors in Fig. D.1(e) and is used in panels (c) and (d). In contrast to the first scenario, $\mathrm{Im}\lambda_3 = \mathrm{Im}c_3 = 0$ are both real-valued, such that the terms with the rate $e^{-2\delta t}$ do not contribute, as can be seen from Eqs. (D.1) and (D.2). Instead, the asymptotes are given by,

$$\gamma_q = \delta\left(\alpha + \eta\cot(\eta t - \zeta)\right), \tag{D.7}$$

$$\gamma_p = \alpha + \delta + \eta\cot(\eta t - \zeta), \tag{D.8}$$

provided $c_3 \neq 0$ and with ζ being the complex phase of $c_1[\alpha-\delta+\mathrm{i}\eta]^2 \equiv |c_1|^2[(\alpha-\eta)^2+\eta^2]e^{\mathrm{i}\zeta}$. In this regime, the asymptotes are not well defined, as the coefficients are periodically diverging, see Fig. D.1(c) and Fig. D.1(d), respectively.

Lastly, in the particular case $\alpha = \delta$, one arrives at,

$$\gamma_q = \frac{(\alpha^2+\eta^2)\,2|c_1|^2 + c_3\mathrm{Re}\left[\alpha(\alpha+\mathrm{i}\eta)c_1 e^{-\mathrm{i}\eta t}\right]}{2|c_1|^2 + c_3\mathrm{Re}\left[c_1 e^{-\mathrm{i}\eta t}\right]}, \tag{D.9}$$

$$\gamma_p = \frac{2\alpha\,2|c_1|^2 + c_3\mathrm{Re}\left[(\alpha+\delta+\mathrm{i}\eta)c_1 e^{-\mathrm{i}\eta t}\right]}{2|c_1|^2 + c_3\mathrm{Re}\left[c_1 e^{-\mathrm{i}\eta t}\right]}. \tag{D.10}$$

Thus, in general, for finite asymptotes γ_q and γ_p, we have to assume that the decay time of the Green's function is given by the real part of a root, which has a non-zero imaginary part, i.e., for the Drude bath $\alpha < \delta$. In Fig. D.1(e) we plot the difference $\alpha - \delta$ as a function of coupling strength γ and cutoff frequency ω_D and see that for large enough cutoffs it is guaranteed to have $\alpha < \delta$.

The temperature-dependent coefficients in the exact master equation depend on the integral quantities $K_q(t)$ and $K_p(t)$ given in Eqs. (2.109) and (2.110), respectively,

$$K_q(t) = \frac{1}{M}\int_0^\infty J(\omega)\coth(\beta\omega/2)\left|\int_0^t e^{-\mathrm{i}\omega\tau}\chi(\tau)d\tau\right|^2\frac{d\omega}{\pi}, \tag{D.11}$$

$$K_p(t) = \frac{1}{M}\int_0^\infty J(\omega)\coth(\beta\omega/2)\left|e^{-\mathrm{i}\omega t}\chi(t) + \mathrm{i}\omega\int_0^t e^{-\mathrm{i}\omega\tau}\chi(\tau)d\tau\right|^2\frac{d\omega}{\pi}, \tag{D.12}$$

where for $K_p(t)$ we perform integration by parts for $\dot{\chi}(\tau)$ and note the initial condition $\chi(t = 0) = 0$.

Since $\dot{K}_q(t)$, $\ddot{K}_q(t)$ and $\dot{K}_p(t)$ are also relevant, for completeness, we state the time derivatives of the integrals,

$$\partial_t\left|\int_0^t e^{-\mathrm{i}\omega\tau}\chi(\tau)d\tau\right|^2 = 2\chi(t)\mathrm{Re}\left[e^{-\mathrm{i}\omega t}\int_0^t e^{-\mathrm{i}\omega\tau}\chi(\tau)d\tau\right], \tag{D.13}$$

$$\begin{aligned}\partial_t^2\left|\int_0^t e^{-\mathrm{i}\omega\tau}\chi(\tau)d\tau\right|^2 &= 2\chi(t)^2\cos(2\omega t) + 2\dot{\chi}(t)\mathrm{Re}\left[e^{-\mathrm{i}\omega t}\int_0^t e^{-\mathrm{i}\omega\tau}\chi(\tau)d\tau\right]\\ &\quad + 2\chi(t)\omega\mathrm{Im}\left[e^{-\mathrm{i}\omega t}\int_0^t e^{-\mathrm{i}\omega\tau}\chi(\tau)d\tau\right].\end{aligned} \tag{D.14}$$

Here, all terms are proportional to the exponentially decaying functions $\chi(t)$ or $\dot{\chi}(t)$, respectively. We find that in the asymptotic limit all time derivatives vanish, $\dot{K}_q(t), \ddot{K}_q(t), \dot{K}_p(t) \overset{t\to\infty}{\longrightarrow}$

0. Furthermore, the asymptotic integral quantities are given by

$$K_q \equiv K_q(t\to\infty) = \frac{1}{M}\int_0^\infty J(\omega)\coth(\beta\omega/2)\,|\bar{\chi}(\mathrm{i}\omega)|^2\,\frac{d\omega}{\pi}, \tag{D.15}$$

$$K_p \equiv K_p(t\to\infty) = \frac{1}{M}\int_0^\infty J(\omega)\coth(\beta\omega/2)\omega^2\,|\bar{\chi}(\mathrm{i}\omega)|^2\,\frac{d\omega}{\pi}, \tag{D.16}$$

where $\bar{\chi}(\mathrm{i}\omega) = \int_0^\infty e^{-z\tau}\chi(\tau)d\tau\big|_{z=\mathrm{i}\omega}$ is the Laplace-transform of the Green's function evaluated at the complex frequency $\mathrm{i}\omega$. The remaining frequency integrals are listed in reference [140] as Fourier representation of $\langle q^2\rangle$ and $\langle p^2\rangle$, respectively. Equivalently, the integrals can be formulated as a Matsubara series [140],

$$K_q = M\langle q^2\rangle = \frac{1}{\beta}\sum_{l=-\infty}^{\infty}\frac{1}{\Omega^2+\nu_l^2+|\nu_l|\bar{\kappa}(|\nu_l|)}, \tag{D.17}$$

$$K_p = \frac{1}{M}\langle p^2\rangle = \frac{1}{\beta}\sum_{l=-\infty}^{\infty}\frac{\Omega^2+|\nu_l|\bar{\kappa}(|\nu_l|)}{\Omega^2+\nu_l^2+|\nu_l|\bar{\kappa}(|\nu_l|)}, \tag{D.18}$$

with $\nu_l = 2\pi l/\beta$ and $\bar{\kappa}(z) = \int_0^t e^{-z\tau}\kappa(\tau)d\tau$ being the Laplace-transform of the damping kernel.

As discussed in the main text, for the Hu-Paz-Zhang master equation there is a sufficient condition, Eq. (2.82), which guarantees positivity of the equilibrium state. Since the exact equilibrium state is positive, we make the consistency check, of whether the positivity condition holds. For the exact asymptotic parameters it reads,

$$1 \le \frac{4}{\Omega^2}\frac{1}{M}\langle p^2\rangle M\gamma_q\langle q^2\rangle \equiv h_{\mathrm{krit}}, \tag{D.19}$$

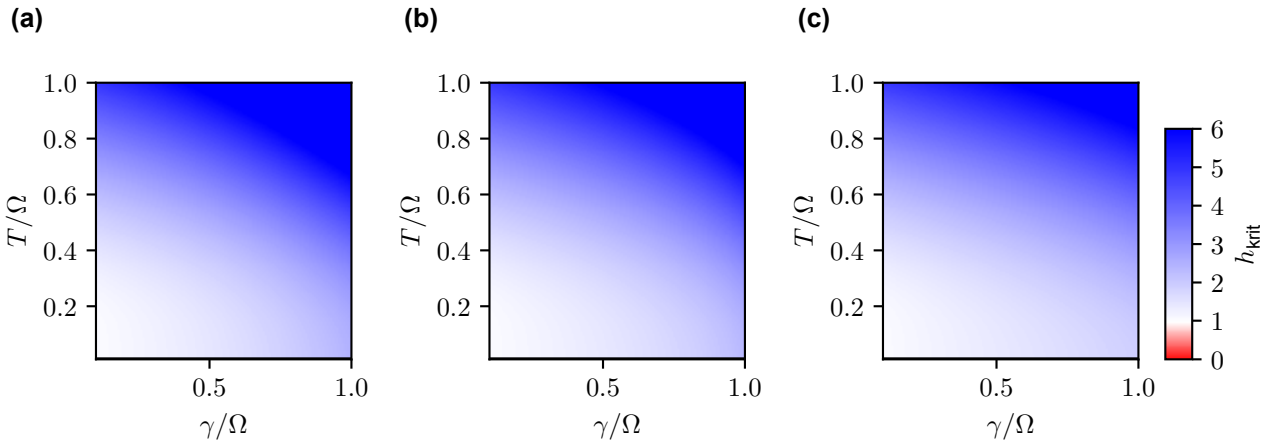

Figure D.2: Analogous to Fig. 2.4. Check of the positivity condition (2.82) for the exact Hu-Paz-Zhang master equation, as a function of coupling strength and temperature for different Drude cutoff frequencies $\omega_D = 2\Omega$ in (a), $\omega_D = 3\Omega$ in (b) and $\omega_D = 5\Omega$ in (c), respectively.

for which we calculate the right-hand side as a function of coupling strength and temperature for different cutoff frequencies in Fig. D.2, and find that it holds for all parameters considered.

D.1 Two-fold time integral for diffusion coefficients

As discussed in the main text, the frequency integrals for $K_q(t)$ and $K_p(t)$ in Eqs. (2.109) and (2.110), respectively, can be transformed into time integrals,

$$K_q(t) = \frac{1}{M}\int_0^t ds \int_0^t du\ \mathrm{Re}\left[C(s-u)\right]\ \chi(s)\chi(u), \tag{D.20}$$

$$K_p(t) = \frac{1}{M}\int_0^t ds \int_0^t du\ \mathrm{Re}\left[C(s-u)\right]\ \dot{\chi}(s)\dot{\chi}(u), \tag{D.21}$$

which agree with the expressions in Ref. [111]. These integrals can be solved explicitly by employing $\chi(t) = \sum_i c_i e^{-\lambda_i t}$ and the Matsubara series of the bath correlation $C(t)$ for the Drude spectral density, which is discussed in Section 2.2,

$$C(t) = M\frac{\gamma\omega_D^2}{2}\left[\cot(\beta\omega_D/2) - \mathrm{i}\right]e^{-\omega_D t} - M\frac{2\gamma}{\beta}\sum_{l=1}^{\infty}\frac{\nu_l\, e^{-\nu_l t}}{1-(\nu_l/\omega_D)^2}. \tag{D.22}$$

Altogether, the time dependence of $\chi(t)$ and $C(t)$ enter only via the argument of the exponential functions. Using the integral identity,

$$\begin{aligned} I_{ij}(x,t) &\equiv \int_0^t ds \int_0^t du\ e^{-x|s-u|}\ e^{-\lambda_i s}\ e^{-\lambda_j u}, \\ &= \frac{2x+\lambda_i+\lambda_j}{(\lambda_i+x)(\lambda_j+x)(\lambda_i+\lambda_j)} + \frac{-2x+\lambda_i+\lambda_j}{(\lambda_i-x)(\lambda_j-x)(\lambda_i+\lambda_j)}e^{-(\lambda_i+\lambda_j)t} \\ &\quad - \frac{1}{(\lambda_i+x)(\lambda_j-x)}e^{-(\lambda_i+x)t} - \frac{1}{(\lambda_j+x)(\lambda_i-x)}e^{-(\lambda_j+x)t}, \end{aligned} \tag{D.23}$$

one arrives at

$$K_q(t) = \frac{\gamma\omega_D^2}{2}\Big(\cot(\beta\omega_D/2)\sum_{ij}\quad c_i c_j\quad I_{ij}(\omega_D,t) + \frac{4}{\beta}\sum_{l=1}^{\infty}\frac{\nu_l}{\nu_l^2-\omega_D^2}\sum_{ij}\quad c_i c_j\quad I_{ij}(\nu_l,t)\Big), \tag{D.24}$$

$$K_p(t) = \frac{\gamma\omega_D^2}{2}\Big(\cot(\beta\omega_D/2)\sum_{ij} c_i c_j\lambda_i\lambda_j I_{ij}(\omega_D,t) + \frac{4}{\beta}\sum_{l=1}^{\infty}\frac{\nu_l}{\nu_l^2-\omega_D^2}\sum_{ij} c_i c_j\lambda_i\lambda_j I_{ij}(\nu_l,t)\Big). \tag{D.25}$$

Evaluating these expressions in the asymptotic limit $I_{ij}(x) \equiv I_{ij}(x, t\to\infty)$, one has to be careful about the contributing terms, e.g., in case $\lambda_i + \lambda_j = 0$. However, as compared to the frequency integrals, the implementation of the Matsubara series might be easier and

numerically more stable.

E Perturbative expansion of the exact Hu-Paz-Zhang master equation

Starting from the equilibrium dispersions Eqs. (D.17) and (D.18), we perform a perturbative expansion for weak coupling using $\bar{\kappa} = O(\gamma)$,

$$M\langle q^2\rangle \simeq \frac{1}{\Omega}\frac{1}{2}\coth(\beta\Omega/2) - \frac{1}{\beta}\sum_{l=-\infty}^{\infty}\frac{|\nu_l|\bar{\kappa}(|\nu_l|)}{(\Omega^2+\nu_l^2)^2}, \tag{E.1}$$

$$\frac{1}{M}\langle p^2\rangle \simeq \Omega\frac{1}{2}\coth(\beta\Omega/2) + \frac{1}{\beta}\sum_{l=-\infty}^{\infty}\frac{|\nu_l|^3\bar{\kappa}(|\nu_l|)}{(\Omega^2+\nu_l^2)^2}, \tag{E.2}$$

where in zeroth-order it is used $\frac{1}{2}\coth(\beta\Omega/2) = \frac{\Omega}{\beta}\sum_{l=-\infty}^{\infty} 1/(\Omega^2+\nu_l^2)$. For the diffusion coefficients in Eqs. (2.107) and (2.108) of the Hu-Paz-Zhang master equation, it follows that

$$D_q \simeq \frac{1}{M}\frac{\gamma_q-\Omega^2}{\Omega}\frac{1}{2}\coth(\beta\Omega/2) - \frac{1}{\beta}\frac{1}{M}\sum_{l=-\infty}^{\infty}\frac{\nu_l^2+\gamma_q}{(\nu_l^2+\Omega^2)^2}|\nu_l|\bar{\kappa}(|\nu_l|), \tag{E.3}$$

$$D_p \simeq \frac{1}{M}\gamma_p\frac{\Omega}{2}\coth(\beta\Omega/2). \tag{E.4}$$

Using $\gamma_q \simeq \Omega^2 + O(\gamma)$, the second term in the former equation can be further approximated,

$$\begin{aligned} -\frac{1}{\beta}\frac{1}{M}\sum_{l=-\infty}^{\infty}\frac{\nu_l^2+\gamma_q}{(\nu_l^2+\Omega^2)^2}|\nu_l|\bar{\kappa}(|\nu_l|) &\simeq -\frac{1}{\beta}\frac{1}{M}\sum_{l=-\infty}^{\infty}\frac{|\nu_l|\bar{\kappa}(|\nu_l|)}{\nu_l^2+\Omega^2}, \\ &= -\frac{2}{M^2}\int_0^{\infty}\frac{J(\omega)}{\omega}\frac{1}{\beta}\sum_{l=-\infty}^{\infty}\frac{\nu_l^2}{(\nu_l^2+\omega^2)(\nu_l^2+\Omega^2)}\frac{d\omega}{\pi}, \end{aligned} \tag{E.5}$$

where in the second line the definition of the damping kernel in Eq. (2.97) is used. The series can be evaluated explicitly,[10]

$$\frac{1}{\beta}\sum_{l=-\infty}^{\infty}\frac{\nu_l^2}{(\nu_l^2+\omega^2)(\nu_l^2+\Omega^2)} = \frac{1}{\Omega^2-\omega^2}\left(\frac{\Omega}{2}\coth(\beta\Omega/2) - \frac{\omega}{2}\coth(\beta\omega/2)\right), \tag{E.6}$$

[10] $\frac{\nu_l^2+\omega^2-\omega^2}{(\nu_l^2+\omega^2)(\nu_l^2+\Omega^2)} = \frac{1}{\Omega^2-\omega^2}\left(\Omega^2\frac{1}{\nu_l^2+\Omega^2} - \omega^2\frac{1}{\nu_l^2+\omega^2}\right)$.

and one arrives at

$$D_q \simeq \frac{1}{M^2}\mathcal{P}\int_0^\infty \frac{J(\omega)}{\Omega^2-\omega^2}\coth(\beta\omega/2)\frac{d\omega}{\pi} + \frac{1}{M}\frac{1}{\Omega}\left[\gamma_q - \Omega^2 - \Omega^2\frac{2}{M}\mathcal{P}\int_0^\infty \frac{J(\omega)/\omega}{\Omega^2-\omega^2}\frac{d\omega}{\pi}\right]\frac{1}{2}\coth(\beta\omega/2). \tag{E.7}$$

Both integrals are well-known from the Redfield theory for the second-order coefficients $\gamma_q^{(2)}$ and $D_q^{(2)}$ in Eqs. (2.78) and (2.81), respectively.

To finalize the discussion, the temperature-independent coefficients γ_q and γ_p are considered. For these parameters, a model independent perturbative expansion for a generic spectral density is difficult, since it requires the inverse Laplace transform of $\bar{\chi}(z) = 1/(z^2 + z\bar{\kappa}(z) + \Omega^2)$. Hence, the poles, which give rise to γ_q and γ_p, depend on the detailed structure of the damping kernel. However, in the zero-coupling limit, i.e., $\bar{\kappa}(z) = 0$, by inverse Laplace transformation one obtains the result for the Green's function $G^{(0)}(t) = \frac{1}{\Omega}\sin(\Omega t)$. Namely, using Eqs. (2.105) and (2.106) it follows, $\gamma_q^{(0)}(t) = \Omega^2$ and $\gamma_p^{(0)}(t) = 0$.

For weak coupling, we consider the explicit solutions for the Drude spectral density of Appendix C, which read

$$\gamma_q \simeq \Omega^2 + \frac{J(\Omega)\Omega}{M\omega_D}, \tag{E.8}$$

$$\gamma_p \simeq \frac{J(\Omega)}{M\Omega} = \gamma_p^{(2)}, \tag{E.9}$$

and agree with the Redfield results of Eqs. (2.78) and (2.80). In particular, the second line in Eq. (E.7) cancels, such that the diffusion coefficients coincide with the Redfield results, i.e., $D_p \simeq D_p^{(2)}$ and $D_q \simeq D_p^{(2)}$.

F Truncated master equation for high temperature and finite cutoff

The truncated master equation proposed in Chapter 3 is a novel approximation to reduce the Redfield equation to GKSL form. The approximation is to truncate the negative contributions of the pseudo-Lindblad equation. This is expected to be valid in regimes, where the weight of the negative contribution is small. In this section, we discuss the weight in the high-temperature regime.

For high temperatures, we Taylor expand the Bose distribution,

$$n_\beta(\omega) = \frac{1}{\beta\omega} - \frac{1}{2} + \frac{\beta\omega}{12} + O((\beta\omega)^3). \tag{F.1}$$

With this, the real part of the coupling density (2.19) reduces to $G'(\Delta) \simeq J(\Delta)(1/\beta\Delta - 1/2 + \beta\Delta/12)$ and for the imaginary part one obtains $G_0''(\Delta) + G_{\text{th}}''(\Delta) \simeq J(\Delta)\left(\frac{1}{2}\frac{\Delta}{\omega_D} - \frac{1}{\beta\omega_D}\right)$. The relevant quantities reduce to

$$\overline{G'} \simeq \frac{1}{\beta}\overline{\frac{J(\Delta)}{\Delta}} + \frac{\beta}{12}\overline{J(\Delta)\Delta}, \tag{F.2}$$

$$\overline{G'^2} \simeq \frac{1}{\beta^2}\overline{\frac{J(\Delta)^2}{\Delta^2}} + \frac{5}{12}\overline{J(\Delta)^2}, \tag{F.3}$$

$$\overline{[G_0'' + G_{\text{th}}'']^2} \simeq \frac{1}{4\omega_D^2}\overline{J(\Delta)^2\Delta^2} + \frac{1}{\beta^2\omega_D^2}\overline{J(\Delta)^2}, \tag{F.4}$$

$$\overline{G_0''}^2 = \frac{1}{4\omega_D^2}\overline{J(\Delta)\Delta}^2. \tag{F.5}$$

Taking only the terms to leading order in β, the weights of the jump operators read [Eq. (3.62)]

$$\|A_\pm\|^2 \simeq \frac{\|S\|^2}{\beta}\left(\pm\overline{\frac{J(\Delta)}{\Delta}} + \sqrt{\overline{\frac{J(\Delta)^2}{\Delta^2}} + \frac{1}{\omega_D^2}\overline{J(\Delta)^2}} + O(\beta^2)\right). \tag{F.6}$$

Now assuming a large Drude cutoff $\omega_D^2 \gg \overline{J(\Delta)^2}$, it is $\overline{J(\Delta)/\Delta} \simeq \sqrt{\overline{J(\Delta)^2/\Delta^2}} \simeq \gamma$ and

$$\|A_\pm\|^2 \overset{\omega_D \gg |\overline{\Delta}|}{\simeq} \frac{\gamma\|S\|^2}{\beta}\left(1 \pm 1 + O(\beta^2)\right). \tag{F.7}$$

With that, we find $\|A_-\|^2/\|A_+\|^2 = O(\beta^2)$ for the relative rate of the negative contribution.

G Exact solution to non-Markovian dephasing for a single qubit

In this section, we solve the dynamics for the master equation of a single qubit,

$$\partial_t\varrho(t) = \frac{1}{2}\sum_{i=1}^{3}\gamma_i(t)\left(\sigma^i\varrho(t)\sigma^i - \varrho(t)\right), \tag{G.1}$$

with arbitrary time-dependent relaxation strengths $\gamma_i(t)$. The solution is obtained by representing the state with the Bloch-vector $(x(t), y(t), z(t))^T \equiv (\langle\sigma^x\rangle, \langle\sigma^y\rangle, \langle\sigma^z\rangle)^T$ as

$$\varrho(t) = \frac{1}{2}\left(\mathbb{1} + x(t)\,\sigma^x + y(t)\,\sigma^y + z(t)\,\sigma^z\right), \tag{G.2}$$

and identifying the equations of motions for the three components. Using the identity $\sigma^i\varrho(t)\sigma^i - \varrho(t) = \sum_{j,j\neq i} x_j(t)\sigma^j$, the master equation is written as,

$$\begin{aligned}\partial_t\varrho(t) &= \frac{1}{2}\left(\dot{x}(t)\,\sigma^x + \dot{y}(t)\,\sigma^y + \dot{z}(t)\,\sigma^z\right), &\text{(G.3)}\\ &= \frac{1}{2}\left(-(\gamma_y(t)+\gamma_z(t))x(t)\,\sigma^x - (\gamma_x(t)+\gamma_z(t))y(t)\,\sigma^y - (\gamma_x(t)+\gamma_y(t))z(t)\,\sigma^z\right), &\text{(G.4)}\end{aligned}$$

and since the Pauli operators form a basis, by equating the coefficients the equations of motion for the components are obtained. Exemplary, for the x-polarization it follows $\dot{x}(t) = -(\gamma_y(t)+\gamma_z(t))\,x(t)$ which we write as $\partial_t \ln(x(t)) = -\gamma_x(t) - \gamma_z(t)$, and can be directly integrated. Altogether, the solutions are given by

$$\begin{aligned}x(t) &= e^{-\int_0^t(\gamma_y(\tau)+\gamma_z(\tau))d\tau}x(0), &\text{(G.5)}\\ y(t) &= e^{-\int_0^t(\gamma_x(\tau)+\gamma_z(\tau))d\tau}y(0), &\text{(G.6)}\\ z(t) &= e^{-\int_0^t(\gamma_x(\tau)+\gamma_y(\tau))d\tau}z(0), &\text{(G.7)}\\ & &\text{(G.8)}\end{aligned}$$

and are discussed in Section 4.5.

List of terms

asymptotic In this thesis, the term *asymptotic* refers to the limit of large times. For instance, the reduced state $\varrho(t)$ reaches a stationary state $\varrho = \lim_{t\to\infty} \varrho(t)$. The time-dependent convoluted coupling operator $\mathbb{S}_t$ reaches $\mathbb{S} = \lim_{t\to\infty} \mathbb{S}_t$. Other examples are, the coupling density $G(\Delta) = \lim_{t\to\infty} G_t(\Delta)$, the Redfield superoperator $\mathcal{R}^{(2)} = \lim_{t\to\infty} \mathcal{R}_t^{(2)}$, the coefficients in the Caldeira-Legget master equation $\gamma_q = \lim_{t\to\infty} \gamma_q(t)$ and analogous for γ_p, D_q, and D_p, and the superoperator for the CCQME $\mathcal{Q}^{(2)} = \lim_{t\to\infty} \mathcal{Q}_t^{(2)}$. 13, 22, 29, 35, 106, 107, 118

convoluted operator Convolution integral of time dependetent coupling operator and bath correlation, $\mathbb{S}_t = \int_0^t C(\tau)\mathbf{S}(-\tau)d\tau$ with static limit $\lim_{t\to\infty} \mathbb{S}_t \equiv \mathbb{S}$, which appears in the Redfield equation. 21, 22, 129

coupling density Half-sided Fourier integral of bath correlation function, $G_t(\Delta) = \int_0^t e^{-\mathrm{i}\Delta\tau} C(\tau)\mathrm{d}\tau$, with static limit $\lim_{t\to\infty} G_t(\Delta) \equiv G(\Delta)$. The real part $G'(\Delta)$ obeys detailed balance condition. The imaginary part $G''(\Delta)$ describes additional vacuum fluctuations and thermal noise. 8, 12, 13, 15, 22, 55, 144

coupling operator The most general form of the system-bath coupling Hamiltonian is $H_{\mathrm{SB}} = \sum_\alpha (S_\alpha \otimes B_\alpha^\dagger + S_\alpha^\dagger \otimes B_\alpha)$, where S_α define the coupling operators. 7

GKSL Short for Gorini-Kossakowski-Sudarshan-Lindblad. Particular form of a quantum master equation with dissipator $\mathcal{D}(L)[\varrho(t)] = L\varrho(t)L^\dagger - \frac{1}{2}\{L^\dagger L, \varrho(t)\}$ that guarantees positive evolution of the reduced state $\varrho(t)$ and can be efficienlty solved by quantum jump trajectories. 16, 25, 135

Hamiltonian The Hamiltonian of the total system-bath compound is denoted as $H_{\mathrm{tot}} = H_{\mathrm{S}} + H_{\mathrm{SB}} + H_{\mathrm{B}}$ with H_{S} and H_{B} acting solely on the system and bath, respectively. System and bath are coupled via the interaction Hamiltonian H_{SB} acting on the joint Hilbert space of system and bath. . 7

pseudo-Lindblad Quantum master equations of pseudo-Lindblad form agree with the GKSL form, except they include terms with negative relaxation weight. A typical form considered in this thesis is $D^{\mathrm{Red}} = \mathcal{D}(A_+) - \mathcal{D}(A_-)$, which is a representation of the Redfield

dissipator with two jumpoperators A_+ and A_- with relaxation weights $+1$ and -1, respectively. 44, 46, 136

quantum trajectories Quantum master equations can be efficiently unraveled by the simulation of pure quantum states that evolve stochastically. A single realization is referred to as quantum trajectory. For GKSL master equations the Monte Carlo wave function approach is well-known. There, the coherent time evolution is interrupted by spontaneously occuring quantum jumps. In this thesis, a new unraveling for pseudo-Lindblad equations is proposed. 62, 85, 87

Redfield equation Perturbative master equation for the reduced dynamics of the system, which is obtained in second-order perturbation theory. The superoperator of the time-dependent Redfield equation is denoted as $\mathcal{R}_t^{(2)}$. 19

reduced Gibbs state From the full equilibrium state of the total system-bath compound $\varrho_{\mathrm{tot}} = \frac{e^{-\beta(H_0+H_{\mathrm{SB}})}}{Z_{\mathrm{tot}}}$, it follows the reduced Gibbs state by taking the partial trace over the bath's degrees of freedom, $\varrho = \mathrm{tr}_{\mathrm{B}} \frac{e^{-\beta(H_0+H_{\mathrm{SB}})}}{Z_{\mathrm{tot}}}$. 29, 103, 142

reorganization energy Constant offset G''_{RN} of coupling density $G(\Delta)$. In the Redfield and quantum-optical master equation it modifies the coherent dynamics by shifting the Hamiltonian. For instance, in the Caldeira-Leggett model, this shift is compensated by the reorganization Hamiltonian. 14, 22, 39

reorganization Hamiltonian The reorganization Hamiltonian $H_{\mathrm{RN}} = -G''_{\mathrm{RN}} S^2$ is a counter term in the total system-bath Hamiltonian that comensates for the reorganization energy. 22, 31

RWA The rotating-wave approximation (RWA) is used to reduce the Redfield equation to GKSL form. This is justified for ultraweak coupling when fast oscillating terms in the Redfield equation are assumed to average out and are neglected. 8, 24, 136

spectral density Denoted as $J(\omega)$. Determines coupling profile to individual states in the bath. Assumed to be a smooth function. Throughout this thesis, an Ohmic spectral density with Drude cutoff is considered. 9

thermal noise Temperature-dependent part for the imaginary part of the coupling density $G''_{\mathrm{th}}(\Delta)$ that vanishes for zero temperature. It is shown to be antisymmetric, i.e., $G''_{\mathrm{th}}(\Delta) = -G''_{\mathrm{th}}(-\Delta)$. 14

zero-point fluctuation Temperature-independent part for the imaginary part of the coupling density $G''_0(\Delta)$ that is not reorganization energy. 14

List of Figures

Bibliography

[1] R. Labouvie, B. Santra, S. Heun, and H. Ott, Bistability in a Driven-Dissipative Superfluid, Phys. Rev. Lett. **116**, 235302 (2016).

[2] D. Husmann, M. Lebrat, S. Häusler, J.-P. Brantut, L. Corman, and T. Esslinger, Breakdown of the Wiedemann–Franz law in a unitary Fermi gas, Proc. Natl. Acad. Sci. U.S.A. **115**, 8563–8568 (2018).

[3] M. Lebrat, P. Grišins, D. Husmann, S. Häusler, L. Corman, T. Giamarchi, J.-P. Brantut, and T. Esslinger, Band and Correlated Insulators of Cold Fermions in a Mesoscopic Lattice, Phys. Rev. X **8**, 011053 (2018).

[4] I. Georgescu, 25 years of BEC, Nat Rev Phys **2**, 396–396 (2020).

[5] D. Vorberg, W. Wustmann, R. Ketzmerick, and A. Eckardt, Generalized bose-einstein condensation into multiple states in driven-dissipative systems, Phys. Rev. Lett. **111**, 240405 (2013).

[6] D. Vorberg, W. Wustmann, H. Schomerus, R. Ketzmerick, and A. Eckardt, Nonequilibrium steady states of ideal bosonic and fermionic quantum gases, Phys. Rev. E **92**, 062119 (2015).

[7] A. Schnell, D. Vorberg, R. Ketzmerick, and A. Eckardt, High-temperature nonequilibrium bose condensation induced by a hot needle, Phys. Rev. Lett. **119**, 140602 (2017).

[8] R. A. Nyman, H. S. Dhar, J. D. Rodrigues, and F. Mintert, Phase transitions of light in a dye-filled microcavity: Observations and simulations, J. Phys.: Conf. Ser. **1919**, 012006 (2021).

[9] F. E. Öztürk, T. Lappe, G. Hellmann, J. Schmitt, J. Klaers, F. Vewinger, J. Kroha, and M. Weitz, Observation of a non-Hermitian phase transition in an optical quantum gas, Science **372**, 88–91 (2021).

[10] J. Bloch, I. Carusotto, and M. Wouters, Non-equilibrium Bose–Einstein condensation in photonic systems, Nat Rev Phys **4**, 470–488 (2022).

[11] A. Schnell, L.-N. Wu, A. Widera, and A. Eckardt, Floquet-heating-induced Bose condensation in a scarlike mode of an open driven optical-lattice system, Phys. Rev. A **107**, L021301 (2023).

[12] F. Letscher, O. Thomas, T. Niederprüm, M. Fleischhauer, and H. Ott, Bistability Versus Metastability in Driven Dissipative Rydberg Gases, Phys. Rev. X **7**, 021020 (2017).

[13] N. Dogra, M. Landini, K. Kroeger, L. Hruby, T. Donner, and T. Esslinger, Dissipation-induced structural instability and chiral dynamics in a quantum gas, Science **366**, 1496–1499 (2019).

[14] Q. Fontaine, D. Squizzato, F. Baboux, I. Amelio, A. Lemaître, M. Morassi, I. Sagnes, L. Le Gratiet, A. Harouri, M. Wouters, I. Carusotto, A. Amo, M. Richard, A. Minguzzi, L. Canet, S. Ravets, and J. Bloch, Kardar–Parisi–Zhang universality in a one-dimensional polariton condensate, Nature **608**, 687–691 (2022).

[15] L. W. Clark, N. Schine, C. Baum, N. Jia, and J. Simon, Observation of Laughlin states made of light, Nature **582**, 41–45 (2020).

[16] C. K. Andersen, A. Kamal, N. A. Masluk, I. M. Pop, A. Blais, and M. H. Devoret, Quantum Versus Classical Switching Dynamics of Driven Dissipative Kerr Resonators, Phys. Rev. Appl. **13**, 044017 (2020).

[17] A. S. Trushechkin, M. Merkli, J. D. Cresser, and J. Anders, Open quantum system dynamics and the mean force Gibbs state, AVS Quantum Science **4**, 012301 (2022).

[18] C. Cohen-Tannoudji, J. Dupont-Roc, and G. Grynberg, Radiation Considered as a Reservoir: Master Equation for the Particles, in *Atom—Photon Interactions* (1998) Chap. 4, pp. 257–351.

[19] H. J. Carmichael, *Statistical Methods in Quantum Optics 1* (Springer-Verlag, Berlin, 1999).

[20] C. W. Gardiner and P. Zoller, *Quantum Noise*, 3rd ed. (Springer-Verlag, Berlin, 2004).

[21] H.-P. Breuer and F. Petruccione, *The Theory of Open Quantum Systems* (Oxford University Press, New York, 2007).

[22] D. Walls and G. J. Milburn, eds., *Quantum Optics* (Springer, Berlin, Heidelberg, 2008).

[23] U. Weiss, *Quantum Dissipative Systems*, 4th ed. (World Scientific, 2012).

[24] A. G. Redfield, The theory of relaxation processes, Adv. Magn. Reson. **1**, 1–32 (1965).

[25] F. E. Figueirido and R. M. Levy, Vibrational relaxation and Bloch–Redfield theory, J. Chem. Phys. **97**, 703–706 (1992).

[26] A. Dodin, T. Tscherbul, R. Alicki, A. Vutha, and P. Brumer, Secular versus nonsecular Redfield dynamics and Fano coherences in incoherent excitation: An experimental proposal, Phys. Rev. A **97**, 013421 (2018).

[27] F. Benatti, D. Chruściński, and R. Floreanini, Local Generation of Entanglement with Redfield Dynamics, Open Syst. Inf. Dyn. **29**, 2250001 (2022).

[28] H. Grabert, P. Talkner, and P. Hänggi, Microdynamics and time-evolution of macroscopic non-Markovian systems, Z Physik B **26**, 389–395 (1977).

[29] F. Shibata, Y. Takahashi, and N. Hashitsume, A generalized stochastic liouville equation. Non-Markovian versus memoryless master equations, J. Stat. Phys. **17**, 171–187 (1977).

[30] S. Nakajima, On quantum theory of transport phenomena: Steady diffusion, Prog. Th. Phys. **20**, 948–959 (1958).

[31] R. Zwanzig, Ensemble method in the theory of irreversibility, J. Chem. Phys. **33**, 1338–1341 (1960).

[32] G. Schaller and T. Brandes, Preservation of positivity by dynamical coarse graining, Phys. Rev. A **78**, 022106 (2008).

[33] C. Majenz, T. Albash, H.-P. Breuer, and D. A. Lidar, Coarse graining can beat the rotating-wave approximation in quantum Markovian master equations, Phys. Rev. A **88**, 012103 (2013).

[34] E. Mozgunov and D. Lidar, Completely positive master equation for arbitrary driving and small level spacing, Quantum **4**, 227 (2020).

[35] T. V. Tscherbul and P. Brumer, Partial secular Bloch-Redfield master equation for incoherent excitation of multilevel quantum systems, J. Chem. Phys. **142**, 104107 (2015).

[36] D. Farina and V. Giovannetti, Open-quantum-system dynamics: Recovering positivity of the Redfield equation via the partial secular approximation, Phys. Rev. A **100**, 012107 (2019).

[37] R. Hartmann and W. T. Strunz, Accuracy assessment of perturbative master equations: Embracing nonpositivity, Phys. Rev. A **101**, 012103 (2020).

[38] V. Romero-Rochin and I. Oppenheim, Relaxation properties of two-level systems in condensed phases, Physica A **155**, 52–72 (1989).

[39] E. Geva, E. Rosenman, and D. Tannor, On the second-order corrections to the quantum canonical equilibrium density matrix, J. Chem. Phys. **113**, 1380–1390 (2000).

[40] C. H. Fleming and N. I. Cummings, Accuracy of perturbative master equations, Phys. Rev. E **83**, 031117 (2011).

[41] J. Thingna, J.-S. Wang, and P. Hänggi, Generalized Gibbs state with modified Redfield solution: Exact agreement up to second order, J. Chem. Phys. **136**, 194110 (2012).

[42] J. Thingna, J.-S. Wang, and P. Hänggi, Reduced density matrix for nonequilibrium steady states: A modified Redfield solution approach, Phys. Rev. E **88**, 052127 (2013).

[43] M. Łobejko, M. Winczewski, G. Suárez, R. Alicki, and M. Horodecki, Towards reconciliation of completely positive open system dynamics with the equilibration postulate (2022), arxiv:2204.00643 .

[44] G. M. Timofeev and A. S. Trushechkin, Hamiltonian of mean force in the weak-coupling and high-temperature approximations and refined quantum master equations, Int. J. Mod. Phys. A **37**, 2243021 (2022).

[45] A. Suárez, R. Silbey, and I. Oppenheim, Memory effects in the relaxation of quantum open systems, J. Chem. Phys. **97**, 5101–5107 (1992).

[46] P. Pechukas, Reduced dynamics need not be completely positive, Phys. Rev. Lett. **73**, 1060–1062 (1994).

[47] A. Montoya-Castillo, T. C. Berkelbach, and D. R. Reichman, Extending the applicability of Redfield theories into highly non-Markovian regimes, J. Chem. Phys. **143**, 194108 (2015).

[48] M.-D. Choi, Positive Linear Maps on C*-Algebras, Canadian Journal of Mathematics **24**, 520–529 (1972).

[49] V. Gorini, A. Kossakowski, and E. C. G. Sudarshan, Completely positive dynamical semigroups of N-level systems, J. Math. Phys. **17**, 821–825 (1976).

[50] G. Lindblad, On the generators of quantum dynamical semigroups, Commun. Math. Phys. **48**, 119–130 (1976).

[51] J. Dalibard, Y. Castin, and K. Mølmer, Wave-function approach to dissipative processes in quantum optics, Phys. Rev. Lett. **68**, 580–583 (1992).

[52] K. Mølmer, Y. Castin, and J. Dalibard, Monte Carlo wave-function method in quantum optics, J. Opt. Soc. Am. B **10**, 524–538 (1993).

[53] C. W. Gardiner, A. S. Parkins, and P. Zoller, Wave-function quantum stochastic differential equations and quantum-jump simulation methods, Phys. Rev. A **46**, 4363–4381 (1992).

[54] R. Dum, A. S. Parkins, P. Zoller, and C. W. Gardiner, Monte Carlo simulation of master equations in quantum optics for vacuum, thermal, and squeezed reservoirs, Phys. Rev. A **46**, 4382–4396 (1992).

[55] N. Gisin and I. C. Percival, Wave-function approach to dissipative processes: Are there quantum jumps?, Phys. Lett. A **167**, 315–318 (1992).

[56] N. Gisin and I. C. Percival, The quantum-state diffusion model applied to open systems, J. Phys. A **25**, 5677–5691 (1992).

[57] A. J. Daley, Quantum trajectories and open many-body quantum systems, Adv. Phys. **63**, 77–149 (2014).

[58] I. I. Rabi, J. R. Zacharias, S. Millman, and P. Kusch, A New Method of Measuring Nuclear Magnetic Moment, Phys. Rev. **53**, 318–318 (1938).

[59] E. Jaynes and F. Cummings, Comparison of quantum and semiclassical radiation theories with application to the beam maser, Proceedings of the IEEE **51**, 89–109 (1963).

[60] W. J. Munro and C. W. Gardiner, Non-rotating-wave master equation, Phys. Rev. A **53**, 2633–2640 (1996).

[61] H. Wichterich, M. J. Henrich, H.-P. Breuer, J. Gemmer, and M. Michel, Modeling heat transport through completely positive maps, Phys. Rev. E **76**, 031115 (2007).

[62] A. Vrajitoarea, R. Belyansky, R. Lundgren, S. Whitsitt, A. V. Gorshkov, and A. A. Houck, Ultrastrong light-matter interaction in a photonic crystal (2022), arxiv:2209.14972 .

[63] D. W. Hone, R. Ketzmerick, and W. Kohn, Statistical mechanics of Floquet systems: The pervasive problem of near degeneracies, Phys. Rev. E **79**, 051129 (2009).

[64] T. Shirai, J. Thingna, T. Mori, S. Denisov, P. Hänggi, and S. Miyashita, Effective Floquet-Gibbs states for dissipative quantum systems, New J. Phys. **18**, 053008 (2016).

[65] A. Eckardt, Colloquium: Atomic quantum gases in periodically driven optical lattices, Rev. Mod. Phys. **89**, 011004 (2017).

[66] G. Engelhardt, G. Platero, and J. Cao, Discontinuities in driven spin-boson systems due to coherent destruction of tunneling: Breakdown of the floquet-gibbs distribution, Phys. Rev. Lett. **123**, 120602 (2019).

[67] H.-P. Breuer, B. Kappler, and F. Petruccione, Stochastic wave-function method for non-Markovian quantum master equations, Phys. Rev. A **59**, 1633–1643 (1999).

[68] I. Kondov, U. Kleinekathöfer, and M. Schreiber, Stochastic unraveling of Redfield master equations and its application to electron transfer problems, J. Chem. Phys. **119**, 6635–6646 (2003).

[69] H.-P. Breuer, Genuine quantum trajectories for non-Markovian processes, Phys. Rev. A **70**, 012106 (2004).

[70] J. Piilo, S. Maniscalco, K. Härkönen, and K.-A. Suominen, Non-Markovian Quantum Jumps, Phys. Rev. Lett. **100**, 180402 (2008).

[71] J. Piilo, K. Härkönen, S. Maniscalco, and K.-A. Suominen, Open system dynamics with non-Markovian quantum jumps, Phys. Rev. A **79**, 062112 (2009).

[72] K. Härkönen, Jump probabilities in the non-Markovian quantum jump method, J. Phys. A **43**, 065302 (2010).

[73] K. Luoma, W. T. Strunz, and J. Piilo, Diffusive limit of non-Markovian quantum jumps, Phys. Rev. Lett. **125**, 150403 (2020).

[74] Y. Tanimura and R. Kubo, Time evolution of a quantum system in contact with a nearly gaussian-markoffian noise bath, Phys. Soc. Jpn. **58**, 101–114 (1989).

[75] A. Fruchtman, N. Lambert, and E. M. Gauger, When do perturbative approaches accurately capture the dynamics of complex quantum systems?, Sci. Rep. **6**, 28204 (2016).

[76] M. Xu and J. Ankerhold, About the performance of perturbative treatments of the spin-boson dynamics within the hierarchical equations of motion approach, Eur. Phys. J. Spec. Top. 10.1140/epjs/s11734-023-01000-6 (2023).

[77] D. Suess, A. Eisfeld, and W. T. Strunz, Hierarchy of stochastic pure states for open quantum system dynamics, Phys. Rev. Lett. **113**, 150403 (2014).

[78] L. Diósi, N. Gisin, J. Halliwell, and I. C. Percival, Decoherent histories and quantum state diffusion, Phys. Rev. Lett. **74**, 203–207 (1995).

[79] M. Topaler and N. Makri, System-specific discrete variable representations for path integral calculations with quasi-adiabatic propagators, Chem. Phys. Lett. **210**, 448–457 (1993).

[80] N. Makri and D. E. Makarov, Tensor propagator for iterative quantum time evolution of reduced density matrices. I. Theory, J. Chem. Phys. **102**, 4600–4610 (1995).

[81] M. Richter and B. P. Fingerhut, Coarse-grained representation of the quasi adiabatic propagator path integral for the treatment of non-Markovian long-time bath memory, J. Chem. Phys. **146**, 214101 (2017).

[82] A. Imamoḡlu, Stochastic wave-function approach to non-Markovian systems, Phys. Rev. A **50**, 3650–3653 (1994).

[83] B. M. Garraway, Nonperturbative decay of an atomic system in a cavity, Phys. Rev. A **55**, 2290–2303 (1997).

[84] L. Mazzola, S. Maniscalco, J. Piilo, K.-A. Suominen, and B. M. Garraway, Sudden death and sudden birth of entanglement in common structured reservoirs, Phys. Rev. A **79**, 042302 (2009).

[85] J. Cerrillo and J. Cao, Non-markovian dynamical maps: Numerical processing of open quantum trajectories, Phys. Rev. Lett. **112**, 110401 (2014).

[86] B. L. Hu, J. P. Paz, and Y. Zhang, Quantum Brownian motion in a general environment: Exact master equation with nonlocal dissipation and colored noise, Phys. Rev. D **45**, 2843–2861 (1992).

[87] A. Garg, J. N. Onuchic, and V. Ambegaokar, Effect of friction on electron transfer in biomolecules, J. Chem. Phys. **83**, 4491–4503 (1985).

[88] A. Nazir and G. Schaller, The reaction coordinate mapping in quantum thermodynamics, in *Thermodynamics in the Quantum Regime: Fundamental Aspects and New Directions*, edited by F. Binder, L. A. Correa, C. Gogolin, J. Anders, and G. Adesso (Springer International Publishing, Cham, 2018) pp. 551–577.

[89] S. Alipour, A. T. Rezakhani, A. P. Babu, K. Mølmer, M. Möttönen, and T. Ala-Nissila, Correlation-picture approach to open-quantum-system dynamics, Phys. Rev. X **10**, 041024 (2020).

[90] F. Nathan and M. S. Rudner, Universal Lindblad equation for open quantum systems, Phys. Rev. B **102**, 115109 (2020).

[91] A. Trushechkin, Quantum master equations and steady states for the ultrastrong-coupling limit and the strong-decoherence limit, (2021), arxiv:2109.01888 .

[92] R. Alicki, Comment on "Reduced Dynamics Need Not Be Completely Positive", Phys. Rev. Lett. **75**, 3020–3020 (1995).

[93] A. Shaji and E. Sudarshan, Who's afraid of not completely positive maps?, Phys. Lett. A **341**, 48–54 (2005).

[94] D. Tupkary, A. Dhar, M. Kulkarni, and A. Purkayastha, Fundamental limitations in Lindblad descriptions of systems weakly coupled to baths, Phys. Rev. A **105**, 032208 (2022).

[95] R. Kubo, M. Toda, and N. Hashitsume, *Statistical Physics II* (Springer Berlin Heidelberg, 1991).

[96] S. Mukamel, *Principles of Nonlinear Optical Spectroscopy* (Oxford University Press, New York, 1995).

[97] A. Ishizaki and G. R. Fleming, Unified treatment of quantum coherent and incoherent hopping dynamics in electronic energy transfer: Reduced hierarchy equation approach, J. Chem. Phys. **130**, 234111 (2009).

[98] G. Ritschel and A. Eisfeld, Analytic representations of bath correlation functions for ohmic and superohmic spectral densities using simple poles, J. Chem. Phys. **141**, 094101 (2014).

[99] M. Kaltak and G. Kresse, Minimax isometry method: A compressive sensing approach for Matsubara summation in many-body perturbation theory, Phys. Rev. B **101**, 205145 (2020).

[100] S. Valleau, A. Eisfeld, and A. Aspuru-Guzik, On the alternatives for bath correlators and spectral densities from mixed quantum-classical simulations, J. Chem. Phys. **137**, 224103 (2012).

[101] P. Hänggi, H. Grabert, P. Talkner, and H. Thomas, Bistable systems: Master equation versus fokker-planck modeling, Phys. Rev. A **29**, 371–378 (1984).

[102] T. Albash, S. Boixo, D. A. Lidar, and P. Zanardi, Quantum adiabatic Markovian master equations, New J. Phys. **14**, 123016 (2012).

[103] J.-M. Zhang, B. Chen, and J. Jing, Trapping quantum coherence with a dissipative thermal bath (2022), arXiv:2209.01781 .

[104] R. Alicki and K. Lendi, *Quantum Dynamical Semigroups and Applications* (Springer, Berlin, 2007).

[105] S. Diehl, A. Micheli, A. Kantian, B. Kraus, H. P. Büchler, and P. Zoller, Quantum states and phases in driven open quantum systems with cold atoms, Nat. Phys. **4**, 878–883 (2008).

[106] K. H. Lee, V. Balachandran, R. Tan, C. Guo, and D. Poletti, Giant spin current rectification due to the interplay of negative differential conductance and a non-uniform magnetic field, Entropy **22**, 1311 (2020).

[107] M. Reh, M. Schmitt, and M. Gärttner, Time-Dependent Variational Principle for Open Quantum Systems with Artificial Neural Networks, Phys. Rev. Lett. **127**, 230501 (2021).

[108] S. Denisov, T. Laptyeva, W. Tarnowski, D. Chruściński, and K. Życzkowski, Universal Spectra of Random Lindblad Operators, Phys. Rev. Lett. **123**, 140403 (2019).

[109] J. C. Flack, Coarse-graining as a downward causation mechanism, Phil. Trans. R. Soc. A. **375**, 20160338 (2017).

[110] L. Dávila Romero and J. Pablo Paz, Decoherence and initial correlations in quantum Brownian motion, Phys. Rev. A **55**, 4070–4083 (1997).

[111] R. Karrlein and H. Grabert, Exact time evolution and master equations for the damped harmonic oscillator, Phys. Rev. E **55**, 153–164 (1997).

[112] C. Timm, Time-convolutionless master equation for quantum dots: Perturbative expansion to arbitrary order, Phys. Rev. B **83**, 115416 (2011).

[113] J. P. Paz, Physical origins of time asymmetry, in *Decoherence in Quantum Brownian Motion*, Vol. 1 (Cambridge University Press, 1994) pp. 213–220.

[114] H.-P. Breuer, E.-M. Laine, J. Piilo, and B. Vacchini, Colloquium: Non-Markovian dynamics in open quantum systems, Rev. Mod. Phys. **88**, 021002 (2016).

[115] J. Thingna, Steady-state transport properties of anharmonic systems, PhD thesis (2013).

[116] A. Colla and H.-P. Breuer, Open-system approach to nonequilibrium quantum thermodynamics at arbitrary coupling, Phys. Rev. A **105**, 052216 (2022).

[117] F. Haake and R. Reibold, Strong damping and low-temperature anomalies for the harmonic oscillator, Phys. Rev. A **32**, 2462–2475 (1985).

[118] D. Burgarth, P. Facchi, R. Hillier, and M. Ligabò, Taming the Rotating Wave Approximation (2023), arxiv:2301.02269 .

[119] P. Hänggi and G.-L. Ingold, Fundamental aspects of quantum Brownian motion, Chaos **15**, 026105 (2005).

[120] L. D'Alessio, Y. Kafri, A. Polkovnikov, and M. Rigol, From quantum chaos and eigenstate thermalization to statistical mechanics and thermodynamics, Adv. Phys. **65**, 239–362 (2016).

[121] D. A. Abanin, E. Altman, I. Bloch, and M. Serbyn, Colloquium: Many-body localization, thermalization, and entanglement, Rev. Mod. Phys. **91**, 021001 (2019).

[122] T. Mori and S. Miyashita, Dynamics of the density matrix in contact with a thermal bath and the quantum master equation, Phys. Soc. Jpn. **77**, 124005 (2008).

[123] J. M. Deutsch, Eigenstate thermalization hypothesis, Rep. Prog. Phys. **81**, 082001 (2018).

[124] M. Campisi, P. Talkner, and P. Hänggi, Fluctuation Theorem for Arbitrary Open Quantum Systems, Phys. Rev. Lett. **102**, 210401 (2009).

[125] P. Talkner and P. Hänggi, Colloquium: Statistical mechanics and thermodynamics at strong coupling: Quantum and classical, Rev. Mod. Phys. **92**, 041002 (2020).

[126] S. Jang, J. Cao, and R. J. Silbey, Fourth-order quantum master equation and its Markovian bath limit, J. Chem. Phys. **116**, 2705–2717 (2002).

[127] J. Thingna, H. Zhou, and J.-S. Wang, Improved Dyson series expansion for steady-state quantum transport beyond the weak coupling limit: Divergences and resolution, J. Chem. Phys. **141**, 194101 (2014).

[128] H. Grabert, U. Weiss, and P. Talkner, Quantum theory of the damped harmonic oscillator, Z. Phys. B **55**, 87 (1984).

[129] A. O. Caldeira and A. J. Leggett, Quantum tunnelling in a dissipative system, Ann. Phys. **149**, 374–456 (1983).

[130] S. Maniscalco, J. Piilo, F. Intravaia, F. Petruccione, and A. Messina, Lindblad- and non-Lindblad-type dynamics of a quantum Brownian particle, Phys. Rev. A **70**, 032113 (2004).

[131] G. Homa, A. Csordás, M. A. Csirik, and J. Z. Bernád, Range of applicability of the Hu-Paz-Zhang master equation, Phys. Rev. A **102**, 022206 (2020).

[132] G. Homa, J. Z. Bernád, and L. Lisztes, Positivity violations of the density operator in the Caldeira-Leggett master equation, Eur. Phys. J. D **73**, 53 (2019).

[133] A. Tameshtit and J. E. Sipe, Positive Quantum Brownian Evolution, Phys. Rev. Lett. **77**, 2600–2603 (1996).

[134] F. Cerisola, M. Berritta, S. Scali, S. A. R. Horsley, J. D. Cresser, and J. Anders, Quantum-classical correspondence in spin-boson equilibrium states at arbitrary coupling, (2022), arxiv:2204.10874 .

[135] J. D. Cresser and J. Anders, Weak and Ultrastrong Coupling Limits of the Quantum Mean Force Gibbs State, Phys. Rev. Lett. **127**, 250601 (2021).

[136] G.-L. Ingold, *Dissipative Quantum Systems* (Universität Augsburg, 2018).

[137] G.-L. Ingold, Path integrals and their application to dissipative quantum systems, in *Coherent Evolution in Noisy Environments* (Springer Berlin Heidelberg, 2002) pp. 1–53.

[138] H. B. Callen and T. A. Welton, Irreversibility and generalized noise, Phys. Rev. **83**, 34–40 (1951).

[139] S. Maniscalco, F. Intravaia, J. Piilo, and A. Messina, Misbeliefs and misunderstandings about the non-Markovian dynamics of a damped harmonic oscillator, J. Opt. B: Quantum Semiclass. Opt. **6**, S98–S103 (2004).

[140] H. Grabert, P. Schramm, and G.-L. Ingold, Quantum Brownian motion: The functional integral approach, Physics Reports **168**, 115–207 (1988).

[141] T. Becker, L.-N. Wu, and A. Eckardt, Lindbladian approximation beyond ultraweak coupling, Phys. Rev. E **104**, 014110 (2021).

[142] T. Becker and A. Eckardt, Optimal form of time-local non-Lindblad master equations (2023), arxiv:2312.15066 .

[143] C. Gneiting, Disorder-dressed quantum evolution, Phys. Rev. B **101**, 214203 (2020).

[144] P. Groszkowski, A. Seif, J. Koch, and A. A. Clerk, Simple master equations for describing driven systems subject to classical non-Markovian noise, Quantum **7**, 972 (2023).

[145] J. H. P. Colpa, Diagonalization of the quadratic boson hamiltonian, Physica A: Statistical Mechanics and its Applications **93**, 327–353 (1978).

[146] P. F. Palmer, The singular coupling and weak coupling limits, J. Math. Phys. **18**, 527–529 (1977).

[147] J. M. Zhang and R. X. Dong, Exact diagonalization: The Bose–Hubbard model as an example, Eur. J. Phys. **31**, 591–602 (2010).

[148] V. V. Dodonov, O. V. Man'ko, V. I. Man'ko, and A. Wünsche, Hilbert-Schmidt distance and non-classicality of states in quantum optics, J. of Mod. Opt. **47**, 633–654 (2000).

[149] A. Gilchrist, N. K. Langford, and M. A. Nielsen, Distance measures to compare real and ideal quantum processes, Phys. Rev. A **71**, 062310 (2005).

[150] J. R. Johansson, P. D. Nation, and F. Nori, QuTiP 2: A Python framework for the dynamics of open quantum systems, Comput. Phys. Commun. **184**, 1234–1240 (2013).

[151] I. de Vega and D. Alonso, Dynamics of non-Markovian open quantum systems, Rev. Mod. Phys. **89**, 015001 (2017).

[152] B. Balzer and G. Stock, Modeling of decoherence and dissipation in nonadiabatic photoreactions by an effective-scaling nonsecular Redfield algorithm, Chem. Phys. **310**, 33–41 (2005).

[153] H. J. Goldsmid, *Introduction to Thermoelectricity* (Springer-Verlag, Berlin, 2010).

[154] P. Talkner and P. Hänggi, Open system trajectories specify fluctuating work but not heat, Phys. Rev. E **94**, 022143 (2016).

[155] S. Deffner, J. P. Paz, and W. H. Zurek, Quantum work and the thermodynamic cost of quantum measurements, Phys. Rev. E **94**, 010103 (2016).

[156] K. Singh, C. J. Fujiwara, Z. A. Geiger, E. Q. Simmons, M. Lipatov, A. Cao, P. Dotti, S. V. Rajagopal, R. Senaratne, T. Shimasaki, M. Heyl, A. Eckardt, and D. M. Weld, Quantifying and Controlling Prethermal Nonergodicity in Interacting Floquet Matter, Phys. Rev. X **9**, 041021 (2019).

[157] N. M. Myers, O. Abah, and S. Deffner, Quantum thermodynamic devices: From theoretical proposals to experimental reality, AVS Quantum Science **4**, 027101 (2022).

[158] L. Wu and A. Eckardt, Quantum engineering of a synthetic thermal bath for bosonic atoms in a one-dimensional optical lattice via Markovian feedback control, SciPost Physics **13**, 059 (2022).

[159] M. L. Alamo, F. Petiziol, and A. Eckardt, A minimal quantum heat pump based on high-frequency driving and non-Markovianity (2023), arxiv:2307.14892 .

[160] M. Langemeyer and M. Holthaus, Energy flow in periodic thermodynamics, Phys. Rev. E **89**, 012101 (2014).

[161] J. S. Lee and J. Yeo, Perturbative steady states of completely positive quantum master equations, Phys. Rev. E **106**, 054145 (2022).

[162] M. B. Plenio and P. L. Knight, The quantum-jump approach to dissipative dynamics in quantum optics, Rev. Mod. Phys. **70**, 101–144 (1998).

[163] Th. Basché, S. Kummer, and C. Bräuchle, Direct spectroscopic observation of quantum jumps of a single molecule, Nature **373**, 132–134 (1995).

[164] S. Gleyzes, S. Kuhr, C. Guerlin, J. Bernu, S. Deléglise, U. Busk Hoff, M. Brune, J.-M. Raimond, and S. Haroche, Quantum jumps of light recording the birth and death of a photon in a cavity, Nature **446**, 297–300 (2007).

[165] Z. K. Minev, S. O. Mundhada, S. Shankar, P. Reinhold, R. Gutiérrez-Jáuregui, R. J. Schoelkopf, M. Mirrahimi, H. J. Carmichael, and M. H. Devoret, To catch and reverse a quantum jump mid-flight, Nature **570**, 200–204 (2019).

[166] T. Becker, C. Netzer, and A. Eckardt, Quantum Trajectories for Time-Local Non-Lindblad Master Equations, Phys. Rev. Lett. **131**, 160401 (2023).

[167] N. Megier, D. Chruściński, J. Piilo, and W. T. Strunz, Eternal non-Markovianity: From random unitary to Markov chain realisations, Sci. Rep. **7**, 6379 (2017).

[168] A. McDonald and A. A. Clerk, Third quantization of open quantum systems: New dissipative symmetries and connections to phase-space and Keldysh field theory formulations, (2023), arxiv:2302.14047 .

[169] A. Smirne, M. Caiaffa, and J. Piilo, Rate operator unraveling for open quantum system dynamics, Phys. Rev. Lett. **124**, 190402 (2020).

[170] G. Chiriacò, M. Tsitsishvili, D. Poletti, R. Fazio, and M. Dalmonte, Diagrammatic method for many-body non-Markovian dynamics: Memory effects and entanglement transitions, Phys. Rev. B **108**, 075151 (2023).

[171] M. R. Hush, I. Lesanovsky, and J. P. Garrahan, Generic map from non-Lindblad to Lindblad master equations, Phys. Rev. A **91**, 032113 (2015).

[172] T. Felbinger and M. Wilkens, Stochastic wave-function simulation of two-time correlation functions, J. of Mod. Opt. **46**, 1401–1420 (1999).

[173] B. Donvil and P. Muratore-Ginanneschi, Quantum trajectory framework for general time-local master equations, Nat. Commun. **13**, 4140 (2022).

[174] M. J. W. Hall, J. D. Cresser, L. Li, and E. Andersson, Canonical form of master equations and characterization of non-Markovianity, Phys. Rev. A **89**, 042120 (2014).

[175] E. Guardado-Sanchez, B. M. Spar, P. Schauss, R. Belyansky, J. T. Young, P. Bienias, A. V. Gorshkov, T. Iadecola, and W. S. Bakr, Quench dynamics of a Fermi gas with strong nonlocal interactions, Phys. Rev. X **11**, 021036 (2021).

[176] A. Schnell, Global becomes local: Efficient many-body dynamics for global master equations (2023), arxiv:2309.07105 .

[177] F. Verstraete, V. Murg, and J. Cirac, Matrix product states, projected entangled pair states, and variational renormalization group methods for quantum spin systems, Advances in Physics **57**, 143–224 (2008).

[178] U. Schollwöck, The density-matrix renormalization group in the age of matrix product states, Annals of Physics **326**, 96–192 (2011).

[179] X. Xu, J. Thingna, C. Guo, and D. Poletti, Many-body open quantum systems beyond Lindblad master equations, Phys. Rev. A **99**, 012106 (2019).

[180] H. Weimer, A. Kshetrimayum, and R. Orús, Simulation methods for open quantum many-body systems, Rev. Mod. Phys. **93**, 015008 (2021).

[181] D. Tupkary, A. Dhar, M. Kulkarni, and A. Purkayastha, Fundamental limitations in Lindblad descriptions of systems weakly coupled to baths, Phys. Rev. A **105**, 032208 (2022).

[182] K. Nestmann and C. Timm, Time-convolutionless master equation: Perturbative expansions to arbitrary order and application to quantum dots (2019), arxiv:1903.05132 .

[183] E. B. Davies, Markovian master equations, Comm. Math. Phys. **39**, 91–110 (1974).

[184] T. Becker, A. Schnell, and J. Thingna, Canonically Consistent Quantum Master Equation, Phys. Rev. Lett. **129**, 200403 (2022).

[185] M. M. Wolf, J. Eisert, T. S. Cubitt, and J. I. Cirac, Assessing non-markovian quantum dynamics, Phys. Rev. Lett. **101**, 150402 (2008).

[186] N. Li, J. Ren, L. Wang, G. Zhang, P. Hänggi, and B. Li, Colloquium: Phononics: Manipulating heat flow with electronic analogs and beyond, Rev. Mod. Phys. **84**, 1045–1066 (2012).

[187] M. Thoss and F. Evers, Perspective: Theory of quantum transport in molecular junctions, J. Chem. Phys. **148**, 030901 (2018).

[188] I. Knezevic and B. Novakovic, Time-dependent transport in open systems based on quantum master equations, J. Comput. Electron. **12**, 363–374 (2013).

[189] J. E. Elenewski, D. Gruss, and M. Zwolak, Communication: Master equations for electron transport: The limits of the Markovian limit, J. Chem. Phys. **147**, 151101 (2017).

[190] D. K. Ferry, J. Weinbub, M. Nedjalkov, and S. Selberherr, A review of quantum transport in field-effect transistors, Semicond. Sci. Technol. **37**, 043001 (2022).

[191] E. Crowder, L. Lampert, G. Manchanda, B. Shoffeitt, S. Gadamsetty, Y. Pei, S. Chaudhary, and D. Davidović, Application of the Fourth-Order Time Convolutionless Master Equation to Open Quantum Systems with Infrared Diverging Dynamics (2023), arxiv:2310.15089 .

[192] B. B. Laird, J. Budimir, and J. L. Skinner, Quantum-mechanical derivation of the Bloch equations: Beyond the weak-coupling limit, J. Chem. Phys. **94**, 4391–4404 (1991).

[193] N. Anto-Sztrikacs and D. Segal, Strong coupling effects in quantum thermal transport with the reaction coordinate method, New J. Phys. **23**, 063036 (2021).

[194] M. Esposito, M. A. Ochoa, and M. Galperin, Nature of heat in strongly coupled open quantum systems, Phys. Rev. B **92**, 235440 (2015).

[195] C. Jarzynski, Stochastic and macroscopic thermodynamics of strongly coupled systems, Phys. Rev. X **7**, 011008 (2017).

[196] P. Strasberg and M. Esposito, Stochastic thermodynamics in the strong coupling regime: An unambiguous approach based on coarse graining, Phys. Rev. E **95**, 062101 (2017).

[197] D. Newman, F. Mintert, and A. Nazir, Performance of a quantum heat engine at strong reservoir coupling, Phys. Rev. E **95**, 032139 (2017).

[198] J.-S. Wang, B. K. Agarwalla, H. Li, and J. Thingna, Nonequilibrium Green's function method for quantum thermal transport, Front. Phys. **9**, 673–697 (2014).

[199] N. Bergmann and M. Galperin, A Green's function perspective on the nonequilibrium thermodynamics of open quantum systems strongly coupled to baths, Eur. Phys. J. Spec. Top. **230**, 859–866 (2021).

[200] G. T. Landi, D. Poletti, and G. Schaller, Nonequilibrium boundary-driven quantum systems: Models, methods, and properties, Rev. Mod. Phys. **94**, 045006 (2022).

[201] N. Anto-Sztrikacs, A. Nazir, and D. Segal, Effective-Hamiltonian Theory of Open Quantum Systems at Strong Coupling, PRX Quantum **4**, 020307 (2023).

[202] A. Schnell, A. Eckardt, and S. Denisov, Is there a floquet lindbladian?, Phys. Rev. B **101**, 100301 (2020).

[203] M. Reitter, J. Näger, K. Wintersperger, C. Sträter, I. Bloch, A. Eckardt, and U. Schneider, Interaction dependent heating and atom loss in a periodically driven optical lattice, Phys. Rev. Lett. **119**, 200402 (2017).

[204] R. Blümel, A. Buchleitner, R. Graham, L. Sirko, U. Smilansky, and H. Walther, Dynamical localization in the microwave interaction of Rydberg atoms: The influence of noise, Phys. Rev. A **44**, 4521–4540 (1991).

[205] J. Dziarmaga, Dynamics of a quantum phase transition and relaxation to a steady state, Advances in Physics **59**, 1063–1189 (2010).

[206] D. Poletti and C. Kollath, Slow quench dynamics of periodically driven quantum gases, Phys. Rev. A **84**, 013615 (2011).

[207] A. Polkovnikov, K. Sengupta, A. Silva, and M. Vengalattore, Colloquium: Nonequilibrium dynamics of closed interacting quantum systems, Rev. Mod. Phys. **83**, 863–883 (2011).

[208] A. Russomanno, A. Silva, and G. E. Santoro, Periodic Steady Regime and Interference in a Periodically Driven Quantum System, Phys. Rev. Lett. **109**, 257201 (2012).

[209] A. Lazarides, A. Das, and R. Moessner, Periodic Thermodynamics of Isolated Quantum Systems, Phys. Rev. Lett. **112**, 150401 (2014).

[210] A. Eckardt and E. Anisimovas, High-frequency approximation for periodically driven quantum systems from a Floquet-space perspective, New J. Phys. **17**, 093039 (2015).

[211] T. Shirai, T. Mori, and S. Miyashita, Floquet–Gibbs state in open quantum systems, Eur. Phys. J. Special Topics **277**, 323–333 (2018).

[212] C. Zerbe and P. Hänggi, Brownian parametric quantum oscillator with dissipation, Phys. Rev. E **52**, 1533–1543 (1995).

Acknowledgements

I thank all my collaborators: Alexander Schnell, Camilo Santiago Tello Breuer, Ché Netzer, Juzar Thingna, and Ling-Na Wu. A special thanks goes to my supervisor André Eckardt for scientific and mental support throughout the years as a Master's and doctoral student.

As a scientific supervisor André does not only push me to have good results, but also to present them in the best way possible. He has taught me everything I know about scientific writing. He never cuts short on rehearsing talks for scientific conferences and to give detailed feedback on manuscripts. Apart from his excellent expertise, he is also very supportive when things are difficult. On the one hand, before I get lost in technical details, he reminds me of the bigger picture. On the other hand, he keeps me motivated for the well-invested effort into scientific projects.

In 2018 as a Master's student, I joined André's group at the Max Planck institute for the physics of complex systems in Dresden. There, I was also co-supervised by Ling-Na Wu and successfully finished my Master's thesis in April 2019. Ling-Na was also the first person, who pointed out that the diagonalization of the Redfield equation was not unique, which has had a great impact on the course of the subsequent projects ever since.

In May 2019 I continued as a doctoral student and was given the chance to attend international conferences. An exceptional great experience was the 709. WE-Heraeus-Seminar on *Quantization of Dissipative Chaos: Ideas and Means*, in December 2019, where I was given the chance to contribute with a talk. During this seminar, I was able to get to know scientists, with a great impact in the field of open quantum systems. Here, I would like to mention Juzar Thingna, who is not only an excellent researcher, but also became effectively my second supervisor and my scientific role model. Throughout the years, and together with Alexander Schnell, we held weekly discussions for several hours. Juzar not only contributed excellent scientific guidance, especially, for the CCQME project, but also provided encouraging mental support. Without him, the thesis in this form would not have been possible.

Equally, I thank Alexander Schnell for his contributions. He has a great expertise in the field of open quantum systems. From Alex, I also learned how important it is to reach out to people in a scientific environment, e.g., to ask questions after a talk or in a poster session.

During my time as a research assistant at the TU Berlin, starting from March 2020, I was also entitled to co-supervise several Bacherlor's and Master's theses. Here, I want to thank Abdul Wasay, Camilo Santiago Tello Breuer, Charlotte Maurer, Ché Netzer, Dorian Wenzel, Jerome Wiesemann, Johann Frederik Aßmuss, Juan Mateo Rodriguez Umbarila, and Sarah Spaulding. From my perspective all of them did an excellent work, for which some of them were even acknowledged by scientific publications. Furthermore, from co-supervising, I have learned a lot of things that I will carry on to my future career.

For carefully reading this manuscript and for their feedback I want to thank André Eckardt, Andy Knoll, Francesco Petiziol, Isaac Tesfaye, Robert Fuchs, and Robert Salzwedel.

Selbstständigkeitserklärung

Diese Arbeit wurde unter der wissenschaftlichen Betreuung von Prof. Dr. André Eckardt durchgeführt.

Hiermit versichere ich, dass ich die vorliegende Arbeit ohne unzulässige Hilfe Dritter und ohne Benutzung anderer als der angegebenen Hilfsmittel angefertigt habe; die aus fremden Quellen direkt oder indirekt übernommenen Gedanken sind als solche kenntlich gemacht. Die Arbeit wurde bisher weder im Inland noch im Ausland in gleicher oder ähnlicher Form einer anderen Prüfungsbehörde vorgelegt.